A Bioimpedance Simulator

A dissertation
submitted in partial fulfilment of
the requirements for the degree of

Master of Technology
in Biomedical Engineering

by

Shibam Debbarma
(143300020)

under the supervision of

Prof. P. C. Pandey

Department of Biosciences and Bioengineering
Indian Institute of Technology Bombay
June 2016

Indian Institute of Technology Bombay

M. Tech. Dissertation Approval

Dissertation entitled "**A bioimpedance simulator**" by **Shibam Debbarma** (Roll No. **143300020**) is approved, after the successful completion of *viva voce* examination, for the award of the degree of **Master of Technology** in **Biomedical Engineering**.

Supervisor ..... PCPandey 4/7/2016
(Prof. P. C. Pandey)

Examiners .....
(Prof. D. K. Sharma)

.....
(Prof. L. R. Subramanyan)

Chairperson .....
(Prof. Joseph John)

Date: July 4, 2016

Place: Mumbai

Declaration

I declare that this dissertation represents my own ideas and words. I have cited and referenced the original sources adequately wherever other's ideas and words are included. I also declare that I have adhered to all principles of academic honesty and integrity and have not mispresented or fabricated or falsified any idea/data/fact/source in my submission. I understand any violation of the above will be a cause for disciplinary action by the institute and can also evoke penal action from the sources which have thus not been properly cited or from whom proper permission has not been taken when needed.

Shibam Debbarma

(Shibam Debbarma)

143300020
(Roll No.)

Date: July 4, 2016

Place: Mumbai

Shibam Debbarma/ Prof. P. C. Pandey (supervisor), “A bioimpedance simulator”, M.Tech. Dissertation, Biomedical Engineering, Indian Institute of Technology Bombay, June 2016.

ABSTRACT

Impedance cardiography is a non-invasive technique for monitoring the time-varying thoracic impedance during the cardiac cycle and is used for diagnosing cardiovascular disorders. The thoracic impedance has a basal impedance and a time-varying component. A bioimpedance simulator with a settable basal value and time-varying component with selectable waveform and settable parameters is developed for testing and calibration of impedance cardiograph and other bioimpedance measuring instruments. It has four blocks: impedance variation circuit for realizing the time-varying thoracic impedance, the controller circuit for controlling the impedance variation, a wireless module connected to the controller with serial interface for setting the parameters of the control waveforms, and a battery powered power supply block. The simulator is electrically isolated from the mains. A PC-based GUI for setting the control parameters through wireless link is also developed. The impedance variation circuit consists of switch-resistor network to provide to fix basal impedance connected in parallel with a voltage-controlled resistor (VCR) circuit to provide the time-varying component. The VCR circuit has to provide precise linear variation in resistance in response to control voltages applied to it. Circuits using matched JFET and MOSFET pairs for realizing a floating precision linear VCR are studied and tested using simulation and practical implementation. For the simulator, a matched JFET pair based VCR with SD bootstrapped gate and self-tracking arrangement is implemented to extend the range of linear operation and to reduce device-parameter dependency. The switch-resistor is implemented using analog switches connected in parallel with fixed resistors. The control parameters for the switch-resistor network and the VCR circuit is set from the controller.

CONTENTS

ABSTRACT		**i**
LIST OF ABBREVIATIONS		**iv**
LIST OF SYMBOLS		**v**
LIST OF FIGURES		**vi**
LIST OF TABLES		**xi**
Chapter 1	**INTRODUCTION**	**1**
1.1	Background	1
1.2	Project objective	1
1.3	Dissertation outline	2
Chapter 2	**BASICS OF IMPEDANCE CARDIOGRAPHY**	**3**
2.1	Introduction	3
2.2	The ICG waveform	3
2.3	The parallel column model of thoracic impedance	4
2.4	The impedance cardiograph	6
2.5	Electrode configurations	7
2.6	Bioimpedance simulator	8
Chapter 3	**JFET BASED VOLTAGE-CONTROLLED RESISTOR**	**9**
3.1	Introduction	9
3.2	JFET basics	9
3.3	JFET based VCR circuits	11
3.4	Simulation results for JFET as a voltage-controlled resistor	19
3.5	Practical results for the floating precision linear VCR proposed by Holani et al. [26]	26
3.6	Conclusion	28
Chapter 4	**MOSFET BASED VOLTAGE-CONTROLLED RESISTOR**	**30**
4.1	Introduction	30
4.2	MOSFET device basics	30
4.3	MOSFET based VCR circuits	32
4.4	Simulation results for the floating precision linear VCR circuit using matched MOSFET device pair	39
4.5	Practical results for the floating precision linear VCR circuit using matched MOSFET device pair	43

4.6	Conclusion	45
Chapter 5	**BIOIMPEDANCE SIMULATOR**	**46**
5.1	Introduction	47
5.2	The thoracic impedance model	48
5.3	Realization of the bioimpedance simulator	43
5.4	Microcontroller program	57
5.5	PC-based GUI for real-time parameter setting	62
Chapter 6	**TEST RESULTS**	**64**
6.1	Introduction	64
6.2	Validation of the power supply circuit	64
6.3	Validation of the controller circuit	65
6.4	Validation of the impedance variation circuit	70
6.5	Conclusion	72
Chapter 7	**SUMMARY AND CONCLUSION**	**82**
APPENDICES		**83**
A	Simulation results for JFET based VCR circuits	83
B	Practical results for JFET based VCR circuits	119
C	Simulation and Practical Results for MOSFET Based VCR Circuits	123
D	Schematic of bioimpedance simulator	128
E	PCB layout of bioimpedance simulator	131
F	Component list for bioimpedance simulator	135
REFERENCES		**138**
ACKNOWLEDGEMENT		**142**
AUTHOR'S RESUME		**143**

LIST OF ABBREVIATIONS

Abbreviation	Explanation
ASCII	American Standard Code for Information Interchange
COM	communication
DAC	digital-to-analog converter
ECG	electrocardiogram
EGG	electro-glottography
GUI	graphical user interface
IC	integrated circuit
ICG	impedance cardiogram
IO	input-output
ISR	interrupt service routine
JFET	junction field-effect transistor
LDO	low drop-out
MOSFET	metal-oxide-semiconductor field-effect transistor
PC	personal computer
SD	source-drain
SV	stroke volume
UART	universal asynchronous receiver/transmitter
VCR	voltage-controlled resistor

LIST OF SYMBOLS

Symbol	Explanation
i_D	drain current
i_X	current through terminal X
I_{DSS}	drain saturation current
R_{DS}	drain-source channel resistance
R_{XY}	resistance across X-Y terminal
R_o	fixed resistance in the simulator model of thorax
R_v	variable resistance in the simulator model of thorax
R_{E1E2}	resistance across the terminals E1 and E2
v_B	substrate voltage
v_{BS}	substrate-source voltage
v_C	control voltage
v_{DS}	drain-source voltage
v_G	gate voltage
v_{GS}	gate-source voltage
V_P	pinch-off voltage
v_{REF}	reference voltage in the VCR circuit
V_{T0}	threshold voltage without body effect
V_T	threshold voltage
v_X	X-terminal voltage
v_Y	Y-terminal voltage
V_{BB}	substrate bias voltage

LIST OF FIGURES

Figure 2.1: The thoracic impedance waveform ($\Delta Z = Z(t) - Z_0$), where Z_0 is the basal impedance, ICG ($-dZ/dt$) , and ECG waveform, adapted from [7]. 4

Figure 2.2: Parallel column model of thoracic impedance [3]. 5

Figure 2.3: Block diagram for impedance cardiograph instrument with tetra-polar electrode configuration. 6

Figure 2.4: Various Spot Electrode Array configuration [102]. 7

Figure 3.1: An n-channel JFET and its v_{DS} vs i_D characteristics [15] 10

Figure 3.2: JFET based floating linear VCR devised by Senani [21]. 12

Figure 3.3: R_{XY} as a function of v_C and v_{XY} for linear operation of the JFET-based floating VCR proposed by Senani [21]. 13

Figure 3.4: Matched JFET pair based VCR circuit proposed by Clarke [22]. 14

Figure 3.5: VCR circuit reported by Tadic [23] using matched device pair and multiplier-divider, schematic redrawn on the basis of Figures 1 and 2 of [23]. 16

Figure 3.6: Floating linear precision VCR circuit proposed by Holani et al. [24]. 17

Figure 3.7: Effect of device parameter variation (33% change in I_{DSS} and V_P) on R_{XY} vs. v_{XY} response of JFET based VCR circuits with $\lambda = 0$. Circuits: (a) single JFET as VCR, (b) VCR circuit of Senani [21], and (c) VCR circuits of Holani et al. [24]. Device parameters: (i) I_{DSS} = 15 mA, $V_P = -3$ V, (ii) I_{DSS} = 20 mA, $V_P = -3$ V, (iii) I_{DSS} = 10 mA, $V_P = -3$ V, (iv) I_{DSS} = 15 mA, $V_P = -4$ V, and (v) I_{DSS} = 15 mA, $V_P = -2$ V. 23

Figure 3.8: Effect of device parameter variation (33% change in I_{DSS} and V_P) on R_{XY} vs. v_{XY} response of JFET based VCR circuits with $\lambda = 0.03$. Circuits: (a) single JFET as VCR, (b) VCR circuit of Senani [21], and (c) VCR circuits of Holani et al. [24]. Device parameters: (i) I_{DSS} = 15 mA, $V_P = -3$ V, (ii) I_{DSS} = 20 mA, $V_P = -3$ V, (iii) I_{DSS} = 10 mA, $V_P = -3$ V, (iv) I_{DSS} = 15 mA, $V_P = -4$ V, and (v) I_{DSS} = 15 mA, $V_P = -2$ V. 24

Figure 3.9: Effect of λ on R_{XY} vs. v_{XY} response for the floating precision linear VCR using matched JFET pair. Device parameters (with ±33 % variation): (i) I_{DSS} = 15 mA, $V_P = -3$ V, (ii) I_{DSS} = 20 mA, $V_P = -3$ V, (iii) I_{DSS} = 10 mA, $V_P = -3$ V, (iv) I_{DSS} = 15 mA, $V_P = -4$ V, and (v) I_{DSS} = 15 mA, $V_P = -2$ V. 25

Figure 3.10: Simulation results for R_{XY} vs. v_{XY} response for the floating precision linear VCR using matched JFET pair proposed by Holani et al. [24] with the effect of λ. Device parameters: Q1 with I_{DSS} = 0.8987 mA, $V_P = -1.032$ V and Q2 with I_{DSS} = 0.8842 mA, $V_P = -1.028$ V. 27

Figure 3.11: Practical results for R_{XY} vs. v_{XY} response for the floating precision linear VCR using matched JFET pair proposed by Holani et al. [24]. Device parameters: Q1 with I_{DSS} = 0.8987 mA, V_P = −1.032 V and Q2 with I_{DSS} = 0.8842 mA, V_P = −1.028 V. 28

Figure 4.1: An enhancement-type n channel MOSFET and its drain-source voltage vs drain current characteristics [28]. 31

Figure 4.2: Enhancement-type MOSFET-based VCR developed by Moon et.al. [31]. 33

Figure 4.3: MOSFET based VCR circuit proposed by Fort [32]. 34

Figure 4.4: Matched-pair MOSFET-based floating VCR circuit with SD-bootstrapped gate, SD-bootstrapped substrate, and self-tracking. 37

Figure 4.5: R_{XY} as a function of v_A and v_{XY} for linear operation of the MOSFET pair-based floating precision linear VCR. 39

Figure 4.6: Effect of v_{C2} and λ on R_{XY} vs. v_{XY} response of the floating precision linear VCR using matched MOSFET pair based VCR circuit (in Figure 4.4). Device parameters: (a) λ = 0 and (b) λ = 0.03, for two sets of k and V_T as follows: (i) k = 0.52 mA/V^2 and V_T = 0.7 V, (ii) k = 0.28 mA/V^2 and V_T = 0.4 V, V_{BB} = −2 V. 42

Figure 4.7: Effect of V_{BB} and λ on R_{XY} vs. V_{XY} response of the floating precision linear VCR using matched MOSFET pair based VCR circuit (in Figure 4.4). Substrate voltage: (a) V_{BB} = −2 V and (b) V_{BB} = −4 V, Device parameters: k = 0.52 mA/V^2 and V_T = 0.7 V. Control voltages: v_{C1} = 1 V, v_{C2} = −1 V, and v_{C3} = 0 V. 43

Figure 4.8: Effect of device parameters on R_{XY} vs. V_{XY} response of the floating precision linear VCR using matched MOSFET pair based VCR circuit (in Figure 4.4). Device parameters: (a) k = 0.52 mA/V^2 and V_T = 0.7 V and (b) k = 0.28 mA/V^2 and V_T = 0.4 V. Control voltages: v_{C1} = 1 V, v_{C2} = −1 V, and v_{C3} = 0 V. 43

Figure 4.9: Practical results for R_{XY} vs. V_{XY} response of the floating precision linear VCR using matched MOSFET pair based VCR circuit (in Figure 4.4). Device parameters (calculated) : k = 0.575 mA/V^2 and V_T = 0.396 V and k = 0.614 mA/V^2 and V_T = 0.389 V. Substrate voltage: (a) V_{BB} = −2 V and (b) V_{BB} = −4 V. Control voltages: v_{C1} = 1 V, v_{C2} = −0.5 V and −1 V, and v_{C3} = 0 V. 44

Figure 5.1: Thoracic impedance model [13]. 48

Figure 5.2: Block diagram of bioimpedance simulator. 49

Figure 5.3: Switch-Resistor circuit. 50

Figure 5.4: VCR circuit implemented using U441 [25] and LT1499 [46]. 51

Figure 5.5: Controller. 52

Figure 5.6: Differential amplifiers for generating v_1 and v_2 from the two DAC channels of the microcontroller U8. 53

Figure 5.7: Connections of Bluetooth module. 54

Figure 5.8: Power supply circuit. 56

Figure 5.9: Flow chart of the main program of “bioimpedance_simulator_control”. 60

Figure 5.10: Flow chart for U1RXInterrupt ISR of bioimpedance_simulator_control. 61

Figure 5.11: PC based GUI program “Bio-impedance Simulator”: (a) Initial appearance of bioimpedance simulator, (b) GUI connected to the Bluetooth module through COM Port 6, and different parameter values are set for basal resistance, left DAC channel and right DAC channel. 63

Figure 6.1: Control voltage signals with their parameters: (a) Parameter values set by the PC based GUI, and (b) Generated control waveforms for the VCR circuit v_1 (Right DAC Channel) with sinusoidal signal of peak-to-peak voltage 2 V, frequency 100 Hz, offset 0 V (Pink), v_2 (Left DAC Channel)with sinusoidal signal of peak-to-peak voltage 2 V, frequency 100 Hz, offset 0 V (Cyan) around AVREF of 1.65 V (Green). 66

Figure 6.2: Control voltage signals with their parameters: (a) Parameter values set by the PC based GUI, and (b) Generated control waveforms for the VCR circuit v_1 (Right DAC Channel) with triangular signal of peak-to-peak voltage 2 V, frequency 50 Hz, offset −1 V (Pink), v_2 (Left DAC Channel) with square signal of peak-to-peak voltage 2 V, frequency 100 Hz, offset 0.4 V (Cyan) around AVREF of 1.65 V (Green). 67

Figure 6.3: Control voltage signals with their parameters: (a) Parameter values set by the PC based GUI, and (b) Generated control waveforms for the VCR circuit v_1 (Right DAC Channel) with sawtooth signal of peak-to-peak voltage 2 V, frequency 50 Hz, offset 1 V (Pink), v_2 (Left DAC Channel) with sinusoidal signal of peak-to-peak voltage 2 V, frequency 10 Hz, offset −1 V (Cyan) around AVREF of 1.65 V (Green). 68

Figure 6.4: Control voltage signals with their parameters: (a) Parameter values set by the PC based GUI, and (b) Generated control waveforms for the VCR circuit v_1 (Right DAC Channel) with sawtooth signal of peak-to-peak voltage 1.2 V, frequency 0.1 Hz, offset −1 V (Pink), v_2 (Left DAC Channel) with sinusoidal signal of peak-to-peak voltage 1.36 V, frequency 1 Hz, offset 1 V (Cyan) around AVREF of 1.65 V (Green). 69

Figure 6.5: Circuit for testing of the VCR circuit response. Configurations: (a) Testing of DC response for the VCR and (b) Testing of AC response for the VCR. 72

Figure 6.6: Control voltage signals with their parameters: (a) Parameter values set by the PC based GUI, and (b) Generated control waveforms for the VCR circuit v_1 (Right DAC Channel) with sinusoidal signal of peak-to-peak voltage 400 mV, frequency 100 Hz, offset −0.8 V (Pink), v_2 (Left DAC Channel) with sinusoidal signal of amplitude 0 V, frequency 100 Hz, offset 0.4 V (Cyan) and the observed waveform at the floating terminal of the VCR circuit (Green). 73

Figure 6.7: Control voltage signals with their parameters: (a) Parameter values set by the PC based GUI, and (b) Generated control waveforms for the VCR circuit v_1 (Right DAC Channel) with sinusoidal signal of peak-to-peak voltage 200 mV, frequency 100 Hz, offset −0.8 V (Pink), v_2

(Left DAC Channel) with sinusoidal signal of amplitude 0 V, frequency 100 Hz, offset 0.4 V (Cyan) and the observed waveform at the floating terminal of the VCR circuit (Green). 74

Figure 6.8: Control voltage signals with their parameters: (a) Parameter values set by the PC based GUI, and (b) Generated control waveforms for the VCR circuit v_1 (Right DAC Channel) with square signal of peak-to-peak voltage 200 mV, frequency 100 Hz, offset −0.8 V (Pink), v_2 (Left DAC Channel) with sinusoidal signal of amplitude 0 V, frequency 100 Hz, offset 0.4 V (Cyan) and the observed waveform at the floating terminal of the VCR circuit (Green). 75

Figure 6.9: Control voltage signals with their parameters: (a) Parameter values set by the PC based GUI, and (b) Generated control waveforms for the VCR circuit v_1 (Right DAC Channel) with triangular signal of peak-to-peak voltage 200 mV, frequency 100 Hz, offset −0.8 V (Pink), v_2 (Left DAC Channel) with sinusoidal signal of amplitude 0 V, frequency 100 Hz, offset 0.4 V (Cyan) and the observed waveform at the floating terminal of the VCR circuit (Green). 76

Figure 6.10: Control voltage signals with their parameters: (a) Parameter values set by the PC based GUI, and (b) Generated control waveforms for the VCR circuit v_1 (Right DAC Channel) with sawtooth signal of peak-to-peak voltage 200 mV, frequency 100 Hz, offset −0.8 V (Pink), v_2 (Left DAC Channel) with sinusoidal signal of amplitude 0 V, frequency 100 Hz, offset 0.4 V (Cyan) and the observed waveform at the floating terminal of the VCR circuit (Green). 77

Figure 6.11: Control voltage signals with their parameters v_1 (Right DAC Channel) with sinusoidal signal of peak-to-peak voltage 200 mV, frequency 100 Hz, offset −0.8 V (Pink) and v_2 (Left DAC Channel) with sinusoidal signal of amplitude 0 V, frequency 100 Hz, offset 0.4 V (Cyan): (a) Input sinusoidal signal with frequency 10 kHz (Blue) and observed amplitude modulated signal with frequency 10 kHz (Green), (b) Input sinusoidal signal with frequency 50 kHz (Blue) and observed amplitude modulated signal with frequency 50 kHz (Green), and (c) Input sinusoidal signal with frequency 100 kHz (Blue) and observed amplitude modulated signal with frequency 100 kHz (Green). 78

Figure 6.12: Control voltage signals with their parameters v_1 (Right DAC Channel) with square signal of peak-to-peak voltage 200 mV, frequency 100 Hz, offset −0.8 V (Pink) and v_2 (Left DAC Channel) with sinusoidal signal of amplitude 0 V, frequency 100 Hz, offset 0.4 V (Cyan): (a) Input sinusoidal signal with frequency 10 kHz (Blue) and observed amplitude modulated signal with frequency 10 kHz (Green), (b) Input sinusoidal signal with frequency 50 kHz (Blue) and observed amplitude modulated signal with frequency 50 kHz (Green), and (c) Input sinusoidal signal with frequency 100 kHz (Blue) and observed amplitude modulated signal with frequency 100 kHz (Green). 79

Figure 6.13: Control voltage signals with their parameters v_1 (Right DAC Channel) with triangular signal of peak-to-peak voltage 200 mV, frequency 100 Hz, offset −0.8 V (Pink) and v_2 (Left DAC Channel) with sinusoidal signal of amplitude 0 V, frequency 100 Hz, offset 0.4 V (Cyan): (a) Input sinusoidal signal with frequency 10 kHz (Blue) and observed amplitude modulated signal

with frequency 10 kHz (Green), (b) Input sinusoidal signal with frequency 50 kHz (Blue) and observed amplitude modulated signal with frequency 50 kHz (Green), and (c) Input sinusoidal signal with frequency 100 kHz (Blue) and observed amplitude modulated signal with frequency 100 kHz (Green). 80

Figure 6.14: Control voltage signals with their parameters v_1 (Right DAC Channel) with sawtooth signal of peak-to-peak voltage 200 mV, frequency 100 Hz, offset −0.8 V (Pink) and v_2 (Left DAC Channel) with sinusoidal signal of amplitude 0 V, frequency 100 Hz, offset 0.4 V (Cyan): (a) Input sinusoidal signal with frequency 10 kHz (Blue) and observed amplitude modulated signal with frequency 10 kHz (Green), (b) Input sinusoidal signal with frequency 50 kHz (Blue) and observed amplitude modulated signal with frequency 50 kHz (Green), and (c) Input sinusoidal signal with frequency 100 kHz (Blue) and observed amplitude modulated signal with frequency 100 kHz (Green). 81

Figure D.1: The power supply circuit. 128

Figure D.2: The controller circuit. 129

Figure D.3: The impedance variation circuit. 130

Figure E.1: Top overlay of PCB. 131

Figure E.2: Bottom overlay of PCB. 132

Figure E.3: Top layer of PCB. 133

Figure E.4: Bottom layer of PCB. 134

LIST OF TABLES

Table 3.1: JFET parameters of U441 [25]. 19

Table 4.1: Device parameters of MOSFETs in ALD1106 [37]. 40

Table 5.1: Nominal values of R_{SW} for different switch combination. 50

Table 5.2: Estimated current requirement for each IC used in the bioimpedance simulator circuit. 55

Table 5.3: **S**imulation parameters for the bioimpedance simulator. 58

Table 6.1: Output voltage levels of the power supply circuit. 65

Table 6.2: Values of the digitally controlled basal resistance obtained from the switch-R circuit. 70

Table 6.3: Test results for the matched JFET pair based VCR circuit implemented on PCB for the bioimpedance simulator circuit. 71

Table A.1: Circuit simulation (LT Spice) results for JFET-based grounded VCR using single device (Circuit in Figure 3.1, with $v_C = v_{GS}$, $v_{XY} = v_{DS}$, and $i_X = i_D$): i_X and R_{XY} as a function of v_{XY}, with $v_C = 0$ V and λ as a parameter. (i) $V_P = -1$ V and $I_{DSS} = 6$ mA, (ii) $V_P = -1$ V and $I_{DSS} = 15$ mA, (iii) $V_P = -3.5$ V and $I_{DSS} = 6$ mA, and (iv) $V_P = -3.5$ V and $I_{DSS} = 15$ mA. 83

Table A.2: Circuit simulation (LT Spice) results for JFET-based grounded VCR using single device (Circuit in Figure 3.1, with $v_C = v_{GS}$, $v_{XY} = v_{DS}$, and $i_X = i_D$): R_{XY} as a function of v_{XY}, with different values of v_C and λ as a parameter. (i) $V_P = -1$ V and $I_{DSS} = 6$ mA, (ii) $V_P = -1$ V and $I_{DSS} = 15$ mA, (iii) $V_P = -3.5$ V and $I_{DSS} = 6$ mA, and (iv) $V_P = -3.5$ V and $I_{DSS} = 15$ mA. 87

Tabe A.3: Circuit simulation (LT Spice) results for JFET-based floating VCR using single device with SD-bootstrapped gate (Circuit in Figure 3.2 with $R_1 = R_2 = R_3 = R_5 = 10$ kΩ, $R_4 = 5$ kΩ): R_{XY} as a function of v_{XY}, with different values of v_C and λ as a parameter. (i) $V_P = -1$ V and $I_{DSS} = 6$ mA, (ii) $V_P = -1$ V and $I_{DSS} = 15$ mA, (iii) $V_P = -3.5$ V and $I_{DSS} = 6$ mA, and (iv) $V_P = -3.5$ V and $I_{DSS} = 15$ mA. 91

Table A.4: Circuit simulation (LT Spice) results for a floating precision linear VCR using matched JFET device pair with SD-bootstrapped gate and self-tracking arrangement (Circuit in Figure 3.6 with $R_2 = R_3 = 1$ MΩ, $R_4 = R_5 = R_7 = 10$ kΩ, $R_8 = 5$ kΩ): R_{XY} as a function of v_{XY}, with $v_{C1} = -0.5$ V, $v_{C2} = 0.5$ V, and λ as a parameter. (i) $V_P = -1$ V and $I_{DSS} = 6$ mA, (ii) $V_P = -1$ V and $I_{DSS} = 15$ mA, (iii) $V_P = -3.5$ V and $I_{DSS} = 6$ mA, and (iv) $V_P = -3.5$ V and $I_{DSS} = 15$ mA. Values of R_1 selected as the values of R_{XY} of the bootstrapped JFET circuit for λ = 0 and values of V_C as given in parentheses. 95

Table A.5: Circuit simulation (LT Spice) results for JFET-based grounded VCR using single device (Circuit in Figure 3.1, with $v_C = v_{GS}$, $v_{XY} = v_{DS}$, and $i_X = i_D$): R_{XY} as a function of v_{XY}, with

different values of v_C, and λ for devices with ±33% variation in V_P and I_{DSS}, λ = 0 and 0.03. H.Z. = high impedance (cut-off region). 99

Table A.6: Circuit simulation (LT Spice) results for JFET-based floating VCR using single device with SD-bootstrapped gate (Circuit in Figure 3.2 with $R_1 = R_2 = R_3 = R_5 = 10$ kΩ, $R_4 = 5$ kΩ): R_{XY} as a function of v_{XY}, with different values of v_C and λ for devices with ±33% variation in V_P and I_{DSS}, λ = 0 and 0.03. H.Z. = high impedance (cut-off region). 104

Table A.7: Circuit simulation (LT Spice) results for a floating precision linear VCR using matched JFET device pair with SD-bootstrapped gate and self-tracking arrangement (Circuit in Figure 3.6 with $R_2 = R_3 = 1$ MΩ, $R_4 = R_5 = R_7 = 10$ kΩ, $R_8 = 5$ kΩ): R_{XY} as a function of v_{XY}, with $R_1 = 300$ Ω, $v_{C2} = 0.5$ V, and v_{C1} as the voltage for devices with ±33% variation in V_P and I_{DSS}, λ = 0 and 0.03. 109

Table A.8 Circuit simulation (LT Spice) results for a precision linear floating VCR using matched JFET device pair with SD-bootstrapped gate and self-tracking arrangement considering the effect of mismatch in the device pair (Circuit in Figure 3.6 with $R_2 = R_3 = 1$ MΩ, $R_4 = R_5 = R_7 = 10$ kΩ, $R_8 = 5$ kΩ): R_{XY} as a function of v_{XY}, with $R_1 = 210$ Ω, $v_{C2} = 0.5$ V, and v_{C1} as the voltage for controlling the VCR value. Q1 has $V_P = -1$ V and $I_{DSS} = 6$ mA while Q2 has V_P and I_{DSS} with mismatch of ±20 mV and ±0.18 mA, respectively. 114

Table B.1: Circuit simulation (LT Spice) results for JFET-based floating VCR using single device with SD-bootstrapped gate (Circuit in Figure 3.2 with $R_1 = R_2 = R_3 = R_5 = 10$ kΩ, $R_4 = 5$ kΩ): R_{XY} as a function of v_{XY}, with different values of v_C and λ as a parameter. (i) $V_P = -1.032$ V & $I_{dss} = 0.8987$ mA, and (ii) $V_P = -1.028$ V & $I_{dss} = 0.8842$ mA. 119

Table B.2: Circuit simulation (LT Spice) results for a floating precision linear VCR using matched JFET device pair with SD-bootstrapped gate and self-tracking arrangement (Circuit in Figure 3.6 with $R_2 = R_3 = 1$ MΩ, $R_4 = R_5 = R_7 = 10$ kΩ, $R_8 = 5$ kΩ): R_{XY} as a function of v_{XY}, with $R_1 = 1000$ Ω, $v_{C2} = 0.5$ V, and v_{C1} as the voltage for controlling the VCR value. Device Pair: Q1 with $V_P = -1.032$ V and $I_{DSS} = 0.8987$ mA and Q2 with $V_P = -1.028$ V and $I_{DSS} = 0.8842$ mA. 121

Table B.3: Practical results for a precision linear floating VCR using matched JFET device pair with SD-bootstrapped gate and self-tracking arrangement (Circuit in Figure 3.6 with $R_2 = R_3 = 1$ MΩ, $R_4 = R_5 = R_7 = 10$ kΩ, $R_8 = 5$ kΩ, two 10 kΩ in parallel): R_{XY} as a function of v_{XY}, with $R_1 = 992$ Ω (measured value), $v_{C2} = 0.5$ V, and v_{C1} as the voltage for controlling the VCR value. Device Pair: Q1 with $V_P = -1.032$ V and $I_{DSS} = 0.8987$ mA and Q2 with $V_P = -1.028$ V and $I_{DSS} = 0.8842$ mA. 122

Table C.1: Circuit simulation (LT Spice) results for a floating precision linear VCR using matched MOSFET device pair with SD-bootstrapped gate, SD-bootstrapped substrate and self-tracking arrangement (Circuit in Figure 4.4 with $R_1 = 1$ kΩ, R_2 to $R_4 = R_6$ to $R_9 = R_{11}$ to $R_{14} = R_{16}$ to $R_{19} = R_{21} = 10$ kΩ, $R_5 = R_{10} = R_{15} = R_{20} = 5$ kΩ) for v_{C2} and λ: R_{XY} as a function of V_{XY}, $R_1 = 1000$ Ω, $v_{C1} = 1$ V, $v_{C3} = 0$ V, $V_{BB} = -2$ V. Device parameters: (i) $V_T = 0.7$ V and $k = 0.52$ mA/V^2, and (ii) $V_T = 0.4$ V and $k = 0.28$ mA/V^2. 123

Table C.2: Circuit simulation (LT Spice) results for a floating precision linear VCR using matched MOSFET device pair with SD-bootstrapped gate, SD-bootstrapped substrate and self-tracking arrangement (Circuit in Figure 4.4 with R_1 = 1 kΩ, R_2 to R_4 = R_6 to R_9 = R_{11} to R_{14} = R_{16} to R_{19} = R_{21} = 10 kΩ, R_5 = R_{10} = R_{15} = R_{20} = 5 kΩ) for V_{BB} and λ: R_{XY} as a function of v_{XY}, R_1 = 1000 Ω, v_{C1} = 1 V, v_{C2} = –1 V, v_{C3} = 0 V. Device parameters: V_T = 0.7 V and k = 0.52 mA/V^2. 125

Table C.3: Circuit simulation (LT Spice) results for a floating precision linear VCR using matched MOSFET device pair with SD-bootstrapped gate, SD-bootstrapped substrate and self-tracking arrangement (Circuit in Figure 4.4 with R_1 = 1 kΩ, R_2 to R_4 = R_6 to R_9 = R_{11} to R_{14} = R_{16} to R_{19} = R_{21} = 10 kΩ, R_5 = R_{10} = R_{15} = R_{20} = 5 kΩ) : R_{XY} as a function of v_{XY}, R_1 = 1000 Ω, v_{C1} = 1 V, v_{C2} = –1 V, v_{C3} = 0 V, and V_{BB} = –2 V. To observe the effect of device parameters V_T, k, and λ. Device parameters: (i) V_T = 0.7 V and k = 0.52 mA/V^2 and (ii) V_T = 0.4 V and k = 0.28 mA/V^2. 126

Table C.4: Practical results for a floating precision linear VCR using matched MOSFET device pair with SD-bootstrapped gate, SD-bootstrapped substrate and self-tracking arrangement (Circuit in Figure 4.4 with R_1 = 1 kΩ, R_2 to R_4 = R_6 to R_9 = R_{11} to R_{14} = R_{16} to R_{19} = R_{21} = 10 kΩ, R_5 = R_{10} = R_{15} = R_{20} = 5 kΩ) for v_{C2} and V_{BB} : R_{XY} as a function of v_{XY}, R_1 = 992 Ω, v_{C1} = 1 V, and v_{C3} = 0 V. Measured device parameter for the device pair with mismatch: M1: V_T = 0.396 V and k = 0.575 mA/V^2 and M2: V_T = 0.389 V and k = 0.614 mA/V^2. 127

Table F.1: Component list for the bioimpedance simulator 135

Chapter 1
INTRODUCTION

1.1 Background

Electrical impedance of biological materials (e.g. tissues, blood, body fluids etc.) is known as bioimpedance and its measurement is used in many different diagnostic techniques for extracting information about abnormalities present in the human body, such as fluid accumulation, vocal chord dynamics, cardiac disorders etc. [1], [2], [3]. Out of different types of biological materials, blood has the highest conductivity and variation in the amount of the blood in the thorax region causes impedance variation during the cardiac cycle [1], [2]. Impedance cardiography (ICG) is a noninvasive technique for monitoring of the thoracic impedance [3]. The impedance variation in the thorax region occurs mainly due to the volumetric changes in the blood vessels during the cardiac cycle and in the lungs during ventilation [5], [6]. The impedance variation is used for the assessment of hemodynamic parameters (e.g. blood ejection time, maximum blood ejection velocity, stroke volume, cardiac output etc.) and may be useful in the diagnosis of cardiac disorders (e.g. mitral stenonis) [4]. A current of low amplitude (< 5 mA) and high frequency (20 – 100 kHz) is injected through a pair of electrodes in the thorax and the resulting amplitude modulated voltage is sensed using the same or another pair of electrodes [3], [6], [7]. The envelope of the amplitude modulated voltage signal is obtained by demodulation to retrieve the impedance variation. Some of the commercially available ICG instruments are Niccomo [11] and Philips ICG [12].

A bioimpedance simulator is needed to generate time-varying impedance in order to determine the overall performance of the ICG instrument. It is used to test the linearity, sensitivity, frequency response, and dynamic behavior of the impedance sensing instrument using various test waveforms [13], [14]. It should be able to simulate the impedance variation of the thorax by providing a very small impedance variation (0.1 – 2 %) with different test waveforms superimposed on a base value, and should have the facility for selecting the base value, amplitude, frequency of variation and the waveform.

1.2 Project Objective

The objective of this project is to devise a bioimpedance simulator which can be used for testing the ICG instruments. The simulator should be capable of generating various test waveform (sine, square, triangular, sawtooth, and thoracic impedance waveform) with appropriate ranges of frequency and impedance variation. For realizing time-varying impedance with an arbitrarily controlled waveshape, precision floating voltage controlled

resistor (VCR) circuits using JFETs and MOSFETs are studied and tested. A matched JFET pair based VCR circuit is selected for use in the bioimpedance simulator. The designed simulator circuit has four blocks: impedance variation circuit for realizing the time varying thoracic impedance, the controller circuit for controlling the impedance variation, a wireless module connected to the controller with serial interface for setting the parameters of the control waveforms, and a battery powered power supply block. The simulator is electrically isolated from the mains. A PC-based GUI for setting the control parameter through wireless link is also developed.

1.3 Dissertation Outline

Chapter 2 provides a review of impedance cardiography. Chapters 3 and 4 present the study of JFET and MOSFET based VCR circuits, respectively. The bioimpedance simulator is presented in the fifth chapter and the test results are presented in the sixth chapter. The last chapter provides the summary and conclusions along with some suggestion for future work.

Chapter 2

BASICS OF IMPEDANCE CARDIOGRAPHY

2.1 Introduction

Impedance cardiography is a noninvasive technique useful for estimating various cardiovascular indices such as blood ejection time, maximum blood ejection rate, stroke volume, etc, by assessing the impedance variation across the thorax region [3], [6]. The variation in the thoracic impedance takes place due to volumetric change of blood in the blood vessels and change in blood resistivity as a function of its velocity during the cardiac cycle and due to variation of air volume inside the lungs due to ventilation [1], [2], [5]. An excitation current having low amplitude (< 5 mA) and high frequency (20 – 100 kHz) is injected in the thorax region through a pair of electrodes. The resulting voltage across the thorax gets amplitude modulated due to variation in the thoracic impedance. It is picked up using the current injecting or another pair of electrodes [3], [5], [6], [9] and is demodulated to get the impedance signal. The excitation strength is kept low in order to avoid any possibility of sensation and physiological effects [3], [6], [9]. The frequency of greater than 20 kHz results in low skin-electrode contact impedance and the thoracic impedance becomes almost resistive, resulting in better response in terms of thoracic impedance variation. Use of high frequency also results in lower carrier ripple after demodulation. However, at high frequency (> 500 kHz), the current does not pass through the deeper region of the thorax and the variable component of the impedance decreases. Further, the precision of the impedance detector circuit decreases at higher excitation frequency. Hence, the frequency range of 20 – 100 kHz is considered to be most appropriate The impedance offered by the thorax region has two components: a basal impedance due to the presence of bones, organs and tissues which remains almost constant and a time-varying component due to volumetric changes in blood volume during cardiac cycles superimposed on the basal impedance [3], [6], [7]. The basal impedance ranges from 20 – 200 Ω, depending on the height, weight, age, and thoracic fluid volume. The time-varying component ranges from 0.1 – 2 % of the basal impedance and hence extracting the impedance variation signal is a challenging task [3] – [9].

2.2 The ICG Waveform

A typical thoracic impedance waveform is shown in Figure 2.1 along with the impedance cardiogram (ICG) which is negative first derivative of the thoracic impedance $\left(dZ/dt\right)$ [7]. The ECG waveform sensed using the ICG electrodes is also shown in the figure to indicate the time relationship of the ICG with the cardiac cycle. The ICG waveform is shown

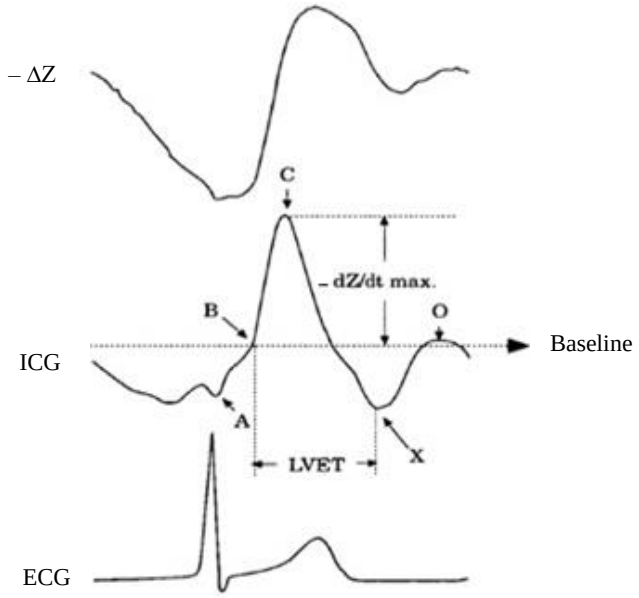

Figure 2.1: The thoracic impedance waveform ($\Delta Z = Z(t) - Z_0$), where Z_0 is the basal impedance, ICG ($-dZ/dt$) , and ECG waveform, adapted from [8].

with its characteristic points (A, B, C, O, and X) which are related to cardiac activities during a cardiac cycle [6], [7]. The A point is a downward deflection indicating the atrial contraction; the B point is the starting of blood ejection signifying aortic valve opening; the C point is the maximum upward deflection occurring during the systole where the blood flow in the aorta increases and maximum impedance variation takes place; the X point indicates the aortic valve closure; and the O point coincides with diastolic upward deflection with mitral valve opening snap [7]. The time duration between the B point and the X point is called left ventricular ejection time (LVET) and is used along with $\left(-dZ/dt\right)_{\max}$ for calculating the stroke volume. Examination of the elevation of the O point can be useful in diagnosing mitral stenosis. Thus a careful observation of variations in the ICG signal can be helpful in diagnosis of several cardiac disorders at early stage.

2.3 The Parallel Column Model of Thoracic Impedance

In order to calculate various cardiovascular indices of the thorax, the parallel column model of thoracic impedance is commonly used [3]. This model, as shown in Figure 2.2, has a constant impedance Z_0 in parallel with a cylindrical column representing the variable impedance Z_{var} [4], [11]. This cylindrical column, with a fixed length L, a fixed resistivity ρ , and a uniform variable cross sectional area A, is assumed to be placed in a homogenous electric field. The maximum change in the volume of the cylinder is proportional to the impedance variation and the relation is given by

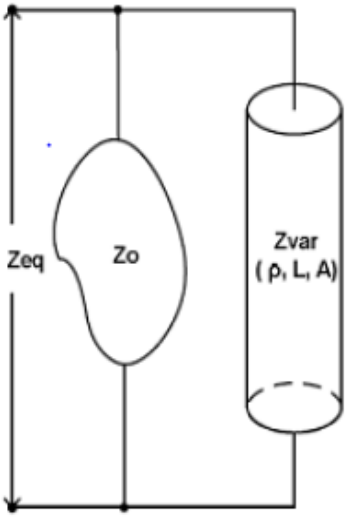

Figure 2.2: Parallel column model of thoracic impedance [3].

$$\Delta V = \left(\frac{\rho L^2}{Z_0^{\,2}} \right) \Delta Z \tag{2.1}$$

It is difficult to estimate the value of ρ and L as these are different for different individuals. Based on the parallel column model of the thoracic impedance, Kubicek et al. [7] assumed ΔV to be the stroke volume SV and estimated ΔZ due to ventricular ejection as $\left(-dZ/dt\right)_{\max}$ T_{LVET} , thus giving the formula for stroke volume as

$$\mathrm{SV} = \left(\frac{\rho L^2}{Z_0^{\,2}} \right) \left(-dZ/dt\right)_{\max} T_{LVET} \tag{2.2}$$

The Kubicek's equation for SV was modified by Sramek [6] by considering the thorax region as a truncated cone and relating L to person's height H as

$$\mathrm{SV} = \left(\frac{(0.17H)^3}{4.25 Z_0} \right) \left(-dZ/dt\right)_{\max} T_{LVET} \tag{2.3}$$

Later Bernstein introduced a weighting factor δ and the SV equation was modified as Sramek-Bernstein [7], [8] equation

$$\mathrm{SV} = \delta \left(\frac{(0.17H)^3}{4.25 Z_0} \right) \left(-dZ/dt\right)_{\max} T_{LVET} \tag{2.4}$$

Bernstein [8] further modified the SV equation with a new parameter as given below

$$\mathrm{SV} = \frac{V_{ITBV}}{\xi^2} \sqrt{\frac{\left(-dZ/dt\right)_{\max}}{Z_0}} \; T_{LVET} \tag{2.5}$$

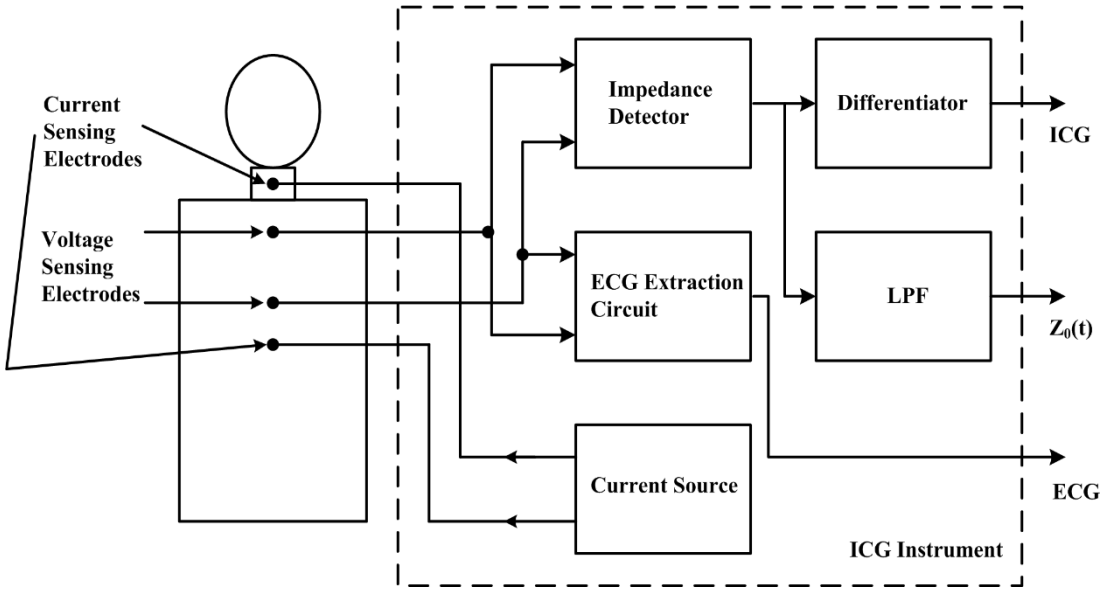

Figure 2.3: Block diagram for impedance cardiograph instrument with tetra-polar electrode configuration.

where V_{ITBV} is introduced as intra-thoracic blood volume and can be related to body weight W (Kg) as $V_{ITBV} = 16\,W^{1.02}$ and ξ as the index of trans-thoracic aberrant conduction which can be given as

$$\xi = \frac{Z_C^2 - Z_C Z_0 + K}{2Z_C^2 + {Z_0}^2 - 3Z_C Z_0 + K} \tag{2.6}$$

where Z_C is the critical level of basal impedance (~ 20 Ω), Z_0 is the measured trans-thoracic quasi static basal impedance (Ω), $0 < \xi < 1$ for all $Z_0 < Z_C$, $\xi = 1$ for all $Z_0 \geq Z_C$, and $K \rightarrow 0$.

2.4 The Impedance Cardiograph

Figure 2.3 shows a block diagram of impedance cardiograph instrument. It consists of an AC current source, two pair of electrodes (one for injecting the excitation current and another for sensing the voltage across the thorax), impedance detector, differentiator and an ECG extraction circuit. Two different electrode pairs are used to inject the current inside the thorax region and to sense the amplitude modulated voltage signal developed across the thorax [3], [9], [10]. The electrodes are connected in such a way that the outer electrode pair provides the AC current and the inner electrode pair senses the developed voltage in order to reduce the error related to skin-electrode contact impedance. The AC current source is used to inject the low amplitude (< 5 mA), high frequency (20 – 100 kHz) current in the thorax region through the outer electrode pair [9], [10]. The impedance variation is superimposed on the basal impedance. It is detected by demodulating the amplitude modulated voltage. The modulation index is about 0.1 – 2 % of the basal value [3]. The amplitude of this current needs to be stable, as any

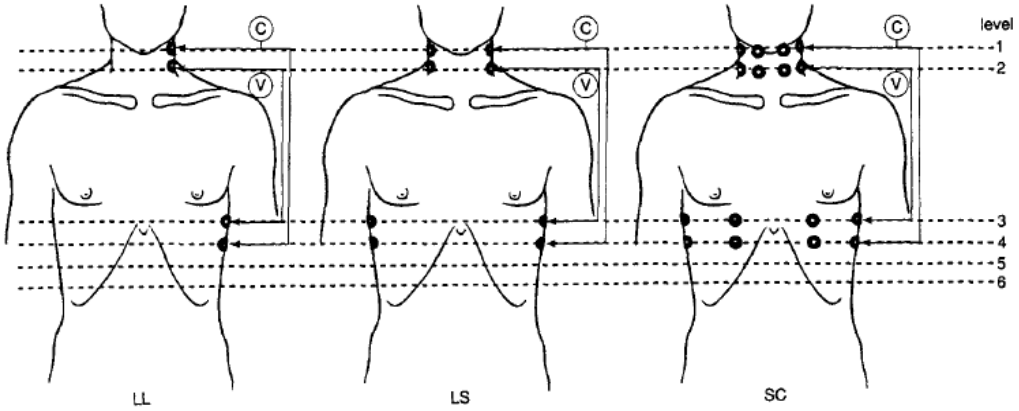

Figure 2.4: Various Spot Electrode Array configuration [10].

amplitude instability appears as noise in the envelope of the sensed voltage and hence contributes noise to the demodulator output.

The impedance detector consists of an AC differential amplifier and amplitude demodulator, which is usually realized using a precision full-wave rectifier and a low-pass filter. The low-pass cutoff frequency is chosen to allow all the frequencies of the signal band while rejecting the higher frequencies, including the carrier ripple. The output is passed through a differentiator to provide the ICG signal and through a low-pass filter to provide the basal impedance. High order low-pass and high-pass filters may be used to increase the stop-band and to get a sharp transition. However these filters introduce phase distortion, and phase-correction filters are often employed in the digital processing stage. An ECG signal is also generated as a reference signal to correlate cardiac electrical activity with the ICG signal. This signal is obtained from the voltage sensing electrodes using a differential amplifier and low-pass filter.

2.5 Electrode Configurations

Electrode pairs are used for injecting the excitation current in the thorax region and for sensing the developed voltage across it. Two types of electrode configurations can be used. In bipolar configuration, the same electrode pair is used for both current injection and voltage sensing. In this configuration, the voltage drop across the skin-electrode contact impedance gets added to the voltage developed across the thoracic impedance and thus contributes to the sensed voltage. In tetra-polar configuration, different electrode pairs are used for injecting the current and the sensing voltage [7], [10]. In this configuration, the error due to skin-electrode contact impedance is reduced as a different electrode pair along with high input impedance amplifier is used to sense the voltage.

Homogeneous electric field is helpful for impedance measurement [9], [10]. So, the electrodes used in ICG instrument should provide a uniform current density in the thorax region.

Two types of electrodes namely spot electrodes and band electrodes are used. The spot electrodes are easy to place onto the skin but provide non-uniform current density whereas band electrodes provide more uniform current density but are difficult to place on the body [9]. Use of an array of spot electrodes is an alternate option to achieve both uniform current density and ease during placement. Figure 2.4 shows some of the spot electrode array configurations used in impedance cardiography: LL (left lateral) tetra-polar spot electrode array configuration given in the left, LS (lateral spot) spot electrode array with 8 laterally placed spot electrodes used by Bernstein given in the middle, and SC (semi-circle) electrode array in the right with 16 spot electrode array proposed by Woltjar [10].

2.6 Bioimpedance Simulator

To validate the overall performance, such as linearity, sensitivity, accuracy, dynamic behavior, and frequency response of the ICG instrument, a bioimpedance simulator is needed which can provide an arbitrarily varying impedance signal along with standard test waveforms such as sine, square, triangular and thoracic impedance signal. The simulator requires a linear precision voltage-controlled resistor (VCR) circuit to provide a continuous impedance variation superimposed on a basal impedance. The VCR circuit can be realized using JFETs and MOSFETs which are descried in Chapter 3 and 4, respectively. Development of the bioimpedance simulator is described in Chapter 5.

Chapter 3
JFET BASED VOLTAGE-CONTROLLED RESISTOR

3.1 Introduction

A thoracic bioimpedance simulator provides a time-varying impedance in accordance with a control voltage in order to mimic the thoracic impedance. Hence it can be realized using a voltage-controlled resistor (VCR). A JFET can be used as a VCR when it is operated in ohmic region, with its drain-source channel resistance controlled by the gate-source voltage. It acts as a linear resistance if the drain-source voltage is limited to tens of mV. Moreover the relationship between the control voltage and the channel resistance varies with process-dependent device parameters and temperature. For use in bioimpedance simulator, we need a VCR which acts as a linear resistor for a larger range of drain-source voltage and variation in the resistance is not dependent on device parameters. Another desirable feature of the VCR for this application is that it should be a floating resistor, i.e. neither of its two terminals is grounded. Several circuits meeting some of these requirements have been reported and some of them are reviewed in the subsequent sections. Apart from realizing the thoracic bioimpedance simulator, the applications of the VCR circuit also include analog multipliers, modulators, demodulators and tunable circuits. MOSFETs can also act as a VCR and the design approach for MOSFET based VCR circuits are described in the next chapter.

3.2 JFET Basics

A JFET has three terminals: gate (G), source (S), and drain (D) [15], [16]. It can be used as a voltage-controlled resistor, with the voltage v_{GS} controlling the channel resistance R_{DS}. The drain and source terminals are interchangeable, with the more positive of the two terminals acting as the drain in case of of n-channel device. Figure 3.1 shows an n-channel JFET with its typical drain current versus drain-source voltage characteristics [15]. With $v_{DS} > 0$, the device is normally operated by keeping the gate-source junction reversed biased, i.e. $v_{GS} \leq 0$ with $i_G \approx 0$. As v_{GS} becomes more negative, i_D decreases and becomes zero for $v_{GS} \leq V_P$, known as the pinch-off voltage. The region with $v_{GS} \leq V_P$ is known as the cut-off region. For $v_{GS} > V_P$ and $v_{GD} > V_P$, i.e. $v_{DS} < v_{GS} - V_P$, the current i_D increases with v_{DS}, and this region is known as the ohmic, triode, or non-saturation region. In this region, the device acts as a linear resistor for v_{DS} below tens of mV. For $v_{DS} > v_{GS} - V_P$, i_D reaches a saturation level

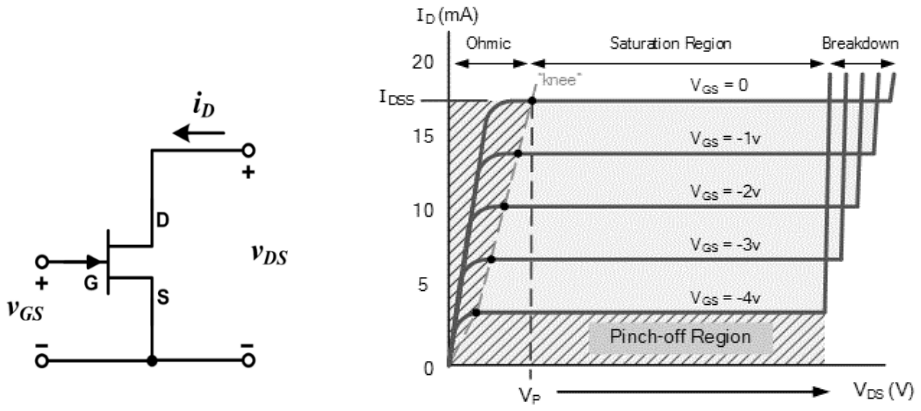

Figure 3.1: An n-channel JFET and its v_{DS} vs i_D characteristics [15].

and becomes almost independent of v_{DS}. This region is known as the saturation region. The saturation current at $v_{GS} = 0$ is termed as I_{DSS}. If v_{DS} is further increased, the channel breaks down resulting in a large current, marked as the breakdown region.

The relationship between i_D and v_{DS} [17] can be approximately given as

$$i_D = \begin{cases} 0, & v_{GS} \le V_P \\ I_{DSS}\left(\dfrac{2(v_{GS}-V_P)v_{DS}-v_{DS}^2}{V_P^2}\right), & V_P \le v_{GS} \le 0 \quad \text{and} \quad 0 \le v_{DS} \le v_{GS}-V_P \\ I_{DSS}\left(1-\dfrac{v_{GS}}{V_P}\right)^2, & V_P \le v_{GS} \le 0 \quad \text{and} \quad v_{DS} \ge v_{GS}-V_P \end{cases} \tag{3.1}$$

In the saturation region, i_D remains slightly dependent on v_{DS} and this effect is modelled by channel length modulation, which is not considered in (3.1).

In the ohmic region, the channel resistance $R_{DS} = v_{DS}/i_D$ is given as

$$R_{DS} = V_P^2/[2I_{DSS}(v_{GS}-V_P-v_{DS}/2)], \quad 0 \le v_{DS} \le v_{GS}-V_P \tag{3.2}$$

As R_{DS} is a function of v_{GS}, the device acts as a VCR. For small values of v_{DS}, R_{DS} can be approximated as

$$R_{DS} = V_P^2/[2I_{DSS}(v_{GS}-V_P)], \quad 0 \le v_{DS} << v_{GS}-V_P \tag{3.3}$$

and the device acts as a linear resistance. Its smallest value is at $v_{GS} = 0$, given as

$$R_{DS,ON} = |V_P|/(2I_{DSS}) \tag{3.4}$$

The dynamic resistance $r_{ds} = \dfrac{v_{ds}}{i_{ds}} = \dfrac{\partial v_{DS}}{\partial i_{DS}}$ is given as

$$r_{ds} = V_P^2/[2I_{DSS}(v_{GS}-V_P-v_{DS})] \tag{3.5}$$

We see that the dynamic resistance also varies with v_{DS} and becomes infinite as $v_{DS} \to v_{GS} - V_P$.

The equation for the drain current i_D in (3.1) can also be written as

$$i_D = \begin{cases} 0, & v_{GS} \le V_P \\ k[(v_{GS} - V_P)v_{DS} - {v_{DS}}^2/2], & V_P \le v_{GS} < 0 \quad \text{and} \quad 0 < v_{DS} < v_{GS} - V_P \\ k[(v_{GS} - V_P)^2/2], & V_P \le v_{GS} < 0 \quad \text{and} \quad v_{DS} > v_{GS} - V_P \end{cases} \quad (3.6)$$

where k is given as

$$k = 2I_{DSS}/V_P^2 \quad (3.7)$$

and hence $R_{DS,ON}$ in terms of k is given as

$$R_{DS,ON} = 1/(k|V_P|) \quad (3.8)$$

The values of the pinch-off voltage V_P and $R_{DS,ON}$ can be expressed in terms of device parameters as

$$|V_P| = qN_D a^2/2\varepsilon \quad (3.9)$$

$$R_{DS,ON} = l/(2awqN_D\mu) \quad (3.10)$$

where q = electronic charge, N_D = concentration of donor ions, a = channel thickness, ε = dielectric constant of material of the channel, l = channel length, w = channel width, and μ = carrier mobility in the device channel [15]. Using (3.4), (3.9), and (3.10), the formula for k in (3.7) can be rewritten as:

$$k = 4\mu\varepsilon w/(al) \quad (3.11)$$

The parameters V_P and k are process dependent and also vary with temperature. Thus the channel resistance R_{DS} of a JFET can be controlled by varying v_{GS}, but the resistance is nonlinear and is dependent on process-dependent parameters and temperature. Further, the source terminal of the device is common and hence the single JFET device cannot be used as a floating VCR.

3.3 JFET Based VCR Circuits

In many electronic circuits, a VCR may be needed to act as a linear resistance for a large voltage range, and should act as a precision resistance with minimal effect of process and temperature dependent parameters on its resistance. The VCR circuit may be needed to provide a floating resistor in some applications. Some applications may require a resistance mirror i.e. a resistance-controlled resistance. Several circuits [17] – [24] have been proposed to meet some of these requirements. Some of them are reviewed in this section.

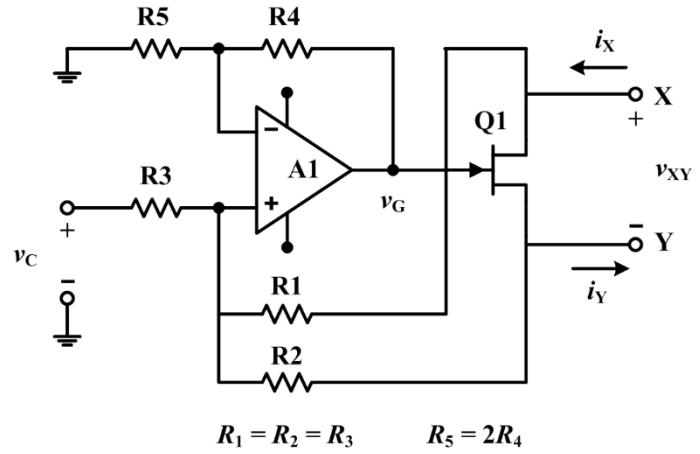

Figure 3.2: JFET based floating linear VCR reported by Senani [21].

3.3.1 JFET based floating linear VCR circuit, reported by Senani [21]

In a grounded JFET based VCR, addition of the drain voltage to the control voltage for generating the gate voltage has been used for expanding the range of v_{DS} for linear operation [17]. In a floating linear VCR circuit proposed by Senani [21], the gate voltage is obtained by adding the drain and source voltages to the control voltage. In the schematic shown in Figure 3.2, X and Y are the terminals of the controlled floating resistance and v_C is the control voltage. The op amp A1 is used to generate v_G as the following:

$$v_G = (v_C + v_X + v_Y)/2 \tag{3.12}$$

The resistances R_1, R_2, and R_3 may be selected as 1 MΩ to decrease the loading on the terminals X and Y, and to ensure $i_X \approx i_Y$. For $v_X > v_Y$, the terminals X and Y act as the drain and source, respectively. Therefore, $v_{DS} = v_X - v_Y = v_{XY}$ and $v_{GS} = v_G - v_Y$. Assuming the device Q1 to be operating in the ohmic region, the drain current can be given as

$$i_X = k[(v_G - v_Y - V_P)v_{XY} - {v_{XY}}^2/2], \quad 0 \geq v_G - v_Y \geq V_P \text{ and } 0 \geq v_G - v_X \geq V_P \tag{3.13}$$

By putting the value of v_G as in (3.12) in (3.13), the quadratic term gets eliminated and i_X can be expressed as

$$i_X = k(v_C/2 - V_P)v_{XY}, \quad 0 \geq v_C + v_{XY} \geq 2V_P \text{ and } 0 \geq v_C - v_{XY} \geq 2V_P \tag{3.14}$$

It can be shown that the relation in (3.14) is applicable for $v_Y > v_X$ also. Thus the circuit works as a floating VCR for either polarity of v_{XY}. The constraints on v_{XY} can be

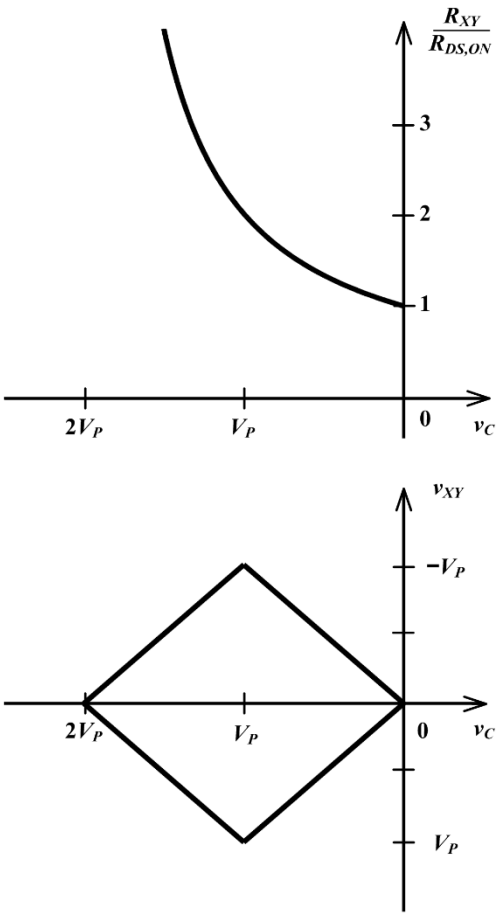

Figure 3.3: R_{XY} as a function of v_C and v_{XY} for linear operation of the JFET-based floating VCR proposed by Senani [21].

written as $|v_{XY}| \le \min(-v_C, v_C - 2V_P)$. Therefore the resistance of the VCR, $R_{XY} = v_{XY} / i_X$, is given as

$$R_{XY} = \frac{1}{k(v_C/2 - V_P)}, \quad 0 \ge v_C \ge 2V_P \quad \text{and} \quad |v_{XY}| \le \min(-v_C, v_C - 2V_P) \quad (3.15)$$

In terms of $R_{DS,ON}$ of the device, as given in (3.8), the VCR resistance is given as

$$R_{XY} = \frac{R_{DS,ON}}{1 - 0.5\, v_C / V_P}, \quad 0 \ge v_C \ge 2V_P \quad \text{and} \quad |v_{XY}| \le \min(-v_C, v_C - 2V_P) \quad (3.16)$$

The variation in the resistance with v_C and the range of v_{XY} for the linear operation as given in (3.16) are graphically represented in Figure 3.3. The maximum range for v_{XY} is $\pm V_P$ for $v_C = V_P$ and it results in $R_{XY} = 2R_{DS,ON}$. The range of v_{XY} for linear operation becomes much smaller for resistances significantly differing from this value. This limitation on the range of linearity has not been stated in [23].

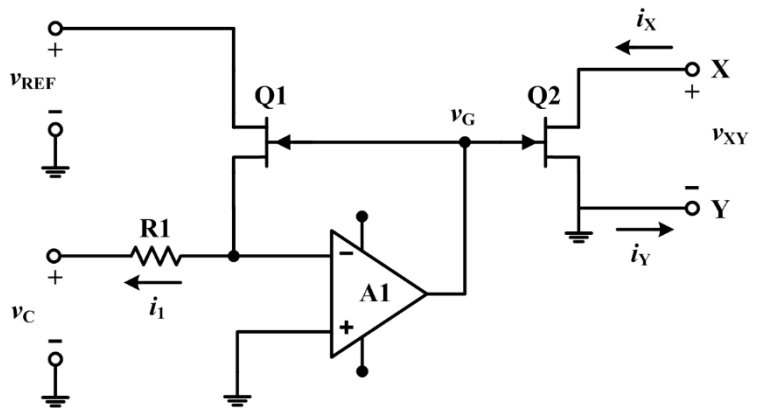

Figure 3.4: Matched JFET pair based VCR circuit reported by Clarke [22].

In this floating VCR circuit, the value of the resistance and its relation with the control voltage depend on the device parameters. Hence the circuit cannot be used in applications requiring a precision VCR.

3.3.2 Grounded precision VCR circuit using matched JFET pair, reported by Clarke [22]

Using two matched JFETs and an op amp, Clarke [22] reported a set of four circuits for realizing a grounded VCR whose resistance value is compensated against the variations in device parameters using a negative feedback. One of the circuits is shown in Figure 3.4 with an op amp A1 and two matched n-channel JFETs Q1 and Q2 operating in the ohmic region. X and Y are the terminals of the controlled grounded resistance and v_C is the controlled voltage. To provide a negative feedback through A1 and Q1, the JFET terminal connected to the inverting input of A1 should be the source terminal, i.e. $v_{REF} \geq 0$ and $i_1 > 0$. The current i_1 is controlled by v_C as

$$i_1 = -v_C / R_1 \tag{3.17}$$

Assuming Q1 to be operating in the ohmic region, i_1 is related to v_G as

$$i_1 = k_1(v_G - V_{P1} - v_{REF}/2)v_{REF}, \quad 0 \geq v_G \geq V_{P1} \text{ and } 0 \geq v_G - v_{REF} \geq V_{P1} \tag{3.18}$$

The voltage v_G is set by the feedback loop to maintain the current i_1 through Q1. Using (3.17) and (3.18), v_G is given as

$$v_G = \frac{-v_C}{k_1 R_1 v_{REF}} + V_{P1} + \frac{v_{REF}}{2} \tag{3.19}$$

The voltage v_G is also given to Q2 as the gate voltage. Considering Q2 also to be in the ohmic region, the current i_X $(=i_Y)$ through Q2 can be given as

$$i_X = k_2(v_G - V_{P2} - v_{XY}/2)v_{XY}, \quad 0 \geq v_G \geq V_{P2} \text{ and } 0 \geq v_G - v_X \geq V_{P2} \quad (3.20)$$

Using (3.19) and (3.20), we get

$$i_X = \left[k_2 \left(\frac{-v_C}{k_1 R_1 v_{REF}} + V_{P1} + \frac{v_{REF}}{2} - V_{P2} - \frac{v_{XY}}{2} \right) \right] v_{XY} \quad (3.21)$$

Therefore, the resistance $R_{XY} = v_{XY}/i_X$ for the VCR is given as

$$R_{XY} = \left[k_2 \left(\frac{-v_C}{k_1 R_1 v_{REF}} + V_{P1} - V_{P2} + \frac{v_{REF} - v_{XY}}{2} \right) \right]^{-1} \quad (3.22)$$

For VCR operation, v_{REF} is kept constant and a negative v_C is applied as the control voltage. With Q1 and Q2 as matched pair, $k_1 = k_2 = k$ and $V_{P1} = V_{P2} = V_P$, and the expression for R_{XY} can be written as

$$R_{XY} = \left[\left(-\frac{v_C}{R_1 v_{REF}} + k(v_{REF} - v_{XY})/2 \right) \right]^{-1} \quad (3.23)$$

Assuming v_{REF} and v_{XY} to be small, the resistance R_{XY} can be approximated as

$$R_{XY} = \frac{v_{REF}}{-v_C} R_1 \quad (3.24)$$

Thus R_{XY} does not depend on the device parameters I_{DSS} and V_P and the circuit can be used as a precision VCR.

This circuit realizes a grounded precision VCR which acts as a linear resistance for small values of v_{XY}.

3.3.3 Precision linear VCR circuit using matched JFET pair and multiplier-divider, reported by Tadic [23]

A precision VCR circuit with extended range of linear operation using a matched JFET pair, an op amp, a current mirror, a current-to-voltage converter, a summer, and a multiplier-divider has been proposed by Tadic [23]. The circuit is shown in Figure 3.5 with the matched devices Q1 and Q2 operating in either the ohmic region or the saturation region. X and Y are the resistance terminals of the grounded VCR and v_C is the control voltage. A current mirror is used to provide $i_F = i_X$. The gate voltage v_{G1} required for i_F as the drain current of Q1 is generated by the negative feedback loop formed by A1 and Q1. A current-to-voltage converter

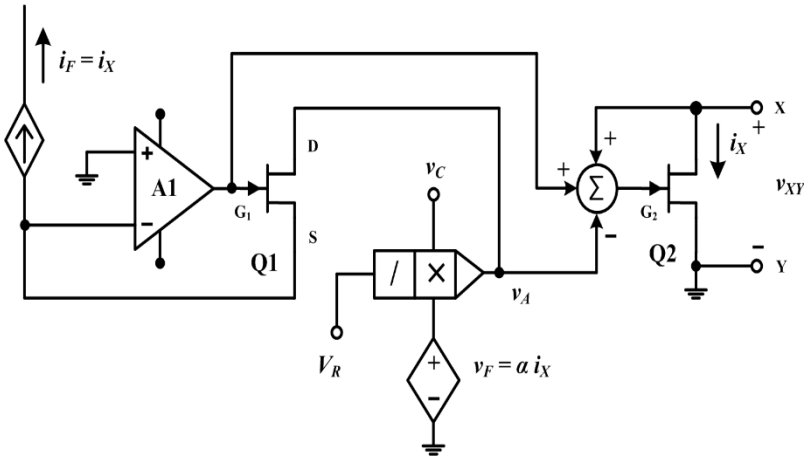

Figure 3.5: VCR circuit reported by Tadic [23] using matched device pair and multiplier-divider, schematic redrawn on the basis of Figures 1 and 2 of [23].

generates $v_F = \alpha\, i_X$ and the multiplier-divider generates $v_A = v_C\, v_F / V_R$ which is applied as the drain voltage of Q1. The resistance across the drain-source terminals of Q1 is given as

$$R_{DS} = v_A / i_F = \{v_C\, (\alpha\, i_X) / V_R\} / (i_X) = \alpha\, v_C / V_R$$

The gate voltage for Q2 is generated by the summer as $v_{G2} = v_{G1} + v_X - v_A$. It is seen that the two devices have the same drain current and the same gate-drain voltage and hence will have the same drain-source resistances. Therefore

$$R_{XY} = \alpha\, v_C / V_R \tag{3.25}$$

and circuit acts as a grounded precision linear VCR. A modification of the circuit has been proposed for floating VCR.

The main feature of the circuit is that the two matched devices can operate either in the ohmic or saturation regions and hence it can be used for varying the resistance over a very wide range. As Q1 is part of the negative feedback loop, it is required that $i_F > 0$ and hence it is required that $v_{XY} > 0$. Therefore the VCR is linear only for unipolar voltages. Its applications get further restricted as it requires a multiplier-divider for its realization.

3.3.4 Floating precision linear VCR circuit using matched JFET pair, reported by Holani et al. [26]

The JFET based VCR circuit reported by Senani [21] can operate as a linear floating or grounded VCR for an extended voltage range but its resistance is dependent on device parameters. The VCR circuit proposed by Clarke [22] uses a matched pair of devices and negative feedback to realize a grounded precision VCR. The resistance does not depend on device parameters, but it acts as a linear resistance only for very small voltages. The VCR circuit proposed by Tadic [23] uses a matched pair of devices to realize precision VCR with a

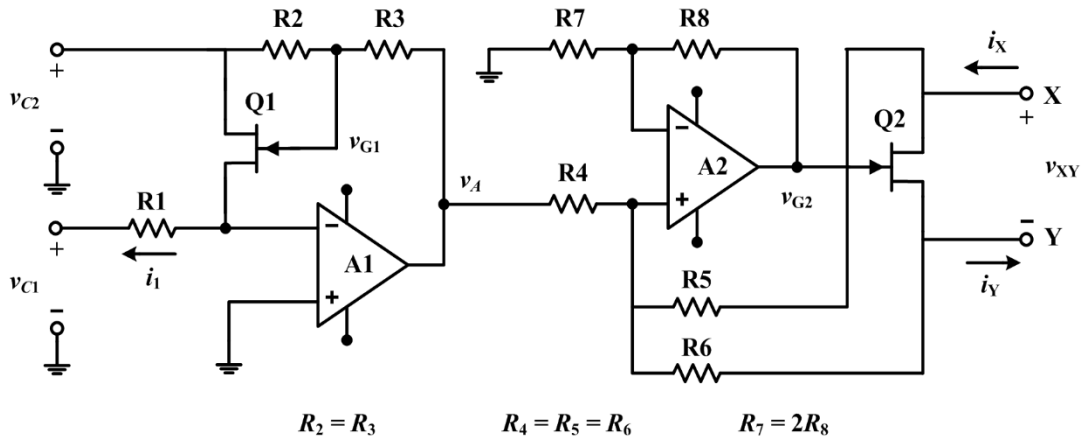

Figure 3.6: Floating linear precision VCR circuit proposed by Holani et al. [24].

large dynamic range of resistance. However, the circuit requires a multiplier-divider and acts as linear resistor only for unipolar voltages. Holani et. al. [24] proposed a circuit using a matched pair of devices and negative feedback to realize a floating precision VCR which acts as a linear resistor for an extended range of voltages and without polarity restriction. The circuit is shown in Figure 3.6. The matched n-channel JFETs Q1 and Q2 are operated in ohmic region. X and Y are the terminals of the floating VCR, with v_{C1} and v_{C2} as the control voltages. The negative feedback loop formed by A1 and Q1 maintains the inverting input terminal of A1 at virtual ground. It requires $v_{C2} > 0$ and $i_1 > 0$. Since $i_1 = -v_{C1}/R_1$, it is required that $v_{C1} < 0$. The gate voltages are obtained by superimposing the common mode voltages obtained from the respective drain and source voltages on the op amp output v_A, as the following:

$$v_{G1} = (v_A + v_{C2})/2 \tag{3.26}$$

$$v_{G2} = (v_A + v_X + v_Y)/2 \tag{3.27}$$

For the above v_{G1} and v_{G2}, the resistances have to be selected as $R_2 = R_3$, $R_4 = R_5 = R_6$ and $R_7 = 2R_8$. The resistances R_5 and R_6 should be large enough to avoid any loading on the terminals X and Y and to ensure $i_X \approx i_Y$.

The drain-source channel resistance of Q1 is given as

$$R_{DS1} = v_{C2}/i_1 = \frac{v_{C2}}{-v_{C1}} R_1 \tag{3.28}$$

and the voltage v_A is set accordingly by the negative feedback loop. The voltage v_{C2} is such that Q1 operates in the ohmic region and its drain current i_1 is given as

$$i_1 = k_1[(v_{G1} - V_{P1})\, v_{C2} - {v_{C2}}^2 / 2], \qquad 0 \geq v_{G1} \geq V_{P1} \text{ and } v_{G1} - v_{C2} \geq V_{P1} \tag{3.29}$$

Using (3.26) and (3.29), expression for op amp output v_A can be obtained as

$$v_A = 2\left[\frac{-v_{C1}}{k_1 R_1 v_{C2}} + V_{P1}\right], \quad 0 \leq v_{C2} \leq v_A - 2V_{P1} \tag{3.30}$$

For Q2 to be operated in the ohmic region with $v_X > v_Y$, relation between v_X, v_Y and the current $i_X (= i_Y)$ can be given as

$$i_X = k_2[(v_{G2} - v_Y - V_{P2})\, v_{XY} - {v_{XY}}^2 / 2], \qquad 0 \geq v_{G2} - v_Y \geq V_{P2} \text{ and } 0 \geq v_{G2} - v_X \geq V_{P2} \tag{3.31}$$

This relation is valid for the condition $v_X < v_Y$ as well. Using the expression for v_{G2} from (3.27), the current i_X can be given as

$$i_X = k_2[(v_A/2 - V_{P2})v_{XY}], \qquad 0 \geq v_A > 2V_{P2} \text{ and } |v_{XY}| \leq \min(-v_A, v_A - 2V_{P2}) \tag{3.32}$$

Using the expression for op amp output v_A from (3.30), we can obtain

$$i_X = k_2\left[\frac{-v_{C1}}{R_1 k_1 v_{C2}} + V_{P1} - V_{P2}\right] v_{XY} \tag{3.33}$$

Since, transistors Q1 and Q2 are matched, $k_1 = k_2 = k$ and $V_{P1} = V_{P2} = V_P$ and (3.33) can be rewritten as

$$i_X = \left(-v_{C1}/v_{C2}R_1\right) v_{XY}, \qquad 0 \geq v_A > 2V_P \text{ and } |v_{XY}| \leq \min(-v_A, v_A - 2V_P) \tag{3.34}$$

The channel resistance for the device Q2 is $R_{XY} = v_{XY} / i_X$. Its value along with its constraints, from (3.34), is given as the following:

$$R_{XY} = \frac{v_{C2}}{-v_{C1}} R_1, \qquad 0 \geq v_A > 2V_P \text{ and } |v_{XY}| \leq \min(-v_A, v_A - 2V_P) \tag{3.35}$$

The values for v_{C1}, v_{C2}, and R_1 are selected in such a way that $v_A = 2[V_P - v_{C1}/(k R_1 v_{C2})]$ satisfies the condition $0 \geq v_A > 2V_P$. In this circuit, the drain and source voltages are added to the control voltage to obtain the gate voltage and this arrangement is called as source-drain (SD) bootstrapping which is used to extend the range of linearity. Use of matched JFET pair and negative feedback makes it a self-tracking circuit which ensures precision. The limitation of this that the device pair Q1 and Q2 are operated only in ohmic

Table 3.1: JFET parameters of U441 [25].

Parameter	Min.	Typ.	Max.	Test conditions
Device-dependence of V_P (from datasheet)	−1.0 V	−3.5 V	−6.0 V	T = 25 ˚C, I_{DS} = 1 nA, V_{DS} = 10 V
Device-dependence of I_{DSS} (from datasheet)	6 mA	15 mA	30 mA	T = 25 ˚C, V_{GS} = 0 V, V_{DS} = 10 V
Differential gate-source voltage (from datasheet)		6 mV	20 mV	I_D = 5 mA, V_{DG} = 10 V
Saturation drain current ratio (from datasheet)		0.97		V_{GS} = 0 V, V_{DS} = 10 V
Dependence of I_{DSS} on temperature (calc. using temperature coefficient of −0.17% / ºC, as obtained from the transfer characteristics in datasheet)	14.7 mA	15.0 mA	15.3 mA	I_{DSS} (25 ºC) = 15 mA, $T_{\min}$ = 15 ˚C, T_{typ} = 25 ˚C, $T_{\max}$ = 35 ˚C
Dependence of V_P on temperature (calc. using temperature coefficient of −1.7 mV / ºC, as obtained from the transfer characteristics in datasheet)	−3.48 V	−3.50 V	−3.52 V	$V_{GS,OFF}$ (25 ˚C) = 2.0 V, $T_{\min}$ = 15 ˚C, T_{typ} = 25 ˚C, $T_{\max}$ = 35 ˚C
Dependence of $R_{DS,ON}$ on V_P (calc. (3.4))	33 Ω	117 Ω	200 Ω	I_{DSS} = 15 mA, $V_{P\min}$ = −1.0 V, $V_{P typ}$ = −3.5 V, $V_{P\max}$ = −6.0 V, V_{DS} = 0.1 V, V_{GS} = 0 V
Dependence of R_{DS} on I_{DSS} (calc. (3.4))	58 Ω	117 Ω	292 Ω	V_P = −3.5 V, $I_{DSS\min}$ = 6 mA, $I_{DSS typ}$ = 15 mA, $I_{DSS\max}$ = 30 mA, V_{DS} = 0.1 V, V_{GS} = 0 V

region and hence the dynamic range for linear operation is small, as depicted in Figure 3.3 for the VCR circuit proposed by Senani [21].

3.4 Simulation Results for JFET as a Voltage Controlled Resistor (VCR)

A single JFET can be used as a VCR with a control signal v_C $(= v_{GS})$ for controlling its channel resistance R_{DS} and v_{DS} as the terminal voltage [17] – [24]. It acts as a linear resistor only up to tens of mV and then enters into saturation region as shown in Figure 3.1.

The drain current i_D vs v_{DS} characteristics of a JFET depends on its I_{DSS} and V_P parameter. A large value of I_{DSS} indicates rapid increase in i_D with increase in v_{DS}. A large value of V_P indicates that the JFET has a relatively wider ohmic region with respect to its v_{DS}. While carrying out the simulation, the effect of channel length modulation coefficient λ on its channel R_{DS} has also been examined. The parameters I_{DSS} and V_P are taken from the datasheet of a matched JFET pair module U441 (Vishay Siliconix) [25] as shown in Table 3.1. This matched pair device is used to implement the VCR circuit in PCB for the thoracic bioimpedance simulator. The device parameters used for simulation are I_{DSS}, V_P, BETA and λ [26]. BETA for a JFET device can be calculated using the following equation:

$$\text{BETA} = \frac{I_{DSS}}{{V_P}^2} = \frac{k}{2} \tag{3.36}$$

3.4.1 Simulation results for a single JFET as VCR

The characteristics of the single JFET based grounded VCR, as shown in Figure 3.1, was studied using circuit simulation for linearity and precision. Considering the range of I_{DSS} and V_P as in the datasheet, simulation was carried out for different combinations of device parameters as (i) $I_{DSS} = 6$ mA and $V_P = -1$ V, (ii) $I_{DSS} = 15$ mA and $V_P = -1$ V, (iii) $I_{DSS} = 6$ mA and $V_P = -3.5$ V, and (iv) $I_{DSS} = 15$ mA and $V_P = -3.5$ V. The channel length modulation coefficient λ was selected as 0, 0.01, 0.02, and 0.03 to observe its effect on i_D and R_{DS}. The control voltage v_C (= v_{GS}) was varied from 0 to a value closer to V_P for the different devices. The simulation results for i_X versus v_{XY} and R_{XY} versus v_{XY} are given in Table A.1 (Appendix A) for $v_C = 0$ and four values of λ. The results for different values of v_C and two values of λ are given in Table A.2. The tabulated results show that R_{XY} remains almost constant for $v_{DS} = \pm 100$ mV and it decreases slightly for $\lambda = 0.03$. It is also seen that R_{XY} changes significantly with change in the device parameters.

3.4.2 Simulation results for floating linear VCR of Senani [21]

Addition of drain and source terminal voltage to the gate the terminal of the JFET device removes the quadratic term present in the expression for i_X as given in (3.14). The constraints for VCR operation given in (3.15) show that there is no valid range for v_{XY} with $v_C = 0$. However, in practical case, a small range of v_{XY} can be achieved with $v_C = 0$ until

the gate-source junction or the gate-drain junction crosses its turn on voltage V_γ. Therefore, the constraints for linear resistance in (3.15) and can be modified as

$$V_\gamma \geq v_C \geq 2V_P \quad \text{and} \quad |v_{XY}| \leq \min(V_\gamma - v_C, v_C - 2V_P)$$

The simulation for floating linear JFET based VCR circuit in Figure 3.2 with $R_1 = R_2 = R_3 = 1\,\text{M}\Omega$, $R_5 = 10\,\text{k}\Omega$, $R_4 = 5\,\text{k}\Omega$, and supply voltage of ±15 V for the op amp A1 was carried out for different combinations of device parameters as (i) $I_{DSS} = 6$ mA and $V_P = -1$ V, (ii) $I_{DSS} = 15$ mA and $V_P = -1$ V, (iii) $I_{DSS} = 6$ mA and $V_P = -3.5$ V, and (iv) $I_{DSS} = 15$ mA and $V_P = -3.5$ V. The channel length modulation coefficient λ was selected as 0 and 0.03 to observe its effect on R_{XY}. The simulation results for R_{XY} versus v_{XY} are given in Table A.3 (Appendix A). The results show that R_{XY} stabilizes against v_{XY} for an extended range of ± 1 V. The effect of λ causes a variation less than 5 %. R_{XY} remains stable for the highest range of v_{XY} for $v_C \approx V_P$ and the range decreases as v_C significantly differs from V_P on either side as shown in Figure 3.3.

3.4.3 Simulation results for floating precision linear JFET based VCR of Holani et al. [24]

The VCR circuit proposed by Holani et al. [24], as shown in Figure 3.6, uses a matched JFET pair with SD bootstrapped gate for extending v_{XY} range with a self-tracking arrangement for providing precision in channel resistance. Simulation was carried out for four different sets of device parameters as (i) $I_{DSS} = 6$ mA and $V_P = -1$ V, (ii) $I_{DSS} = 15$ mA and $V_P = -1$ V, (iii) $I_{DSS} = 6$ mA and $V_P = -3.5$ V, and (iv) $I_{DSS} = 15$ mA and $V_P = -3.5$ V. The effect of λ was examined for its values of 0 and 0.03. The resistances in the circuit were selected as $R_2 = R_3 = 1\,\text{M}\Omega$, $R_4 = R_5 = R_6 = R_7 = 10\,\text{k}\Omega$, and $R_8 = 5\,\text{k}\Omega$. The supply voltage used for the op amp A1 and A2 was ±15 V. The resistance response of this circuit, given in (3.35), depends on v_{C2}, v_{C1} and R_1. Various values of R_1 were chosen for simulation and the corresponding R_{XY} values were observed keeping $v_{C2}/(-v_{C1}) = 1$. The results are given in Table A.4 (Appendix A). It is seen that depending on the values of R_1, the generated op amp output voltage v_A along with the terminal voltages for both the devices controls the range over which R_{XY} remains stable. The effect of λ causes a variation of up to 5%. If v_A goes above V_P, the stable range of R_{XY} with respect to v_{XY} decreases, as shown in

Figure 3.2. The resistance response of these VCR circuit can be scaled up or scaled down with precision by varying v_{C1} and v_{C2} in a range so that v_A is not significantly different from V_P.

3.4.4 Comparision of the VCR circuits

In the previous simulations, the parameters of the devices taken have large deviation with respect to each other. Therefore those devices do not have linear channel resistance of similar range. To examine the effect of the piece-to piece variation in process-dependent parameters of the devices from a batch, five devices are taken with parameter variation of about $\pm 33\,\%$ around $I_{DSS} = 15$ mA and $V_P = -3$ V. The simulation was carried out for five sets of device parameters as: (i) $I_{DSS} = 15$ mA and $V_P = -3$ V, (ii) $I_{DSS} = 20$ mA and $V_P = -3$ V, (iii) $I_{DSS} = 10$ mA and $V_P = -3$ V, (iv) $I_{DSS} = 15$ mA and $V_P = -4$ V, and (v) $I_{DSS} = 15$ mA and $V_P = -2$ V. The effect of λ was examined for $\lambda = 0$ and $\lambda = 0.03$. The simulation was repeated for the circuits for all three VCR used in the previous section. The results are presented in Tables A.5, A.6, and A.7 (Appendix A). The results of the single JFET based grounded VCR in Figure 3.1, are given in Table A.5. The results for floating linear JFET based VCR circuit in Figure 3.2 with $R_1 = R_2 = R_3 = 1\,\text{M}\Omega$, $R_5 = 10\,\text{k}\Omega$, and $R_4 = 5\,\text{k}\Omega$ are shown in Table A.6. The results presented in Table A.5 and A.6 show significant variations due to process-dependent parameters. The results for the floating precision linear VCR in Figure 3.6 with $R_1 = 210\ \Omega$, $R_2 = R_3 = 1\,\text{M}\Omega$, $R_4 = R_5 = R_6 = R_7 = 10\,\text{k}\Omega$, and $R_8 = 5\,\text{k}\Omega$ are shown in Table A.7. Table A.7 shows that the effect of variation in device parameters are significantly decreased in the floating precision linear VCR circuit as proposed by Holani et al. [24]. Figure 3.7 and Figure 3.8 show a comparative study of these VCR circuit response with $\lambda = 0$ and $\lambda = 0.03$, respectively. Figure 3.9 shows the effect of λ on the floating precision linear VCR. It is seen that $\lambda = 0$ results in constant resistance while $\lambda = 0.03$ results in slight decrease in R_{XY} with increase in $|v_{XY}|$.

3.4.5 A study of the effect of device mismatch

Matched JFET devices have some mismatch present in terms of their process-dependent parameters. These mismatches may contribute variation in the resistance response of the floating precision linear VCR circuit of Figure 3.6. The resistances in the circuit were selected as $R_1 = 300\ \Omega$, $R_2 = R_3 = 1\,\text{M}\Omega$, $R_4 = R_5 = R_6 = R_7 = 10\,\text{k}\Omega$, and $R_8 = 5\,\text{k}\Omega$. We examined the effect of variations of ± 20 mV in V_P and $\pm 3\,\%$ in I_{DSS} by circuit simulation. For Q1, we take five sets of parameters as: (i) $I_{DSS} = 6$ mA, $V_P = -1$ V, (ii) $I_{DSS} = 6$ mA, $V_P = -1$ V, (iii) $I_{DSS} = 6$ mA, $V_P = -1$ V, (iv) $I_{DSS} = 6$ mA, $V_P = -1$ V,

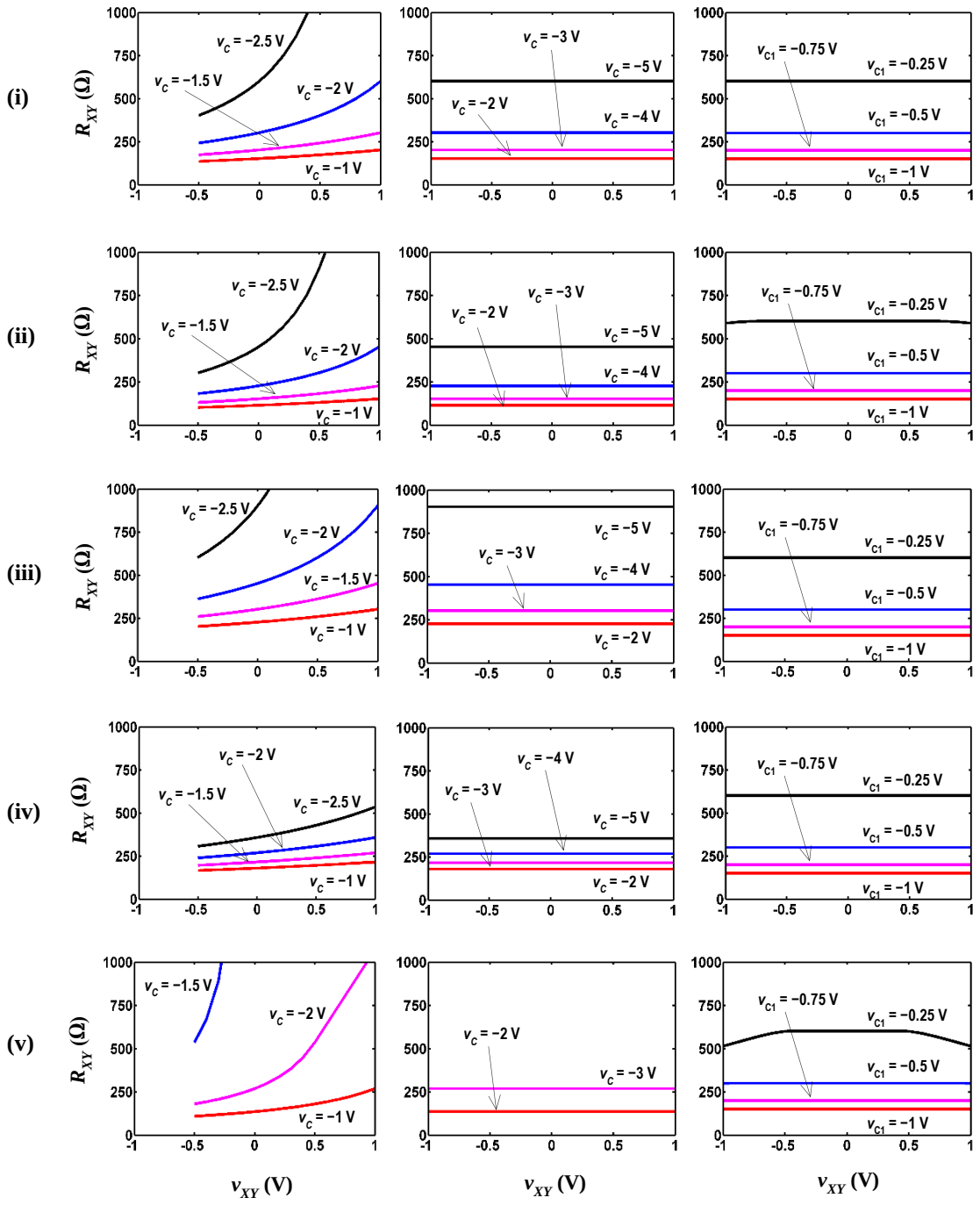

(a) Single JFET VCR

(b) VCR circuit of Senani [21]

(c) VCR circuit of Holani et al. [24]

Figure 3.7: Effect of device parameter variation (33% change in I_{DSS} and V_P) on R_{XY} vs. v_{XY} response of JFET based VCR circuits with λ = 0. Circuits: (a) single JFET as VCR, (b) VCR circuit of Senani [21], and (c) VCR circuits of Holani et al. [24]. Device parameters: (i) I_{DSS} = 15 mA, V_P = −3 V, (ii) I_{DSS} = 20 mA, V_P = −3 V, (iii) I_{DSS} = 10 mA, V_P = −3 V, (iv) I_{DSS} = 15 mA, V_P = −4 V, and (v) I_{DSS} = 15 mA, V_P = −2 V.

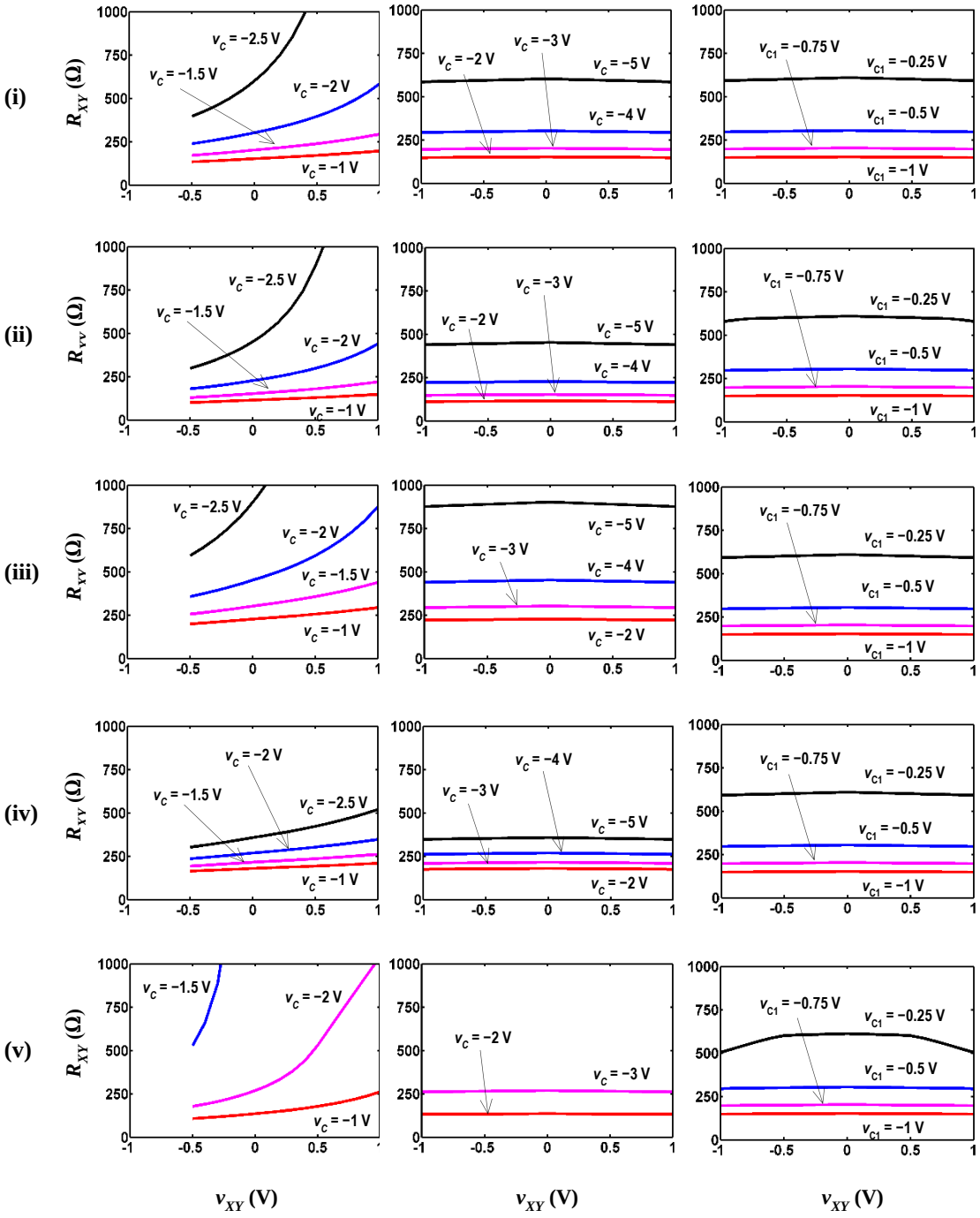

(a) Single JFET VCR

(b) VCR circuit of Senani [21]

(c) VCR circuit of Holani et al. [24]

Figure 3.8: Effect of device parameter variation (33% change in I_{DSS} and V_P) on R_{XY} vs. v_{XY} response of JFET based VCR circuits with λ = 0.03. Circuits: (a) single JFET as VCR, (b) VCR circuit of Senani [21], and (c) VCR circuits of Holani et al. [24]. Device parameters: (i) I_{DSS} = 15 mA, V_P = −3 V, (ii) I_{DSS} = 20 mA, V_P = −3 V, (iii) I_{DSS} = 10 mA, V_P = −3 V, (iv) I_{DSS} = 15 mA, V_P = −4 V, and (v) I_{DSS} = 15 mA, V_P = −2 V.

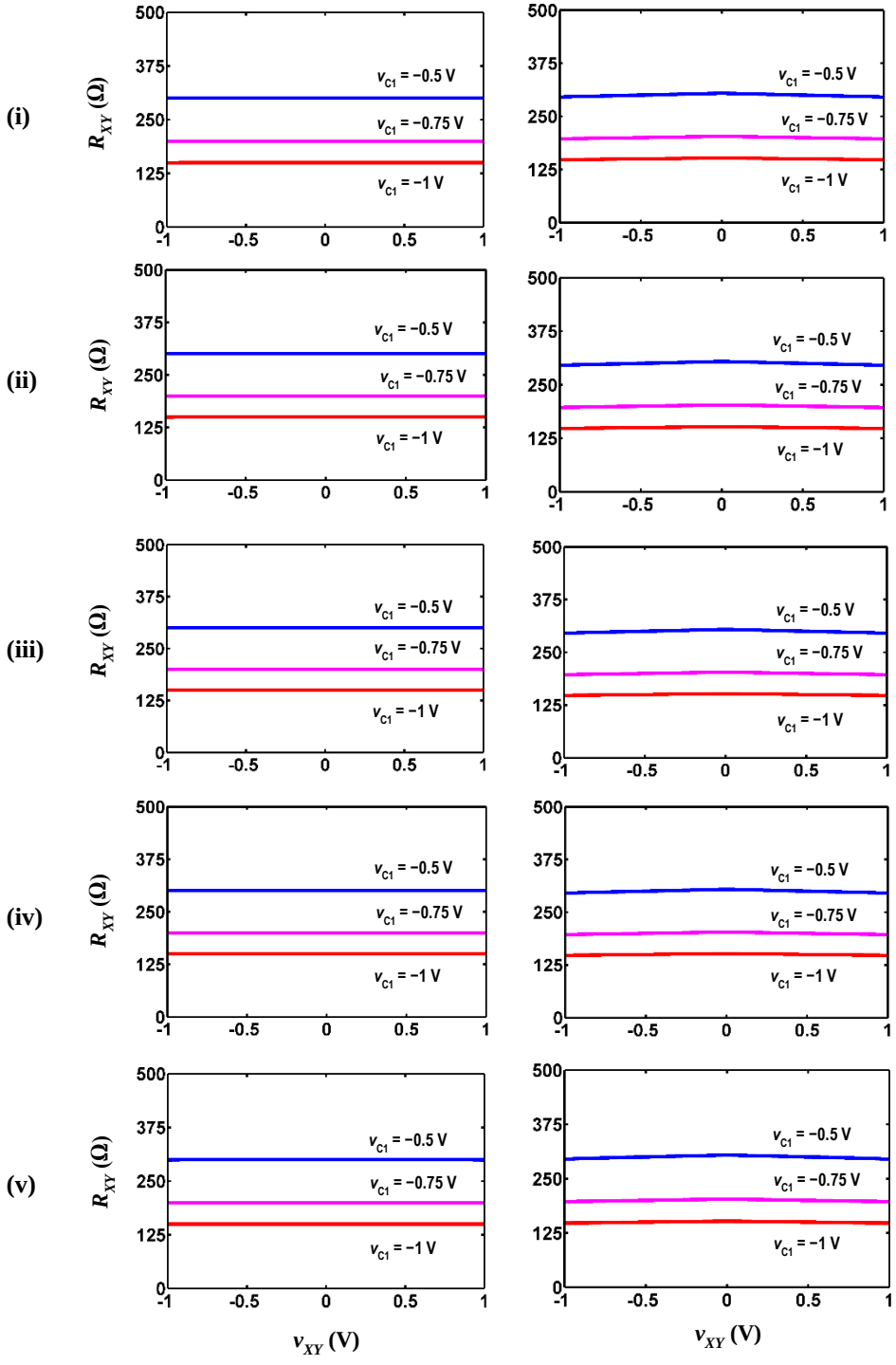

Figure 3.9: Effect of λ on R_{XY} vs. v_{XY} response for the floating precision linear VCR using matched JFET pair. Device parameters (with ±33 % variation): (i) I_{DSS} = 15 mA, V_P = −3 V, (ii) I_{DSS} = 20 mA, V_P = −3 V, (iii) I_{DSS} = 10 mA, V_P = −3 V, (iv) I_{DSS} = 15 mA, V_P = −4 V, and (v) I_{DSS} = 15 mA, V_P = −2 V.

and (v) $I_{DSS} = 6$ mA, $V_P = -1$ V. For Q2, we take five sets of parameters as: (i) $I_{DSS} = 6$ mA, $V_P = -1$ V, (ii) $I_{DSS} = 6$ mA, $V_P = -0.98$ V, (iii) $I_{DSS} = 6$ mA, $V_P = -1.02$ V, (iv) $I_{DSS} = 5.82$ mA, $V_P = -1$ V, and (v) $I_{DSS} = 6.18$ mA, $V_P = -1$ V. The simulation results for this section are given in Table A.8 (Appendix A). The variation in resistance due to device parameter mismatch is limited within $\pm 5\,\%$ for the devices used in simulation.

3.5 Practical Results for the Floating Precision Linear VCR Proposed by Holani et al. [26]

Using a matched JFET pair device U441 [25], resistors and two µA741CN op amp ICs [26], the VCR circuit proposed by Holani et al. [24] and as shown in Figure 3.6 was bread-boarded and tested. Before implementing the VCR circuit, the device parameters of the two devices in the chip were calculated from the measured i_D versus v_{DS} response, with $v_{GS} = 0$. The voltage v_{DS} was increased and the saturation value of i_D was taken as I_{DSS}. Value of i_D measured for v_{DS} of 0.5 V was used to calculate V_P using the following quadratic relation for non-saturation operation as obtained from (3.1):

$$(i_D / I_{DSS}) V_P^2 + 2 v_{DS} . V_P + {v_{DS}}^2 = 0$$

The parameter values were found to be as the following:

Device 1: I_{DSS} = 0.8987 mA, V_P = −1.032 V

Device 2: I_{DSS} = 0.8842 mA, V_P = −1.028 V

Using the above measured parameters, a new set of simulation was carried out for the floating linear VCR of Senani [21] in Figure 3.2 for both the devices. The resistance values in the circuit were the same as in earlier simulation ($R_1 = R_2 = R_3 = 1\,\text{M}\Omega$, $R_5 = 10\,\text{k}\Omega$, and $R_4 = 5\,\text{k}\Omega$). The results are presented in Table B.1 (Appendix B). With $\lambda = 0$ and small v_{XY}, the VCR circuit resistances with Device 1 are 576.2 Ω, 759.2 Ω, 1115.8 Ω, and 2103.3 Ω for v_C of 0 V, −0.5 V, −1.0 V, and −1.5 V, respectively. The corresponding values with Device 2 differ by 7.1 Ω, 10.9 Ω, 18.0 Ω, and 48.3 Ω. The maximum range of linearity is obtained for v_C = −1.0 V which is close to the measured value of V_P. Therefore this devices can be used for VCR circuit with resistance variation around 1 kΩ. For λ = 0 and v_C = −1 V, the resistance remains constant for $|v_{XY}| < 1$ V. For λ = 0.03, the resistance decreases by 3% for variation of v_{XY} in either direction over this range.

Next the floating precision linear JFET based VCR circuit of Holani et al. [24], as shown in Figure 3.6, was simulated with the measured values of parameters of the two devices (Device 1 as Q1 and Device 2 as Q2). The simulation was carried out with R_1 = 1 kΩ, v_{C2} = 0.5 V, and the resistance values in the circuit being same as in the earlier simulation (R_2

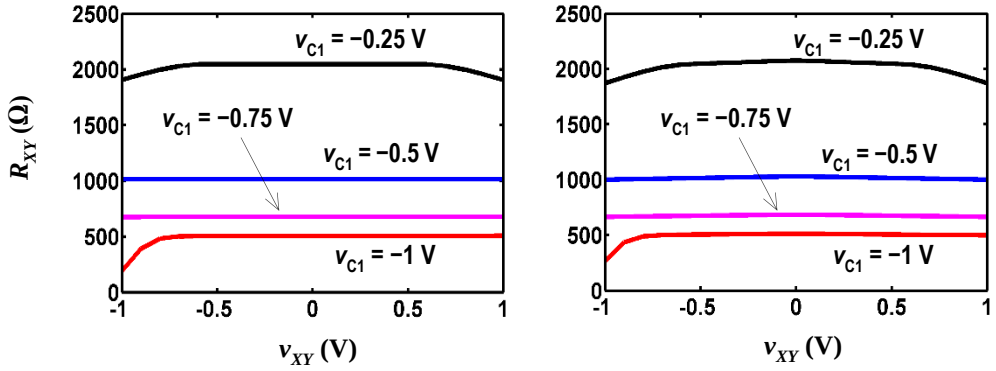

(a) λ = 0 (b) λ = 0.03

Figure 3.10: Simulation results for R_{XY} vs. v_{XY} response for the floating precision linear VCR using matched JFET pair proposed by Holani et al. [24] with the effect of λ. Device parameters: Q1 with I_{DSS} = 0.8987 mA, V_P = −1.032 V and Q2 with I_{DSS} = 0.8842 mA, V_P = −1.028 V.

$= R_3 = 1\ \text{M}\Omega$, $R_4 = R_5 = R_6 = R_7 = 10\ \text{k}\Omega$, $R_8 = 5\ \text{k}\Omega$). The results are shown in Table B.2 (Appendix B) and the corresponding plots are given in Figure 3.10. The calculated values of R_{XY} for v_{C1} of −0.25 V, −0.5 V, −0.75 V, and −1 V are 2000 Ω, 1000 Ω, 666 Ω, and 500 Ω, respectively. The simulation results show R_{XY} values to be close to the corresponding calculated values. For λ = 0 and v_{C1} = −0.5 V, the resistance remains constant at 1015.8 Ω for v_{XY} over the range of ±1 V. The error of 1.5% with reference to the calculated value may be attributed to the mismatch in the parameter values of the two devices. For other values of v_{C1}, there is a decrease in the range of linearity to ±0.6 V for v_{C1} = −0.25 V and ±0.5 V for v_{C1} = −1 V. For small values of v_{XY}, the resistance with λ = 0.03 shows an increase of 1.5% to 2% above the corresponding value with λ = 0 and decreases by up to the same amount for change in v_{XY} in either direction. Thus R_{XY} remains constant with variation in v_{XY} for λ = 0 and shows a variation of up to 4% for λ = 0.03.

For practical testing, the VCR circuit in Figure 3.6 was implemented on bread-board using two µA741CN as the op amps with ±12 V supply. The resistor values were R_1 = 1 kΩ, $R_2 = R_3 = 1\ \text{M}\Omega$, $R_4 = R_5 = R_6 = R_7 = 10\ \text{k}\Omega$, and $R_8 = 5\ \text{k}\Omega$ (two 10 kΩ resistors in parallel). All resistors had 5% tolerance. The measured value of R1 used in the circuit was 992 Ω. The floating terminal voltage v_{XY} was used up to ±1 V. The control voltage v_{C2} was kept at 0.5 V. The control voltage v_{C1} was varied as −0.25 V, −0.5 V, −0.75 V, and −1 V, respectively. The corresponding feedback voltage v_A were found to be −1.354 V, −0.7 V, −0.023 V, and 0.54 V. The practical results for the VCR circuit are given in Table B.3 (Appendix B). The behavior in the resistance variation is found to be unusual when v_{XY} is around ± 100 mV. As the voltage and current readings are compatible to errors of

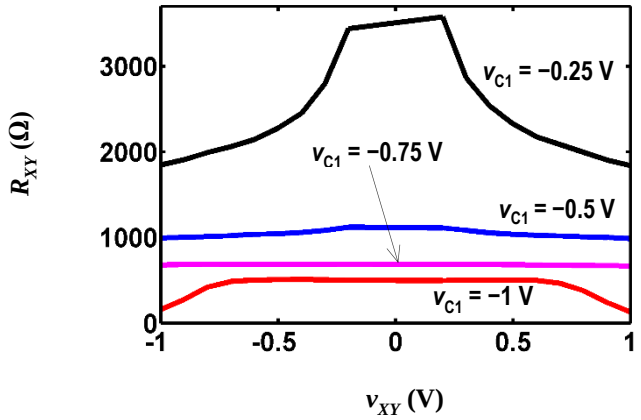

Figure 3.11: Practical results for R_{XY} vs. v_{XY} response for the floating precision linear VCR using matched JFET pair proposed by Holani et al. [24]. Device parameters: Q1 with I_{DSS} = 0.8987 mA, V_P = −1.032 V and Q2 with I_{DSS} = 0.8842 mA, V_P = −1.028 V.

measurements, these readings are not included for further plotting and analysis. For $v_A < V_P$ (−1.354 V), the variation in resistance was found to be ±32.1 % around the midrange of R_{XY}. The resistance varies significantly in this region with small change in v_{XY}. For $V_P < v_A < 0$, (−0.7 V and −0.023 V) the variation in resistances were found to be ±6.4 % and ± 1.6 % around the midrange of R_{XY}, respectively. For $v_A > 0$ (0.54 V), the variation in resistance was found to be ±59.1 % around the midrange of R_{XY}. The circuit cannot be operated in this region as the gate-source or gate-drain junction of the JFET devices may become forward biased and as a result the channel resistance decreases drastically. Figure 3.11 shows the resistance response based on the practical results for the proposed VCR circuit with respect to its v_{XY} and v_{C1}. The practical results in Figure 3.11 follow almost the same pattern as the simulation results in Figure 3.10. The resistance with v_{C1} of −1 V in practical case closely follows the corresponding resistance in simulation, until Q2 gets forward biased for v_{XY} exceeding 0.7 V. The variations in the resistance for practical results with v_{C1} of −0.5 V and −0.75 V are more than the corresponding variations in simulation results with λ = 0.03. This may be because the devices used may have λ of higher than 0.03 as used in simulation. The resistance response with v_{C1} of −0.25 V shows a significant variation in practical case than the simulation result which shows that the VCR cannot be operated in this region as a linear resistor.

3.6 Conclusion

After a study and simulation of the JFET based VCR circuits, the floating precision linear VCR proposed by Holani et al. [24] is found to be suitable for realizing the variable resistance in the bioimpedance simulator. The VCR circuit was tested and verified using both simulation and practical implementation. The practical results for the proposed VCR circuit

were found to be satisfactory when used for obtaining a variable resistance around $2R_{DS,\min}$ of the JFET, the voltage range for linear operation decreasing for the controlled resistance being away on either side of this resistance.

Chapter 4

MOSFET BASED VOLTAGE-CONTROLLED RESISTOR

4.1 Introduction

A MOSFET can be used as a VCR with its gate-source voltage controlling its drain-source channel resistance. It acts as a linear resistance if the drain-source voltage is limited to tens of mV. MOSFETs can also be used to realize the VCR circuits described in the previous chapter. A description of some of these circuits and test results obtained through simulation and practical realization are presented in this chapter.

4.2 MOSFET Device Basics

A MOSFET can be used as a linear voltage-controlled resistor for a small range of drain-source voltage [16], [28], [29]. Figure 4.1 shows an enhancement-type NMOS transistor with its source (S), gate (G), drain (D), and substrate or bulk (B) terminals and its drain-source voltage v_{DS} versus drain current i_D characteristics [28]. It is operated with $v_{DS} > 0$ and $v_{BS} \le 0$ to ensure that the substrate-channel junction is reversed biased. The drain and source terminals are interchangeable, the one at the higher potential acts as the drain in n-channel device. The current $i_D \approx 0$ for $v_{GS} \le V_T$ and this region is known as the cutoff region. For $v_{GD} > V_T$, the current increases with v_{DS} and this region is known as the non-saturation, triode, or linear region. For $v_{GD} < V_T$, the current becomes independent of v_{DS} and this region is known as the saturation region. The current i_D is approximately given as

$$i_D = \begin{cases} 0, & v_{GS} \le V_T \\ k[(v_{GS} - V_T)v_{DS} - {v_{DS}}^2/2], & v_{GS} > V_T \text{ and } v_{GD} > V_T \\ k[(v_{GS} - V_T)^2/2], & v_{GS} > V_T \text{ and } v_{GD} < V_T \end{cases} \tag{4.1}$$

The value of *k* for a MOSFET is given as

$$k = \mu_0 C_{OX} w / l \tag{4.2}$$

where μ_0 is the carrier mobility in the device channel, C_{OX} is the gate oxide layer capacitance per unit area, and l and w are channel length and width, respectively [16]. The carrier mobility μ depends on temperature T and the relation can be given as

$$\mu(T) = \mu_0 (T_0 / T)^m \tag{4.3}$$

where μ_0 is the mobility at the room temperature T_0 (usually 25 ˚C) and m is a constant with a value of 1.2 − 2 [30], [31].

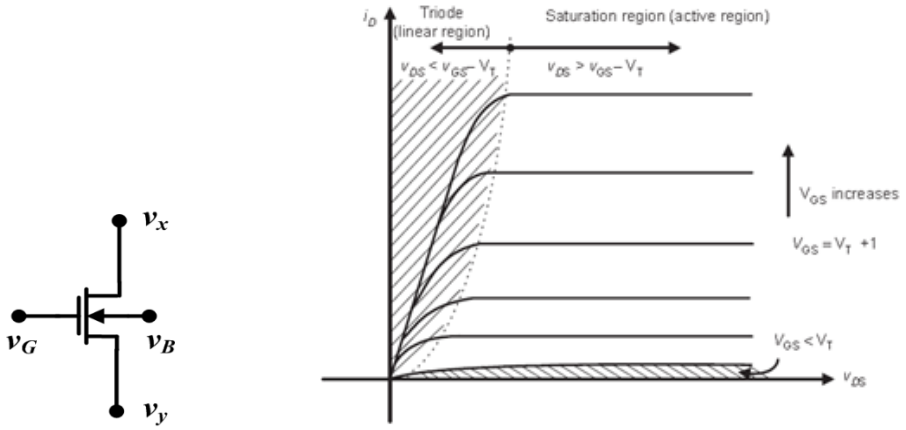

Figure 4.1: An enhancement-type n channel MOSFET and its drain-source voltage vs drain current characteristics [28].

The threshold voltage V_T depends on temperature, device parameters, and substrate-source bias v_{BS} [30]. The effect of temperature on V_T can be given as

$$V_T(T) = V_T(T_0) - K(T - T_0) \tag{4.4}$$

where T is the absolute temperature, T_0 is the room temperature (usually 25 ˚C), and K is the temperature drift coefficient for the threshold voltage [18]. The threshold voltage V_T for $v_{BS} = 0$ is given as

$$V_T(v_{BS} = 0) = V_{FB} + 2\psi_B + \frac{\sqrt{2\varepsilon_{Si} q N_A (2\psi_B)}}{C_{OX}} \tag{4.5}$$

where ψ_B is the body Fermi potential, ε_{Si} is the relative permittivity of silicon, N_A is the doping concentration of the body, V_{FB} is the flat-band voltage, and q is charge on electron [18]. The effect of v_{BS} on the threshold can be modeled as a threshold voltage shift ΔV_T and can be given as the following:

$$V_T(v_{BS}) = V_{T0} + \Delta V_T \tag{4.6}$$

The shift ΔV_T is given as

$$\Delta V_T = \frac{\sqrt{2\varepsilon_{Si} q N_A}}{C_{OX}} \left(\sqrt{|2\psi_B + v_{BS}|} - \sqrt{|2\psi_B|} \right) \tag{4.7}$$

where $(\sqrt{2\varepsilon_{Si} q N_A} / C_{OX})$ is also called GAMMA [16]. The voltage V_{T0} is the threshold voltage without considering the body effect, which refers to a change in the threshold voltage due to substrate bias.

In a model of the drain current which is based on the symmetry of the source and drain terminals [28], [29], the body effect is represented by process-dependent parameter α (typically 1.05 – 1.35). In this model, the thresholds at the source and drain ends of the channel given as

$V_{T0}+(\alpha-1)(v_S-v_B)$ and $V_{T0}+(\alpha-1)(v_D-v_B)$, respectively. For the device to be operated in non-saturation region, the gate-channel voltage should be supra-threshold at the source and drain ends i.e.

$$v_G - v_S \geq V_{T0} + (\alpha - 1)(v_S - v_B)$$

$$\text{and } v_G - v_D \geq V_{T0} + (\alpha - 1)(v_D - v_B)$$

which can be expressed as

$$v_G - v_B \geq V_{T0} + \alpha (v_S - v_B)$$

$$\text{and } v_G - v_B \geq V_{T0} + \alpha (v_D - v_B)$$

In the non-saturation region, the drain current i_D is given as [30]:

$$i_D = \frac{k}{2\alpha}[(v_G - v_S - (V_{T0} + (\alpha-1)(v_S - v_B)))^2 - (v_G - v_D - (V_{T0} + (\alpha-1)(v_D - v_B)))^2], \quad v_G > V_{T0} \text{ and } v_B < 0 \tag{4.8}$$

The expression for i_D, as given in (4.8), can also be written as:

$$i_D = k[v_G - v_B - V_{T0} - \alpha(\frac{v_D + v_S}{2} - v_B)](v_D - v_S) \tag{4.9}$$

The resistance $R_{DS} = (v_D - v_S)/i_D$ can be controlled by the gate voltage v_G but it is nonlinear due to the presence of the common mode voltage $(v_D + v_S)/2$ and v_B. For very small v_{DS}, the term $(v_D + v_S)/2$ can be neglected and the channel resistance R_{DS} can be approximated as a linear resistance as given in the following equation:

$$R_{DS} = \frac{1}{k(v_G - V_T)}, \quad v_{DS} << v_G - V_T \tag{4.10}$$

Since R_{DS} depends on device parameters k and V_{T0}, it varies with process-dependent parameters and also due to changes in temperature and substrate-channel bias v_B. For small value of v_{DS}, the substrate (B) terminal of the MOSFET device may be tied with the source terminal to ensure that the substrate-channel junction is not forward biased. However, the channel potential varies across its length and the variation in channel-substrate voltage introduces variation in the resistance [17], [28], [29].

4.3 MOSFET Based VCR Circuit

A MOSFET device can act as a linear VCR for a small range of drain-source voltages [16], [28], [29]. Several approaches have been reported for improving the performance of a MOSFET as a VCR. Combination of devices operated in linear and saturation region are used to eliminate non-linear terms present in i_D expression. The drain and source terminal voltages can also be added to its gate control voltages to extend the linearity range. Use of matched pair

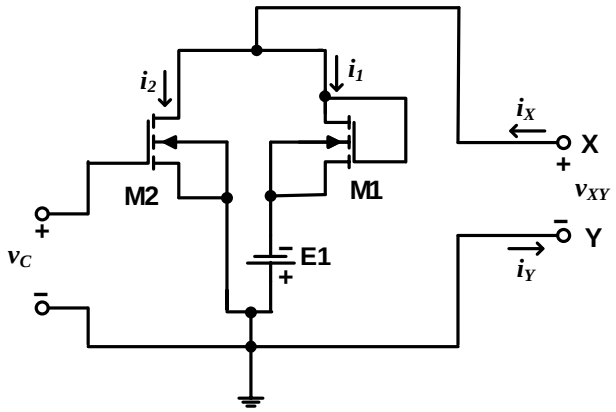

Figure 4.2: Enhancement-type MOSFET-based VCR developed by Moon et.al. [31].

can be used to eliminate device parameter dependency. The VCR can be made either grounded or floating type. Several VCR circuits [31] – [36], based on some of the above mentioned approaches, have been reported and some of them are reviewed here.

4.3.1 Grounded linear VCR using matched pair MOSFETs as reported by Moon et al. [31]

In some circuits, combinations of transistors operating in either non-saturation or saturation regions can be employed to eliminate the nonlinear term present in i_D expression as given in (4.1) and extending the range of linearity for VCR operation [31], [33], [34]. Moon et al. [31] proposed a VCR circuit where a matched pair of enhancement-type MOSFETs was used as shown in Figure 4.2. The transistor M1 with its drain-gate shorted is kept in the saturation region and an external voltage source E_1 is connected at the source terminal of M1 in order to keep gate-source voltage above the threshold voltage for an applied range of drain-source voltage. The drain current i_1 flowing through M1 is given as the following:

$$i_1 = k_1\left(v_{XY} + E_1 - V_{T1}\right)^2 / 2, \quad v_{XY} + E_1 \geq V_{T1} \tag{4.11}$$

The control voltage v_C at the gate terminal of the transistor M2 with respect to v_{XY} is maintained in such a way that M2 operates in the nonsaturation region and its drain current i_2 is given as the following:

$$\begin{aligned} i_2 = k_2[(v_C - V_{T2})v_{XY} - v_{XY}^2/2], \\ v_C > V_{T2},\ v_C \geq v_{XY} + V_{T2} \geq 0 \text{ and } v_{XY} > 0 \end{aligned} \tag{4.12}$$

The total current i_X $(= i_Y)$ is the sum of i_1 and i_2 and can be given as

$$\begin{aligned} i_X = k_1\left(v_{XY} + E_1 - V_{T1}\right)^2/2 + k_2[(v_C - V_{T2})v_{XY} - v_{XY}^2/2], \\ v_C > V_{T2} \text{ and } v_C - V_{T2} \geq v_{XY} \geq V_{T1} - E_1 \end{aligned} \tag{4.13}$$

For matched pair of transistors, $k_1 = k_2 = k$ and $V_{T1} = V_{T2} = V_T$ and the two quadratic terms of v_X present in the (4.13) cancels out each other and we get

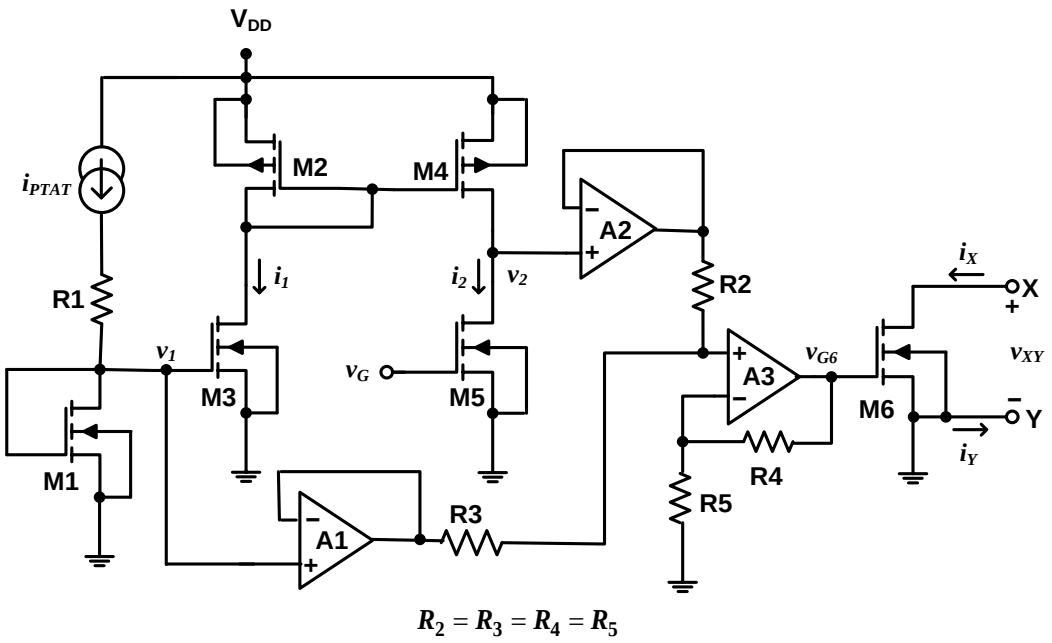

Figure 4.3: MOSFET based VCR circuit proposed by Fort [32].

$$i_X = k[(v_C + E_1 - 2V_T)v_{XY} + (E_1 - V_T)^2/2], \quad v_C > V_T \text{ and } v_C - V_T \geq v_{XY} \geq V_T - E_1 \tag{4.14}$$

The term $(E_1 - V_T)^2$ can be eliminated by selecting $E_1 = V_T$ and the resistance $R_{XY} = v_{XY}/i_X$ becomes:

$$R_{XY} = \frac{1}{k(v_C - V_T)}, \quad v_C > V_T \text{ and } v_C - V_T \geq v_{XY} \geq 0 \tag{4.15}$$

This circuit offers an extended range of $v_{XY} \leq v_C - V_T$ but does not eliminate the effect of the device parameters k and V_T and does not provide a floating resistor. Besides, E_1 has to be matched to V_T of the device.

4.3.2 Grounded precision VCR using NMOS and PMOS devices reported by Fort [32]

Fort [32] proposed a MOSFET-based resistor as shown in Figure 4.3, to reduce the variations occurring due to the device parameters and temperature. A current i_{PTAT} dependent voltage source v_C is used to compensate in mobility of a MOS resistor due to change in temperature. The current i_{PTAT} generated from a current source is proportional to the absolute temperature T which is provided to a voltage generation module, consisting three matched NMOS transistors M1, M3 and M5 and two matched PMOS transistors M2 and M4, for generating two output voltages v_1 and v_2 such that

$$v_1 = V_T + k_1 T \text{ and } v_2 = k_2 T^2$$

These voltages are added using op amps A1, A2, and A3 to provide the gate control voltage as

$$v_{G6} = V_T + k_1 T + k_2 T^2 \tag{4.16}$$

The resistance across the transistor M6 for small values of drain-source voltage, referring (4.9), can be given as

$$R_{XY} = 1/k(v_{G6} - V_{T6}) \tag{4.17}$$

With the threshold voltage of M6 being matched to V_T, the resistance can be written as

$$R_{XY} = 1/k(k_1 T + k_2 T^2) \tag{4.18}$$

The values of k_1 and k_2 are selected to compensate for variation in μ with temperature and resistance value is stabilized with respect to temperature variation.

The circuit cannot be realized as a floating VCR and it does not compensate for V_T variation. It does not extend the range of linearity.

4.3.3 Floating precision linear VCR using a matched MOSFET pair

The matched JFET pair based floating precision linear VCR, as proposed by Holani et al. [24], can also be implemented using an n-channel MOSFET pair with independent substrate terminals. The control voltages for the matched pair of MOSFETs is obtained by source-drain (SD) bootstrapping of the gate (G) and substrate (B) terminals.

The schematic diagram of the MOSFET pair based floating precision linear VCR circuit is shown in Figure 4.4. It uses matched devices M1 and M2 with independent substrate terminals. Three independent voltage sources v_{C1}, v_{C2}, v_{C3}, and resistor R_1 control the channel resistance of the device M1. The op amp A1 forms the negative feedback loop with M1 to generate v_A. The voltage v_{C3} acts as the reference for the whole circuit and it may be shorted to the ground. The op amps A4 and A5 buffer the source and drain voltages of M1. The op amp A3 uses v_A and the drain and source voltages of M1 to generate its gate voltage v_{G1}. The op amp A2 generates v_{B1} by adding source and drain voltages to V_{BB}. The terminals X and Y provide the terminals of the floating VCR. The op amps A7 and A6 generate v_{G2} and v_{B2} by adding the source and drain voltages of M2 to v_A and V_{BB}, respectively. The op amps A8 and A9 buffer the drain and source voltages of M2. The expressions for the gate and substrate voltages for M1 and M2 are given as

$$v_{G1} = (v_A + v_{C1} + v_{C3})/2 \tag{4.19}$$

$$v_{G2} = (v_A + v_X + v_Y)/2 \tag{4.20}$$

$$v_{B1} = (V_{BB} + v_{C1} + v_{C3})/2 \tag{4.21}$$

$$v_{B2} = (V_{BB} + v_X + v_Y)/2 \tag{4.22}$$

These summations are obtained by selecting the resistances as the following:

$$R_7 = R_8 = R_9, \quad R_{11} = 2\,R_{10}$$

$$R_{17} = R_{18} = R_{19}, \quad R_{21} = 2\,R_{20}$$

$$R_2 = R_3 = R_4, \quad R_6 = 2\,R_5$$

$$R_{12} = R_{13} = R_{14}, \quad R_{16} = 2\,R_{15}$$

Both the devices M1 and M2 are operated in the non-saturation region The negative feedback loop formed by A1 and M1 maintains the inverting input terminal of A1 at v_{C3}. It requires $v_{C1} > v_{C3}$ and $i_1 > 0$. The current i_1 through M1 can be given as

$$i_1 = (v_{C3} - v_{C2}) / R_1, \quad v_{C2} < v_{C3} \tag{4.23}$$

The channel resistance of M1 can be given as

$$R_{DS1} = (v_{C1} - v_{C3}) / i_1 \tag{4.24}$$

Using (4.23) and (4.24), we get

$$R_{DS1} = \frac{(v_{C1} - v_{C3})}{(v_{C1} - v_{C3})} R_1 \tag{4.25}$$

Using (4.9), i_1 can be expressed as

$$i_1 = k_1 [v_{G1} - v_{B1} - V_{T01} - \alpha_1 (\frac{v_{C1} + v_{C3}}{2} - v_{B1})](v_{C1} - v_{C3}) \tag{4.26}$$

Using (4.19), (4.21), and (4.26) expression for i_1 can be simplified to

$$i_1 = k_1 [v_A - (V_{T01} + (1 - \alpha_1) V_{BB})](v_{C1} - v_{C3}) / 2 \tag{4.27}$$

Now, using (4.23), (4.24) and (4.27), expression for v_A can be obtained as

$$v_A = \left[\frac{(v_{C3} - v_{C2})}{2 (v_{C1} - v_{C3}) k_1 R_1} + (V_{T01} + (1 - \alpha_1) V_{BB}) \right] \tag{4.28}$$

The current i_X through M2, using (4.9), can be written as

$$i_X = k_2 [v_{G2} - v_{B2} - V_{T02} - \alpha_2 (\frac{v_X + v_Y}{2} - v_{B2})](v_X - v_Y) \tag{4.29}$$

Using (4.20), (4.22), and (4.25) the expression for i_X can be simplified as

$$i_X = k_2 [v_A - (V_{T02} + (1 - \alpha_2) V_{BB})](v_X - v_Y) / 2 \tag{4.30}$$

The channel resistance $R_{DS2} = (v_X - v_Y) / i_X$ which is the resistance across the X and Y terminals of the VCR and hence is given as

$$R_{XY} = 2[v_A - (V_{T02} + (1 - \alpha_2) V_{BB})]^{-1} / k_2 \tag{4.31}$$

Using (4.28) and (4.31), R_{XY} can be expressed as

$$R_{XY} = 2 \left[\frac{(v_{C3} - v_{C2})}{2 (v_{C1} - v_{C3}) k_1 R_1} + V_{T01} - V_{T02} - V_{BB} (\alpha_1 - \alpha_2) \right]^{-1} / k_2 \tag{4.32}$$

Since M1 and M2 are matched, $k_1 = k_2$, $V_{T01} = V_{T02}$, and V_{BB} is same for both the devices, so $\alpha_1 = \alpha_2$. The above equation can be further simplified as

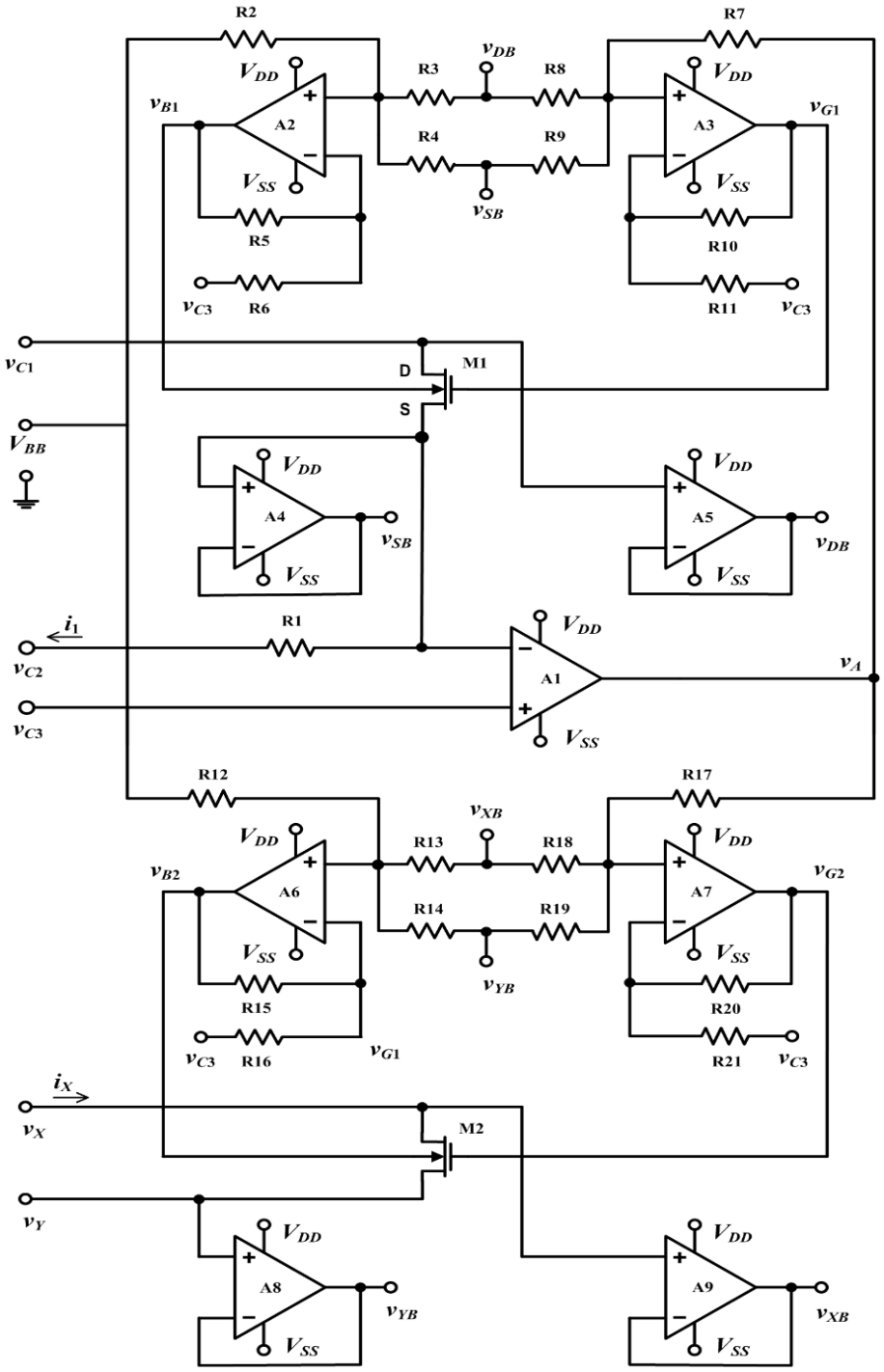

$R_1 = 1\ \text{k}\Omega$
$R_2 = R_7 = R_{12} = R_{17}$
$R_3 = R_4 = R_8 = R_9 = R_{13} = R_{14} = R_{18} = R_{19}$
$R_5 = R_{10} = R_{15} = R_{20}$
$R_6 = R_{11} = R_{16} = R_{21}$

Figure 4.4: Matched-pair MOSFET-based floating VCR circuit with SD-bootstrapped gate, SD-bootstrapped substrate, and self-tracking.

$$R_{XY} = \frac{(v_{C1} - v_{C3})}{(v_{C3} - v_{C2})} R_1 \tag{4.33}$$

The condition for operating M2 in nonsaturation region are

$$\begin{aligned} v_{G2} - v_{B2} &\geq V_{T0} + \alpha(v_X - v_{B2}) \\ \& \quad v_{G2} - v_{B2} &\geq V_{T0} + \alpha(v_Y - v_{B2}) \end{aligned} \tag{4.34}$$

Using (4.20), (4.22), and (4.34), conditions for VCR to be in linear operation can be rewritten as

$$\begin{aligned} v_A &\geq 2V_{T0} + (1-\alpha)V_{BB} + \alpha(v_Y - v_X) \\ \& \quad v_A &\geq 2V_{T0} + (1-\alpha)V_{BB} + \alpha(v_X - v_Y) \end{aligned} \tag{4.35}$$

which can be further simplified to

$$|v_X - v_Y| \leq \frac{1}{\alpha}(v_A - 2V_{T0} - (1-\alpha)V_{BB}) \tag{4.36}$$

For substrate-channel to be reverse biased, we have $v_X > v_B$ and $v_Y > v_B$, which place the following constraints:

$$v_X > \frac{V_{BB} + v_X + v_Y}{2} \text{ and } v_Y > \frac{V_{BB} + v_X + v_Y}{2}$$

And it can be simplified to

$$V_{BB} < -|v_X - v_Y| \tag{4.37}$$

Therefore the constraints for drain-source terminal voltage becomes

$$|v_X - v_Y| < \min[\frac{1}{\alpha}(v_A - 2V_{T0} - (1-\alpha)V_{BB}), -V_{BB}] \tag{4.38}$$

The resistance response of this VCR, as given in (4.33), becomes completely independent of device parameters and V_{BB} provided the condition given in (4.38) is not violated. The range of v_{XY} can be extended by applying a large value of V_{BB}. Since MOSFET is operated with a positive gate-source voltage, there is no restriction on the range of the drain-source voltage as long as the gate-source, the gate-drain, and the channel-substrate junctions remain reversed biased. The variation in the resistance with v_A and the range of v_{XY} for the linear operation as given in (4.38) are graphically represented in Figure 4.5. As we see, v_A and V_{BB} restrict the range of v_{XY} as given in (4.38), and the channel resistance R_{XY} decreases with increase in v_A as given in (4.31).

The minimum value of R_{XY} can be obtained when the constraints given in (4.38) meet the following condition:

$$\frac{1}{\alpha}(v_A - 2V_{T0} - (1-\alpha)V_{BB}) = -V_{BB} \tag{4.39}$$

Using the above relation, expression for v_A to achieve $R_{XY,\min}$ can be given as

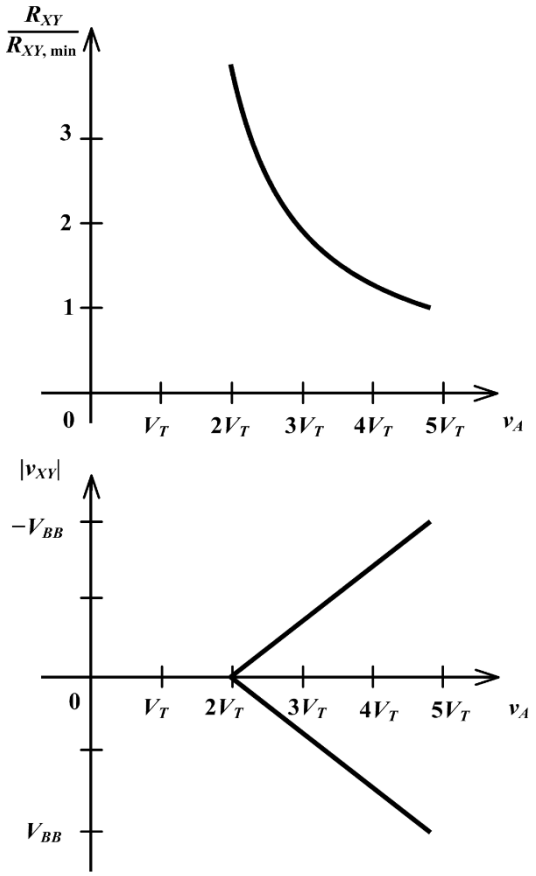

Figure 4.5: R_{XY} as a function of v_A and v_{XY} for linear operation of the MOSFET pair-based floating precision linear VCR.

$$v_A = 2V_{T0} + (1-2\alpha)V_{BB} \tag{4.40}$$

Using (4.31) and (4.40), the expression for $R_{XY,\min}$ can be obtained as

$$R_{XY,\min} = 2[V_{T0} + (1-2\alpha)V_{BB}]^{-1} / k \tag{4.41}$$

In this circuit, the drain and source voltages are added to the control voltage to obtain the gate voltage and this arrangement is called as source-drain (SD) bootstrapping which is used to extend the range of linearity. Use of matched MOSFET pair and negative feedback makes it a self-tracking circuit for realizing a precision resistor with no effect of variation in device parameters.

4.4 Simulation Results for the Floating Precision Linear VCR Circuit using Matched MOSFET Device Pair

The proposed VCR circuit, as described in subsection 4.3.3 and shown in Figure 4.4, requires two matched MOSFET devices with independent substrate terminal. ALD1106 [39] is a quad n-channel MOSFET IC with four matched devices and their substrate terminals shorted

Table 4.1: Device parameters of MOSFETs in ALD1106 [37].

Parameter	Min.	Typ.	Max.	Test conditions
Device-dependence of V_T (datasheet)	0.4 V	0.7 V	1.0 V	T = 25 ˚C, I_{DS} = 1 µA, V_{DS} = V_{GS}
Device-dependence of R_{DS} (datasheet)	–	350 Ω	500 Ω	T = 25 ˚C, V_{GS} = 5 V, V_{DS} = 0.1 V
Device-dependence of k (calc. (4.1))	0.28 mA/V^2	0.52 mA/V^2	–	T = 25 ˚C, I_{DS} = 4.8 mA (typ.), 3.0 mA (min.) for V_{DS} = V_{GS} = 5 V, V_T = 0.7 V
Dependence of V_T on temperature (calc. (4.4))	0.688 V	0.700 V	0.712 V	K = −1.2 mV/ ˚C, V_T (25 ˚C) = 0.7 V, $T_{\min}$ = 15 ˚C, T_{typ} = 15 ˚C, $T_{\max}$ = 35 ˚C
Dependence of k on temperature (calc. (4.2) & (4.3))	0.49 mA/V^2	0.52 mA/V^2	0.55 mA/V^2	m = 1.5, k (25 ˚C) = 0.52 mA/V^2, $T_{\min}$ = 15 ˚C, T_{typ} = 15 ˚C, $T_{\max}$ = 35 ˚C
Dependence of R_{DS} on V_T (calc. (4.9))	1201 Ω	1479 Ω	1923 Ω	k = 0.52 mA/V^2, $V_{T\min}$ = 0.4 V, $V_{T typ}$ = 0.7 V, $V_{T\max}$ = 1.0 V, V_{DS} = 0.1 V, V_{GS} = 2 V
Dependence of R_{DS} on k (calc. (4.9))	–	1479 Ω	2747 Ω	$k_{\min}$ = 0.28 mA/V^2, k_{typ} = 0.52 mA/V^2, V_T = 0.7 V, V_{DS} = 0.1 V, V_{GS} = 2 V

together. ALD1116 is a dual n-channel MOSFET IC with two matched devices and their substrate terminals shorted together. The device parameters for this two ICs are same and presented in Table 4.1. These parameters were used for simulation. The device parameters vary from piece-to-piece and also depend on temperature which are presented in the table.

Simulation for this matched MOSFET pair based VCR was carried out using a SPICE LEVEL 1 model for the MOSFET devices. The device parameters, used for this simulation, were taken from Table 4.1 and from the downloaded SPICE model [38], as the following:

Channel length (l) = 7.8 µm, Channel width (w) = 0.138 mm,

Area of drain diffusion (AD) = 1.61 nm^2,

Area of source diffusion (AS) = 6.03 nm^2,

Perimeter of drain (PD) = 0.478 mm, Perimeter of source (PS) = 0.478 mm.

Other parameters used for simulation were transconductance parameter KP, bulk threshold parameter GAMMA, surface potential PHI, zero-bias threshold voltage VTO, and channel-length modulation parameter LAMBDA (λ). KP can be calculated using the following relation:

$$\text{KP} = kl/w \tag{4.42}$$

The values for GAMMA and PHI were taken from the downloaded SPICE model [38]. The values for k and V_{TO} were taken from Table 4.1. The values for λ were taken as 0 and 0.03. The resistor values in the circuit were taken as $R_1 = 1\,\text{k}\Omega$, $R_2 = R_3 = R_4 = R_6 = R_7 = R_8 = R_9 = R_{11} = R_{12} = R_{13} = R_{14} = R_{16} = R_{17} = R_{18} = R_{19} = R_{21} = 10\,\text{k}\Omega$, and $R_{10} = R_{15} = R_{20} = 5\,\text{k}\Omega$. The op amps used with supply voltage of ±15 V. The reference voltage v_{C3} was connected to ground. Simulation was carried out for two sets of matched device parameters:

$$\text{Device pair 1: } k = 0.52 \text{ mA/V}^2 \text{ and } V_T = 0.7 \text{ V}$$

$$\text{Device pair 2: } k = 0.28 \text{ mA/V}^2 \text{ and } V_T = 0.4 \text{ V}$$

The voltages v_{C1} and V_{BB} were taken as 1 V and –2 V, respectively, and v_{XY} was varied from 0 to ±2 V. The values of v_{C2} and λ were varied to observe their effect on R_{XY} versus v_{XY}.

The simulation results are given in Appendix C. Table C.1 shows the simulation results for examining the effect of varying v_{C2}. With the device pair 1 and $\lambda = 0$, the variations in R_{XY} are $\pm 33.4\%$, $\pm 20.3\%$, $\pm 12.3\%$, and $\pm 6\%$ for v_{C2} of −0.5 V, −1 V, −1.5 V, and −2 V, respectively. The corresponding variations with this device pair and $\lambda = 0.03$, are $\pm 38.5\%$, $\pm 23.7\%$, $\pm 15.3\%$, and $\pm 8.8\%$. With the device pair 2 and $\lambda = 0$, the variations in R_{XY} are $\pm 13.4\%$, $\pm 6.8\%$, $\pm 4.5\%$, and $\pm 3.4\%$ for v_{C2} of −0.5 V, −1 V, −1.5 V, and −2 V, respectively. The corresponding variations with this device pair and $\lambda = 0.03$, are $\pm 16.4\%$, $\pm 9.6\%$, $\pm 7.3\%$, and $\pm 6.2\%$. The resistance response for these two matched pair devices, with the effect of v_{C2} and λ, is shown graphically in Figure 4.6. The simulation results show that when v_{C2} is selected for small R_{XY}, the resistance remains nearly constant with respect to v_{XY}. When v_{C2} is selected for large R_{XY}, the resistance has a significant variation with increase in $|v_{XY}|$. Variation in R_{XY} with increase in $|v_{XY}|$ for λ = 0.03 is larger than that for λ = 0. Thus the simulation results show that (i) the range of linearity decreases for higher values of R_{XY}, (ii) the controlled resistance is not much affected by change in the device parameters for smaller values of R_{XY}, and (iii) the channel length modulation introduces non-linearity.

Table C.2 shows simulation results for the effect of variation in V_{BB} and λ with v_{C1} = 1 V and $v_{C2} = -1$ V for device pair 1. For $V_{BB} = -2$ V, the variations in R_{XY} are $\pm 12.3\%$

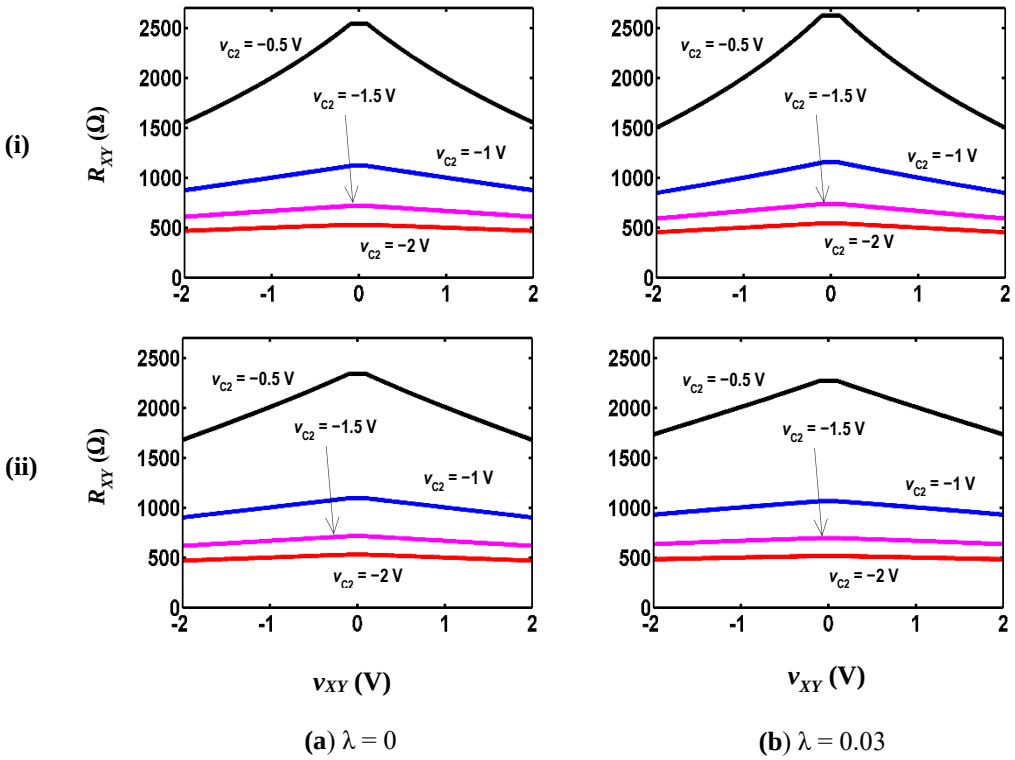

(a) λ = 0 **(b)** λ = 0.03

Figure 4.6: Effect of v_{C2} and λ on R_{XY} vs. v_{XY} response of the floating precision linear VCR using matched MOSFET pair based VCR circuit (in Figure 4.4). Device parameters: (a) λ = 0 and (b) λ = 0.03, for two sets of k and V_T as follows: (i) k = 0.52 mA/V^2 and V_T = 0.7 V, (ii) k = 0.28 mA/V^2 and V_T = 0.4 V, V_{BB} = −2 V.

and $\pm 15.3\,\%$ with $\lambda = 0$ and $\lambda = 0.03$, respectively. The corresponding variations for V_{BB} = −4 V are $\pm 9\,\%$ and $\pm 11.9\,\%$. The resistance response, with the effect of V_{BB} and λ, is shown graphically in Figure 4.7. The plots show that the variation in resistance with $|v_{XY}|$ reduces for more negative value of V_{BB} and λ = 0.03 results in larger variation as compared with λ = 0.

Table C.3 shows simulation results for the two device pairs, with v_{C1} = 1 V, $v_{C2} = -1$ V, and V_{BB} = −2 V. The resistance response for these device pairs are shown graphically in Figure 4.8. With $\lambda = 0$ and $\lambda = 0.03$, the variation in R_{XY} for the first set of parameters were found $\pm 12.3\,\%$ and $\pm 15.3\,\%$, respectively. With $\lambda = 0$ and $\lambda = 0.03$, the variation in R_{XY} for the second set of parameters were found $\pm 6.6\,\%$ and $\pm 9.6\%$, respectively.

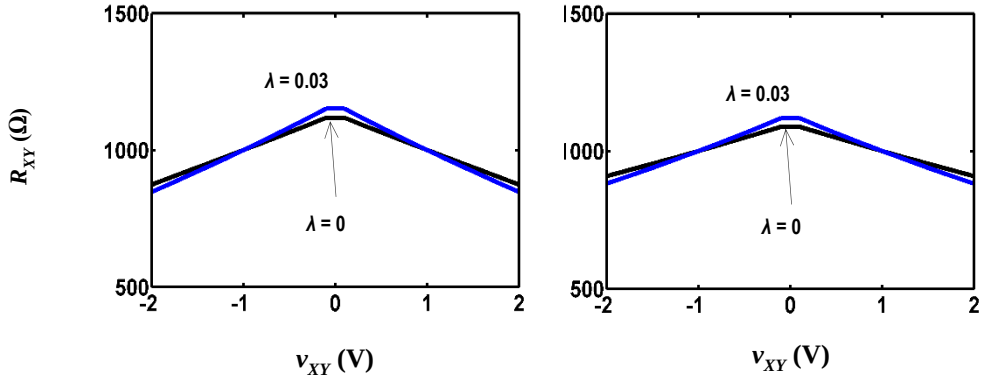

(a) $V_{BB} = -2$ V **(b)** $V_{BB} = -4$ V

Figure 4.7: Effect of V_{BB} and λ on R_{XY} vs. V_{XY} response of the floating precision linear VCR using matched MOSFET pair based VCR circuit (in Figure 4.4). Substrate voltage: (a) $V_{BB} = -2$ V and (b) $V_{BB} = -4$ V, Device parameters: k = 0.52 mA/V^2 and V_T = 0.7 V. Control voltages: v_{C1} = 1 V, v_{C2} = −1 V, and v_{C3} = 0 V.

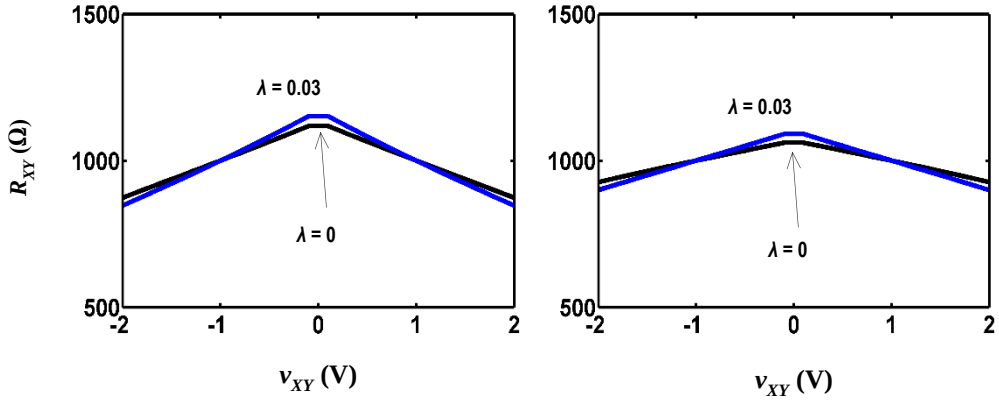

(a) k = 0.52 mA/V^2 and V_T = 0.7 V **(b)** k = 0.28 mA/V^2 and V_T = 0.4 V

Figure 4.8: Effect of device parameters on R_{XY} vs. V_{XY} response of the floating precision linear VCR using matched MOSFET pair based VCR circuit (in Figure 4.4). Device parameters: (a) k = 0.52 mA/V^2 and V_T = 0.7 V and (b) k = 0.28 mA/V^2 and V_T = 0.4 V. Control voltages: v_{C1} = 1 V, v_{C2} = −1 V, and v_{C3} = 0 V.

4.5 Practical Results for the Floating Precision Linear VCR Circuit using Matched MOSFET Device Pair

The quad n-channel MOSFET IC ALD1106 [37] has a common substrate terminal for all the on-chip devices. One device each from two ICs can be used for implementing the proposed MOSFET pair based VCR circuit, with the two devices selected on the basis of matching of their measured parameters. For this purpose, parameters of all devices on two ICs were measured and two devices, one from each IC, with the least device parameter mismatch

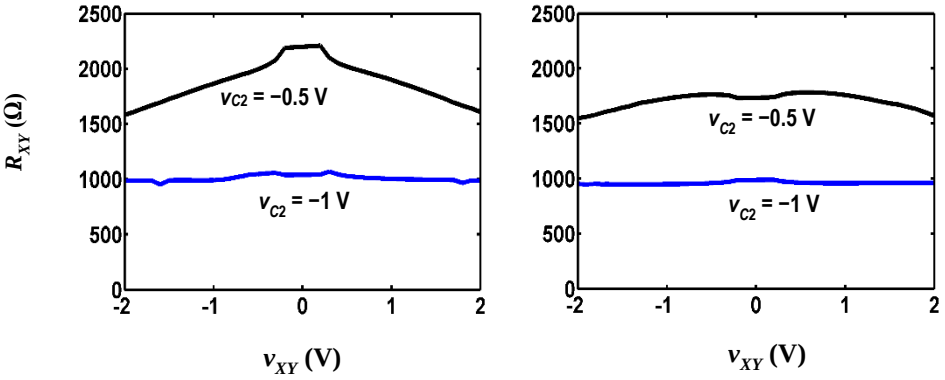

(a) $V_{BB} = -2$ V **(b)** $V_{BB} = -4$ V

Figure 4.9: Practical results for R_{XY} vs. V_{XY} response of the floating precision linear VCR using matched MOSFET pair based VCR circuit (in Figure 4.4). Device parameters (calculated) : k = 0.575 mA/V^2 and V_T = 0.396 V and k = 0.614 mA/V^2 and V_T = 0.389 V. Substrate voltage: (a) $V_{BB} = -2$ V and (b) $V_{BB} = -4$ V. Control voltages: v_{C1} = 1 V, $v_{C2} = -0.5$ V and −1 V, and v_{C3} = 0 V.

were selected. Values of i_D were measured with $v_{GS} = 1$ V and $v_{BS} = 0$ for v_{DS} of 0.1 V and 0.5 V. Assuming $\alpha = 1$, the value of V_T was calculated using the following relation as obtained from (4.8):

$$\frac{i_{D1}}{i_{D2}} = \frac{(v_{GS} - V_T - v_{DS1}/2)\ v_{DS1}}{(v_{GS} - V_T - v_{DS2}/2)\ v_{DS2}}$$

After calculating the value of V_T, the value for k was calculated from the following relation as obtained from (4.8):

$$i_D = k[(v_{GS} - V_T)v_{DS} - \frac{v_{DS}^{\ 2}}{2}]$$

for v_{DS} of 0.1 V. The parameters of the selected devices were selected as the following:

Device 1: $k = 0.575$ mA/V^2 and $V_T = 0.396$ V

Device 2: $k = 0.614$ mA/V^2 and $V_T = 0.389$ V

The circuit was assembled on the bread-board using two ALD1106 ICs (each for one MOSFET), resistors, and five µA741CN ICs as op amps. The value of R_1 was selected as 1 kΩ (measured $R_1 = 992\ \Omega$). The control voltages v_{C1} and v_{C3} were 1 V and 0 V, respectively. The resistors had nominal values as the resistances used for the simulation and with 5% tolerance. The VCR circuit was tested for v_{C2} of −0.5 V and −1 V and V_{BB} of −2 V and −4 V. The measured resistance values were found to be inconsistent for v_{XY} of around ± 100 mV, which can be explained by the measurement errors. Therefore the resistance values at ± 100 mV were excluded for further plotting and analysis.

The results are given Table C.4 (Appendix C). With $V_{BB} = -2$ V, the variations in R_{XY} over $|v_{XY}| < 2$ V are $\pm 16.5\,\%$ and $\pm 5.8\,\%$ for v_{C2} of −0.5 V and −1 V, respectively. With $V_{BB} = -4$ V, the corresponding variations are $\pm 7.1\,\%$ and $\pm 2.2\,\%$. Increase in negative V_{BB} results in larger range of operation for $|v_{XY}|$. The resistance response for the practical results of the VCR circuit is shown graphically in Figure 4.9. It is seen that the values of R_{XY} for the two values V_{BB} are almost the same for v_{C2} of –1 V.

4.6 Conclusion

The proposed MOSFET pair based VCR circuit was tested using both simulation and practical implementation. The simulation results show that (i) the range of linearity decreases for higher values of R_{XY}, (ii) the controlled resistance is not much affected by change in the device parameters for smaller values of R_{XY}, and (iii) the channel length modulation introduces non-linearity. The practical implementation using a selected pair of nearly matched devices confirms that the circuit can be used as a linear floating VCR. Although the practical implementation could not be tested for the effect of device parameter variations, it was seen that the value of the resistance was not much affected by change in V_{BB}. Hence, it may be concluded that implementation of the circuit using a matched pair of devices on the same die and with independent substrates can be used for its intended purpose of providing floating precision linear VCR.

Chapter 5
BIOIMPEDANCE SIMULATOR

5.1 Introduction

Bioimpedance simulator is a circuit which can provide impedance equivalent to human body impedance and can be used to test linearity, sensitivity, and dynamic response of various impedance measuring instruments (e.g. ICG, EGG etc.). The simulator circuit developed here provides an impedance variation equivalent to thoracic impedance and can be used to test and calibrate an ICG instrument. As described in Chapter 2, the thoracic impedance can be modelled as a basal impedance in parallel with a time-varying impedance. The thoracic impedance model is assumed to be purely resistive for the excitation frequency of 20 – 100 kHz as used in ICG instruments.

Several bioimpedance simulator circuits were developed earlier at IIT Bombay. Manigandan [39] developed a simulator using astable multivibrator, analog switches, resistors and potentiometer. The impedance variation was generated in the form of square wave superimposed on a desired basal value. The basal resistance was selected by the manually controlled switches while the time-varying resistance was realized by analog switch controlled by astable multivibrator. The hardware was redesigned by Naidu [40] using a microcontroller to reduce the wiring associated with manually controlled switches and also to generate the variable frequency square wave. Venkatachalam [41] used digital potentiometer instead of analog switches to obtain step variation in the resistance. Patil [42] extended the frequency range of the simulator for making it useful in bioimpedance measuring techniques, e.g., electro-glottography (EGG). The simulator was redesigned by Desai [44] using a digital potentiometer and analog switches which were controlled digitally from the microcontroller and the impedance variation was generated in the form of square wave. But all these simulators provide resistance variation in discrete steps. Therefore, the simulator may not be useful for testing the ICG and several other bioimpedance measuring instruments because of the presence of the differentiator circuit used for signal conditioning. Therefore, Holani redesigned the hardware which had four circuit blocks: resistance variation circuit, controller circuit, serial interface, and power supply [43]. A matched JFET pair based VCR circuit was used to provide continuous impedance variation. The circuit had a serial interface from PC to microcontroller for setting the parameters for basal impedance and control waveforms used to drive the VCR circuit. The VCR is able to provide time-varying resistance in accordance with a control waveform (sine, square, triangular or thoracic impedance), superimposed on a digitally controlled basal

resistance. But the controller circuit did not provide real-time control on the parameters used in the resistance variation circuit.

An impedance simulator was developed by Pandey et al. [13] using a switch-resistor network to generate a time-varying square wave impedance waveform with digitally controlled configuration using microcontroller. A block of digitally controlled analog switches with resistors in series and such three blocks connected in parallel configuration were used to provide basal resistance along with time-varying impedance. A particular block of resistances was realized for basal impedances and the other block to provide variation. The generated impedance variation waveform was in the form of a square wave with selectable range of frequencies. The variation was achieved by using the parallel combination of analog switches with resistances connected in series and the switching action provided the impedance variation depending on the on-resistance of the switches activated at a time. Another simulator using a similar approach and staircase variation using a network of low on-resistance analog switches and precision resistors has been reported by Ulbrich et al. [14] for testing and calibration of ICG instruments with textile electrodes.

After studying all these previous simulators, the bioimpedance simulator is developed with the following considerations:

(i) Realization of the floating precision linear VCR circuit using both matched pair JFET as well as MOSFET devices for the time-varying resistance. The matched MOSFET pair based VCR circuit may have potential for IC fabrication.

(ii) Development of a PC-based GUI for real-time control of parameters for resistance variation circuit over a Bluetooth based wireless link.

(iii) Power supply with a chargeable battery for making the simulator circuit battery operated and electrically isolated from PC.

(iv) In all the simulator circuits, the capacitive component of the time varying bioimpedance is ignored. A voltage controlled capacitor circuit can be added along with the VCR circuit for providing the time-varying capacitive component as well.

5.2 The Thoracic Impedance Model

For ICG, the thoracic impedance can be modeled as a fixed resistance R_O connected in parallel with a variable resistance R_V . The thoracic impedance model with an impedance sensor and bipolar electrode configuration for impedance measurement is shown in Figure 5.1(a) [15]. The resistance R_O refers to the basal resistance offered by bones, tissues and fluids located between the measuring points and remains constant. The time-varying resistance R_V indicates the respiratory and cardiac activities. The resistances R_{E1} and R_{E2} represent the

(a) Bipolar electrode configuration

(b) Tetra-polar electrode configuration

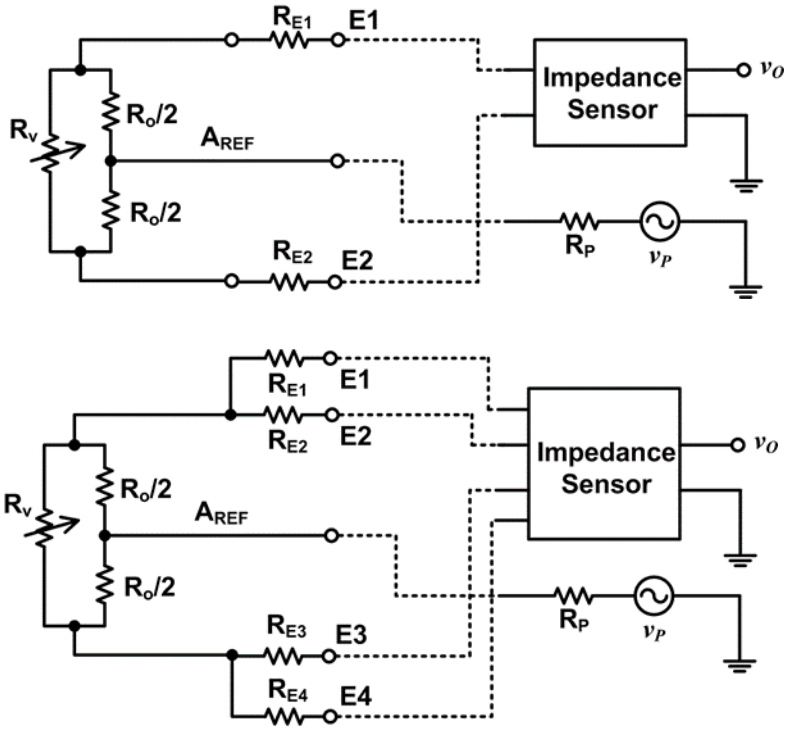

Figure 5.1: Thoracic impedance model [15].

electrode-tissue contact impedances. Therefore, the equivalent resistance across the measuring points E1 and E2 can be given as:

$$R_{E1E2} = R_O \| R_V + R_{E1} + R_{E2} \tag{5.1}$$

In an actual measurement of bioimpedance, the sensed voltage across R_{E1E2} contains both voltage developed by the excitation current and voltages due to various internal bio-signals and external pickups. These interferences can be modeled as a common mode voltage as represented by the voltage v_P in series with resistance R_P between the ground of the impedance sensor and a common mode point A_{REF} (center point of the resistance R_O). It can be used for testing the effect of the common mode interference on the bioimpedance.

The same model using tetra-polar electrode configuration is given in Figure 5.1(b). This configuration is used to reduce the effect of electrode-tissue contact impedances during measurement.

5.3 Realization of the Bioimpedance Simulator

The bioimpedance simulator consists of four blocks: the resistance variation circuit, the controller circuit, Bluetooth module connected to the controller using serial interface, and the power supply module. A PC based GUI is developed for wireless interfacing with the bioimpedance simulator for real-time control of simulation parameters, as shown in Figure 5.2. The resistance variation circuit has a digitally controlled switch-resistor network realizing the

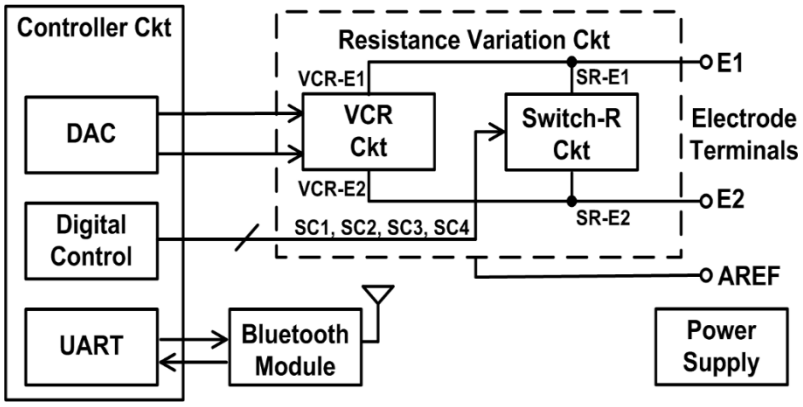

Figure 5.2: Block diagram of bioimpedance simulator.

basal resistance R_O and a voltage-controlled resistor (VCR) circuit realizing the time-varying resistance R_V. The controller circuit is capable of generating various control waveforms (sinusoidal, square, triangular, or a thoracic impedance waveform) for the VCR circuit along with controls for the switch-resistor network. An electrically isolated serial interface using Bluetooth module is used for real-time control of the simulation parameters from PC-based GUI. The power supply circuit uses a rechargeable battery to provide ± 5 V and two 3.3 V supplies. Each of these blocks is described in the following subsections.

5.3.1 Impedance variation circuit

The impedance variation circuit is implemented with a digitally controlled switch-resistor network realizing the basal resistance connected in parallel with the VCR circuit realizing the time-varying component. The switch-resistor network, as shown in Figure 5.3, a quad analog switch IC ADG811 (Analog Devices) [45] as U13 and fixed-value resistors R11, R12, R13, and R14. The analog switch IC is operated at 3.3 V supply with decoupling capacitor C23 and the control voltage levels compatible with the 3.3 V logic levels of a microcontroller. The analog switches are operated with logic zero input. Four fixed-valued resistors are used for setting the basal resistance. The resistors values have the following values:

R_{11} = 10 Ω, R_{12} = 20 Ω (two 10 Ω in series),

R_{13} = 50 Ω (two 100 Ω in parallel), R_{14} = 100 Ω

The total resistance R_{SW} across the terminals X and Y is given as:

$$R_{SW} = S_1 R_{11} + S_2 R_{12} + S_3 R_{13} + S_4 R_{14} \tag{5.2}$$

where the switch status (S_1, S_2, S_3, S_4) is 0 if the corresponding switch is closed and 1 if it is open. The switch combination is controlled by the controller circuit using the general purpose IO pins of the microcontroller. The four switches S1 – S4 are used to set 16 different basal resistance values with nominal values ranging from 0 to 180 Ω, as shown in Table 5.1. The

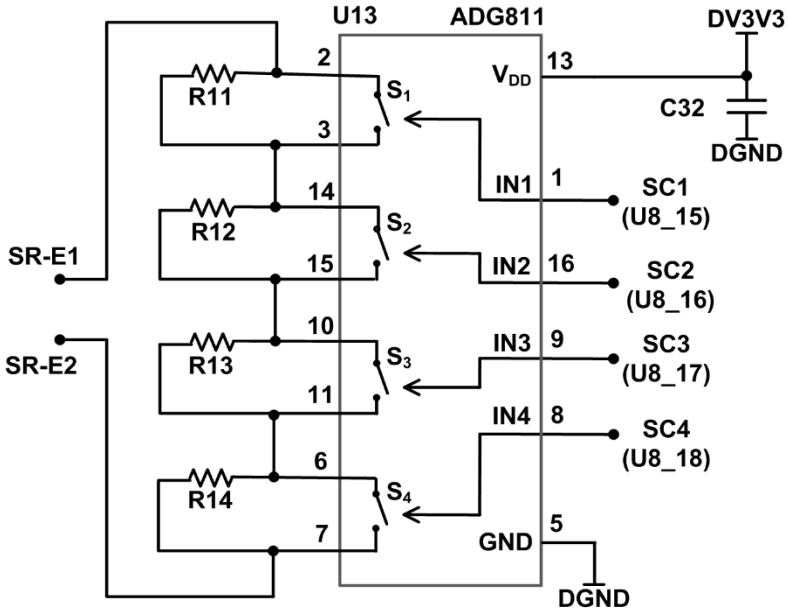

R_{11} = 10 Ω, R_{12} = 20 Ω, R_{13} = 50 Ω, R_{14} = 100 Ω, and C_{32} = 0.1 µF.

Figure 5.3: Switch-Resistor circuit.

Table 5.1: Nominal values of R_{SW} for different switch combination.

Switch control				Resistance R_{SW} (Ω)	Switch on-resistance error(Ω)
S1	S2	S3	S4		
0	0	0	0	0	2.0
1	0	0	0	10	1.5
0	1	0	0	20	1.5
1	1	0	0	30	1.0
0	0	1	0	50	1.5
1	0	1	0	60	1.0
0	1	1	0	70	1.0
1	1	1	0	80	0.5
0	0	0	1	100	1.5
1	0	0	1	110	1.0
0	1	0	1	120	1.0
1	1	0	1	130	0.5
0	0	1	1	150	1.0
1	0	1	1	160	0.5
0	1	1	1	170	0.5
1	1	1	1	180	0.0

switches have on-resistance of less than 0.5 Ω. The off resistance are very large compared to the resistance values. Hence the errors in R_{SW} values are contributed by the on-resistance of the switches as listed in the table.

The schematic of the floating precision linear VCR circuit, as shown in Figure 5.4, is implemented using a matched-pair JFET package U441 (Vishay Siliconix) [25] as U11 and op amp IC LT1499 (Linear Technology) [46] as U10. LT1499 is a quad op amp IC with rail-to-

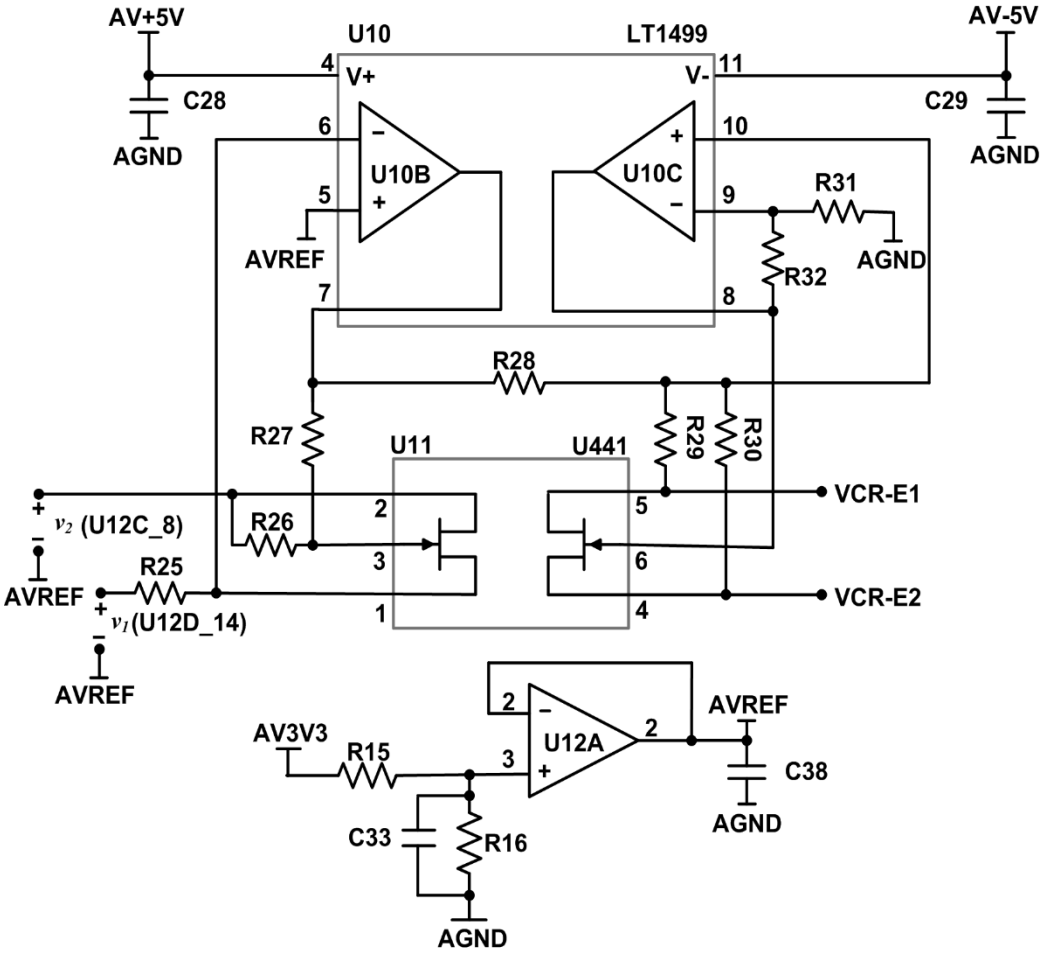

$R_{15} = R_{16} = 100$ kΩ, $R_{25} = 1$ kΩ, $R_{26} = R_{27} = 1$ MΩ, $R_{28} = R_{29} = R_{30} = R_{31} = 10$ kΩ, $R_{32} = 5$ kΩ, and $C_{28} = C_{29} = C_{33} = C_{38} = 0.1$ μF.

Figure 5.4: VCR circuit implemented using U441[27] and LT1499 [46].

rail input and output, operates with supply of ±2.2 V to ±15 V and has typical current consumption of 6.8 mA [46]. In this application, it is powered with ±5 V with decoupling capacitors C28 and C29, each of 0.1 μF, and used for generating the gate voltages for the matched JFET pair. The voltages v_1 and v_2, generated from the controller circuit, are used to control the resistance across the terminals VCR-E1 and VCR-E2. The values of capacitors and resistors used in the circuit are:

$$C_{38} = 0.1\,\mu\text{F},\ R_{26} = R_{27} = 1\ \text{M}\Omega,\ R_{28} = R_{29} = R_{30} = R_{31} = 10\ \text{k}\Omega$$

$$R_{32} = 5\ \text{k}\Omega,\ R_{15} = R_{16} = 100\ \text{k}\Omega.$$

The terminals SR-E1 and SR-E2 of the switch-resistor circuit of Figure 5.3 and the terminals VCR-E1 and VCR-E2 of the VCR circuit of Figure 5.4 are connected in parallel and form the terminals E1 and E2 as shown in Figure 5.2. Therefore, the terminal voltages at E1 and E2 must be within the limits for linear operation of the two circuits. For the VCR circuit,

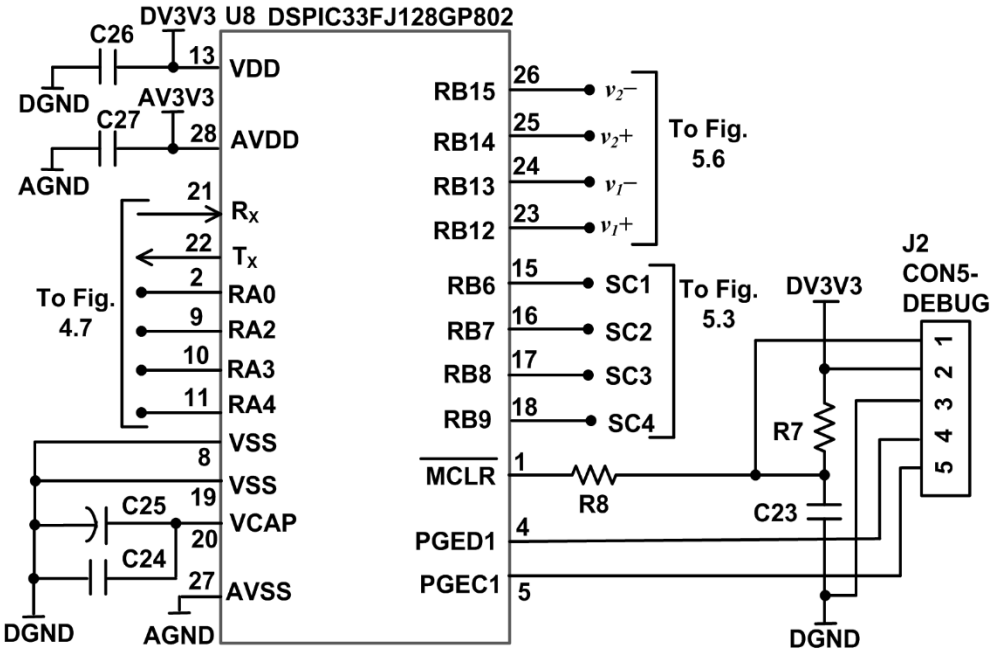

R_7 = 10 kΩ, R_8 = 100 Ω,
$C_{23} = C_{24} = C_{26} = C_{27}$ = 0.1 µF, and C_{25} = 10 µF.

Figure 5.5: Controller.

the limit for linear operation is ±1 V with respect to the analog reference voltage AVREF. For the switch-resistor circuit, this limit is the supply voltage of U13 i.e. from 0 to 3.3 V with respect to DGND. The op amp bias voltages marked as AV+5V and AV−5V are at +5 V and −5 V with respect to AGND. The AGND and DGND tracks are shorted at the power supply ground GND. The value of AVREF is set at half of 3.3 V, i.e. at 1.65 V with respect to AGND. It is generated using R15, R16, bypass capacitor C33, and buffered using U12A and load capacitance C38, as shown in Figure 5.4. The terminals E1 and E2 have a net linear range of ±1 V with reference to AVREF. As the op amps have rail-to-rail input and output voltages, the range for control voltages is [−5 V, +5V] with respect to AGND and [−6.65 V, +3.35 V] with respect to AVREF, thus providing a compatible range for the requirement of negative gate voltages for the JFETs.

5.3.2 Controller

The controller circuit is designed using the microcontroller DSPIC33FJ128GP802 (Microchip) [46] with on-chip DAC as U8 for generating the analog control waveforms for VCR, digital control signals for the switch-resistor network, serial communication over a Bluetooth module for selecting the simulation parameters, as shown in Figure 5.5. DSPIC33FJ128GP802 is a 16-bit microcontroller, with supply voltage of 3 − 3.6 V, with two

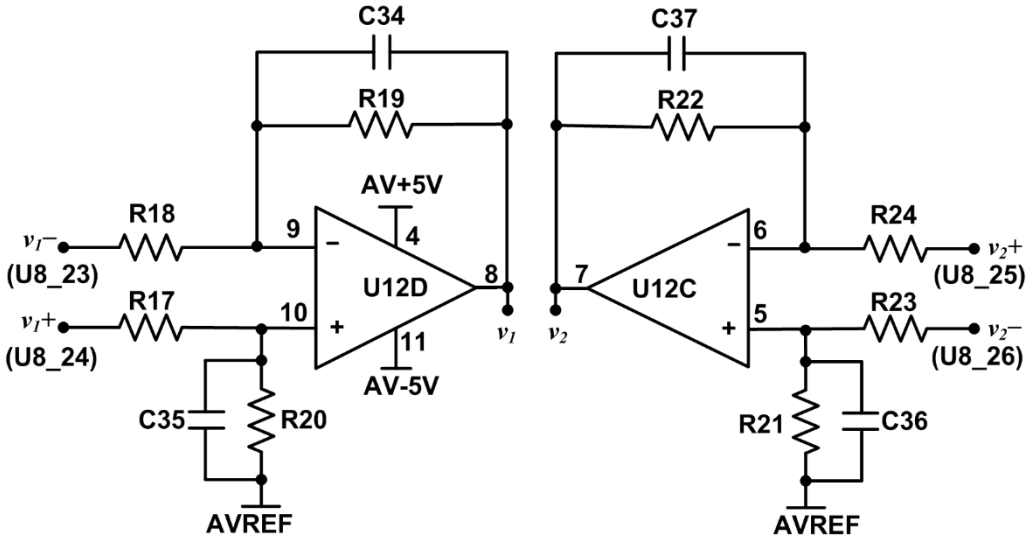

$$R_{19} / R_{18} = R_{20} / R_{17} = \alpha_1, \qquad R_{22} / R_{24} = R_{21} / R_{23} = \alpha_2$$
$$R_{19} C_{34} = R_{20} C_{35} = 1/ (2\pi f_c), \qquad R_{21} C_{36} = R_{22} C_{37} = 1/ (2\pi f_c)$$

$R_{17} = R_{18} = R_{23} = R_{24} = 5$ kΩ, $R_{19} = R_{20} = R_{21} = R_{22} = 10$ kΩ,
and $C_{34} = C_{35} = C_{36} = C_{37} = 12$ nF.

Figure 5.6: Differential amplifiers for generating v_1 and v_2 from the two DAC channels of the microcontroller U8.

UART ports, and an on-chip DAC. In our circuit, it is operated at 3.3 V and its internal RC oscillator with PLL is used for generating clock, so that external oscillator is not needed. The Master Clear pin (MCLR) is used to reset the microcontroller and for programming or debugging. A logic 0 can be applied to this pin to reset the device. Combination of R7 and C23 provides logic 1 for normal operation. The value of R7 is kept large to reduce the current for reset control. The resistor R8 limits the current drawn from C23 to avoid MCLR pin break down. Programming and debugging is done through the connector J2 using the PIC microcontroller programming kit. The first pin of J2 is connected to the MCLR pin and applies reset control (by providing logic 0) followed by logic transitions during programming and debugging. The capacitors C24 and C25 are used at the VCAP pin of the microcontroller to stabilize the regulator present inside the microcontroller. Therefore, these capacitors are often referred as CPU logic filter capacitors. The values of C24 and C25 are 0.1 µF and 10 µF, respectively, as given in the datasheet [47].

The microcontroller U8 has an on-chip DAC with two output channels, each with a differential output, with the range of [1.09 V, 2.36 V]. A differential amplifier is used to get a single ended output with respect to AVREF for providing the analog control voltages for VCR circuit. The op amp IC LT1499 (Linear Technology) as U12 is used to implement these two

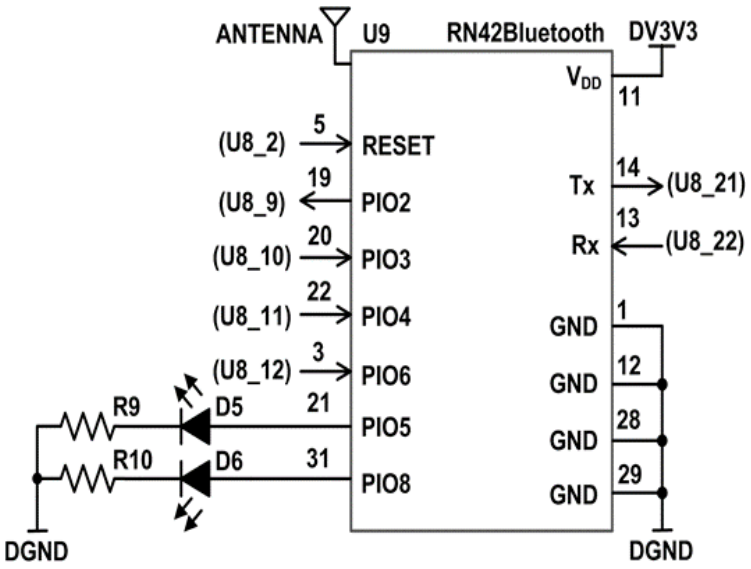

$R_9 = R_{10} = 1\ \text{k}\Omega$.

Figure 5.7: Connections of Bluetooth module.

differential amplifiers for the DAC channels, as shown in Figure 5.6. The differential amplifier outputs are given as

$$v_1 = v_{AVREF} + \alpha_1(v_{1+} - v_{1-}) \tag{5.3}$$

$$v_2 = v_{AVREF} + \alpha_2(v_{2-} - v_{2+}) \tag{5.4}$$

The resistor values, for providing differential gain of $\alpha_1 = \alpha_2 = 2$ for v_1 and v_2, respectively, are selected as

$$R_{19} = R_{20} = R_{21} = R_{22} = 10\ \text{k}\Omega,\ R_{17} = R_{18} = R_{23} = R_{24} = 5\ \text{k}\Omega$$

If the sampling rate for a signal is f_s, the DAC channels of U8 use interpolation for sampling the output signal at an internal sampling rate of 256 f_s. Therefore, a single-order low-pass filter with cutoff f_c one-tenth of the sampling rate i.e. 25.6 f_s is adequate as a smoothening filter for DAC outputs. In our simulator circuit, v_1 and v_2 are generated with sampling frequencies of 64 Hz, 640 Hz, or 6.4 kHz. The capacitorsC34, C35, C36, and C37 are selected as 12 nF for $f_s \approx 1.32$ kHz.

5.3.3 Serial interface

A Bluetooth module RN42 (Microchip) [48] with integrated antenna, as U9, is used to provide wireless serial interface for setting the simulation parameters for the controller circuit as shown in Figure 5.5. The port pin RB.10 of the microcontroller U8 is configured as receiver pin to UART module and the pin RB.11 is configured as transmit pin from UART. The connections for the Bluetooth module is shown in Figure 5.7. The Bluetooth module U9 is

Table 5.2: Estimated current requirement for each IC used in the bioimpedance simulator circuit.

Supply voltage	Component	Current requirement (mA)
DV3V3	U8: DSPIC33FJ128GP802	25.0
	U9: RN42 Bluetooth	50.0
	U13: ADG811	0.016
	Total	75.016
AV3V3	U8: DSPIC33FJ128GP802	9.0
AV+5	U10: LT1499	6.8
	U12: LT1499	6.8
	Total	13.6
AV−5	U10: LT1499	6.8
	U12: LT1499	6.8
	Total	13.6

operated with supply of 3.3 V. It is used through ASCII commands via UART or PIO signals from the microcontroller. It can provide data transfer rate up to 3 Mbps with transmitting or receiving range up to 10 meters. It has an internal UART which is interfaced with the UART module of the microcontroller as shown in Figure 5.7. It also has status pins (PIO2, PIO5, and PIO8) with or without LEDs for indicating the connection status of the device and control pins (RESET, PIO3, PIO4, and PIO6) either for setting the device to a specific discovery mode or to initiate reset command. The resistors R9 and R10 are used to limit the current through the LEDs. The default baud rate of the device over UART is 115.2 kbps. The microcontroller is also set to the same baud rate for handling the serial communication with the Bluetooth module. Details about these configurations are described in section 5.4.

5.3.4 Power

The simulator circuit blocks need ±5 V and 3.3 V supplies. Three supplies of 3.3 V, 5 V, and −5 V needed for the analog operation are labeled as AV3V3, AV+5, and AV−5, respectively. The supply of 3.3 V needed for the digital operations is labeled as DV3V3. The digital part of the microcontroller U8, the Bluetooth module U9, and the analog switch IC U13 are powered with DV3V3. The op amp ICs U10 and U12 are powered with AV+5 and AV−5. The analog part of the microcontroller U8 is powered with AV3V3. The current requirements for the individual chips are given in Table 5.2. The power supply circuit is designed to be operated with a rechargeable battery with nominal output voltage of 3.3 V to 4.7 V as input supply. A battery charging unit consisting of MCP73833 stand-alone linear Li-ion / Li-polymer

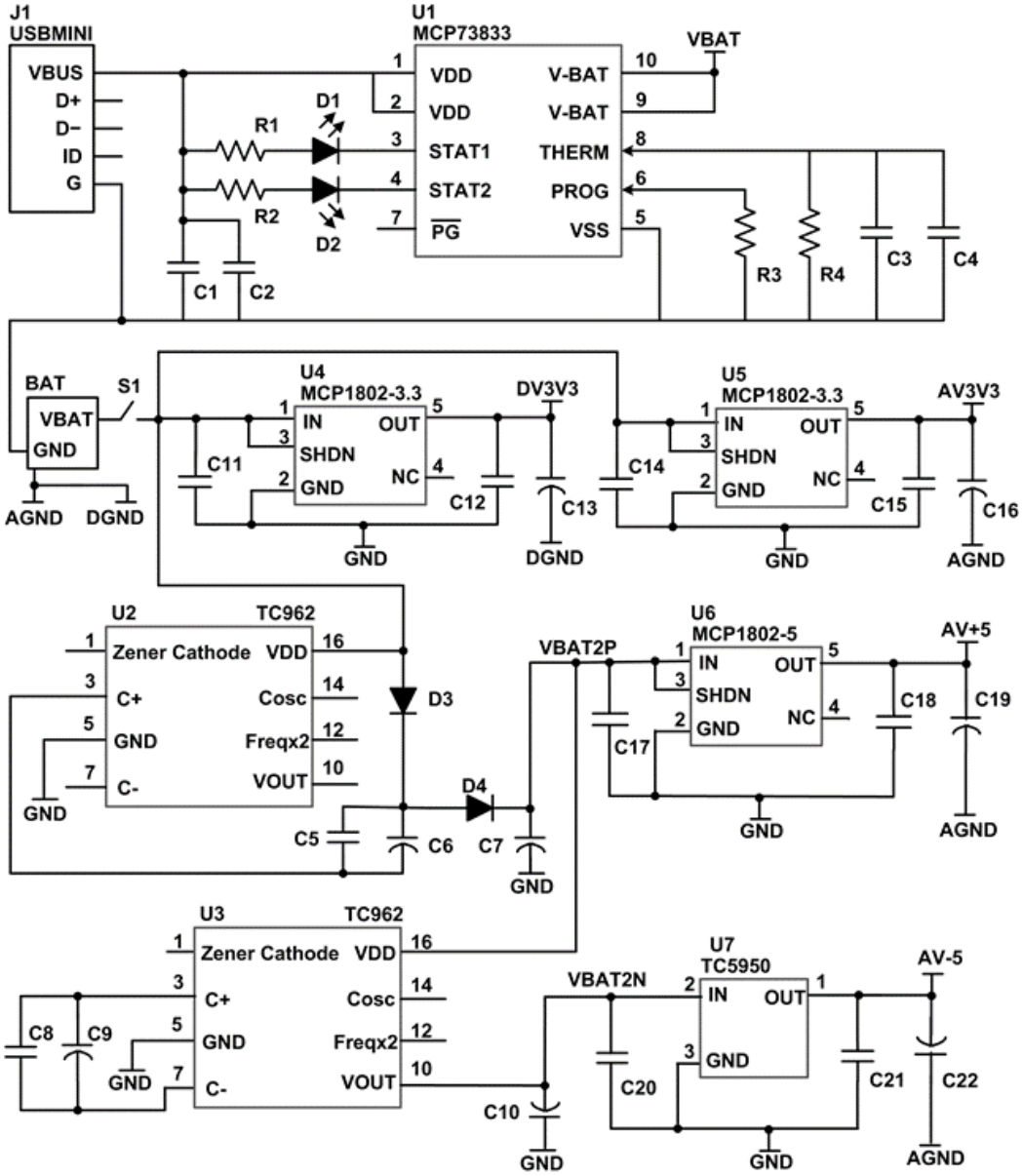

$R_1 = R_2 = 1$ kΩ, $R_3 = 1.8$ kΩ, $R_4 = 10$ kΩ,
$C_1 = C_3 = C_5 = C_8 = C_{11} = C_{12} = C_{14} = C_{15} = C_{17} = C_{18} = C_{20} = C_{21} = 0.1$ µF,
$C_2 = C_4 = 1$ µF, and $C_6 = C_7 = C_9 = C_{10} = C_{13} = C_{16} = C_{19} = C_{22} = 10$ µF.

Figure 5.8: Power supply circuit.

charge management controller IC (Microchip) [49] is used to charge the rechargeable battery from a maximum of 6 V dc input.

The power supply circuit with the battery charging unit is shown in Figure 5.8. It is designed, using charge-pump based dc-dc converters and low-dropout linear regulators, to generate output voltages of ±5 V as AV+5 and AV−5 and two 3.3 V as DV3V3 and AV3V3 from a single Li-ion battery. The analog and digital grounds, labeled as AGND and DGND

respectively, are shorted at a stable point near the negative terminal of the input supply labeled as GND. The Li-ion charge management controller is connected before the battery input terminals to provide adequate connectivity for charging from an external dc power supply.

The Li-ion battery charge management controller IC MCP73833 as U1 is configured to charge the battery used in the bioimpedance simulator circuit. The maximum input of the charger IC is 6 V dc with a programmable charging current up to 1 A. Two LEDs, D1 and D2, are used as charging status indicators (charging/ charged). Resistances R1 and R2 are used to limit the current through the LEDs. A Li-ion battery with nominal voltage of 3.7 V with current drawing capacity of 1000 mA per hour is used in the simulator circuit for testing.

The two 3.3 V supplies, DV3V3 and AV3V3, are obtained using two low-dropout linear regulator ICs MCP1802-3.3 (Microchip) [50] as U4 and U5, respectively. The input voltage range of the ICs is from 3.6 to 16.0 V with a quiescent current of 68 μA. Charge pump based dc-dc converters followed by linear regulators are used to generate ±5 V for the op amp. The charge pump based converter IC TC962 (Microchip) [51] has input voltage range of 3 – 18 V and typical quiescent current of 510 μA. It can be configured as a voltage doubler or inverter as shown in Figure 5.8. One TC962 as U2 is configured as a voltage doubler with a nominal output of $2V_{in}-2V_D$, labeled as VBAT2P. Another TC962 as U3 is used as a voltage inverter with the nominal output of $-(2V_{in}-2V_D)$, labeled as VBAT2N. The supply AV+5 is generated by applying VBAT2P as input to a positive low-dropout linear regulator IC MCP1802-5 (Microchip) [50] as U6. The input voltage range for this IC is 3 – 18 V with quiescent current of 68 μA. The supply AV−5 is generated by applying VBAT2N as input to a negative low-dropout linear regulator IC TC5950 (Microchip) [52] as U7. Input voltage range for this IC is −5.6 V to −10 V with quiescent current of 3.5 μA. The resistors and decoupling capacitor values used in this circuit are as the following:

$$R_1 = R_2 = 1\ \text{k}\Omega,\ R_3 = 1.8\ \text{k}\Omega,\ R_4 = 10\ \text{k}\Omega,$$

$$C_1 = C_3 = C_5 = C_8 = C_{11} = C_{12} = C_{14} = C_{15} = C_{17} = C_{18} = C_{20} = C_{21} = 0.1\,\mu\text{F},$$

$$C_2 = C_4 = 1\,\mu\text{F}, \text{ and } C_6 = C_7 = C_9 = C_{10} = C_{13} = C_{16} = C_{19} = C_{22} = 10\,\mu\text{F}$$

5.4 Microcontroller Program

The microcontroller is used for generating control parameters for the impedance variation circuit. One part of the impedance variation has the switch-resistor network comprising fixed valued resistors and a quad analog switch IC ADG811 [45] as U13 realizing the basal resistance for a range from 0 Ω to 180 Ω. These values are achieved by the combination of resistances and the four analog switches either by activating or deactivating them, by writing to the four IO pins of the DSPIC33FJ128GP802. The other part of the impedance variation circuit is the matched JFET pair based floating VCR circuit which needs

Table 5.3: Simulation parameters for the bioimpedance simulator.

Sl No.	Parameter	ASCII Commands	Parameter values
1	Basal resistance (Ω)	16 different characters	0, 10, 20, 30, 50, 60, 70, 80, 100, 110, 120, 130, 150, 160, 170, 180
2	Frequency Range	3 different characters	0.1 – 1 Hz, 1 – 10 Hz, 10 – 100 Hz
3	Frequency (Hz)	16 different characters	0.1, 0.2, 0.4, 0.5, 0.8, 1, 2, 4, 5, 8, 10, 20, 40, 50, 80, 100
4	V1-waveshape	4 different characters	sine, square, triangular, sawtooth
5	V1-offset (mV), ref.: AREF	11 different characters	1000, 800, 600, 400, 200, 0, −200, −400, −600, −800, −1000
6	V1-amplitude (mV)	11 different characters	0, 100, 200, 300, 400, 500, 600, 700, 800, 900, 1000
7	V2-waveshape	4 different characters	sine, square, triangular, sawtooth
8	V2-offset (mV), ref.: AREF	11 different characters	0, 100, 200, 300, 400, 500, 600, 700, 800, 900, 1000
9	V2-amplitude (mV)	11 different characters	1000, 800, 600, 400, 200, 0, −200, −400, −600, −800, −1000

analog waveforms as control. The analog waveforms are generated by outputting pre-stored digitized samples of the waveform through the two DAC channels as described in Subsection 5.3.2. A periodic waveform is generated by storing the digitized samples of one period and outputting the samples using a loop. If the waveform to be generated has N_p samples in a period and sampling frequency is f_s, the output frequency of the resulting waveform is $f_c = f_s / N_p$.The DAC of the microcontroller uses internal interpolation at a rate of $256\, f_s$. The amplitude, frequency and offset of the generated waveforms are also need to be controlled digitally in real time. The simulation parameters to be controlled by the controller is presented in Table 5.3 along with their range.

Assuming the output waveform has spectral component up to frequency f_m, a first order low-pass filter with cutoff frequency f_c in the range of $f_m < f_c < 256\, f_s - f_m$ will be adequate enough for smoothening the output waveform as well as for preserving the spectral component of the generated waveform. Since $256\, f_s >> f_m$, f_c can be chosen as $10\, f_m < f_s < 25.6\, f_s$ i.e. the condition for f_c can be given as $f_m < f_c / 10$ and

$f_s > \max\ (2\,f_m\,,\, f_c/25.6)$. In the simulator circuit, $f_c \approx 1.32$ kHz and therefore $f_m < 132$ Hz and $f_s > \max\ (2\,f_m\,,\, 52\text{ Hz})$.

Waveforms of different frequencies can be generated by setting the sampling frequency f_s at fixed value and selecting the number of samples N_p for a given frequency as given by the relation $f_o = f_s / N_P$. The sampling frequency f_s can be set by modifying the content of the 'Auxiliary Control Register (ACLKCON)' and 'DAC1 Control Register (DAC1CON)' of the controller associated with the system clock [47]. Using these registers, three sampling frequencies f_s of 64 Hz, 640 Hz, and 6.4 kHz were generated in order to achieve output frequency range of 0.1 Hz to 100 Hz which is discussed below. Modification in N_p can be done in two ways, either we can take samples for highest frequency which will have minimum number of samples or for lowest frequency which will have maximum number of samples. For the first case, to generate lower frequency waveform we need to generate intermediate samples using interpolation for increasing the total number of samples N_p. While for the second case, we shall drop some samples to reduce the total number of N_p using decimation. Here, the decimation method is used for outputting the analog waveforms from the DAC channels.

With N_p = 640 for sine, square, triangular, and sawtooth waveforms and sampling frequency f_s of 64 Hz, 640 Hz, and 6.4 kHz, we have generated waveforms with output frequency f_o from 0.1 Hz to 100 Hz for each type of waveform. The on-chip DAC module, with 4-sample FIFO buffer for each channel and a default buffer, outputs the samples from the corresponding FIFO buffers to the two DAC channels at the fixed sampling frequency. If the FIFO buffers get empty, the value stored in the default buffer is fed to the output of both the channels and this will cause a distortion in the output waveform.

To carry out the required operations discussed above, a program for the PIC microcontroller 'bioimpedance_simulator_control' is written in embedded C using 'Microchip MPLAB X IDE®'. The program has a main function and three interrupt service routines (ISR): 'U1RXInterrupt' ISR for receiving the simulation parameters using the UART interrupt, 'DAC1LInterrupt' ISR for controlling the left DAC channel interrupt, and 'DAC1RInterrupt' ISR for the right DAC channel interrupt. The main program has an initialization part for the clock, UART, and DAC module and an infinite loop for continuously outputting the waveform samples from both DAC channels. The control is sent through ASCII commands a PC-based GUI which are received by the microcontroller over its UART through the Bluetooth based wireless connection. A set of ASCII commands are programmed for controlling the switch-resistor network. On receiving these commands, U1RXInterrupt ISR is involved by the UART interrupt to set the basal resistance in real time. Another set of ASCII commands are used to

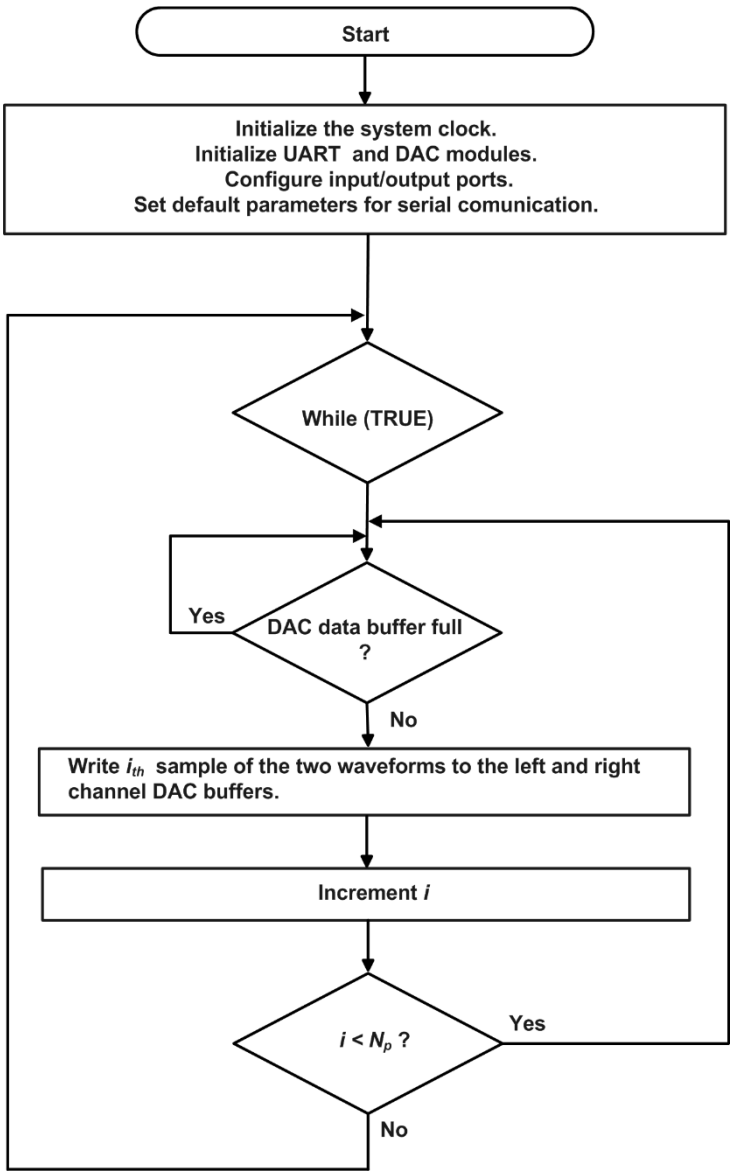

Figure 5.9: Flow chart of the main program of "bioimpedance_simulator_control".

control the waveform parameters (type of waveform, amplitude, frequency, and offset) in real time. In this case, the 'U1RXInterrupt ISR' is invoked by UART interrupt which in turn invokes the DAC interrupt ISRs for modifying the waveforms in real time.

Figure 5.9 represents a flowchart for the main function. It sets the system clock first with internal default oscillator as the clock source configured at f_{clk} of 37 MHz. It initializes the UART module, DAC module, and input/output ports by configuring the appropriate TRIS and PORT registers. An infinite while loop is used for continuously generating the analog waveforms from the DAC channels. While outputting the samples for a period, the DAC buffers are checked each time whether they are full or empty and the samples are sent to the DAC channels from the buffers. The number of samples are counted using a variable 'i' until the

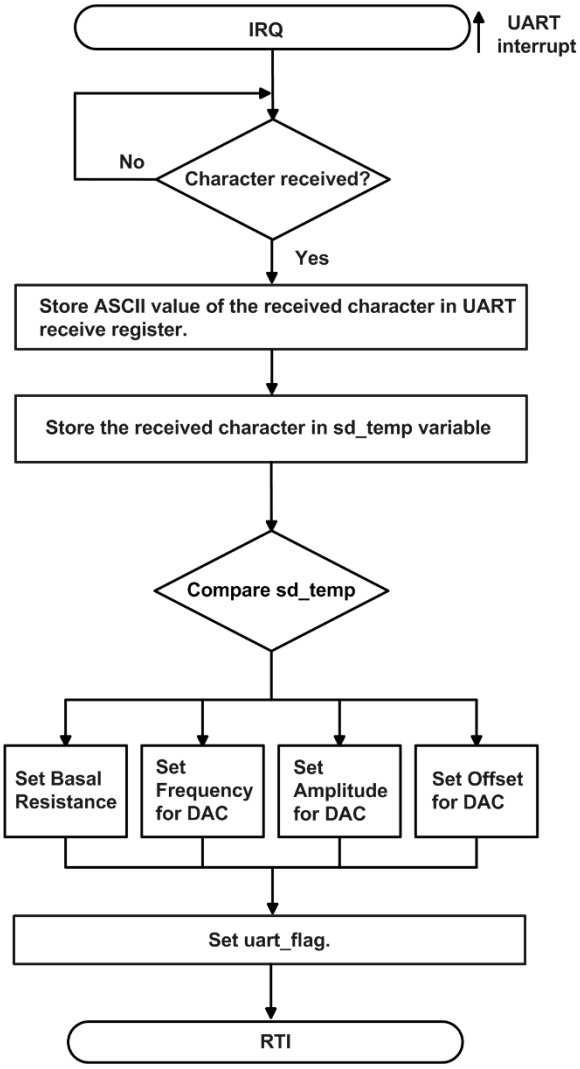

Figure 5.10: Flow chart for U1RXInterrupt ISR of bioimpedance_simulator_control.

samples for one period is transmitted. The operation of the main program is modified in real time when a simulation parameter is sent from the GUI either to set the basal resistance or to modify the parameters of the generated waveforms. When a command is sent for selecting the basal resistance, writing of the waveform samples to the DAC buffers is not affected. When a command is sent to change frequency range or the shape of the waveform, writing of the waveforms samples to the DAC buffers gets suspended for a short time as the contents of the ACLKCON and DAC1CON registers and the waveform sample values are reinitialized. When a command is sent to change the amplitude, frequency in the currently specified range, or offset, the waveform changes in real time as those parameters are directly used in outputting the waveform samples to the DAC buffers.

Figure 5.10 represents a flowchart for the 'U1RXInterrupt' ISR. When the UART receiver receives a character, the 'U1RXInterrupt' ISR is called else it will wait until a character is received by the UART receiver. As soon as the character is received, it is stored in the UART

receiver register. Then the received character is passed to a local variable named ‘sd_temp’ which is compared with various conditions written in the microcontroller program to generate a command only for a single simulation parameter. The parameter may be used for setting the basal resistance or for setting the analog waveform type to be generated as output from the DAC channels or to set the amplitude, frequency, and offset of the generated output. Then the ‘uart_flag’ is set to end the ‘U1RXInterrupt’ ISR and to get ready for receiving the next parameter.

5.5 PC-based GUI for Real-Time Parameter Setting

A PC-based GUI named ‘bioimpedance_simulator_gui’ has been developed in QT framework for setting the simulation parameters such as basal resistance, frequency, waveshape, offset, and amplitude for the two control waveforms of the bioimpedance simulator circuit. The program communicates with the Bluetooth module interfaced with the microcontroller used in the simulator circuit over a serial COM port. The program is initiated by running its executable file and GUI appears on the screen. Bluetooth module needs to be paired with PC before the serial communication is initiated. After pairing, a COM port is given to the paired Bluetooth device, which is identified by the Bluetooth device settings option. Serial communication is established over the assigned COM port and serial data transfer takes place at a rate of 115200 kbps. The GUI window has a drop-down list of available COM ports among which the assigned one needs to be chosen. By clicking on the ‘Connect’ button, connection is established between the simulator and the PC. Four drop-down lists with labels of ‘Basal Resistance’, ‘Frequency Range’, and ‘Waveform Type’ (2 labels) are used for selecting the parameters of basal resistance, frequency range, and shape of waveforms, respectively. Six slider controls (three for each DAC channel) with labels of ‘Amp’, ‘Freq’, and ‘Offset’ are used to control the parameters for each DAC channel separately. The screen of the GUI is shown in Figure 5.11 (a). Values can be chosen for simulation for the basal resistance, frequency range, and the shape of the waveform by selecting any value from the drop-down lists specified for them. The amplitude, frequency, and offset for the control signals can be controlled by dragging the slider control bar up and down specified for these operations. Figure 5.11 (b) shows a screen of the GUI with some selected simulation parameters as described above. Each time the value is changed in the drop-down lists or in slider controls, an ASCII command is sent from PC over the Bluetooth link to the simulator. The ASCII command is received through the UART interrupt of the microcontroller and used for parameter control depending on the program written inside the microcontroller. The ‘Disconnect’ and ‘Connect’ buttons can be used to terminate and reconnect the wireless link over Bluetooth if in case the connection gets lost accidently. The ‘Close’ button closes the GUI window and also terminates the wireless link.

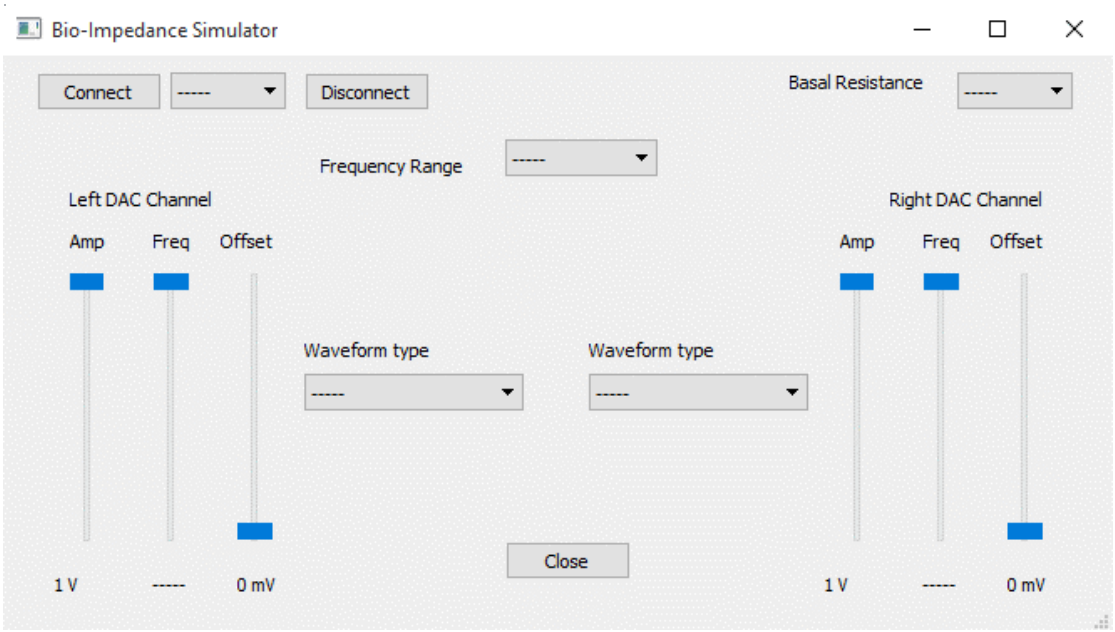

(a)

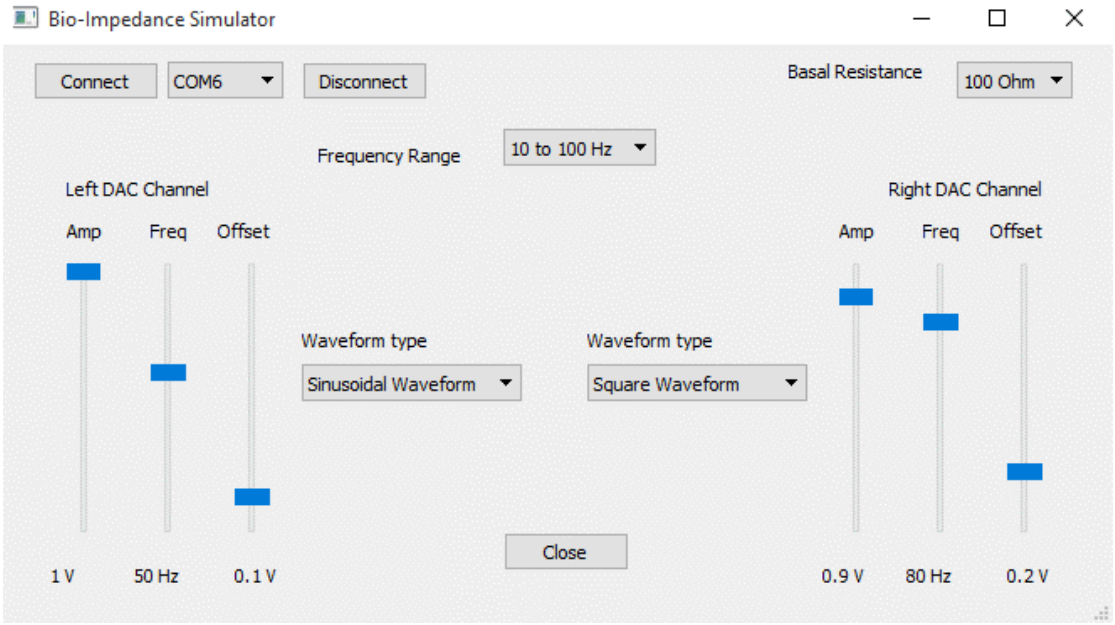

(b)

Figure 5.11: PC based GUI program "Bio-impedance Simulator": (a) Initial appearance of bioimpedance simulator, (b) GUI connected to the Bluetooth module through COM Port 6, and different parameter values are set for basal resistance, left DAC channel and right DAC channel.

Chapter 6
TEST RESULTS

6.1 Introduction

The bioimpedance simulator is designed to provide a time-varying resistance superimposed on a basal resistance. The range of resistance variation is small. The simulator circuit has four blocks: the resistance variation circuit, the controller circuit, the battery powered power supply circuit, and Bluetooth module for wireless control of simulation parameters. It is implemented on a PCB board and tested accordingly. The testing of the bioimepdance simulator was done in four stages. The power supply module was tested in the first stage. The second stage involved the interfacing of the microcontroller with the PC based GUI over a Bluetooth link. The third stage involved testing of the DAC channel outputs. The fourth stage involved testing of the impedance variation circuit which consists of a switch-resistor network for providing basal resistance and the matched JFET pair based VCR circuit providing the time-varying component.

6.2 Validation of the Power Supply Circuit

The power supply circuit (Figure 5.8) was designed to generate ±5 V and two 3.3 V supplies for the simulator circuit. A battery charging unit with a battery charging driver using U1 (MCP73833) was also implemented to make this circuit operated by chargeable battery. The battery charging unit was tested with supplying 5 V dc input (as provided by USB port), two LEDs as status indicator, and a half-charged Li-ion battery (nominal voltage of 3.7 V). The charging operation was found to be satisfactory. The circuit was subsequently powered using the charged Li-ion battery. Two low dropout positive regulators U4 and U5 (MCP1802-3.3) are directly connected to the battery for providing two 3.3 V supplies to serve as DV3V3 and AV3V3 for the digital and analog part of the circuit, respectively. These voltages were found to be correctly generated. Two dc-to-dc charge pump converters U2 and U3 (TC962) are used as voltage doubler and voltage doubler-inverter, respectively. The positive voltage is applied as input to low dropout positive regulator U6 (MCP1802-5) for generating +5 V termed as AV+5 and the negative voltage is given as input to a negative regulator U7 (TC5950) for generating –5 V termed as AV−5. The testing of the circuit showed that the dc-to-dc charge pump converters were unable to drive the load with the battery voltage as the input. Further testing showed that the converter was able to work properly for generating AV+5 with a minimum DC input voltage of 6.3 V. However, generation of AV−5 would require a much larger input voltage which may be unsafe for the regulators used for DV3V3 and AV3V3.

Table 6.1: Output voltage levels of the power supply circuit.

Voltage Source	Expected Value (V)	Measured Value (V)
VBAT (external)	6.367	6.367
DV3V3	3.300	3.291
AV3V3	3.300	3.306
VBAT2P	11.734 (Cal. value with no load)	5.091
VBAT2N	−11.734 (Cal. value with no load)	−5.091
AV+5	5.000	4.972
AV−5 (external)	-5.003	-5.003

Therefore, it was concluded that the charge pump circuit needs to be redesigned and tested. For rest of the testing, the negative charge pump and associated regulator were bypassed and AV−5 was connected to an external −5 V. The positive charge pump was applied with input voltage of 6.3 V which was also used by the regulators generating DV3V3 and AV3V3. With these external supplies, the outputs of different terminals in the supply circuit are given in Table 6.1.

6.3 Validation of the Controller Circuit

The controller circuit (Figure 5.5) has the microcontroller DSPIC33FJ128GP802 as U8 interfaced with the RN42 Bluetooth module as U9. The connection between the Bluetooth and the PC based GUI is tested and varified observing the state of the LEDs. Each parameter received by the Bluetooth from the GUI is sent to the microcontroller and is used in the microcontroller program for controlling the parameters of the impedance variation circuit. The PC based GUI is used to set the control signals of the switch-resistor network which is presented in the next section and to provide the two control waveforms (sine, square, triangular, or sawtooth) used in the matched JFET based VCR circuit. The amplitude, frequency, and offset of the control waveforms can be controlled in real time. The range of amplitude, frequency, and offset for the control waveforms are as given earlier in Table 5.3. Figure 6.1 to 6.4 show some of the observed control waveforms generated for the matched JFET pair based VCR circuit from the controller circuit. The waveforms do not get distorted when their amplitude, frequency, or offset is changed and these parameters are controlled in real time. However the DAC output gets suspended for a very short time when the shape of the waveform or the frequency is changed as in this case new datas are needed to be initialized for the output waveform. This is already discussed in the previous chapter.

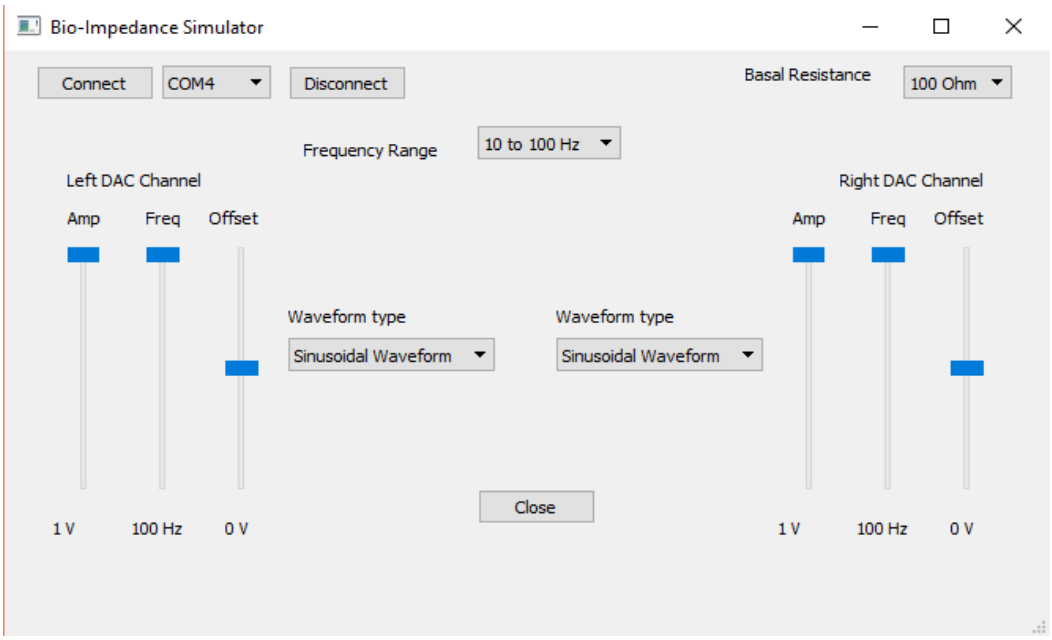

(a)

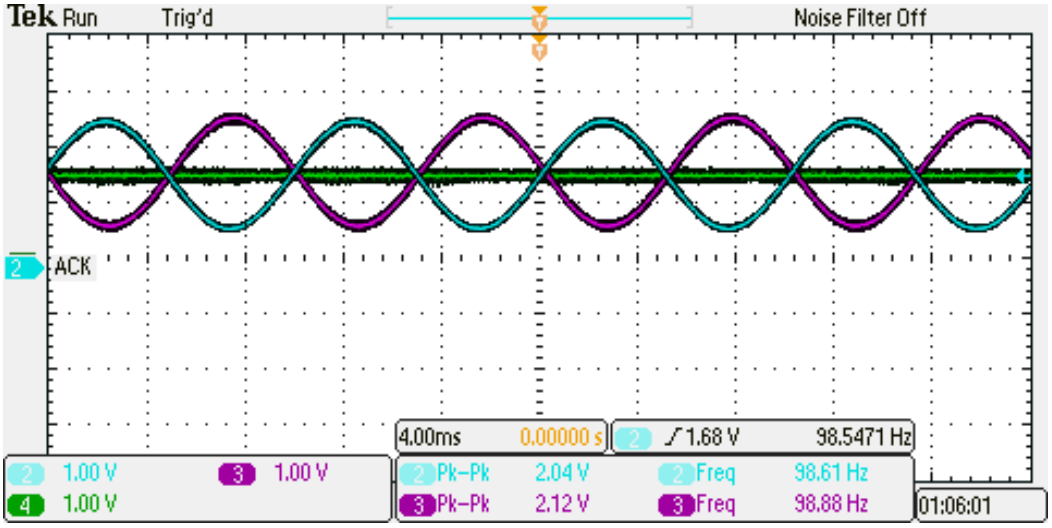

(b)

Figure 6.1: Control voltage signals with their parameters: (a) Parameter values set by the PC based GUI, and (b) Generated control waveforms for the VCR circuit v_1 (Right DAC Channel) with sinusoidal signal of peak-to-peak voltage 2 V, frequency 100 Hz, offset 0 V (Pink), v_2 (Left DAC Channel)with sinusoidal signal of peak-to-peak voltage 2 V, frequency 100 Hz, offset 0 V (Cyan) around AVREF of 1.65 V (Green).

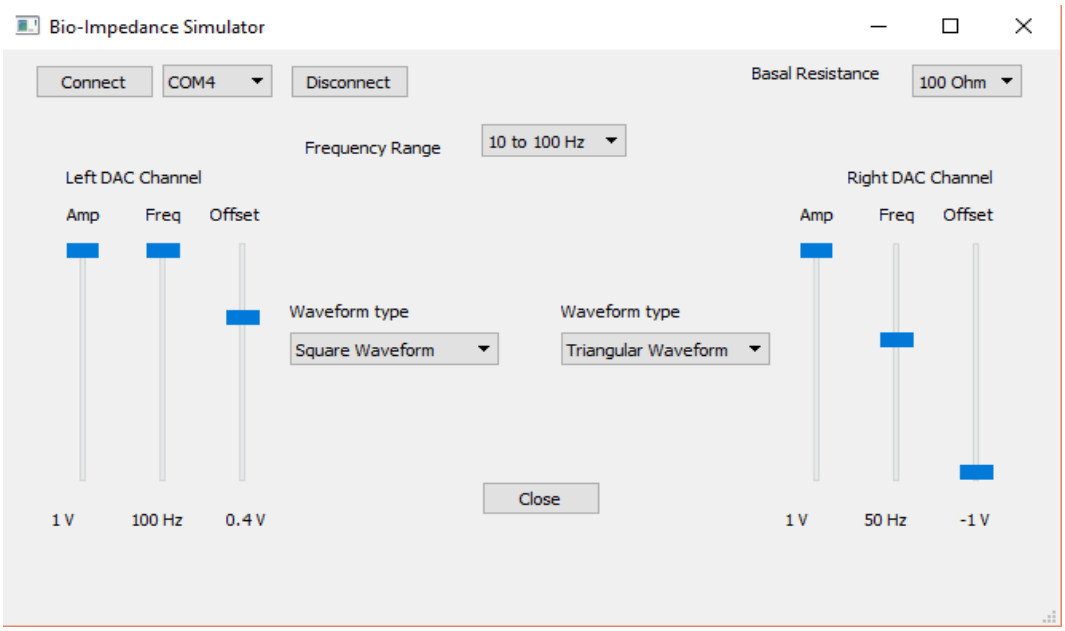

(a)

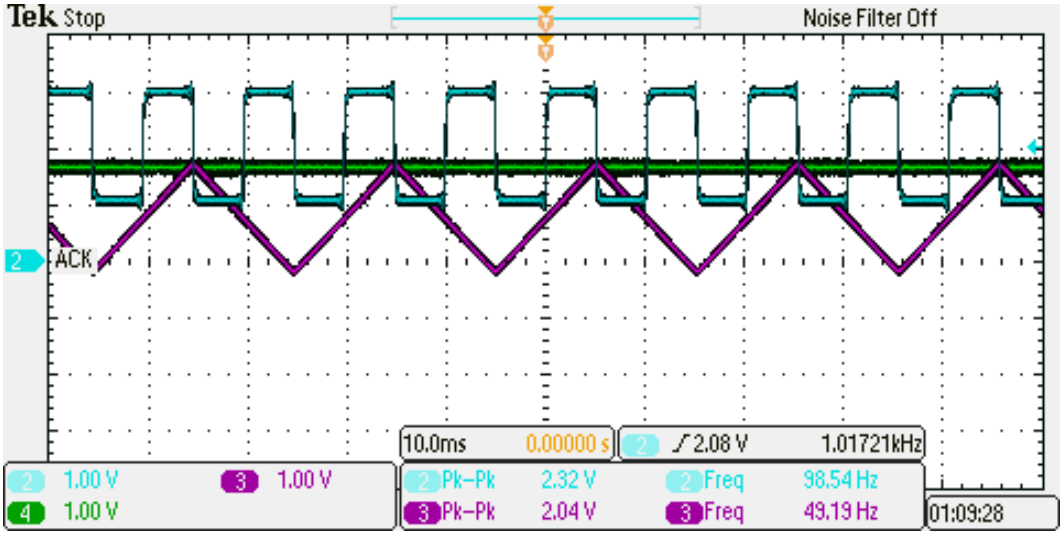

(b)

Figure 6.2: Control voltage signals with their parameters: (a) Parameter values set by the PC based GUI, and (b) Generated control waveforms for the VCR circuit v_1 (Right DAC Channel) with triangular signal of peak-to-peak voltage 2 V, frequency 50 Hz, offset −1 V (Pink), v_2 (Left DAC Channel) with square signal of peak-to-peak voltage 2 V, frequency 100 Hz, offset 0.4 V (Cyan) around AVREF of 1.65 V (Green).

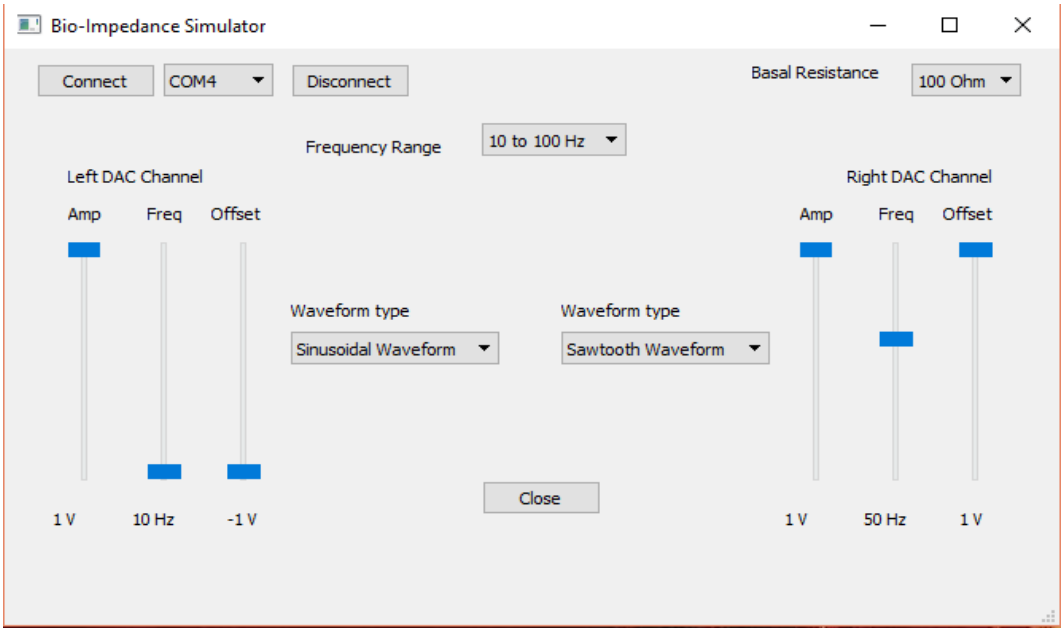

(a)

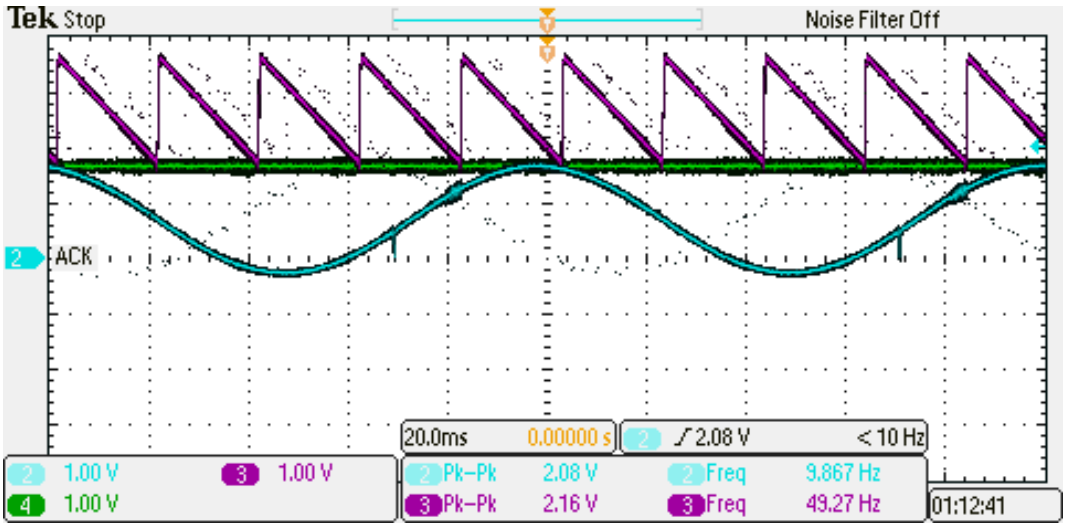

(b)

Figure 6.3: Control voltage signals with their parameters: (a) Parameter values set by the PC based GUI, and (b) Generated control waveforms for the VCR circuit v_1 (Right DAC Channel) with sawtooth signal of peak-to-peak voltage 2 V, frequency 50 Hz, offset 1 V (Pink), v_2 (Left DAC Channel) with sinusoidal signal of peak-to-peak voltage 2 V, frequency 10 Hz, offset −1 V (Cyan) around AVREF of 1.65 V (Green).

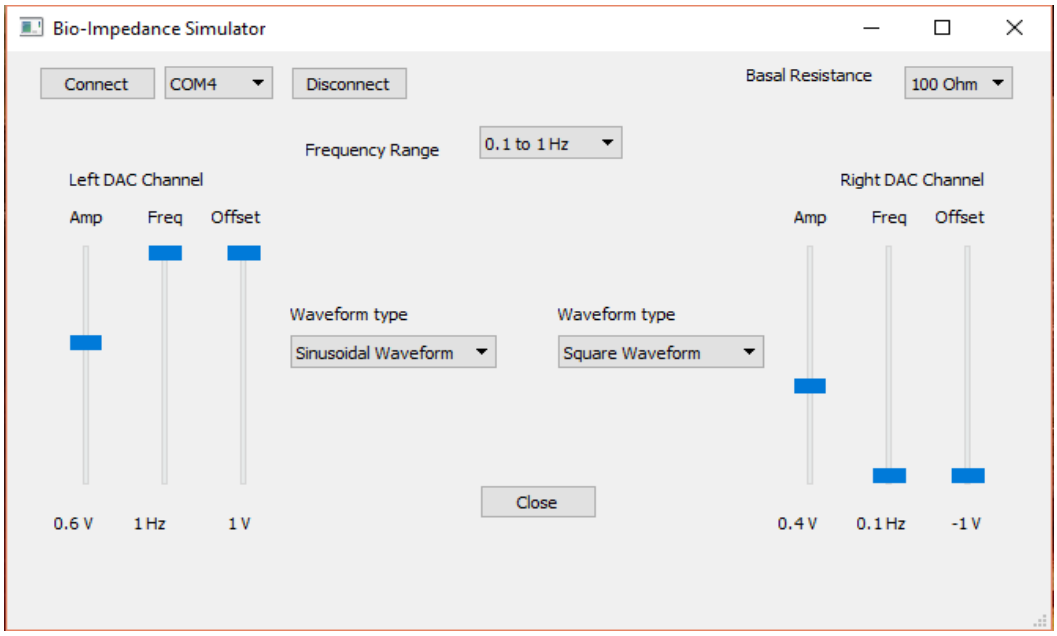

(a)

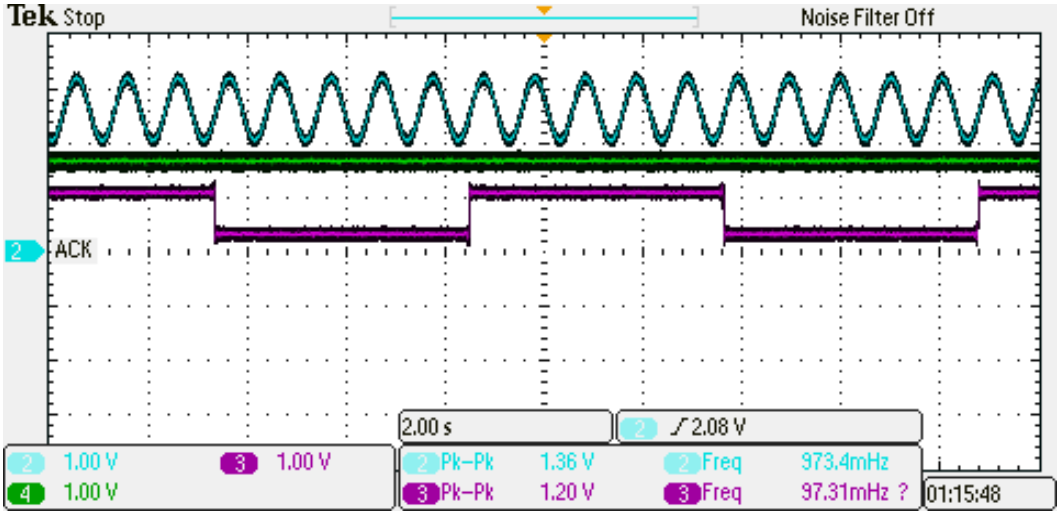

(b)

Figure 6.4: Control voltage signals with their parameters: (a) Parameter values set by the PC based GUI, and (b) Generated control waveforms for the VCR circuit v_1 (Right DAC Channel) with sawtooth signal of peak-to-peak voltage 1.2 V, frequency 0.1 Hz, offset −1 V (Pink), v_2 (Left DAC Channel) with sinusoidal signal of peak-to-peak voltage 1.36 V, frequency 1 Hz, offset 1 V (Cyan) around AVREF of 1.65 V (Green).

Table 6.2: Values of the digitally controlled basal resistance obtained from the switch-R circuit.

Sl. No.	Nominal (Ω)	Measured (Ω)	Error (Ω)
1	0	2.0	2.0
2	10	11.6	1.6
3	20	21.3	1.3
4	30	31.1	1.1
5	50	51.4	1.4
6	60	61.4	1.4
7	70	70.8	0.8
8	80	81.1	1.1
9	100	101.3	1.3
10	110	111.2	1.2
11	120	120.8	0.8
12	130	130.8	0.8
13	150	150.6	0.6
14	160	160.8	0.8
15	170	170.2	0.2
16	180	180.4	0.4

6.4 Validation of the Impedance Variation Circuit

The impedance variation circuit has two parts: the switch-resistor network and the matched JFET pair based VCR circuit. The switch-resistor network is implemented with a quad analog switch IC ADG811 as U13 (Figure 5.3) and four fixed valued resistors for providing the basal resistance in the range from 0 Ω to 180 Ω. The analog switches are controlled digitally through the microcontroller pins assigned to the switches. The test result for the switch resistor network is given in Table 6.2. The deviation of the measured values from the nominal values are close to those estimated on the basis of on-resistance of the analog switches as given in Table 5.1.

The matched JFET based VCR circuit is tested by simulation and practical implementation. On the basis of the simulation and practical results, it was concluded that the control voltage v_2 should be kept fixed at a value less than or equal to 0.5 V to ensure that the feedback voltage v_A does not exceed the value of V_P for the devices and the resistance remains in the stable region (as predicted by Figure 3.3). The variation of the control voltage v_1 is

Table 6.3: Test results for the matched JFET pair based VCR circuit implemented on PCB for the bioimpedance simulator circuit.

v_2 = 0.449 V, R_1 = 1000 Ω				
	R_{E1E2}(Ω)			
E1 − E2 (V)	v_1 = −0.204 V (Calc. R_{E1E2} = 2200.98 Ω, Obsevrd. v_C = –6.30 V)	v_1 = −0.399 V (Calc. R_{E1E2} = 1125.31 Ω, Obsevrd. v_C = –4.82 V)	v_1 = −0.594 V (Calc. R_{E1E2} = 755.89 Ω, Obsevrd. v_C = –2.96 V)	v_1 = −0.791 V (Calc. R_{E1E2} = 567.64 Ω, Obsevrd. v_C = −1.098 V)
−1.0	3337.55	1370.18	705.07	499.20
−0.9	3087.86	1335.80	696.59	498.18
−0.8	2827.02	1296.27	689.97	496.00
−0.7	2547.16	1251.77	678.14	494.51
−0.6	2250.46	1191.06	664.20	491.56
−0.5	1927.78	1125.61	649.77	483.21
−0.4	1597.56	1043.83	625.41	481.00
−0.3	1226.53	903.54	592.27	473.04
−0.2	853.46	732.10	544.91	456.57
−0.1	452.37	471.90	429.42	422.39
0.1	465.05	479.65	430.91	425.08
0.2	868.24	750.36	541.59	455.55
0.3	1245.02	909.09	593.84	470.30
0.4	1629.61	1044.09	626.58	478.09
0.5	1952.34	1139.83	644.61	481.64
0.6	2262.96	1210.49	665.30	485.08
0.7	2548.93	1276.58	678.40	488.13
0.8	2830.69	1335.98	685.52	492.00
0.9	3074.17	1360.11	694.44	491.84
1.0	3287.50	1407.67	705.08	494.25

restricted to a range for operating the VCR in stable region. The floating terminal voltages VCR-E1 and VCR-E2, as given in Figure 5.4, are varied up to ±1 V to test the linearity of the VCR. The device parameters were not measured before soldering the devices and hence the optimal range of control voltage and the value of R25 (which is equivalent to R1 in Figure 3.6) for linear operation of the circuit cannot be calculated. Therefore the circuit was tested using a set of control voltages to find a stable region. The test result for the VCR circuit is given in Table 6.3. It shows that combination of v_2 = 0.449 V and v_1 = −0.791 V was near optimal from linearity consideration.

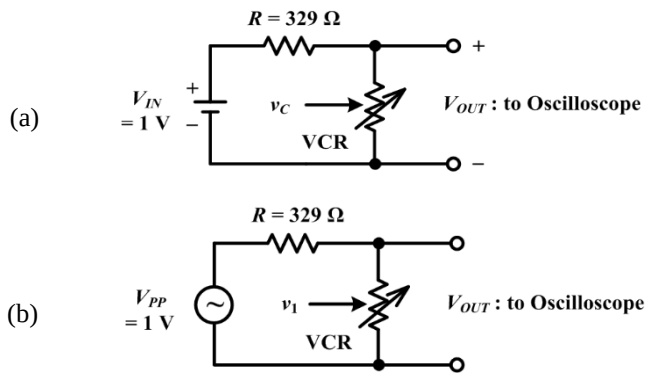

Figure 6.5: Circuit for testing of the VCR circuit response. Configurations: (a) Testing of DC response for the VCR and (b) Testing of AC response for the VCR.

Further testing was carried out with v_2 = 0.449 V and different control waveforms with amplitude of 200 mV and offset of −0.791 V are applied at the control voltage terminal v_1.

To observe the DC response of the VCR circuit, a DC voltage of 1 V followed by series resistance of 329 Ω (to limit the input current) was applied across the floating terminal of the VCR and the developed voltage was observed in oscilloscope. The circuit is shown in Figure 6.6 (a). The observed voltage waveforms across the VCR terminals are shown in Figure 6.6 to Figure 6.10. It was observed that the resistance response of the VCR was linear for control signals with amplitude of 100 mV and offset of −0.791 V.

For observing the AC response, an excitation signal of 1 V peak-to-peak and frequencies of 10 kHz, 50 kHz and 100 kHz, (with series resistance of 329 Ω to limit the input current) with series resistance of 329 Ω (to limit the input current)was applied across the floating terminal of the VCR circuit and the behaviour was observed in oscilloscope. The circuit configuration is shown in Figure 6.6 (b). The control voltage v_2 is kept at 0.449 V and different type of control signals with amplitude of 200 mV and offset of −0.791 V is applied at the control voltage terminal v_1. The response of the VCR circuit is shown in Figure 6.11 to Figure 6.14. The envelope of the voltage modulated signals followed the resistance variation control. A detailed testing of AC response of the simulator circuit has to be carried out. Both the switch-resistor network and the VCR circuit were tested separately on PCB. The use of the combined circuit for testing an ICG instrument needs to be carried out.

6.5 Conclusion

The investigations have contributed to design of floating precision linear VCR and its use for realizing a bioimpedance simulator along with the controller circuit and electrically isolated real-time control of parameters. The bioimepdance simulator was implemented on PCB and tested. The designed power supply circuit was unable to meet –5 V requirement and needs to be redesigned. The controller and PC-based GUI worked satisfactorily.

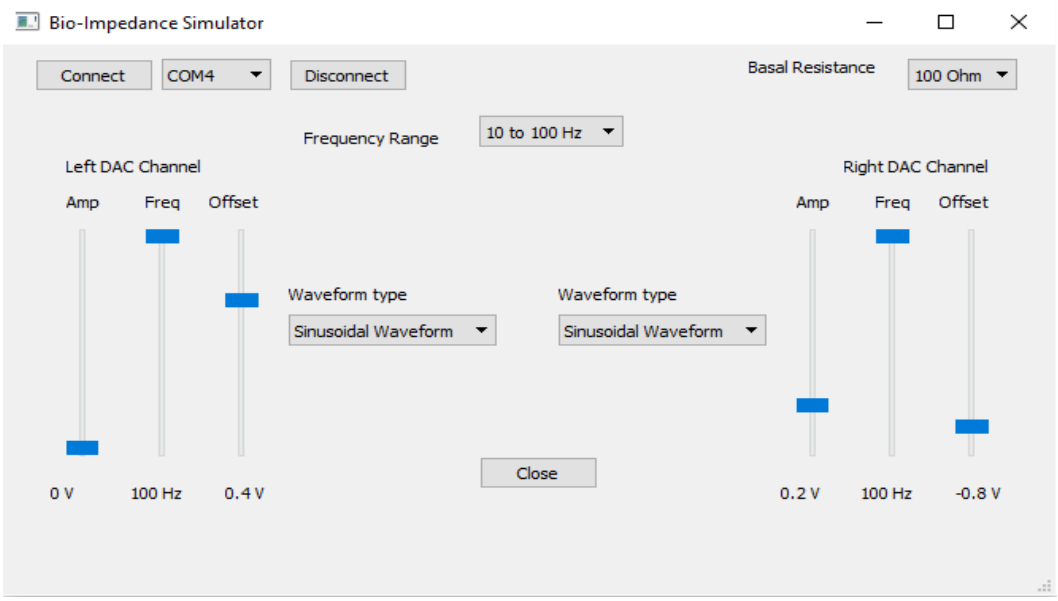

(a)

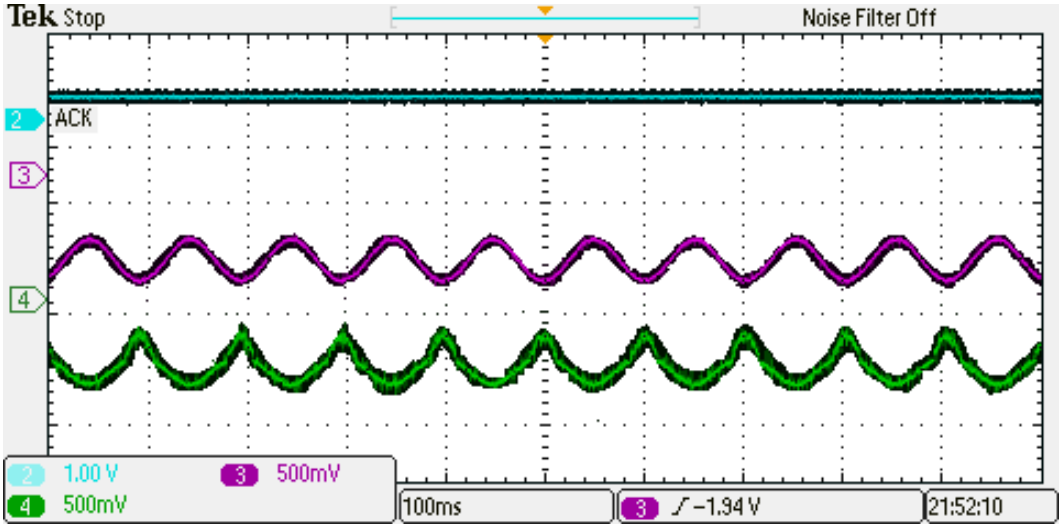

(b)

Figure 6.6: Control voltage signals with their parameters: (a) Parameter values set by the PC based GUI, and (b) Generated control waveforms for the VCR circuit v_1 (Right DAC Channel) with sinusoidal signal of peak-to-peak voltage 400 mV, frequency 100 Hz, offset −0.8 V (Pink), v_2 (Left DAC Channel) with sinusoidal signal of amplitude 0 V, frequency 100 Hz, offset 0.4 V (Cyan) and the observed waveform at the floating terminal of the VCR circuit (Green).

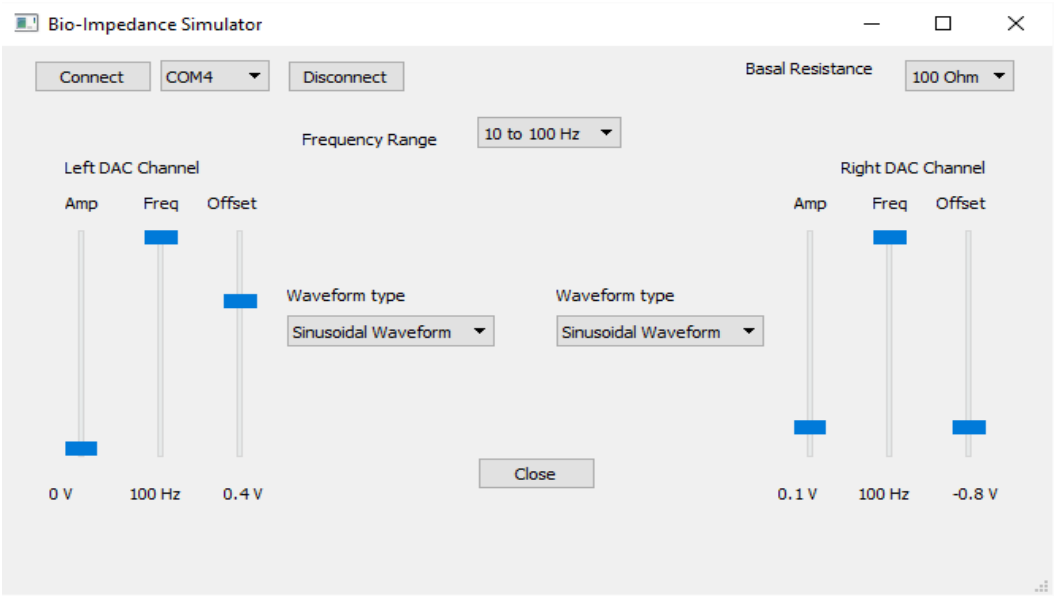

(a)

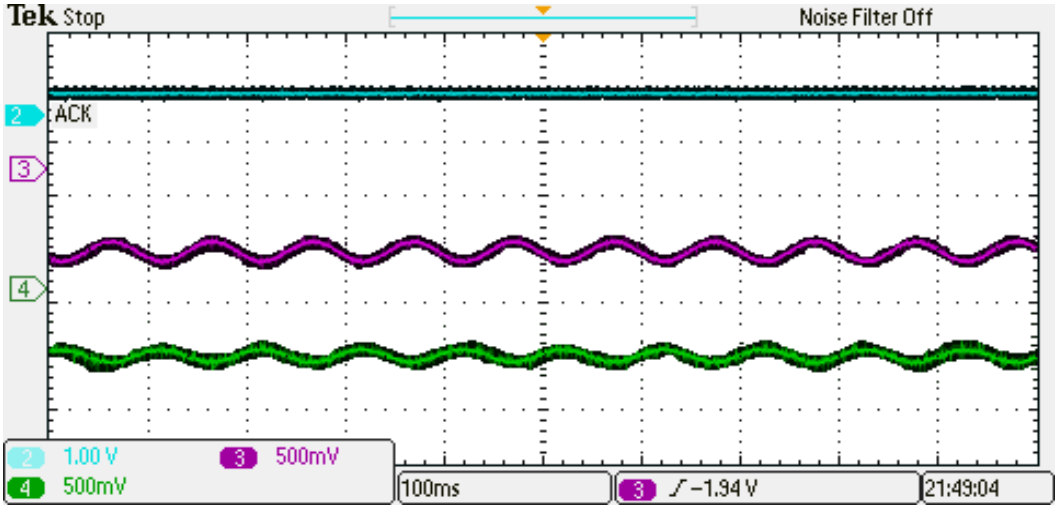

(b)

Figure 6.7: Control voltage signals with their parameters: (a) Parameter values set by the PC based GUI, and (b) Generated control waveforms for the VCR circuit v_1 (Right DAC Channel) with sinusoidal signal of peak-to-peak voltage 200 mV, frequency 100 Hz, offset −0.8 V (Pink), v_2 (Left DAC Channel) with sinusoidal signal of amplitude 0 V, frequency 100 Hz, offset 0.4 V (Cyan) and the observed waveform at the floating terminal of the VCR circuit (Green).

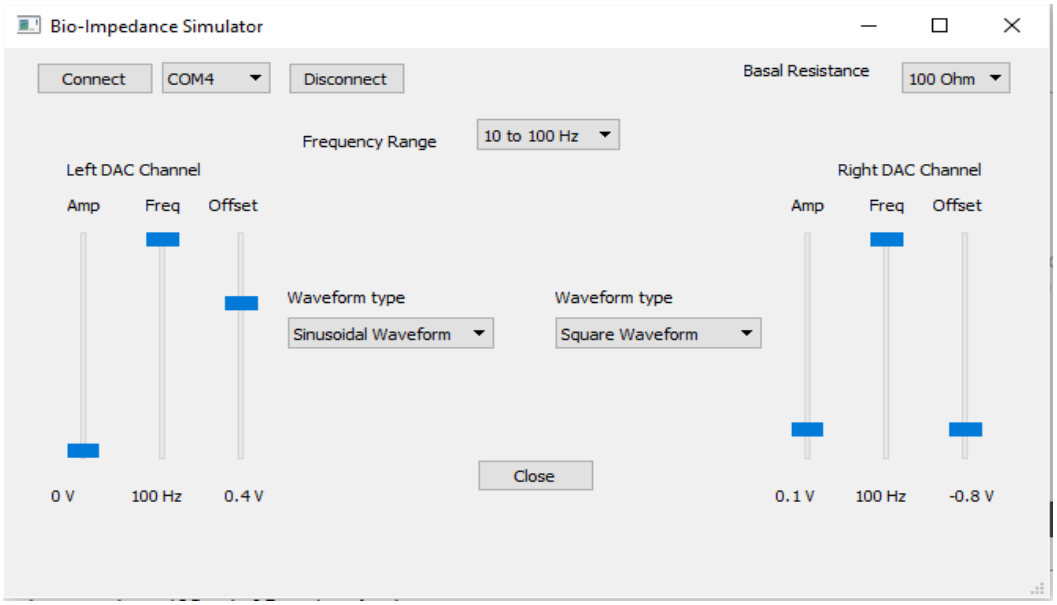

(a)

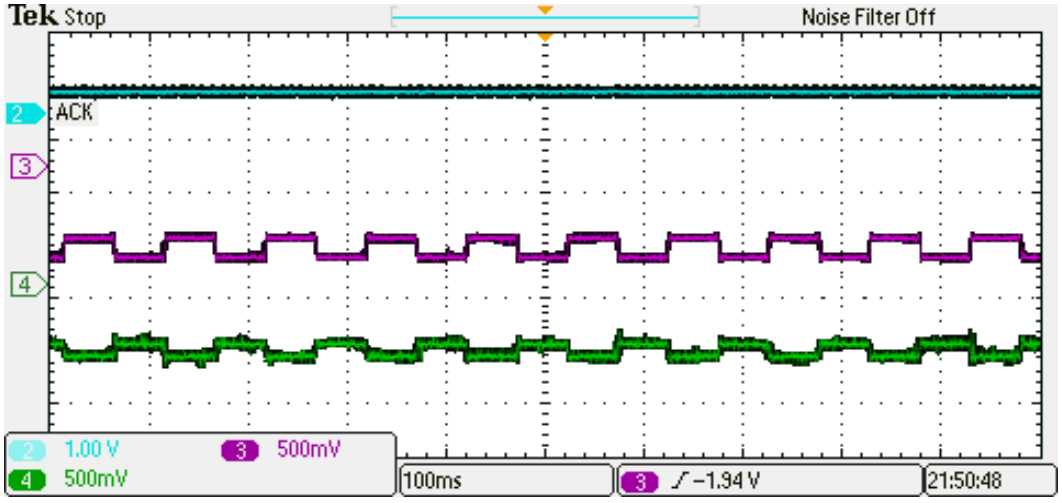

(b)

Figure 6.8: Control voltage signals with their parameters: (a) Parameter values set by the PC based GUI, and (b) Generated control waveforms for the VCR circuit v_1 (Right DAC Channel) with square signal of peak-to-peak voltage 200 mV, frequency 100 Hz, offset −0.8 V (Pink), v_2 (Left DAC Channel) with sinusoidal signal of amplitude 0 V, frequency 100 Hz, offset 0.4 V (Cyan) and the observed waveform at the floating terminal of the VCR circuit (Green).

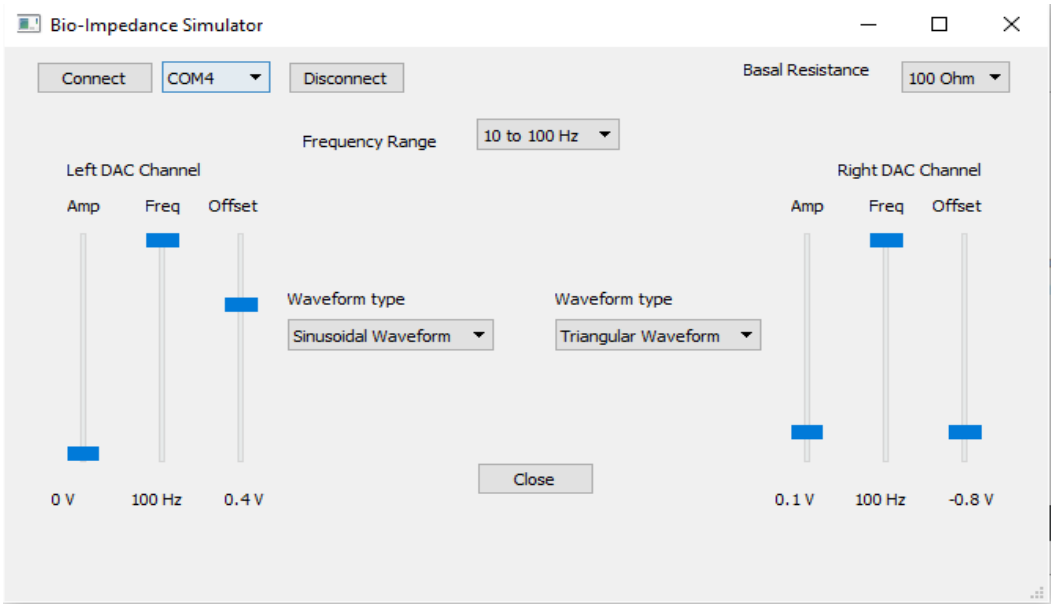

(a)

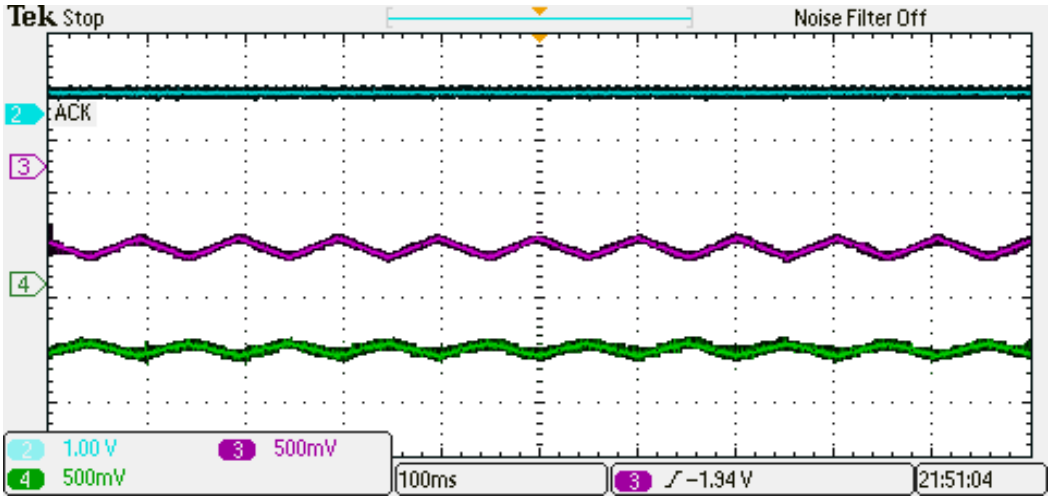

(b)

Figure 6.9: Control voltage signals with their parameters: (a) Parameter values set by the PC based GUI, and (b) Generated control waveforms for the VCR circuit v_1 (Right DAC Channel) with triangular signal of peak-to-peak voltage 200 mV, frequency 100 Hz, offset −0.8 V (Pink), v_2 (Left DAC Channel) with sinusoidal signal of amplitude 0 V, frequency 100 Hz, offset 0.4 V (Cyan) and the observed waveform at the floating terminal of the VCR circuit (Green).

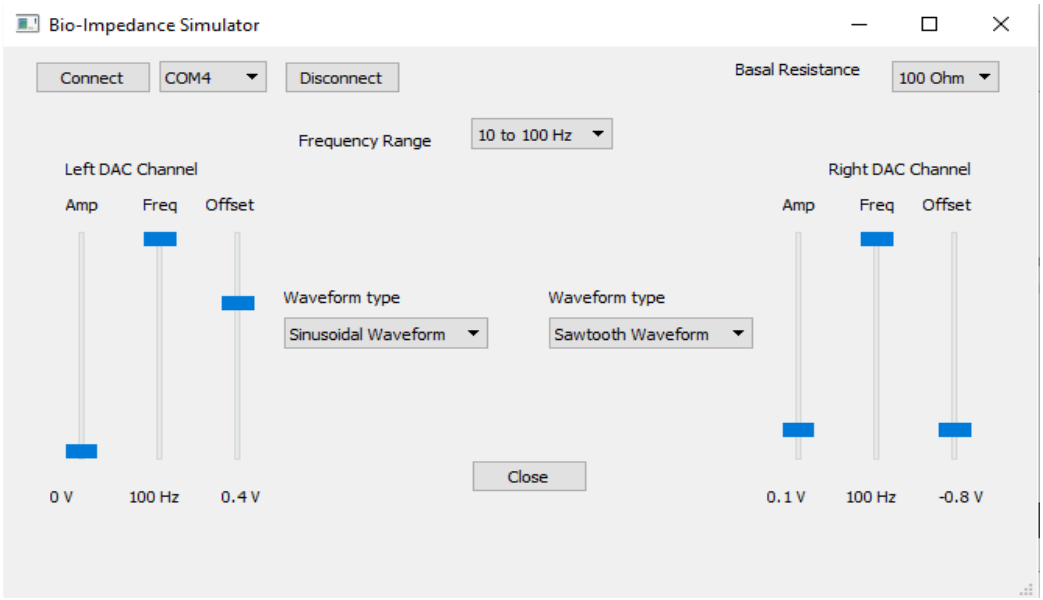

(a)

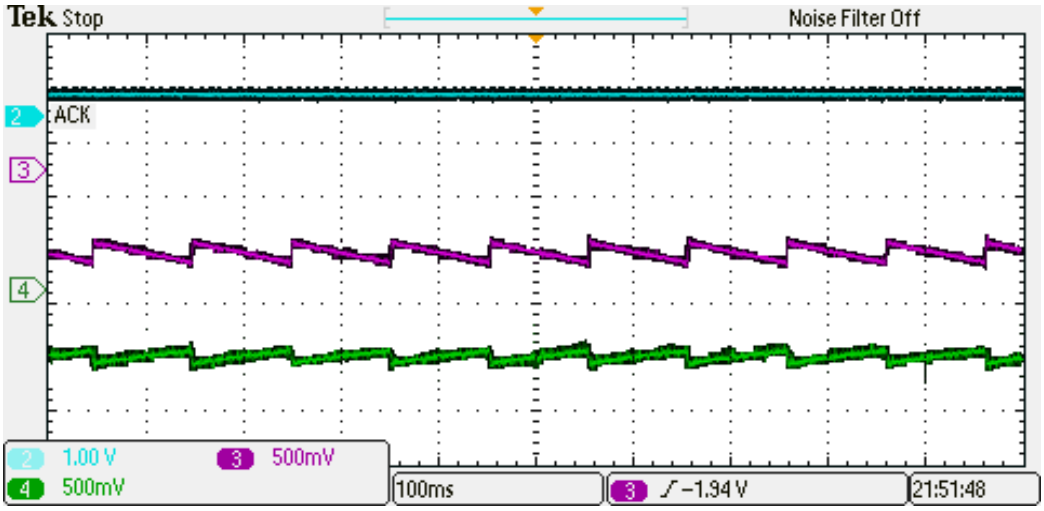

(b)

Figure 6.10: Control voltage signals with their parameters: (a) Parameter values set by the PC based GUI, and (b) Generated control waveforms for the VCR circuit v_1 (Right DAC Channel) with sawtooth signal of peak-to-peak voltage 200 mV, frequency 100 Hz, offset −0.8 V (Pink), v_2 (Left DAC Channel) with sinusoidal signal of amplitude 0 V, frequency 100 Hz, offset 0.4 V (Cyan) and the observed waveform at the floating terminal of the VCR circuit (Green).

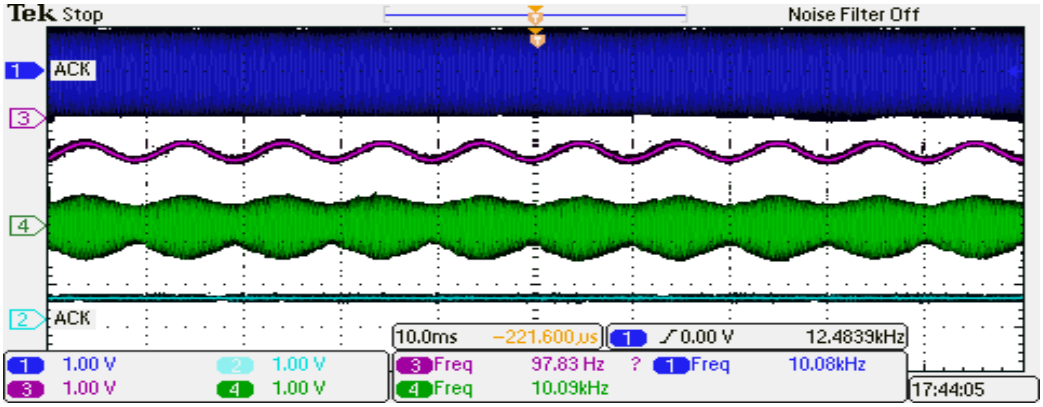

(a)

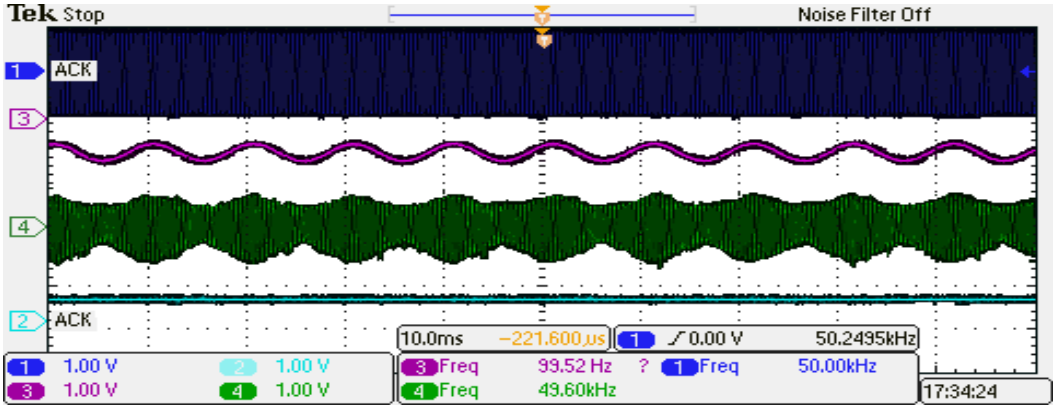

(b)

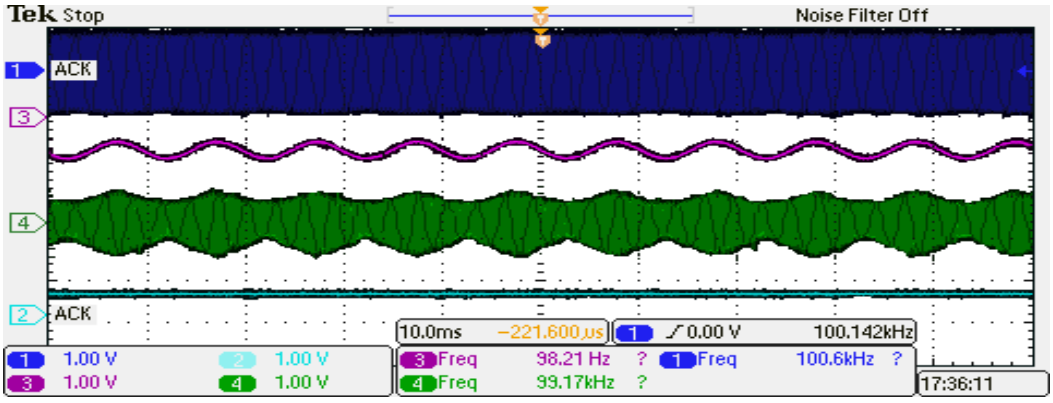

(c)

Figure 6.11: Control voltage signals with their parameters v_1 (Right DAC Channel) with sinusoidal signal of peak-to-peak voltage 200 mV, frequency 100 Hz, offset −0.8 V (Pink) and v_2 (Left DAC Channel) with sinusoidal signal of amplitude 0 V, frequency 100 Hz, offset 0.4 V (Cyan): (a) Input sinusoidal signal with frequency 10 kHz (Blue) and observed amplitude modulated signal with frequency 10 kHz (Green), (b) Input sinusoidal signal with frequency 50 kHz (Blue) and observed amplitude modulated signal with frequency 50 kHz (Green), and (c) Input sinusoidal signal with frequency 100 kHz (Blue) and observed amplitude modulated signal with frequency 100 kHz (Green).

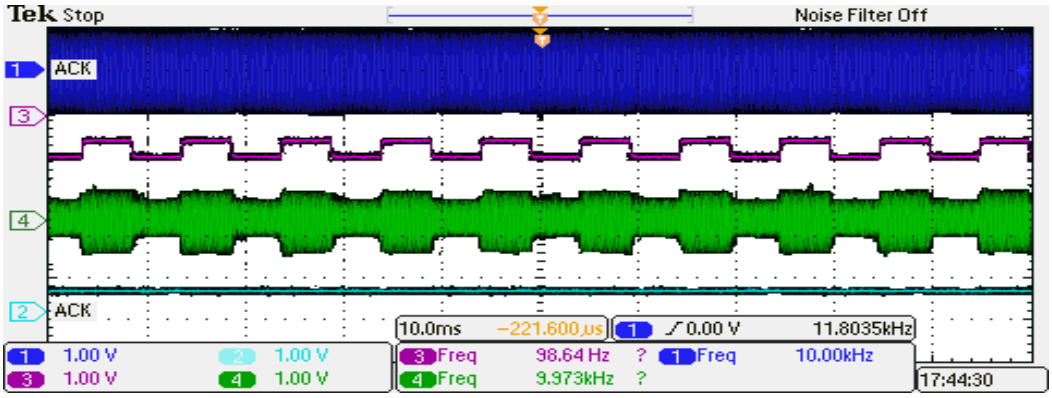

(a)

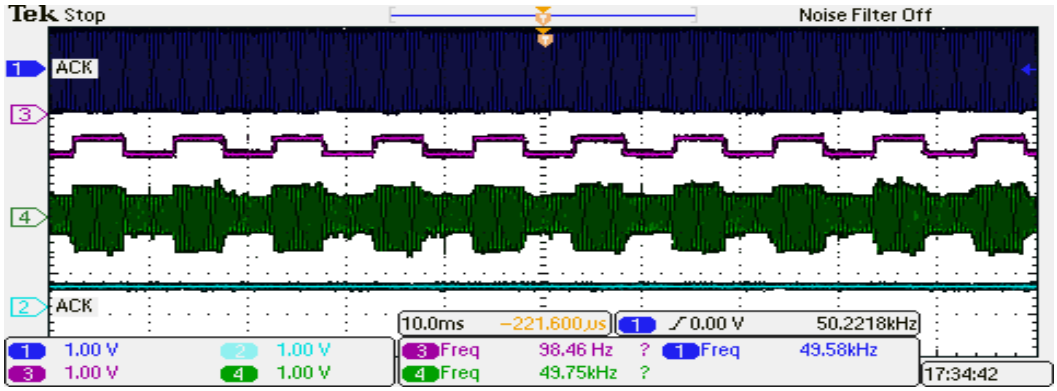

(b)

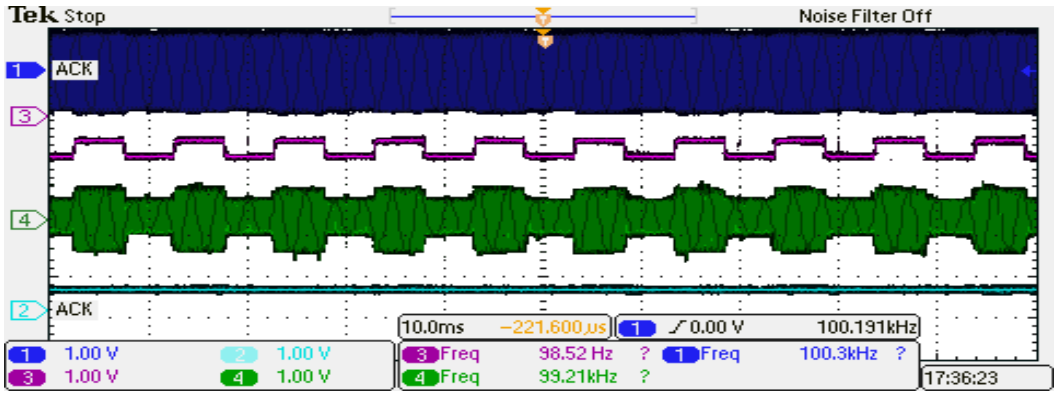

(c)

Figure 6.12: Control voltage signals with their parameters v_1 (Right DAC Channel) with square signal of peak-to-peak voltage 200 mV, frequency 100 Hz, offset −0.8 V (Pink) and v_2 (Left DAC Channel) with sinusoidal signal of amplitude 0 V, frequency 100 Hz, offset 0.4 V (Cyan): (a) Input sinusoidal signal with frequency 10 kHz (Blue) and observed amplitude modulated signal with frequency 10 kHz (Green), (b) Input sinusoidal signal with frequency 50 kHz (Blue) and observed amplitude modulated signal with frequency 50 kHz (Green), and (c) Input sinusoidal signal with frequency 100 kHz (Blue) and observed amplitude modulated signal with frequency 100 kHz (Green).

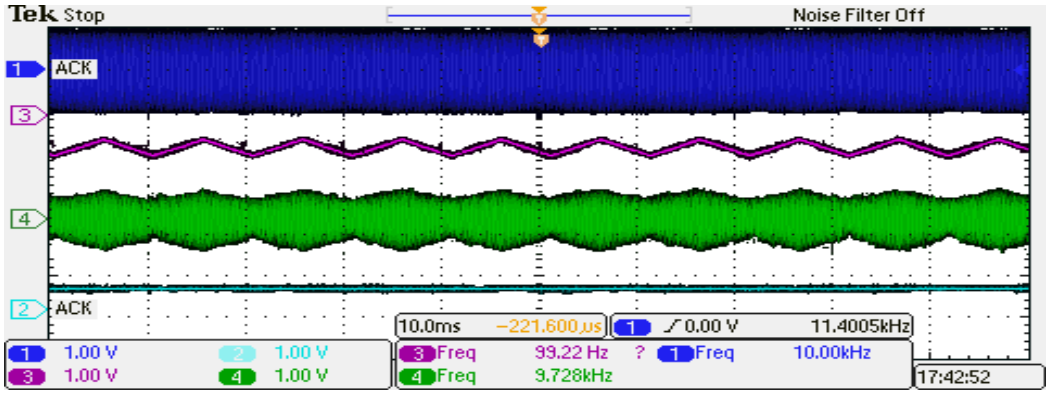

(a)

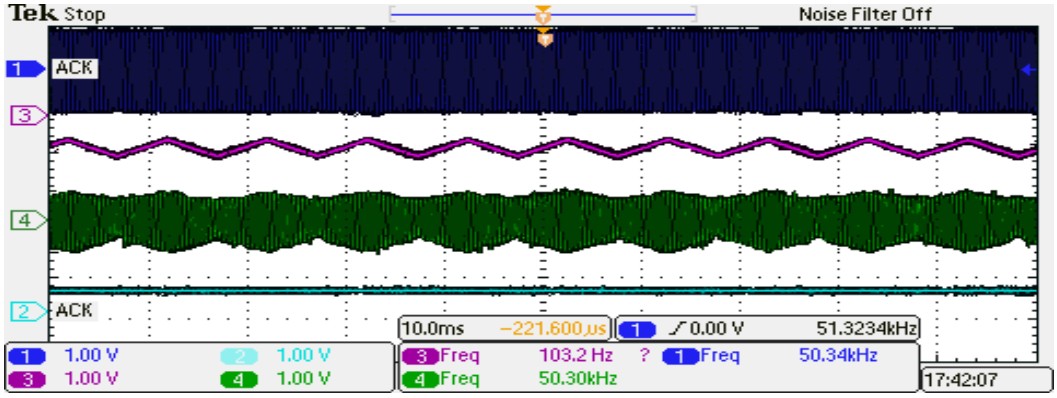

(b)

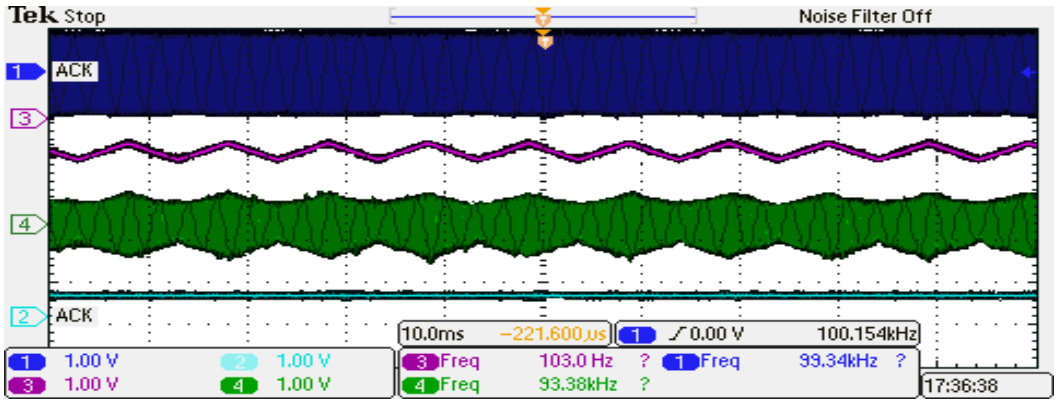

(c)

Figure 6.13: Control voltage signals with their parameters v_1 (Right DAC Channel) with triangular signal of peak-to-peak voltage 200 mV, frequency 100 Hz, offset −0.8 V (Pink) and v_2 (Left DAC Channel) with sinusoidal signal of amplitude 0 V, frequency 100 Hz, offset 0.4 V (Cyan): (a) Input sinusoidal signal with frequency 10 kHz (Blue) and observed amplitude modulated signal with frequency 10 kHz (Green), (b) Input sinusoidal signal with frequency 50 kHz (Blue) and observed amplitude modulated signal with frequency 50 kHz (Green), and (c) Input sinusoidal signal with frequency 100 kHz (Blue) and observed amplitude modulated signal with frequency 100 kHz (Green).

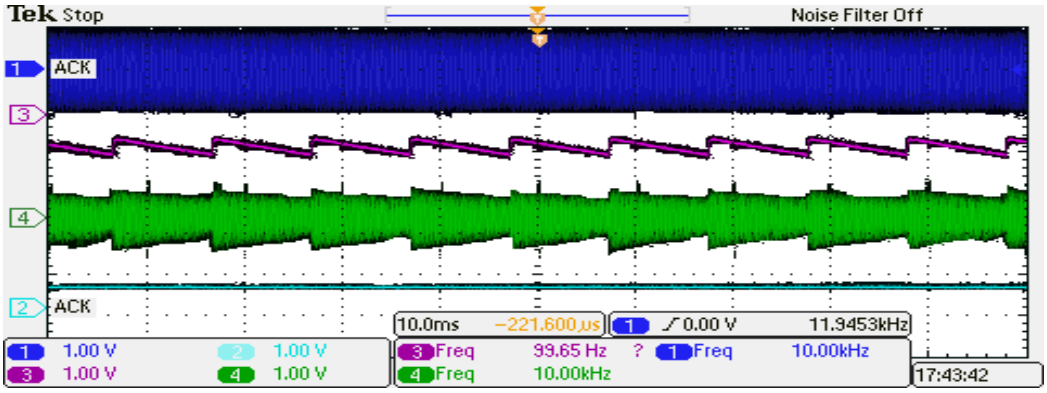

(a)

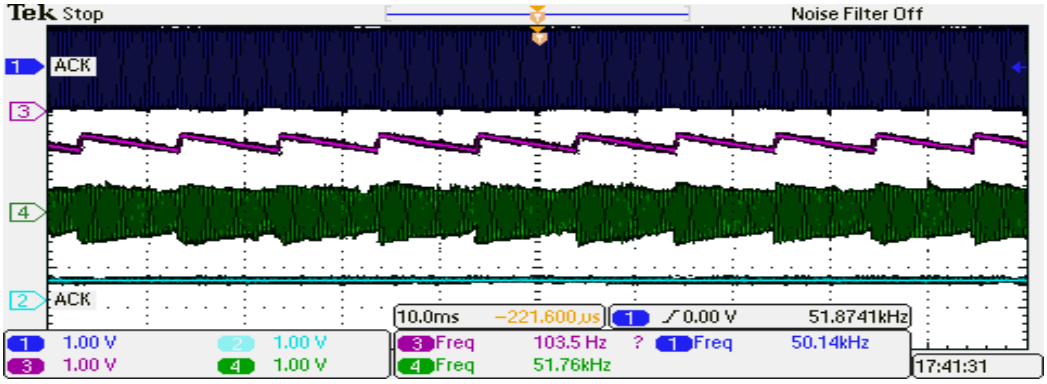

(b)

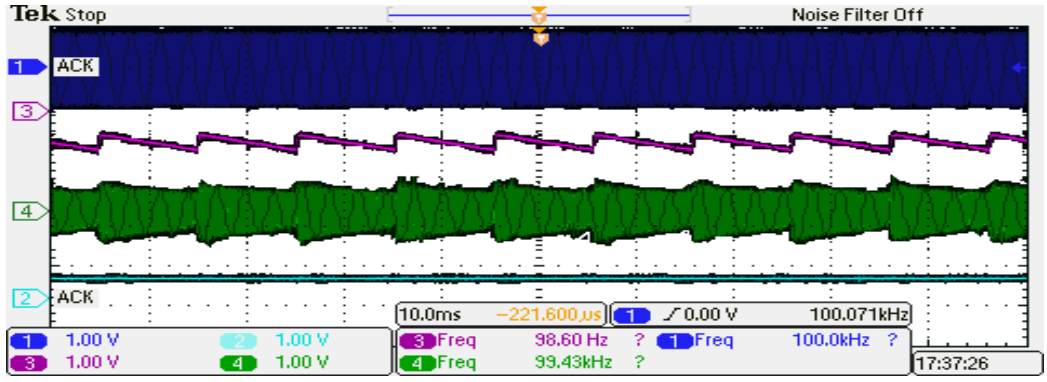

(c)

Figure 6.14: Control voltage signals with their parameters v_1 (Right DAC Channel) with sawtooth signal of peak-to-peak voltage 200 mV, frequency 100 Hz, offset −0.8 V (Pink) and v_2 (Left DAC Channel) with sinusoidal signal of amplitude 0 V, frequency 100 Hz, offset 0.4 V (Cyan): (a) Input sinusoidal signal with frequency 10 kHz (Blue) and observed amplitude modulated signal with frequency 10 kHz (Green), (b) Input sinusoidal signal with frequency 50 kHz (Blue) and observed amplitude modulated signal with frequency 50 kHz (Green), and (c) Input sinusoidal signal with frequency 100 kHz (Blue) and observed amplitude modulated signal with frequency 100 kHz (Green).

Chapter 7

SUMMARY AND CONCLUSSION

The project objective was to design a bioimpedance simulator for testing and calibrating the ICG instruments. The simulator circuit should be capable of generating a continuous, time-varying impedance in response to a control voltage. To meet this requirement, a bioimpedance simulator circuit is developed which has four blocks: the resistance variation circuit, the controller circuit for controlling the impedance variation, a wireless module connected to the controller with serial interface for setting the parameters of the control waveforms, and a battery powered power supply block. The wireless link was implemented using a Bluetooth module interfaced with the controller. The simulator is electrically isolated from the mains. A PC-based GUI was designed for setting the control parameter through wireless link.

The controller circuit consists of a microcontroller and a Bluetooth module configured to work through UART. A program is written for the microcontroller to generate different types of control signals for the resistance variation circuit and for digitally controlling the switch-resistor network. The PC based GUI is developed to control the circuit parameters from PC over the Bluetooth based wireless link. The GUI is capable of controlling the circuit parameters such as amplitude, shape, frequency, and offset of the control voltage generated for the VCR circuit and the digital control for the switch network in real time. The resistance variation circuit is implemented as a parallel combination of a digitally controlled basal resistance obtained using a switch-resistor network and a matched JFET pair based VCR circuit for the time varying component.

The power supply circuit designed for the simulator did not meet the complete requirements and rest of the bioimpedance simulator was tested using external supplies of 6.3 V and −5 V. The switch-resistor network was validated using the controller circuit and the PC based GUI. However, the matched JFET pair based floating precision linear VCR worked linearly for a range of control voltages.

The power supply of the bioimpedance simulator needs to be redesigned. The VCR circuit should be redesigned using a matched MOSFET pair with independent substrate terminal for extending the linear region of operation of the VCR circuit and using op amps with higher frequency response, or possibly designing an analog ASIC using MOSFET based VCR along with MOSFET based op amps. For providing a more realistic simulation of bioimpedance, a voltage-controlled capacitor realized using a VCR and impedance converter may be connected in parallel with the variable resistance.

APPENDIX A

SIMULATION RESULTS FOR JFET BASED VCR CIRCUITS

Table A.1: Circuit simulation (LT Spice) results for JFET-based grounded VCR using single device (Circuit in Figure 3.1, with $v_C = v_{GS}$, $v_{XY} = v_{DS}$, and $i_X = i_D$): i_X and R_{XY} as a function of v_{XY}, with $v_C = 0$ V and λ as a parameter. (i) $V_P = -1$ V and $I_{DSS} = 6$ mA, (ii) $V_P = -1$ V and $I_{DSS} = 15$ mA, (iii) $V_P = -3.5$ V and $I_{DSS} = 6$ mA, and (iv) $V_P = -3.5$ V and $I_{DSS} = 15$ mA.

(i) $V_P = -1$ V and $I_{DSS} = 6$ mA

v_{XY} (V)	i_X (mA)				R_{XY} (Ω)			
	λ = 0	λ = 0.01	λ = 0.02	λ = 0.03	λ = 0	λ = 0.01	λ = 0.02	λ = 0.03
−0.5	−7.29	−7.32	−7.36	−7.39	68.60	68.28	67.96	67.65
−0.4	−5.60	−5.62	−5.64	−5.66	71.44	71.17	70.91	70.64
−0.3	−4.03	−4.04	−4.05	−4.06	74.46	74.25	74.04	73.84
−0.2	−2.57	−2.58	−2.58	−2.59	77.76	77.61	77.46	77.32
−0.1	−1.23	−1.23	−1.23	−1.23	81.37	81.29	81.21	81.13
−0.08	−0.97	−0.99	−0.98	−0.98	82.13	82.07	82.00	81.94
−0.06	−0.72	−0.72	−0.73	−0.73	82.91	82.86	82.81	82.76
−0.04	−0.48	−0.48	−0.48	−0.48	83.70	83.67	83.64	83.60
−0.02	−0.24	−0.24	−0.24	−0.24	84.51	84.49	84.48	84.46
0.02	0.23	0.23	0.23	0.23	86.18	86.16	86.14	86.13
0.04	0.46	0.46	0.46	0.46	87.03	87.00	86.97	86.93
0.06	0.68	0.68	0.68	0.68	87.91	87.86	87.81	87.76
0.08	0.90	0.90	0.90	0.90	88.81	88.74	88.67	88.60
0.1	1.12	1.12	1.12	1.12	89.72	89.63	89.55	89.46
0.2	2.11	2.12	2.12	2.13	94.59	94.41	94.23	94.05
0.3	3.00	3.01	3.02	3.03	100.04	99.75	99.47	99.18
0.4	3.77	3.78	3.80	3.81	106.17	105.76	105.36	104.96
0.5	4.42	4.44	4.46	4.48	113.11	112.57	112.03	111.50
0.6	4.96	4.99	5.01	5.04	121.05	120.35	119.66	118.98
0.7	5.38	5.41	5.45	5.49	130.21	129.33	128.46	127.61
0.8	5.68	5.72	5.77	5.81	140.89	139.80	138.73	137.68
0.9	5.86	5.91	5.97	6.02	153.52	152.18	150.87	149.58
1.0	5.93	5.99	6.05	6.10	168.67	167.04	165.44	163.87
1.1	5.93	5.99	6.06	6.12	185.53	183.55	181.62	179.73
1.2	5.93	6.00	6.07	6.14	202.39	200.05	197.75	195.51
1.3	5.93	6.01	6.08	6.16	219.26	216.50	213.82	211.20
1.4	5.93	6.01	6.09	6.17	236.13	232.93	229.82	226.80
1.5	5.93	6.02	6.10	6.19	252.99	249.33	245.77	242.31
1.6	5.93	6.02	6.12	6.21	269.86	265.69	261.65	257.73
1.7	5.93	6.03	6.13	6.23	286.72	282.02	277.47	273.07
1.8	5.93	6.03	6.14	6.24	303.59	298.32	293.23	288.32
1.9	5.93	6.04	6.15	6.26	320.46	314.59	308.93	303.49
2.0	5.93	6.05	6.16	6.28	337.32	330.82	324.58	318.57

(ii) $V_P = -1$ V and $I_{DSS} = 15$ mA

v_{XY} (V)	i_X (mA)				R_{XY} (Ω)			
	λ = 0	λ = 0.01	λ = 0.02	λ = 0.03	λ = 0	λ = 0.01	λ = 0.02	λ = 0.03
−0.5	−17.45	−17.52	−17.60	−17.67	28.66	28.54	28.41	28.29
−0.4	−13.43	−13.48	−13.53	−13.57	29.78	29.67	29.57	29.47
−0.3	−9.68	−9.71	−9.73	−9.76	30.99	30.90	30.82	30.74
−0.2	−6.19	−6.20	−6.21	−6.22	32.30	32.25	32.19	32.13
−0.1	−2.96	−2.97	−2.97	−2.97	33.75	33.72	33.69	33.66
−0.08	−2.35	−2.35	−2.35	−2.35	34.05	34.03	34.00	33.98
−0.06	−1.75	−1.75	−1.75	−1.75	34.36	34.34	34.33	34.31
−0.04	−1.15	−1.15	−1.15	−1.16	34.68	34.67	34.66	34.64
−0.02	−0.57	−0.57	−0.57	−0.57	35.00	35.00	34.99	34.99
0.02	0.56	0.56	0.56	0.56	35.67	35.66	35.66	35.65
0.04	1.11	1.11	1.11	1.11	36.01	36.00	35.99	35.98
0.06	1.65	1.65	1.65	1.65	36.36	36.35	36.33	36.31
0.08	2.18	2.18	2.18	2.18	36.72	36.70	36.67	36.64
0.1	2.70	2.70	2.70	2.70	37.09	37.06	37.02	36.99
0.2	5.12	5.13	5.14	5.15	39.04	38.97	38.90	38.83
0.3	7.28	7.30	7.32	7.34	41.22	41.10	40.99	40.88
0.4	9.16	9.19	9.23	9.26	43.67	43.51	43.35	43.20
0.5	10.77	10.82	10.86	10.91	46.44	46.23	46.02	45.82
0.6	12.09	12.16	12.23	12.29	49.62	49.35	49.08	48.81
0.7	13.14	13.22	13.31	13.39	53.28	52.94	52.60	52.27
0.8	13.90	14.00	14.11	14.21	57.56	57.13	56.71	56.30
0.9	14.38	14.50	14.62	14.74	62.61	62.08	61.57	61.06
1.0	14.56	14.70	14.84	14.97	68.67	68.03	67.40	66.78
1.1	14.57	14.72	14.87	15.02	75.52	74.74	73.98	73.24
1.2	14.57	14.73	14.90	15.06	82.38	81.46	80.55	79.67
1.3	14.57	14.75	14.93	15.11	89.25	88.16	87.10	86.07
1.4	14.57	14.76	14.95	15.15	96.11	94.85	93.62	92.43
1.5	14.57	14.77	14.98	15.19	102.98	101.53	100.12	98.76
1.6	14.57	14.79	15.01	15.23	109.84	108.19	106.60	105.05
1.7	14.57	14.80	15.04	15.27	116.71	114.85	113.05	111.30
1.8	14.57	14.82	15.07	15.32	123.57	121.49	119.47	117.52
1.9	14.57	14.83	15.10	15.36	130.44	128.11	125.87	123.71
2.0	14.57	14.85	15.12	15.40	137.30	134.73	132.25	129.87

(iii) $V_P = -3.5$ V and $I_{DSS} = 6$ mA

v_{XY} (V)	i_X (mA)				R_{XY} (Ω)			
	λ = 0	λ = 0.01	λ = 0.02	λ = 0.03	λ = 0	λ = 0.01	λ = 0.02	λ = 0.03
−0.5	−1.83	−1.84	−1.85	−1.86	272.97	271.64	270.32	269.01
−0.4	−1.44	−1.45	−1.45	−1.46	277.86	276.77	275.69	274.62
−0.3	−1.07	−1.07	−1.07	−1.07	281.68	280.85	280.02	279.20
−0.2	−0.70	−0.70	−0.70	−0.71	285.56	285.00	284.44	283.88
−0.1	−0.35	−0.35	−0.35	−0.35	289.56	289.27	288.99	288.70
−0.08	−0.28	−0.28	−0.28	−0.28	290.37	290.14	289.91	289.68
−0.06	−0.21	−0.21	−0.21	−0.21	291.19	291.01	290.84	290.67
−0.04	−0.14	−0.14	−0.14	−0.14	292.01	291.89	291.78	291.66
−0.02	−0.07	−0.07	−0.07	−0.07	292.83	292.78	292.72	292.66
0.02	0.07	0.07	0.07	0.07	294.50	294.44	294.38	294.33
0.04	0.14	0.14	0.14	0.14	295.34	295.22	295.11	294.99
0.06	0.20	0.20	0.20	0.20	296.19	296.01	295.84	295.66
0.08	0.27	0.27	0.27	0.27	297.04	296.80	296.57	296.33
0.1	0.34	0.34	0.34	0.34	297.89	297.60	297.31	297.01
0.2	0.66	0.66	0.66	0.67	302.24	301.65	301.05	300.46
0.3	0.98	0.98	0.98	0.99	306.72	305.82	304.92	304.02
0.4	1.29	1.29	1.30	1.30	311.34	310.12	308.90	307.70
0.5	1.58	1.59	1.60	1.61	316.10	314.55	313.01	311.49
0.6	1.87	1.88	1.89	1.90	321.01	319.12	317.25	315.40
0.7	2.15	2.16	2.18	2.19	326.07	323.83	321.63	319.45
0.8	2.42	2.43	2.45	2.47	331.30	328.70	326.14	323.63
0.9	2.67	2.70	2.72	2.74	336.70	333.73	330.81	327.95
1.0	2.92	2.95	2.98	3.01	342.28	338.93	335.64	332.42
1.1	3.16	3.20	3.23	3.26	348.04	344.30	340.64	337.05
1.2	3.39	3.43	3.47	3.51	354.01	349.86	345.81	341.85
1.3	3.61	3.66	3.70	3.75	360.18	355.61	351.16	346.81
1.4	3.82	3.87	3.93	3.98	366.58	361.57	356.70	351.97
1.5	4.02	4.08	4.14	4.20	373.21	367.75	362.46	357.31
1.6	4.21	4.28	4.34	4.41	380.08	374.16	368.42	362.86
1.7	4.39	4.46	4.54	4.61	387.22	380.81	374.62	368.62
1.8	4.56	4.64	4.72	4.81	394.63	387.72	381.05	374.61
1.9	4.72	4.81	4.90	4.99	402.32	394.90	387.74	380.84
2.0	4.87	4.97	5.07	5.16	410.33	402.36	394.70	387.33

(iv) $V_P = -3.5$ V and $I_{DSS} = 15$ mA

v_{XY} (V)	i_X (mA)				R_{XY} (Ω)			
	λ = 0	λ = 0.01	λ = 0.02	λ = 0.03	λ = 0	λ = 0.01	λ = 0.02	λ = 0.03
−0.5	−4.52	−4.54	−4.56	−4.58	110.70	110.17	109.65	109.13
−0.4	−3.56	−3.57	−3.59	−3.60	112.35	111.92	111.49	111.07
−0.3	−2.64	−2.64	−2.65	−2.66	113.87	113.54	113.22	112.89
−0.2	−1.73	−1.74	−1.74	−1.74	115.43	115.20	114.98	114.76
−0.1	−0.86	−0.86	−0.86	−0.86	117.02	116.91	116.80	116.68
−0.08	−0.68	−0.68	−0.68	−0.68	117.35	117.26	117.17	117.07
−0.06	−0.51	−0.51	−0.51	−0.51	117.67	117.61	117.54	117.47
−0.04	−0.34	−0.34	−0.34	−0.34	118.00	117.96	117.91	117.87
−0.02	−0.17	−0.17	−0.17	−0.17	118.33	118.31	118.29	118.27
0.02	0.17	0.17	0.17	0.17	119.00	118.98	118.95	118.93
0.04	0.34	0.34	0.34	0.34	119.34	119.29	119.24	119.20
0.06	0.50	0.50	0.50	0.50	119.67	119.61	119.54	119.47
0.08	0.67	0.67	0.67	0.67	120.01	119.92	119.83	119.74
0.1	0.83	0.83	0.83	0.83	120.36	120.24	120.12	120.01
0.2	1.64	1.64	1.64	1.65	122.10	121.86	121.63	121.39
0.3	2.42	2.43	2.44	2.44	123.89	123.53	123.17	122.82
0.4	3.18	3.19	3.21	3.22	125.74	125.25	124.77	124.29
0.5	3.92	3.94	3.96	3.97	127.64	127.03	126.42	125.81
0.6	4.63	4.66	4.68	4.71	129.60	128.85	128.11	127.38
0.7	5.32	5.35	5.39	5.43	131.63	130.74	129.87	129.00
0.8	5.98	6.03	6.08	6.12	133.72	132.69	131.68	130.68
0.9	6.62	6.68	6.74	6.80	135.88	134.70	133.55	132.41
1.0	7.24	7.31	7.38	7.45	138.11	136.78	135.48	134.20
1.1	7.83	7.92	8.00	8.09	140.42	138.93	137.48	136.06
1.2	8.40	8.50	8.60	8.70	142.80	141.16	139.55	137.98
1.3	8.95	9.06	9.18	9.29	145.27	143.46	141.69	139.97
1.4	9.47	9.60	9.73	9.86	147.83	145.85	143.91	142.03
1.5	9.97	10.11	10.26	10.40	150.48	148.32	146.22	144.17
1.6	10.44	10.60	10.77	10.93	153.23	150.88	148.61	146.40
1.7	10.89	11.07	11.25	11.43	156.09	153.54	151.09	148.71
1.8	11.32	11.52	11.71	11.91	159.05	156.31	153.66	151.11
1.9	11.72	11.94	12.15	12.37	162.13	159.18	156.34	153.60
2.0	12.10	12.33	12.57	12.80	165.33	162.17	159.13	156.20

Table A.2: Circuit simulation (LT Spice) results for JFET-based grounded VCR using single device (Circuit in Figure 3.1, with $v_C = v_{GS}$, $v_{XY} = v_{DS}$, and $i_X = i_D$): R_{XY} as a function of v_{XY}, with different values of v_C and λ as a parameter. (i) $V_P = -1$ V and $I_{DSS} = 6$ mA, (ii) $V_P = -1$ V and $I_{DSS} = 15$ mA, (iii) $V_P = -3.5$ V and $I_{DSS} = 6$ mA, and (iv) $V_P = -3.5$ V and $I_{DSS} = 15$ mA.

(i) $V_P = -1$ V and $I_{DSS} = 6$ mA

	$R_{XY}(\Omega)$							
v_{XY} (V)	$v_C = 0$ V		$v_C = -0.25$ V		$v_C = -0.5$ V		$v_C = -0.75$ V	
	λ = 0	λ = 0.03	λ = 0	λ = 0.03	λ = 0	λ = 0.03	λ = 0	λ = 0.03
−0.5	68.60	67.65	85.33	84.13	113.11	111.50	168.67	166.23
−0.4	71.44	70.64	89.72	88.70	121.05	119.66	187.19	185.01
−0.3	74.46	73.84	94.59	93.78	130.21	129.08	210.33	208.49
−0.2	77.76	77.32	100.04	99.47	140.89	140.07	240.10	238.69
−0.1	81.37	81.13	106.17	105.86	153.52	153.07	279.78	278.95
−0.08	82.13	81.94	107.49	107.24	156.32	155.96	289.36	288.67
−0.06	82.91	82.76	108.84	108.65	159.23	158.95	299.62	299.09
−0.04	83.70	83.60	110.23	110.10	162.26	162.07	310.64	310.27
−0.02	84.51	84.46	111.65	111.59	165.40	165.30	322.51	322.32
0.02	86.18	86.13	114.61	114.55	172.07	171.97	349.22	349.02
0.04	87.03	86.93	116.16	116.02	175.61	175.41	364.32	363.89
0.06	87.91	87.76	117.74	117.54	179.31	178.99	380.79	380.11
0.08	88.81	88.60	119.37	119.10	183.16	182.73	398.83	397.88
0.1	89.72	89.46	121.05	120.70	187.19	186.64	418.67	417.43
0.2	94.59	94.05	130.21	129.45	210.33	209.10	557.56	554.25
0.3	100.04	99.18	140.89	139.67	240.10	237.99	802.40	795.28
0.4	106.17	104.96	153.52	151.74	279.78	276.51	1069.9	1057.2
0.5	113.11	111.50	168.67	166.23	335.33	330.44	1337.3	1317.7
0.6	121.05	118.98	187.19	183.95	402.40	395.36	1604.8	1576.5
0.7	130.21	127.61	210.33	206.09	469.46	459.91	1872.3	1833.9
0.8	140.89	137.68	239.17	233.66	536.53	524.08	2139.7	2089.8
0.9	153.52	149.58	269.06	262.10	603.60	587.87	2407.2	2344.2
1.0	168.67	163.87	298.96	290.39	670.66	651.30	2674.7	2597.1
1.1	185.53	179.73	328.85	318.50	737.73	714.36	2942.1	2848.5
1.2	202.39	195.51	358.75	346.46	804.79	777.06	3209.6	3098.5
1.3	219.26	211.20	388.64	374.26	871.86	839.40	3477.1	3347.0
1.4	236.13	226.80	418.54	401.90	938.93	901.39	3744.5	3594.1
1.5	252.99	242.31	448.44	429.38	1006.0	963.01	4012.0	3839.8
1.6	269.86	257.73	478.33	456.71	1073.1	1024.3	4279.5	4084.1
1.7	286.72	273.07	508.23	483.88	1140.1	1085.2	4546.9	4327.0
1.8	303.59	288.32	538.12	510.90	1207.2	1145.8	4814.4	4568.6
1.9	320.46	303.49	568.02	537.77	1274.3	1206.1	5081.9	4808.7
2.0	337.32	318.57	597.91	564.48	1341.3	1266.0	5349.3	5047.6

(ii) $V_P = -1$ V and $I_{DSS} = 15$ mA

v_{XY} (V)	$R_{XY}(\Omega)$							
	$v_C = 0$ V		$v_C = -0.25$ V		$v_C = -0.5$ V		$v_C = -0.75$ V	
	λ = 0	λ = 0.03	λ = 0	λ = 0.03	λ = 0	λ = 0.03	λ = 0	λ = 0.03
−0.5	28.66	28.29	35.33	34.87	46.44	45.82	68.67	67.71
−0.4	29.78	29.47	37.09	36.69	49.62	49.08	76.07	75.22
−0.3	30.99	30.74	39.04	38.72	53.28	52.84	85.33	84.61
−0.2	32.30	32.13	41.22	40.99	57.56	57.24	97.24	96.68
−0.1	33.75	33.66	43.67	43.55	62.61	62.43	113.11	112.78
−0.08	34.05	33.98	44.19	44.10	63.73	63.59	116.94	116.67
−0.06	34.36	34.31	44.74	44.66	64.89	64.78	121.05	120.84
−0.04	34.68	34.64	45.29	45.24	66.10	66.03	125.46	125.31
−0.02	35.00	34.98	45.86	45.83	67.36	67.32	130.21	130.13
0.02	35.67	35.65	47.05	47.02	70.03	69.99	140.89	140.81
0.04	36.01	35.98	47.66	47.61	71.44	71.36	146.93	146.76
0.06	36.36	36.31	48.30	48.22	72.92	72.80	153.52	153.25
0.08	36.72	36.64	48.95	48.84	74.46	74.29	160.73	160.35
0.1	37.09	36.99	49.62	49.48	76.07	75.86	168.67	168.17
0.2	39.04	38.83	53.28	52.99	85.33	84.85	224.22	222.91
0.3	41.22	40.88	57.56	57.08	97.24	96.41	322.40	319.56
0.4	43.67	43.20	62.61	61.91	113.11	111.82	429.86	424.82
0.5	46.44	45.82	68.67	67.71	135.33	133.39	537.33	529.47
0.6	49.62	48.81	76.07	74.80	162.39	159.60	644.79	633.51
0.7	53.28	52.27	85.33	83.66	189.46	185.66	752.26	736.94
0.8	57.56	56.30	96.94	94.76	216.52	211.57	859.72	839.77
0.9	62.61	61.06	109.05	106.30	243.59	237.33	967.19	942.00
1.0	68.67	66.78	121.17	117.78	270.65	262.94	1074.7	1043.6
1.1	75.52	73.24	133.29	129.18	297.72	288.41	1182.1	1144.0
1.2	82.38	79.67	145.40	140.53	324.78	313.73	1289.6	1245.2
1.3	89.25	86.07	157.52	151.81	351.85	338.91	1397.1	1345.1
1.4	96.11	92.43	169.64	163.03	378.91	363.94	1504.5	1444.4
1.5	102.98	98.75	181.76	174.18	405.98	388.84	1612.0	1543.2
1.6	109.84	105.05	193.87	185.28	433.04	413.59	1719.4	1641.4
1.7	116.71	111.30	205.99	196.31	460.11	438.20	1826.9	1739.0
1.8	123.57	117.52	218.11	207.28	487.17	462.68	1934.4	1836.1
1.9	130.44	123.71	230.22	218.18	514.24	487.02	2041.8	1932.7
2.0	137.30	129.87	242.34	229.03	541.30	511.22	2149.3	2028.7

(iii) $V_P = -3.5$ V and $I_{DSS} = 6$ mA

v_{XY} (V)	$R_{XY}(\Omega)$							
	$v_C = 0$ V		$v_C = -1$ V		$v_C = -2$ V		$v_C = -3$ V	
	λ = 0	λ = 0.03	λ = 0	λ = 0.03	λ = 0	λ = 0.03	λ = 0	λ = 0.03
−0.5	272.97	269.01	373.21	367.75	585.33	576.74	1363.1	1343.0
−0.4	277.86	274.62	380.08	375.62	602.49	595.39	1460.3	1443.1
−0.3	281.68	279.20	387.22	383.80	620.68	615.18	1572.5	1558.5
−0.2	285.56	283.88	394.62	392.30	640.02	636.22	1703.4	1693.2
−0.1	289.56	288.70	402.32	401.13	660.60	658.63	1858.1	1852.5
−0.08	290.37	289.68	403.90	402.94	664.87	663.29	1892.4	1887.9
−0.06	291.19	290.67	405.49	404.77	669.21	668.01	1928.1	1924.6
−0.04	292.01	291.66	407.09	406.61	673.60	672.79	1965.1	1962.8
−0.02	292.83	292.66	408.70	408.46	678.04	677.64	2003.6	2002.4
0.02	294.50	294.33	411.97	411.73	687.12	686.71	2085.3	2084.1
0.04	295.34	294.99	413.62	413.13	691.75	690.92	2128.7	2126.2
0.06	296.19	295.66	415.29	414.55	696.44	695.19	2174.0	2170.1
0.08	297.04	296.33	416.97	415.98	701.20	699.53	2221.2	2215.9
0.1	297.89	297.01	418.66	417.42	706.02	703.92	2270.5	2263.7
0.2	302.24	300.46	427.34	424.82	731.16	726.82	2554.1	2538.9
0.3	306.72	304.02	436.39	432.54	758.17	751.44	2918.6	2892.7
0.4	311.34	307.70	445.84	440.60	787.25	777.96	3404.8	3364.4
0.5	316.10	311.49	455.70	449.02	818.66	806.62	4085.3	4025.0
0.6	321.01	315.40	466.01	457.84	852.69	837.68	4902.4	4815.8
0.7	326.07	319.45	476.80	467.08	889.67	871.46	5719.4	5601.9
0.8	331.30	323.63	488.11	476.76	930.02	908.32	6536.5	6383.4
0.9	336.70	327.95	499.96	486.92	974.21	948.71	7353.5	7160.4
1.0	342.27	332.42	512.41	497.60	1022.8	993.15	8170.6	7932.8
1.1	348.04	337.05	525.50	508.84	1076.6	1042.3	8987.7	8700.7
1.2	354.01	341.85	539.28	520.68	1136.3	1096.9	9804.7	9464.3
1.3	360.18	346.81	553.80	533.16	1203.0	1158.0	10622	10223
1.4	366.58	351.97	569.12	546.35	1278.0	1226.7	11439	10978
1.5	373.21	357.31	585.33	560.29	1363.1	1304.6	12256	11729
1.6	380.08	362.86	602.49	575.07	1454.0	1387.6	13073	12475
1.7	387.22	368.62	620.68	590.76	1544.9	1470.1	13890	13216
1.8	394.62	374.61	640.02	607.43	1635.7	1552.1	14707	13954
1.9	402.32	380.84	660.60	625.19	1726.6	1633.7	15524	14686
2.0	410.33	387.33	682.55	644.14	1817.5	1714.9	16341	15417

(iv) $V_P = -3.5$ V and $I_{DSS} = 15$ mA

v_{XY} (V)	$R_{XY}(\Omega)$							
	$v_C = 0$ V		$v_C = -1$ V		$v_C = -2$ V		$v_C = -3$ V	
	λ = 0	λ = 0.03	λ = 0	λ = 0.03	λ = 0	λ = 0.03	λ = 0	λ = 0.03
−0.5	110.70	109.13	150.48	148.32	235.33	231.91	546.44	538.42
−0.4	112.35	111.07	153.23	151.46	242.19	239.37	585.33	578.44
−0.3	113.87	112.89	156.09	154.73	249.47	247.28	630.20	624.61
−0.2	115.43	114.76	159.05	158.13	257.21	255.70	682.55	678.50
−0.1	117.02	116.68	162.13	161.66	265.44	264.66	744.42	742.20
−0.08	117.35	117.07	162.76	162.38	267.15	266.52	758.17	756.36
−0.06	117.67	117.47	163.40	163.11	268.88	268.41	772.43	771.05
−0.04	118.00	117.87	164.04	163.84	270.64	270.32	787.25	786.31
−0.02	118.33	118.27	164.68	164.59	272.42	272.26	802.65	802.17
0.02	119.00	118.93	165.99	165.89	276.05	275.88	835.33	834.83
0.04	119.34	119.20	166.65	166.45	277.90	277.57	852.69	851.67
0.06	119.67	119.47	167.32	167.02	279.78	279.28	870.79	869.23
0.08	120.01	119.74	167.99	167.60	281.68	281.01	889.67	887.55
0.1	120.36	120.01	168.67	168.17	283.61	282.77	909.40	906.69
0.2	122.10	121.39	172.14	171.14	293.66	291.94	1022.8	1016.8
0.3	123.89	122.82	175.76	174.23	304.47	301.79	1168.7	1158.3
0.4	125.74	124.29	179.54	177.45	316.10	312.40	1363.1	1347.0
0.5	127.64	125.81	183.48	180.83	328.66	323.87	1635.3	1611.2
0.6	129.60	127.38	187.61	184.36	342.28	336.29	1962.4	1927.8
0.7	131.63	129.00	191.92	188.06	357.07	349.81	2289.5	2242.5
0.8	133.72	130.68	196.44	191.93	373.21	364.56	2616.5	2555.3
0.9	135.88	132.41	201.19	196.00	390.89	380.71	2943.6	2866.3
1.0	138.11	134.20	206.17	200.28	410.33	398.50	3270.6	3175.6
1.1	140.42	136.06	211.40	204.77	431.82	418.15	3597.7	3483.0
1.2	142.80	137.98	216.91	209.51	455.70	440.00	3924.8	3788.6
1.3	145.27	139.97	222.72	214.51	482.39	464.43	4251.8	4092.5
1.4	147.83	142.03	228.85	219.79	512.41	491.92	4578.9	4394.6
1.5	150.48	144.17	235.33	225.37	546.44	523.08	4906.0	4695.0
1.6	153.23	146.40	242.19	231.28	582.87	556.36	5233.0	4993.7
1.7	156.09	148.71	249.47	237.56	619.30	589.45	5560.1	5290.7
1.8	159.05	151.11	257.21	244.23	655.73	622.36	5887.2	5586.0
1.9	162.13	153.60	265.44	251.34	692.16	655.07	6214.2	5879.6
2.0	165.33	156.20	274.22	258.92	728.58	687.61	6541.3	6171.6

Table A.3: Circuit simulation (LT Spice) results for JFET-based floating VCR using single device with SD-bootstrapped gate (Circuit in Figure 3.2 with $R_1 = R_2 = R_3 = R_5 = 10$ kΩ, $R_4 = 5$ kΩ): R_{XY} as a function of v_{XY}, with different values of v_C and λ as a parameter. (i) $V_P = -1$ V and $I_{DSS} = 6$ mA, (ii) $V_P = -1$ V and $I_{DSS} = 15$ mA, (iii) $V_P = -3.5$ V and $I_{DSS} = 6$ mA, and (iv) $V_P = -3.5$ V and $I_{DSS} = 15$ mA.

(i) $V_P = -1$ V and $I_{DSS} = 6$ mA

	$R_{XY}(\Omega)$							
v_{XY} (V)	$v_C = 0$ V		$v_C = -1$ V		$v_C = -2$ V		$v_C = -3$ V	
	λ = 0	λ = 0.03	λ = 0	λ = 0.03	λ = 0	λ = 0.03	λ = 0	λ = 0.03
−1.0	85.29	82.93	113.11	109.93	168.67	163.87	298.96	290.38
−0.9	85.33	83.19	113.11	110.24	168.67	164.34	308.69	300.69
−0.8	85.33	83.43	113.11	110.55	168.67	164.81	318.04	310.69
−0.7	85.33	83.66	113.11	110.87	168.67	165.28	326.40	319.78
−0.6	85.33	83.89	113.11	111.18	168.67	165.76	332.76	326.95
−0.5	85.33	84.13	113.11	111.50	168.67	166.23	335.33	330.44
−0.4	85.33	84.37	113.11	111.82	168.67	166.71	335.33	331.40
−0.3	85.33	84.61	113.11	112.14	168.67	167.20	335.33	332.38
−0.2	85.33	84.85	113.11	112.46	168.67	167.68	335.33	333.36
−0.1	85.33	85.09	113.11	112.79	168.67	168.17	335.33	334.34
−0.08	85.33	85.14	113.11	112.85	168.67	168.27	335.33	334.54
−0.06	85.33	85.19	113.11	112.92	168.67	168.37	335.33	334.74
−0.04	85.33	85.24	113.11	112.98	168.67	168.47	335.33	334.94
−0.02	85.33	85.29	113.11	113.05	168.67	168.57	335.33	335.13
0.02	85.33	85.29	113.11	113.05	168.67	168.57	335.33	335.13
0.04	85.33	85.24	113.11	112.98	168.67	168.47	335.33	334.94
0.06	85.33	85.19	113.11	112.92	168.67	168.37	335.33	334.74
0.08	85.33	85.14	113.11	112.85	168.67	168.27	335.33	334.54
0.1	85.33	85.09	113.11	112.79	168.67	168.17	335.33	334.34
0.2	85.33	84.85	113.11	112.46	168.67	167.68	335.33	333.36
0.3	85.33	84.61	113.11	112.14	168.67	167.20	335.33	332.38
0.4	85.33	84.37	113.11	111.82	168.67	166.71	335.33	331.40
0.5	85.33	84.13	113.11	111.50	168.67	166.23	335.33	330.44
0.6	85.33	83.89	113.11	111.18	168.67	165.76	332.76	326.95
0.7	85.33	83.66	113.11	110.87	168.67	165.28	326.40	319.78
0.8	85.33	83.43	113.11	110.55	168.67	164.81	318.04	310.69
0.9	85.33	83.19	113.11	110.24	168.67	164.34	308.69	300.69
1.0	85.33	82.96	113.11	109.93	168.67	163.87	298.96	290.39

(ii) $V_P = -1$ V and $I_{DSS} = 15$ mA

	$R_{XY}(\Omega)$							
v_{XY} (V)	$v_C = 0$ V		$v_C = -1$ V		$v_C = -2$ V		$v_C = -3$ V	
	λ = 0	λ = 0.03	λ = 0	λ = 0.03	λ = 0	λ = 0.03	λ = 0	λ = 0.03
−1.0	35.33	34.41	46.44	45.21	68.67	66.78	121.17	117.77
−0.9	35.33	34.51	46.44	45.33	68.67	66.96	125.01	121.84
−0.8	35.33	34.60	46.44	45.45	68.67	67.15	128.68	125.77
−0.7	35.33	34.69	46.44	45.57	68.67	67.34	131.95	129.33
−0.6	35.33	34.78	46.44	45.69	68.67	67.52	134.40	132.10
−0.5	35.33	34.87	46.44	45.82	68.67	67.71	135.33	133.39
−0.4	35.33	34.96	46.44	45.94	68.67	67.90	135.33	133.78
−0.3	35.33	35.05	46.44	46.07	68.67	68.09	135.33	134.16
−0.2	35.33	35.15	46.44	46.19	68.67	68.28	135.33	134.55
−0.1	35.33	35.24	46.44	46.32	68.67	68.47	135.33	134.94
−0.08	35.33	35.26	46.44	46.34	68.67	68.51	135.33	135.02
−0.06	35.33	35.28	46.44	46.37	68.67	68.55	135.33	135.10
−0.04	35.33	35.30	46.44	46.39	68.67	68.59	135.33	135.18
−0.02	35.33	35.31	46.44	46.42	68.67	68.63	135.33	135.25
0.02	35.33	35.31	46.44	46.42	68.67	68.63	135.33	135.25
0.04	35.33	35.30	46.44	46.39	68.67	68.59	135.33	135.18
0.06	35.33	35.28	46.44	46.37	68.67	68.55	135.33	135.10
0.08	35.33	35.26	46.44	46.34	68.67	68.51	135.33	135.02
0.1	35.33	35.24	46.44	46.32	68.67	68.47	135.33	134.94
0.2	35.33	35.15	46.44	46.19	68.67	68.28	135.33	134.55
0.3	35.33	35.05	46.44	46.07	68.67	68.09	135.33	134.16
0.4	35.33	34.96	46.44	45.94	68.67	67.90	135.33	133.78
0.5	35.33	34.87	46.44	45.82	68.67	67.71	135.33	133.39
0.6	35.33	34.78	46.44	45.69	68.67	67.52	134.40	132.10
0.7	35.33	34.69	46.44	45.57	68.67	67.34	131.95	129.33
0.8	35.33	34.60	46.44	45.45	68.67	67.15	128.68	125.77
0.9	35.33	34.51	46.44	45.33	68.67	66.96	125.01	121.84
1.0	35.33	34.42	46.44	45.21	68.67	66.78	121.17	117.78

(iii) $V_P = -3.5$ V and $I_{DSS} = 6$ mA

	$R_{XY}(\Omega)$							
v_{XY} (V)	$v_C = 0$ V		$v_C = -2$ V		$v_C = -4$ V		$v_C = -6$ V	
	λ = 0	λ = 0.03	λ = 0	λ = 0.03	λ = 0	λ = 0.03	λ = 0	λ = 0.03
−1.0	292.99	284.59	410.33	398.49	682.55	662.79	2043.6	1984.2
−0.9	293.55	285.94	410.33	399.65	682.55	664.71	2043.6	1990.0
−0.8	293.65	286.86	410.33	400.81	682.55	666.65	2043.6	1995.8
−0.7	293.66	287.70	410.33	401.97	682.55	668.59	2043.6	2001.7
−0.6	293.66	288.54	410.33	403.15	682.55	670.55	2043.6	2007.6
−0.5	293.66	289.38	410.33	404.32	682.55	672.52	2043.7	2013.5
−0.4	293.66	290.23	410.33	405.51	682.55	674.50	2043.7	2019.5
−0.3	293.66	291.08	410.33	406.71	682.55	676.50	2043.7	2025.5
−0.2	293.66	291.94	410.33	407.91	682.55	678.50	2043.7	2031.5
−0.1	293.66	292.80	410.33	409.11	682.55	680.52	2043.7	2037.5
−0.08	293.66	292.97	410.33	409.36	682.55	680.92	2043.7	2038.8
−0.06	293.66	293.14	410.33	409.60	682.55	681.33	2043.7	2040.0
−0.04	293.66	293.32	410.33	409.84	682.55	681.74	2043.7	2041.2
−0.02	293.66	293.49	410.33	410.09	682.55	682.14	2043.7	2042.4
0.02	293.66	293.49	410.33	410.09	682.55	682.14	2043.7	2042.4
0.04	293.66	293.32	410.33	409.84	682.55	681.74	2043.7	2041.2
0.06	293.66	293.14	410.33	409.60	682.55	681.33	2043.7	2040.0
0.08	293.66	292.97	410.33	409.36	682.55	680.92	2043.7	2038.8
0.1	293.66	292.80	410.33	409.11	682.55	680.52	2043.7	2037.5
0.2	293.66	291.94	410.33	407.91	682.55	678.50	2043.7	2031.5
0.3	293.66	291.08	410.33	406.71	682.55	676.50	2043.7	2025.5
0.4	293.66	290.23	410.33	405.51	682.55	674.50	2043.7	2019.5
0.5	293.66	289.38	410.33	404.32	682.55	672.52	2043.7	2013.5
0.6	293.66	288.54	410.33	403.15	682.55	670.55	2043.7	2007.6
0.7	293.66	287.71	410.33	401.97	682.55	668.59	2043.7	2001.7
0.8	293.66	286.88	410.33	400.81	682.55	666.65	2043.7	1995.8
0.9	293.66	286.05	410.33	399.65	682.55	664.71	2043.7	1990.0
1.0	293.67	285.23	410.33	398.49	682.55	662.79	2043.7	1984.2

(iv) $V_P = -3.5$ V and $I_{DSS} = 15$ mA

v_{XY} (V)	$R_{XY}(\Omega)$							
	$v_C = 0$ V		$v_C = -2$ V		$v_C = -4$ V		$v_C = -6$ V	
	λ = 0	λ = 0.03	λ = 0	λ = 0.03	λ = 0	λ = 0.03	λ = 0	λ = 0.03
−1.0	118.58	115.24	165.33	160.63	274.22	266.35	818.66	794.93
−0.9	118.65	115.64	165.33	161.09	274.22	267.12	818.66	797.24
−0.8	118.66	115.98	165.33	161.55	274.22	267.89	818.66	799.56
−0.7	118.67	116.31	165.33	162.01	274.22	268.66	818.66	801.90
−0.6	118.67	116.64	165.33	162.48	274.22	269.44	818.66	804.25
−0.5	118.67	116.97	165.33	162.95	274.22	270.23	818.66	806.62
−0.4	118.67	117.31	165.33	163.42	274.22	271.02	818.66	809.00
−0.3	118.67	117.64	165.33	163.89	274.22	271.81	818.66	811.39
−0.2	118.67	117.98	165.33	164.37	274.22	272.61	818.66	813.80
−0.1	118.67	118.32	165.33	164.85	274.22	273.41	818.66	816.22
−0.08	118.67	118.39	165.33	164.95	274.22	273.57	818.66	816.71
−0.06	118.67	118.46	165.33	165.04	274.22	273.73	818.66	817.19
−0.04	118.67	118.53	165.33	165.14	274.22	273.90	818.66	817.68
−0.02	118.67	118.60	165.33	165.24	274.22	274.06	818.66	818.17
0.02	118.67	118.60	165.33	165.24	274.22	274.06	818.66	818.17
0.04	118.67	118.53	165.33	165.14	274.22	273.90	818.66	817.68
0.06	118.67	118.46	165.33	165.04	274.22	273.73	818.66	817.19
0.08	118.67	118.39	165.33	164.95	274.22	273.57	818.66	816.71
0.1	118.67	118.32	165.33	164.85	274.22	273.41	818.66	816.22
0.2	118.67	117.98	165.33	164.37	274.22	272.61	818.66	813.80
0.3	118.67	117.64	165.33	163.89	274.22	271.81	818.66	811.39
0.4	118.67	117.31	165.33	163.42	274.22	271.02	818.66	809.00
0.5	118.67	116.97	165.33	162.95	274.22	270.23	818.66	806.62
0.6	118.67	116.64	165.33	162.48	274.22	269.44	818.66	804.25
0.7	118.67	116.31	165.33	162.01	274.22	268.66	818.66	801.90
0.8	118.67	115.98	165.33	161.55	274.22	267.89	818.66	799.57
0.9	118.67	115.65	165.33	161.09	274.22	267.12	818.66	797.24
1.0	118.67	115.33	165.33	160.63	274.22	266.35	818.66	794.93

Table A.4: Circuit simulation (LT Spice) results for a floating precision linear VCR using matched JFET device pair with SD-bootstrapped gate and self-tracking arrangement (Circuit in Figure 3.6 with $R_2 = R_3 = 1$ MΩ, $R_4 = R_5 = R_7 = 10$ kΩ, $R_8 = 5$ kΩ): R_{XY} as a function of v_{XY}, with $v_{C1} = -0.5$ V, $v_{C2} = 0.5$ V, and λ as a parameter. (i) $V_P = -1$ V and $I_{DSS} = 6$ mA, (ii) $V_P = -1$ V and $I_{DSS} = 15$ mA, (iii) $V_P = -3.5$ V and $I_{DSS} = 6$ mA, and (iv) $V_P = -3.5$ V and $I_{DSS} = 15$ mA. Values of R_1 selected as the values of R_{XY} of the bootstrapped JFET circuit for λ = 0 and values of V_C as given in parentheses.

(i) $V_P = -1$ V and $I_{DSS} = 6$ mA

	R_{XY} (Ω)							
	$R_1 = 85.33$ Ω ($v_A = 0.0$ V)		$R_1 = 113.11$ Ω ($v_A = -0.5$ V)		$R_1 = 168.67$ Ω ($v_A = -1.0$ V)		$R_1 = 335.33$ Ω ($v_A = -1.5$ V)	
v_{XY} (V)	λ = 0 (Obsrvd. v_A = 0.00 V)	λ = 0.03 (Obsrvd. v_A = −0.03 V)	λ = 0 (Obsrvd. v_A = −0.50 V)	λ = 0.03 (Obsrvd. v_A = −0.52 V)	λ = 0 (Obsrvd. v_A = −1.00 V)	λ = 0.03 (Obsrvd. v_A = −1.01 V)	λ = 0 (Obsrvd. v_A = −1.50 V)	λ = 0.03 (Obsrvd. v_A = −1.51 V)
−1.0	85.29	84.13	113.12	111.53	168.68	166.28	298.99	293.27
−0.9	85.33	84.38	113.12	111.84	168.68	166.76	308.72	303.90
−0.8	85.33	84.62	113.12	112.16	168.68	167.24	318.08	314.26
−0.7	85.33	84.86	113.12	112.47	168.68	167.72	326.45	323.76
−0.6	85.33	85.09	113.12	112.79	168.68	168.20	332.80	331.39
−0.5	85.33	85.33	113.12	113.12	168.68	168.68	335.39	335.39
−0.4	85.33	85.57	113.12	113.44	168.68	169.17	335.39	336.37
−0.3	85.33	85.82	113.12	113.77	168.68	169.66	335.39	337.36
−0.2	85.33	86.06	113.12	114.09	168.68	170.16	335.39	338.36
−0.1	85.33	86.31	113.12	114.42	168.68	170.65	335.39	339.36
−0.08	85.33	86.36	113.12	114.49	168.68	170.75	335.39	339.56
−0.06	85.33	86.41	113.12	114.55	168.68	170.85	335.39	339.76
−0.04	85.33	86.46	113.12	114.62	168.68	170.95	335.39	339.96
−0.02	85.33	86.50	113.12	114.69	168.68	171.05	335.39	340.16
0.02	85.33	86.50	113.12	114.69	168.68	171.05	335.39	340.16
0.04	85.33	86.46	113.12	114.62	168.68	170.95	335.39	339.96
0.06	85.33	86.41	113.12	114.55	168.68	170.85	335.39	339.76
0.08	85.33	86.36	113.12	114.49	168.68	170.75	335.39	339.56
0.1	85.33	86.31	113.12	114.42	168.68	170.65	335.39	339.36
0.2	85.33	86.06	113.12	114.09	168.68	170.16	335.39	338.36
0.3	85.33	85.82	113.12	113.77	168.68	169.66	335.39	337.36
0.4	85.33	85.57	113.12	113.44	168.68	169.17	335.39	336.37
0.5	85.33	85.33	113.12	113.12	168.68	168.68	335.39	335.39
0.6	85.33	85.09	113.12	112.79	168.68	168.20	332.80	331.39
0.7	85.33	84.86	113.12	112.47	168.68	167.72	326.45	323.76
0.8	85.33	84.62	113.12	112.16	168.68	167.24	318.08	314.26
0.9	85.33	84.38	113.12	111.84	168.68	166.76	308.72	303.90
1.0	85.33	84.15	113.12	111.53	168.68	166.29	298.99	293.27

(ii) $V_P = -1$ V and $I_{DSS} = 15$ mA

	$R_{XY}(\Omega)$							
	$R_1 = 35.33\ \Omega$ ($v_A = 0.0$ V)		$R_1 = 46.44\ \Omega$ ($v_A = -0.5$ V)		$R_1 = 68.67\ \Omega$ ($v_A = -1.0$ V)		$R_1 = 135.33\ \Omega$ ($v_A = -1.5$ V)	
v_{XY} (V)	λ = 0 (Obsrvd. v_A = 0.00 V)	λ = 0.03 (Obsrvd. v_A = −0.03 V)	λ = 0 (Obsrvd. v_A = −0.50 V)	λ = 0.03 (Obsrvd. v_A = −0.52 V)	λ = 0 (Obsrvd. v_A = −1.00 V)	λ = 0.03 (Obsrvd. v_A = −1.01 V)	λ = 0 (Obsrvd. v_A = −1.50 V)	λ = 0.03 (Obsrvd. v_A = −1.51 V)
−1.0	35.33	34.87	46.44	45.82	68.67	67.73	121.17	118.92
−0.9	35.33	34.96	46.44	45.94	68.67	67.92	125.01	123.11
−0.8	35.33	35.05	46.44	46.07	68.67	68.10	128.69	127.18
−0.7	35.33	35.15	46.44	46.19	68.67	68.29	131.96	130.90
−0.6	35.33	35.24	46.44	46.32	68.67	68.48	134.41	133.86
−0.5	35.33	35.33	46.44	46.44	68.67	68.67	135.34	135.34
−0.4	35.33	35.42	46.44	46.57	68.67	68.86	135.34	135.73
−0.3	35.33	35.52	46.44	46.69	68.67	69.06	135.34	136.12
−0.2	35.33	35.61	46.44	46.82	68.67	69.25	135.34	136.51
−0.1	35.33	35.71	46.44	46.95	68.67	69.45	135.34	136.91
−0.08	35.33	35.73	46.44	46.98	68.67	69.49	135.34	136.99
−0.06	35.33	35.74	46.44	47.00	68.67	69.53	135.34	137.07
−0.04	35.33	35.76	46.44	47.03	68.67	69.56	135.34	137.15
−0.02	35.33	35.78	46.44	47.05	68.67	69.60	135.34	137.23
0.02	35.33	35.78	46.44	47.05	68.67	69.60	135.34	137.23
0.04	35.33	35.76	46.44	47.03	68.67	69.56	135.34	137.15
0.06	35.33	35.74	46.44	47.00	68.67	69.53	135.34	137.07
0.08	35.33	35.73	46.44	46.98	68.67	69.49	135.34	136.99
0.1	35.33	35.71	46.44	46.95	68.67	69.45	135.34	136.91
0.2	35.33	35.61	46.44	46.82	68.67	69.25	135.34	136.51
0.3	35.33	35.52	46.44	46.69	68.67	69.06	135.34	136.12
0.4	35.33	35.42	46.44	46.57	68.67	68.86	135.34	135.73
0.5	35.33	35.33	46.44	46.44	68.67	68.67	135.34	135.34
0.6	35.33	35.24	46.44	46.32	68.67	68.48	134.41	133.86
0.7	35.33	35.15	46.44	46.19	68.67	68.29	131.96	130.90
0.8	35.33	35.05	46.44	46.07	68.67	68.10	128.69	127.18
0.9	35.33	34.96	46.44	45.94	68.67	67.92	125.01	123.11
1.0	35.33	34.87	46.44	45.82	68.67	67.73	121.17	118.92

(iii) $V_P = -3.5$ V and $I_{DSS} = 6$ mA

	$R_{XY}(\Omega)$							
	$R_1 = 293.66\ \Omega$ ($v_A = 0.0$ V)		$R_1 = 410.33\ \Omega$ ($v_A = -2.0$ V)		$R_1 = 682.55\ \Omega$ ($v_A = -4.0$ V)		$R_1 = 2043.7\ \Omega$ ($v_A = -6.0$ V)	
v_{XY} (V)	λ = 0 (Obsrvd. v_A = 0.00 V)	λ = 0.03 (Obsrvd. v_A = −0.10 V)	λ = 0 (Obsrvd. v_A = −2.00 V)	λ = 0.03 (Obsrvd. v_A = −2.07 V)	λ = 0 (Obsrvd. v_A = −4.00 V)	λ = 0.03 (Obsrvd. v_A = −4.05 V)	λ = 0 (Obsrvd. v_A = −6.00 V)	λ = 0.03 (Obsrvd. v_A = −6.02 V)
−1.0	293.04	289.40	410.41	404.49	682.78	672.89	2045.8	2015.9
−0.9	293.59	290.30	410.41	405.66	682.78	674.85	2045.8	2021.9
−0.8	293.69	291.15	410.41	406.84	682.78	676.81	2045.8	2027.8
−0.7	293.70	292.00	410.41	408.02	682.78	678.79	2045.8	2033.8
−0.6	293.70	292.85	410.41	409.22	682.78	680.78	2045.8	2039.8
−0.5	293.70	293.70	410.41	410.41	682.78	682.78	2045.8	2045.8
−0.4	293.70	294.56	410.41	411.62	682.78	684.79	2045.8	2051.8
−0.3	293.70	295.43	410.41	412.83	682.78	686.82	2045.8	2057.9
−0.2	293.70	296.30	410.41	414.05	682.78	688.85	2045.8	2064.0
−0.1	293.70	297.17	410.41	415.28	682.78	690.90	2045.8	2070.2
−0.08	293.70	297.34	410.41	415.52	682.78	691.31	2045.8	2071.4
−0.06	293.70	297.52	410.41	415.77	682.78	691.72	2045.8	2072.7
−0.04	293.70	297.70	410.41	416.02	682.78	692.14	2045.8	2073.9
−0.02	293.70	297.87	410.41	416.26	682.78	692.55	2045.8	2075.2
0.02	293.70	297.87	410.41	416.26	682.78	692.55	2045.8	2075.2
0.04	293.70	297.70	410.41	416.02	682.78	692.14	2045.8	2073.9
0.06	293.70	297.52	410.41	415.77	682.78	691.72	2045.8	2072.7
0.08	293.70	297.34	410.41	415.52	682.78	691.31	2045.8	2071.4
0.1	293.70	297.17	410.41	415.28	682.78	690.90	2045.8	2070.2
0.2	293.70	296.30	410.41	414.05	682.78	688.85	2045.8	2064.0
0.3	293.70	295.43	410.41	412.83	682.78	686.82	2045.8	2057.9
0.4	293.70	294.56	410.41	411.62	682.78	684.79	2045.8	2051.8
0.5	293.70	293.70	410.41	410.41	682.78	682.78	2045.8	2045.8
0.6	293.70	292.85	410.41	409.22	682.78	680.78	2045.8	2039.8
0.7	293.70	292.00	410.41	408.02	682.78	678.79	2045.8	2033.8
0.8	293.70	291.16	410.41	406.84	682.78	676.81	2045.8	2027.8
0.9	293.70	290.32	410.41	405.66	682.78	674.85	2045.8	2021.9
1.0	293.71	289.48	410.41	404.49	682.78	672.89	2045.8	2015.9

(iv) $V_P = -3.5$ V and $I_{DSS} = 15$ mA

	$R_{XY}(\Omega)$							
	$R_1 = 118.67\ \Omega$ ($v_A = 0.0$ V)		$R_1 = 165.33\ \Omega$ ($v_A = -2.0$ V)		$R_1 = 274.22\ \Omega$ ($v_A = -4.0$ V)		$R_1 = 818.66\ \Omega$ ($v_A = -6.0$ V)	
v_{XY} (V)	λ = 0 (Obsrvd. v_A = 0.00 V)	λ = 0.03 (Obsrvd. v_A = −0.10 V)	λ = 0 (Obsrvd. v_A = −2.00 V)	λ = 0.03 (Obsrvd. v_A = −2.07 V)	λ = 0 (Obsrvd. v_A = −4.00 V)	λ = 0.03 (Obsrvd. v_A = −4.04 V)	λ = 0 (Obsrvd. v_A = −6.00 V)	λ = 0.03 (Obsrvd. v_A = −6.02 V)
−1.0	118.59	116.99	165.34	162.99	274.26	270.32	818.99	807.09
−0.9	118.66	117.33	165.34	163.46	274.26	271.10	818.99	809.47
−0.8	118.67	117.67	165.34	163.93	274.26	271.88	818.99	811.83
−0.7	118.68	118.00	165.34	164.40	274.26	272.67	818.99	814.20
−0.6	118.68	118.34	165.34	164.87	274.26	273.46	818.99	816.59
−0.5	118.68	118.68	165.34	165.34	274.26	274.26	818.99	818.99
−0.4	118.68	119.02	165.34	165.82	274.26	275.06	818.99	821.40
−0.3	118.68	119.36	165.34	166.30	274.26	275.86	818.99	823.83
−0.2	118.68	119.70	165.34	166.79	274.26	276.67	818.99	826.28
−0.1	118.68	120.05	165.34	167.27	274.26	277.49	818.99	828.74
−0.08	118.68	120.12	165.34	167.37	274.26	277.65	818.99	829.23
−0.06	118.68	120.19	165.34	167.47	274.26	277.82	818.99	829.73
−0.04	118.68	120.26	165.34	167.57	274.26	277.98	818.99	830.22
−0.02	118.68	120.33	165.34	167.67	274.26	278.15	818.99	830.72
0.02	118.68	120.33	165.34	167.67	274.26	278.15	818.99	830.72
0.04	118.68	120.26	165.34	167.57	274.26	277.98	818.99	830.22
0.06	118.68	120.19	165.34	167.47	274.26	277.82	818.99	829.73
0.08	118.68	120.12	165.34	167.37	274.26	277.65	818.99	829.23
0.1	118.68	120.05	165.34	167.27	274.26	277.49	818.99	828.74
0.2	118.68	119.70	165.34	166.79	274.26	276.67	818.99	826.28
0.3	118.68	119.36	165.34	166.30	274.26	275.86	818.99	823.84
0.4	118.68	119.02	165.34	165.82	274.26	275.06	818.99	821.40
0.5	118.68	118.68	165.34	165.34	274.26	274.26	818.99	818.99
0.6	118.68	118.34	165.34	164.87	274.26	273.46	818.99	816.59
0.7	118.68	118.00	165.34	164.40	274.26	272.67	818.99	814.20
0.8	118.68	117.67	165.34	163.93	274.26	271.88	818.99	811.83
0.9	118.68	117.34	165.34	163.46	274.26	271.10	818.99	809.47
1.0	118.68	117.01	165.34	162.99	274.26	270.32	818.99	807.09

Table A.5: Circuit simulation (LT Spice) results for JFET-based grounded VCR using single device (Circuit in Figure 3.1, with $v_C = v_{GS}$, $v_{XY} = v_{DS}$, and $i_X = i_D$): R_{XY} as a function of v_{XY}, with different values of v_C, and λ for devices with ±33% variation in V_P and I_{DSS}, λ = 0 and 0.03. H.Z. = high impedance (cut-off region).

(i) $V_P = -2$ V and $I_{DSS} = 15$ mA

	$R_{XY}(\Omega)$							
v_{XY} (V)	$v_C = -2.5$ V		$v_C = -2.0$ V		$v_C = -1.5$ V		$v_C = -1.0$ V	
	λ = 0	λ = 0.03	λ = 0	λ = 0.03	λ = 0	λ = 0.03	λ = 0	λ = 0.03
−0.5	H.Z.	H.Z.	535.33	527.48	179.78	177.18	108.67	107.12
−0.4	H.Z.	H.Z.	668.67	660.79	192.48	190.24	113.11	111.82
−0.3	H.Z.	H.Z.	890.89	882.98	207.13	205.32	117.94	116.93
−0.2	H.Z.	H.Z.	1335.3	1327.4	224.22	222.91	123.21	122.50
−0.1	H.Z.	H.Z.	2668.7	2660.7	244.42	243.71	128.98	128.61
−0.08	H.Z.	H.Z.	3335.3	3327.4	248.91	248.33	130.21	129.90
−0.06	H.Z.	H.Z.	4446.5	4438.5	253.57	253.12	131.45	131.22
−0.04	H.Z.	H.Z.	6668.7	6660.7	258.41	258.11	132.72	132.56
−0.02	H.Z.	H.Z.	13335	13327	263.44	263.28	134.01	133.94
0.02	H.Z.	H.Z.	H.Z.	H.Z.	274.11	273.95	136.68	136.60
0.04	H.Z.	H.Z.	H.Z.	H.Z.	279.78	279.45	138.05	137.89
0.06	H.Z.	H.Z.	H.Z.	H.Z.	285.69	285.18	139.46	139.21
0.08	H.Z.	H.Z.	H.Z.	H.Z.	291.86	291.17	140.89	140.56
0.1	H.Z.	H.Z.	H.Z.	H.Z.	298.30	297.42	142.35	141.94
0.2	H.Z.	H.Z.	H.Z.	H.Z.	335.33	333.36	150.15	149.28
0.3	H.Z.	H.Z.	H.Z.	H.Z.	382.95	379.57	158.86	157.48
0.4	H.Z.	H.Z.	H.Z.	H.Z.	446.44	441.20	168.67	166.71
0.5	H.Z.	H.Z.	H.Z.	H.Z.	535.33	527.48	179.78	177.18
0.6	H.Z.	H.Z.	H.Z.	H.Z.	642.40	631.12	192.48	189.14
0.7	H.Z.	H.Z.	H.Z.	H.Z.	749.46	734.15	207.13	202.95
0.8	H.Z.	H.Z.	H.Z.	H.Z.	856.53	836.58	224.22	219.06
0.9	H.Z.	H.Z.	H.Z.	H.Z.	963.60	938.41	244.42	238.10
1.0	H.Z.	H.Z.	H.Z.	H.Z.	1070.7	1039.7	268.67	260.96
1.1	H.Z.	H.Z.	H.Z.	H.Z.	1177.7	1140.3	295.53	286.22
1.2	H.Z.	H.Z.	H.Z.	H.Z.	1284.8	1240.4	322.40	311.34
1.3	H.Z.	H.Z.	H.Z.	H.Z.	1391.9	1339.9	349.26	336.32
1.4	H.Z.	H.Z.	H.Z.	H.Z.	1498.9	1438.8	376.13	361.16
1.5	H.Z.	H.Z.	H.Z.	H.Z.	1606.0	1537.2	402.99	385.85
1.6	H.Z.	H.Z.	H.Z.	H.Z.	1713.1	1635.0	429.86	410.41
1.7	H.Z.	H.Z.	H.Z.	H.Z.	1820.1	1732.2	456.73	434.82
1.8	H.Z.	H.Z.	H.Z.	H.Z.	1927.2	1828.9	483.59	459.10
1.9	H.Z.	H.Z.	H.Z.	H.Z.	2034.3	1925.1	510.46	483.24
2.0	H.Z.	H.Z.	H.Z.	H.Z.	2141.3	2020.7	537.33	507.25

(ii) $V_P = -3$ V and $I_{DSS} = 15$ mA

v_{XY} (V)	$R_{XY}(\Omega)$							
	$v_C = -2.5$ V		$v_C = -2.0$ V		$v_C = -1.5$ V		$v_C = -1.0$ V	
	λ = 0	λ = 0.03	λ = 0	λ = 0.03	λ = 0	λ = 0.03	λ = 0	λ = 0.03
−0.5	401.99	396.11	242.00	238.48	173.43	170.92	135.33	133.39
−0.4	430.56	425.50	252.00	249.05	178.47	176.40	138.36	136.77
−0.3	463.53	459.43	262.86	260.56	183.81	182.21	141.53	140.31
−0.2	501.99	499.02	274.72	273.11	189.50	188.39	144.85	144.01
−0.1	547.44	545.82	287.71	286.86	195.54	194.97	148.34	147.91
−0.08	557.54	556.22	290.46	289.77	196.80	196.34	149.06	148.71
−0.06	568.03	567.01	293.26	292.74	198.07	197.73	149.78	149.52
−0.04	578.91	578.22	296.11	295.76	199.36	199.13	150.51	150.34
−0.02	590.22	589.87	299.02	298.85	200.67	200.55	151.25	151.16
0.02	614.23	613.87	305.02	304.84	203.34	203.22	152.75	152.66
0.04	626.99	626.24	308.12	307.75	204.70	204.46	153.51	153.33
0.06	640.29	639.14	311.27	310.72	206.08	205.71	154.28	154.01
0.08	654.16	652.60	314.49	313.75	207.48	206.99	155.06	154.70
0.1	668.65	666.67	317.78	316.84	208.89	208.28	155.84	155.39
0.2	751.98	747.52	335.33	333.35	216.28	215.02	159.89	158.96
0.3	859.13	851.50	354.93	351.80	224.22	222.25	164.16	162.73
0.4	1002.0	990.15	376.99	372.57	232.76	230.05	168.66	166.71
0.5	1202.0	1184.3	401.99	396.11	242.00	238.48	173.43	170.92
0.6	1442.4	1416.9	430.56	423.02	251.99	247.61	178.47	175.38
0.7	1682.8	1648.3	463.53	454.08	262.86	257.54	183.81	180.12
0.8	1923.2	1878.2	501.99	490.32	274.72	268.38	189.50	185.15
0.9	2163.6	2106.8	547.44	533.16	287.71	280.25	195.54	190.51
1.0	2404.0	2334.1	601.99	584.57	301.99	293.31	202.00	196.23
1.1	2644.3	2560.1	662.19	641.16	317.78	307.76	208.89	202.35
1.2	2884.7	2784.7	722.38	697.43	335.33	323.81	216.28	208.90
1.3	3125.1	3008.1	782.58	753.38	354.93	341.76	224.22	215.95
1.4	3365.5	3230.2	842.78	809.00	376.99	361.96	232.76	223.54
1.5	3605.9	3451.0	902.98	864.31	401.99	384.85	242.00	231.75
1.6	3846.3	3670.5	963.18	919.30	428.79	409.34	252.00	240.64
1.7	4086.7	3888.8	1023.4	973.98	455.59	433.69	262.86	250.30
1.8	4327.1	4105.9	1083.6	1028.3	482.39	457.90	274.72	260.85
1.9	4567.5	4321.7	1143.8	1082.4	509.19	481.97	287.71	272.41
2.0	4807.9	4536.3	1204.0	1136.2	535.99	505.91	301.99	285.13

(iii) $V_P = -4$ V and $I_{DSS} = 15$ mA

v_{XY} (V)	$R_{XY}(\Omega)$							
	$v_C = -2.5$ V		$v_C = -2.0$ V		$v_C = -1.5$ V		$v_C = -1.0$ V	
	λ = 0	λ = 0.03	λ = 0	λ = 0.03	λ = 0	λ = 0.03	λ = 0	λ = 0.03
−0.5	306.76	302.29	239.04	235.56	195.94	193.10	166.10	163.71
−0.4	315.73	312.03	244.42	241.57	199.53	197.21	168.67	166.71
−0.3	325.23	322.37	250.06	247.87	203.26	201.48	171.31	169.82
−0.2	335.33	333.36	255.97	254.47	207.13	205.92	174.04	173.03
−0.1	346.09	345.06	262.16	261.39	211.15	210.53	176.86	176.35
−0.08	348.32	347.50	263.44	262.82	211.97	211.48	177.44	177.02
−0.06	350.58	349.96	264.73	264.26	212.80	212.43	178.02	177.70
−0.04	352.88	352.46	266.03	265.71	213.64	213.39	178.60	178.39
−0.02	355.20	354.99	267.34	267.18	214.48	214.36	179.19	179.08
0.02	359.94	359.73	270.01	269.85	216.19	216.06	180.37	180.27
0.04	362.36	361.93	271.36	271.04	217.05	216.80	180.97	180.76
0.06	364.81	364.16	272.73	272.24	217.92	217.54	181.57	181.25
0.08	367.30	366.43	274.11	273.46	218.80	218.29	182.18	181.75
0.1	369.82	368.72	275.50	274.69	219.69	219.04	182.79	182.26
0.2	382.95	380.69	282.70	281.04	224.22	222.91	185.91	184.82
0.3	397.06	393.56	290.29	287.73	228.95	226.94	189.13	187.48
0.4	412.26	407.42	298.30	294.81	233.88	231.16	192.48	190.24
0.5	428.67	422.39	306.76	302.29	239.04	235.56	195.94	193.10
0.6	446.44	438.62	315.73	310.21	244.42	240.17	199.53	196.07
0.7	465.77	456.27	325.23	318.62	250.06	245.00	203.26	199.16
0.8	486.85	475.53	335.33	327.57	255.97	250.06	207.13	202.37
0.9	509.94	496.64	346.09	337.09	262.16	255.38	211.15	205.70
1.0	535.33	519.86	357.56	347.26	268.67	260.96	215.33	209.18
1.1	563.40	545.53	369.82	358.13	275.50	266.83	219.69	212.80
1.2	594.59	574.07	382.95	369.78	282.70	273.02	224.22	216.57
1.3	629.45	605.97	397.06	382.31	290.29	279.54	228.95	220.51
1.4	668.67	641.88	412.26	395.80	298.30	286.43	233.88	224.62
1.5	713.11	682.57	428.67	410.38	306.76	293.72	239.04	228.92
1.6	760.65	726.00	446.44	426.18	315.73	301.45	244.42	233.41
1.7	808.19	769.18	465.77	443.36	325.23	309.64	250.06	238.12
1.8	855.73	812.11	486.85	462.11	335.33	318.36	255.97	243.06
1.9	903.27	854.81	509.94	482.65	346.09	327.64	262.16	248.24
2.0	950.81	897.26	535.33	505.26	357.56	337.54	268.67	253.68

(iv) $V_P = -3$ V and $I_{DSS} = 10$ mA

v_{XY} (V)	$R_{XY}(\Omega)$							
	$v_C = -2.5$ V		$v_C = -2.0$ V		$v_C = -1.5$ V		$v_C = -1.0$ V	
	λ = 0	λ = 0.03	λ = 0	λ = 0.03	λ = 0	λ = 0.03	λ = 0	λ = 0.03
−0.5	602.01	593.17	362.00	356.71	259.15	255.37	202.00	199.08
−0.4	644.86	637.26	377.00	372.58	266.71	263.59	206.55	204.15
−0.3	694.31	688.16	393.31	389.84	274.73	272.32	211.30	209.46
−0.2	752.01	747.55	411.10	408.67	283.25	281.59	216.29	215.02
−0.1	820.19	817.75	430.58	429.30	292.33	291.46	221.51	220.86
−0.08	835.34	833.35	434.70	433.67	294.21	293.52	222.59	222.07
−0.06	851.07	849.54	438.90	438.12	296.12	295.60	223.68	223.28
−0.04	867.39	866.36	443.18	442.65	298.06	297.70	224.77	224.51
−0.02	884.36	883.83	447.55	447.28	300.02	299.84	225.88	225.75
0.02	920.38	919.83	456.55	456.28	304.02	303.84	228.13	228.00
0.04	939.51	938.39	461.19	460.64	306.06	305.69	229.27	229.00
0.06	959.46	957.74	465.92	465.09	308.13	307.58	230.43	230.02
0.08	980.27	977.93	470.75	469.64	310.22	309.49	231.59	231.05
0.1	1002.0	999.02	475.69	474.28	312.35	311.43	232.77	232.09
0.2	1127.0	1120.3	502.01	499.03	323.43	321.53	238.84	237.44
0.3	1287.7	1276.3	531.42	526.71	335.34	332.38	245.25	243.09
0.4	1502.0	1484.3	564.51	557.86	348.16	344.08	252.00	249.06
0.5	1802.0	1775.4	602.01	593.17	362.00	356.71	259.15	255.37
0.6	2162.4	2124.3	644.86	633.53	377.00	370.41	266.71	262.06
0.7	2522.8	2471.0	694.31	680.12	393.31	385.30	274.73	269.16
0.8	2883.2	2815.8	752.01	734.48	411.10	401.55	283.25	276.71
0.9	3243.6	3158.5	820.19	798.73	430.58	419.36	292.33	284.74
1.0	3604.0	3499.2	902.01	875.85	452.00	438.96	302.00	293.32
1.1	3964.4	3838.0	992.21	960.65	475.69	460.62	312.35	302.50
1.2	4324.8	4174.8	1082.4	1044.9	502.01	484.70	323.43	312.33
1.3	4685.2	4509.7	1172.6	1128.8	531.42	511.62	335.34	322.90
1.4	5045.6	4842.6	1262.8	1212.1	564.51	541.91	348.16	334.28
1.5	5406.1	5173.6	1353.0	1295.0	602.01	576.25	362.00	346.59
1.6	5766.5	5502.7	1443.2	1377.3	642.14	612.92	377.00	359.92
1.7	6126.9	5830.0	1533.4	1459.3	682.27	649.37	393.31	374.42
1.8	6487.3	6155.4	1623.6	1540.7	722.41	685.62	411.09	390.24
1.9	6847.7	6478.9	1713.8	1621.7	762.54	721.66	430.58	407.57
2.0	7208.1	6800.6	1804.0	1702.2	802.67	757.50	452.00	426.65

(v) $V_P = -3$ V and $I_{DSS} = 20$ mA

v_{XY} (V)	$R_{XY}(\Omega)$							
	$v_C = -2.5$ V		$v_C = -2.0$ V		$v_C = -1.5$ V		$v_C = -1.0$ V	
	λ = 0	λ = 0.03	λ = 0	λ = 0.03	λ = 0	λ = 0.03	λ = 0	λ = 0.03
−0.5	302.00	297.60	182.00	179.37	130.57	128.70	102.00	100.55
−0.4	323.43	319.64	189.50	187.30	134.35	132.81	104.27	103.08
−0.3	348.16	345.09	197.65	195.93	138.37	137.17	106.65	105.74
−0.2	377.00	374.78	206.55	205.34	142.63	141.80	109.14	108.52
−0.1	411.09	409.88	216.29	215.65	147.16	146.73	111.76	111.43
−0.08	418.67	417.68	218.35	217.84	148.11	147.76	112.30	112.04
−0.06	426.53	425.77	220.45	220.06	149.06	148.80	112.84	112.64
−0.04	434.70	434.18	222.59	222.33	150.03	149.85	113.39	113.26
−0.02	443.18	442.92	224.77	224.64	151.01	150.92	113.94	113.88
0.02	461.19	460.91	229.28	229.14	153.01	152.92	115.07	115.00
0.04	470.75	470.20	231.59	231.32	154.03	153.85	115.64	115.50
0.06	480.73	479.87	233.96	233.55	155.06	154.79	116.21	116.01
0.08	491.14	489.97	236.38	235.82	156.11	155.75	116.80	116.53
0.1	502.01	500.52	238.84	238.14	157.17	156.72	117.39	117.05
0.2	564.51	561.16	252.00	250.52	162.72	161.77	120.42	119.73
0.3	644.86	639.15	266.71	264.37	168.67	167.20	123.62	122.56
0.4	752.01	743.14	283.25	279.94	175.08	173.05	127.00	125.54
0.5	902.01	888.74	302.00	297.60	182.00	179.37	130.57	128.70
0.6	1082.4	1063.3	323.43	317.78	189.50	186.22	134.35	132.05
0.7	1262.8	1236.9	348.16	341.08	197.65	193.67	138.36	135.60
0.8	1443.2	1409.5	377.00	368.26	206.55	201.80	142.63	139.38
0.9	1623.6	1581.1	411.09	400.39	216.29	210.71	147.16	143.40
1.0	1804.0	1751.6	452.00	438.96	227.00	220.51	152.00	147.69
1.1	1984.4	1921.2	497.20	481.45	238.84	231.34	157.17	152.28
1.2	2164.8	2089.8	542.40	523.71	252.00	243.38	162.72	157.20
1.3	2345.2	2257.5	587.60	565.72	266.71	256.85	168.67	162.49
1.4	2525.6	2424.1	632.80	607.49	283.25	272.00	175.08	168.18
1.5	2706.0	2589.8	678.00	649.02	302.00	289.17	182.00	174.34
1.6	2886.4	2754.6	723.20	690.32	322.13	307.57	189.50	181.00
1.7	3066.8	2918.4	768.40	731.38	342.27	325.86	197.65	188.26
1.8	3247.2	3081.3	813.60	772.21	362.40	344.06	206.55	196.17
1.9	3427.6	3243.3	858.80	812.80	382.53	362.15	216.29	204.84
2.0	3608.0	3404.4	904.00	853.17	402.67	380.14	227.00	214.38

Table A.6: Circuit simulation (LT Spice) results for JFET-based floating VCR using single device with SD-bootstrapped gate (Circuit in Figure 3.2 with $R_1 = R_2 = R_3 = R_5 = 10$ kΩ, $R_4 = 5$ kΩ): R_{XY} as a function of v_{XY}, with different values of v_C and λ for devices with ±33% variation in V_P and I_{DSS}, λ = 0 and 0.03. H.Z. = high impedance (cut-off region).

(i) $V_P = -2$ V and $I_{DSS} = 15$ mA

	R_{XY} (Ω)							
v_{XY} (V)	$v_C = -5.0$ V		$v_C = -4.0$ V		$v_C = -3.0$ V		$v_C = -2.0$ V	
	λ = 0	λ = 0.03	λ = 0	λ = 0.03	λ = 0	λ = 0.03	λ = 0	λ = 0.03
−1.0	H.Z.	H.Z.	1070.7	1039.6	268.67	260.96	135.33	131.51
−0.9	H.Z.	H.Z.	1189.2	1158.1	268.67	261.71	135.33	131.88
−0.8	H.Z.	H.Z.	1337.3	1306.1	268.67	262.46	135.33	132.25
−0.7	H.Z.	H.Z.	1527.8	1496.5	268.67	263.22	135.33	132.63
−0.6	H.Z.	H.Z.	1781.8	1750.4	268.67	263.99	135.33	133.01
−0.5	H.Z.	H.Z.	2137.3	2105.8	268.67	264.75	135.33	133.39
−0.4	H.Z.	H.Z.	2670.6	2639.0	268.67	265.53	135.33	133.78
−0.3	H.Z.	H.Z.	3559.5	3527.8	268.67	266.31	135.33	134.16
−0.2	H.Z.	H.Z.	5337.2	5305.4	268.67	267.09	135.33	134.55
−0.1	H.Z.	H.Z.	10670	10638	268.67	267.87	135.33	134.94
−0.08	H.Z.	H.Z.	13337	13305	268.67	268.03	135.33	135.02
−0.06	H.Z.	H.Z.	17781	17749	268.67	268.19	135.33	135.10
−0.04	H.Z.	H.Z.	26669	26637	268.67	268.35	135.33	135.18
−0.02	H.Z.	H.Z.	53329	53297	268.67	268.51	135.33	135.25
0.02	H.Z.	H.Z.	53329	53297	268.67	268.51	135.33	135.25
0.04	H.Z.	H.Z.	26669	26637	268.67	268.35	135.33	135.18
0.06	H.Z.	H.Z.	17781	17749	268.67	268.19	135.33	135.10
0.08	H.Z.	H.Z.	13337	13305	268.67	268.03	135.33	135.02
0.1	H.Z.	H.Z.	10670	10638	268.67	267.87	135.33	134.94
0.2	H.Z.	H.Z.	5337.3	5305.5	268.67	267.09	135.33	134.55
0.3	H.Z.	H.Z.	3559.5	3527.8	268.67	266.31	135.33	134.16
0.4	H.Z.	H.Z.	2670.6	2639.1	268.67	265.53	135.33	133.78
0.5	H.Z.	H.Z.	2137.3	2105.8	268.67	264.75	135.33	133.39
0.6	H.Z.	H.Z.	1781.8	1750.4	268.67	263.99	135.33	133.01
0.7	H.Z.	H.Z.	1527.8	1496.5	268.67	263.22	135.33	132.63
0.8	H.Z.	H.Z.	1337.3	1306.1	268.67	262.46	135.33	132.25
0.9	H.Z.	H.Z.	1189.2	1158.1	268.67	261.71	135.33	131.88
1.0	H.Z.	H.Z.	1070.7	1039.7	268.67	260.96	135.33	131.51

(ii) $V_P = -3$ V and $I_{DSS} = 15$ mA

v_{XY} (V)	$R_{XY}(\Omega)$							
	$v_C = -5.0$ V		$v_C = -4.0$ V		$v_C = -3.0$ V		$v_C = -2.0$ V	
	λ = 0	λ = 0.03	λ = 0	λ = 0.03	λ = 0	λ = 0.03	λ = 0	λ = 0.03
−1.0	601.99	584.57	301.99	293.31	202.00	196.23	152.00	147.69
−0.9	601.99	586.26	301.99	294.16	202.00	196.79	152.00	148.10
−0.8	601.99	587.97	301.99	295.01	202.00	197.35	152.00	148.53
−0.7	601.99	589.69	301.99	295.86	202.00	197.92	152.00	148.95
−0.6	601.99	591.41	301.99	296.72	202.00	198.49	152.00	149.38
−0.5	601.99	593.15	301.99	297.59	202.00	199.07	152.00	149.81
−0.4	601.99	594.90	301.99	298.46	202.00	199.65	152.00	150.24
−0.3	601.99	596.65	301.99	299.34	202.00	200.23	152.00	150.68
−0.2	601.99	598.42	301.99	300.22	202.00	200.81	152.00	151.11
−0.1	601.99	600.20	301.99	301.10	202.00	201.40	152.00	151.55
−0.08	601.99	600.55	301.99	301.28	202.00	201.52	152.00	151.64
−0.06	601.99	600.91	301.99	301.46	202.00	201.64	152.00	151.73
−0.04	601.99	601.27	301.99	301.64	202.00	201.76	152.00	151.82
−0.02	601.99	601.63	301.99	301.82	202.00	201.88	152.00	151.91
0.02	601.99	601.63	301.99	301.82	202.00	201.88	152.00	151.91
0.04	601.99	601.27	301.99	301.64	202.00	201.76	152.00	151.82
0.06	601.99	600.91	301.99	301.46	202.00	201.64	152.00	151.73
0.08	601.99	600.56	301.99	301.28	202.00	201.52	152.00	151.64
0.1	601.99	600.20	301.99	301.10	202.00	201.40	152.00	151.55
0.2	601.99	598.42	301.99	300.22	202.00	200.81	152.00	151.11
0.3	601.99	596.65	301.99	299.34	202.00	200.23	152.00	150.68
0.4	601.99	594.90	301.99	298.46	202.00	199.65	152.00	150.24
0.5	601.99	593.15	301.99	297.59	202.00	199.07	152.00	149.81
0.6	601.99	591.41	301.99	296.72	202.00	198.49	152.00	149.38
0.7	601.99	589.69	301.99	295.86	202.00	197.92	152.00	148.95
0.8	601.99	587.97	301.99	295.01	202.00	197.35	152.00	148.53
0.9	601.99	586.27	301.99	294.16	202.00	196.79	152.00	148.11
1.0	601.99	584.57	301.99	293.31	202.00	196.23	152.00	147.69

(iii) $V_P = -4$ V and $I_{DSS} = 15$ mA

	$R_{XY}(\Omega)$							
v_{XY} (V)	$v_C = -5.0$ V		$v_C = -4.0$ V		$v_C = -3.0$ V		$v_C = -2.0$ V	
	λ = 0	λ = 0.03	λ = 0	λ = 0.03	λ = 0	λ = 0.03	λ = 0	λ = 0.03
−1.0	357.56	347.26	268.67	260.96	215.33	209.18	179.78	174.66
−0.9	357.56	348.26	268.67	261.71	215.33	209.78	179.78	175.16
−0.8	357.56	349.27	268.67	262.46	215.33	210.38	179.78	175.66
−0.7	357.56	350.28	268.67	263.22	215.33	210.99	179.78	176.16
−0.6	357.56	351.30	268.67	263.99	215.33	211.60	179.78	176.67
−0.5	357.56	352.33	268.67	264.76	215.33	212.21	179.78	177.18
−0.4	357.56	353.36	268.67	265.53	215.33	212.83	179.78	177.69
−0.3	357.56	354.40	268.67	266.31	215.33	213.45	179.78	178.21
−0.2	357.56	355.45	268.67	267.09	215.33	214.07	179.78	178.73
−0.1	357.56	356.50	268.67	267.87	215.33	214.70	179.78	179.25
−0.08	357.56	356.71	268.67	268.03	215.33	214.83	179.78	179.36
−0.06	357.56	356.92	268.67	268.19	215.33	214.95	179.78	179.46
−0.04	357.56	357.13	268.67	268.35	215.33	215.08	179.78	179.57
−0.02	357.56	357.34	268.67	268.51	215.33	215.21	179.78	179.67
0.02	357.56	357.34	268.67	268.51	215.33	215.21	179.78	179.67
0.04	357.56	357.13	268.67	268.35	215.33	215.08	179.78	179.57
0.06	357.56	356.92	268.67	268.19	215.33	214.95	179.78	179.46
0.08	357.56	356.71	268.67	268.03	215.33	214.83	179.78	179.36
0.1	357.56	356.50	268.67	267.87	215.33	214.70	179.78	179.25
0.2	357.56	355.45	268.67	267.09	215.33	214.07	179.78	178.73
0.3	357.56	354.40	268.67	266.31	215.33	213.45	179.78	178.21
0.4	357.56	353.36	268.67	265.53	215.33	212.83	179.78	177.69
0.5	357.56	352.33	268.67	264.76	215.33	212.21	179.78	177.18
0.6	357.56	351.30	268.67	263.99	215.33	211.60	179.78	176.67
0.7	357.56	350.28	268.67	263.22	215.33	210.99	179.78	176.16
0.8	357.56	349.27	268.67	262.46	215.33	210.38	179.78	175.66
0.9	357.56	348.26	268.67	261.71	215.33	209.78	179.78	175.16
1.0	357.56	347.26	268.67	260.96	215.33	209.18	179.78	174.66

(iv) $V_P = -3$ V and $I_{DSS} = 10$ mA

	$R_{XY}(\Omega)$							
v_{XY} (V)	$v_C = -5.0$ V		$v_C = -4.0$ V		$v_C = -3.0$ V		$v_C = -2.0$ V	
	λ = 0	λ = 0.03	λ = 0	λ = 0.03	λ = 0	λ = 0.03	λ = 0	λ = 0.03
−1.0	902.01	875.85	452.00	438.96	302.00	293.32	227.00	220.51
−0.9	902.01	878.40	452.00	440.23	302.00	294.17	227.00	221.14
−0.8	902.01	880.96	452.00	441.50	302.00	295.02	227.00	221.78
−0.7	902.01	883.54	452.00	442.79	302.00	295.87	227.00	222.42
−0.6	902.01	886.13	452.00	444.08	302.00	296.73	227.00	223.06
−0.5	902.01	888.74	452.00	445.38	302.00	297.60	227.00	223.71
−0.4	902.01	891.36	452.00	446.69	302.00	298.47	227.00	224.36
−0.3	902.01	894.00	452.00	448.01	302.00	299.34	227.00	225.01
−0.2	902.01	896.65	452.00	449.33	302.00	300.23	227.00	225.67
−0.1	902.01	899.32	452.00	450.66	302.00	301.11	227.00	226.34
−0.08	902.01	899.86	452.00	450.93	302.00	301.29	227.00	226.47
−0.06	902.01	900.39	452.00	451.20	302.00	301.47	227.00	226.60
−0.04	902.01	900.93	452.00	451.47	302.00	301.65	227.00	226.73
−0.02	902.01	901.47	452.00	451.74	302.00	301.82	227.00	226.87
0.02	902.01	901.47	452.00	451.74	302.00	301.82	227.00	226.87
0.04	902.01	900.93	452.00	451.47	302.00	301.65	227.00	226.73
0.06	902.01	900.39	452.00	451.20	302.00	301.47	227.00	226.60
0.08	902.01	899.86	452.00	450.93	302.00	301.29	227.00	226.47
0.1	902.01	899.32	452.00	450.66	302.00	301.11	227.00	226.34
0.2	902.01	896.65	452.00	449.33	302.00	300.23	227.00	225.67
0.3	902.01	894.00	452.00	448.01	302.00	299.34	227.00	225.01
0.4	902.01	891.36	452.00	446.69	302.00	298.47	227.00	224.36
0.5	902.01	888.74	452.00	445.38	302.00	297.60	227.00	223.71
0.6	902.01	886.13	452.00	444.08	302.00	296.73	227.00	223.06
0.7	902.01	883.54	452.00	442.79	302.00	295.87	227.00	222.42
0.8	902.01	880.96	452.00	441.50	302.00	295.02	227.00	221.78
0.9	902.01	878.40	452.00	440.23	302.00	294.17	227.00	221.14
1.0	902.01	875.85	452.00	438.96	302.00	293.32	227.00	220.51

(v) $V_P = -3$ V and $I_{DSS} = 20$ mA

v_{XY} (V)	$R_{XY}(\Omega)$							
	$v_C = -2.5$ V		$v_C = -2.0$ V		$v_C = -1.5$ V		$v_C = -1.0$ V	
	λ = 0	λ = 0.03	λ = 0	λ = 0.03	λ = 0	λ = 0.03	λ = 0	λ = 0.03
−1.0	452.00	438.95	227.00	220.51	152.00	147.69	114.50	111.28
−0.9	452.00	440.22	227.00	221.14	152.00	148.11	114.50	111.59
−0.8	452.00	441.50	227.00	221.78	152.00	148.53	114.50	111.91
−0.7	452.00	442.79	227.00	222.41	152.00	148.96	114.50	112.23
−0.6	452.00	444.08	227.00	223.06	152.00	149.38	114.50	112.55
−0.5	452.00	445.38	227.00	223.71	152.00	149.81	114.50	112.87
−0.4	452.00	446.69	227.00	224.36	152.00	150.25	114.50	113.19
−0.3	452.00	448.01	227.00	225.01	152.00	150.68	114.50	113.52
−0.2	452.00	449.33	227.00	225.67	152.00	151.12	114.50	113.84
−0.1	452.00	450.66	227.00	226.34	152.00	151.56	114.50	114.17
−0.08	452.00	450.93	227.00	226.47	152.00	151.65	114.50	114.24
−0.06	452.00	451.20	227.00	226.60	152.00	151.74	114.50	114.30
−0.04	452.00	451.47	227.00	226.73	152.00	151.82	114.50	114.37
−0.02	452.00	451.74	227.00	226.87	152.00	151.91	114.50	114.43
0.02	452.00	451.73	227.00	226.87	152.00	151.91	114.50	114.43
0.04	452.00	451.47	227.00	226.73	152.00	151.82	114.50	114.37
0.06	452.00	451.20	227.00	226.60	152.00	151.74	114.50	114.30
0.08	452.00	450.93	227.00	226.47	152.00	151.65	114.50	114.24
0.1	452.00	450.66	227.00	226.34	152.00	151.56	114.50	114.17
0.2	452.00	449.33	227.00	225.67	152.00	151.12	114.50	113.84
0.3	452.00	448.01	227.00	225.01	152.00	150.68	114.50	113.52
0.4	452.00	446.69	227.00	224.36	152.00	150.25	114.50	113.19
0.5	452.00	445.38	227.00	223.71	152.00	149.81	114.50	112.87
0.6	452.00	444.08	227.00	223.06	152.00	149.38	114.50	112.55
0.7	452.00	442.79	227.00	222.42	152.00	148.96	114.50	112.23
0.8	452.00	441.50	227.00	221.78	152.00	148.53	114.50	111.91
0.9	452.00	440.23	227.00	221.14	152.00	148.11	114.50	111.60
1.0	452.00	438.95	227.00	220.51	152.00	147.69	114.50	111.28

Table A.7: Circuit simulation (LT Spice) results for a floating precision linear VCR using matched JFET device pair with SD-bootstrapped gate and self-tracking arrangement (Circuit in Figure 3.6 with $R_2 = R_3 = 1$ MΩ, $R_4 = R_5 = R_7 = 10$ kΩ, $R_8 = 5$ kΩ): R_{XY} as a function of v_{XY}, with $R_1 = 300$ Ω, $v_{C2} = 0.5$ V, and v_{C1} as the voltage for devices with ±33% variation in V_P and I_{DSS}, λ = 0 and 0.03.

(i) $V_P = -2$ V and $I_{DSS} = 15$ mA

	R_{XY} (Ω)							
	$v_{C1} = -0.25$ V (Calc. $R_{XY} = 600$ Ω)		$v_{C1} = -0.50$ V (Calc. $R_{XY} = 300$ Ω)		$v_{C1} = -0.75$ V (Calc. $R_{XY} = 200$ Ω)		$v_{C1} = -1.00$ V (Calc. $R_{XY} = 150$ Ω)	
v_{XY} (V)	λ = 0 (Obsrvd. v_A = −3.56 V)	λ = 0.03 (Obsrvd. v_A = −3.56 V)	λ = 0 (Obsrvd. v_A = −3.11 V)	λ = 0.03 (Obsrvd. v_A = −3.12 V)	λ = 0 (Obsrvd. v_A = −2.65 V)	λ = 0.03 (Obsrvd. v_A = −2.67 V)	λ = 0 (Obsrvd. v_A = −2.20 V)	λ = 0.03 (Obsrvd. v_A = −2.22 V)
−1.0	514.08	504.09	299.23	294.69	200.02	197.16	150.01	147.88
−0.9	533.87	525.38	300.04	296.57	200.02	197.73	150.01	148.30
−0.8	553.68	546.91	300.04	297.44	200.02	198.30	150.01	148.73
−0.7	572.63	567.82	300.04	298.30	200.02	198.87	150.01	149.15
−0.6	589.11	586.55	300.04	299.17	200.02	199.44	150.01	149.58
−0.5	600.17	600.17	300.04	300.04	200.02	200.02	150.01	150.01
−0.4	602.14	604.50	300.04	300.92	200.02	200.60	150.01	150.44
−0.3	602.14	606.29	300.04	301.80	200.02	201.19	150.01	150.88
−0.2	602.14	608.08	300.04	302.69	200.02	201.77	150.01	151.32
−0.1	602.14	609.89	300.04	303.59	200.02	202.36	150.01	151.76
−0.08	602.14	610.25	300.04	303.76	200.02	202.48	150.01	151.85
−0.06	602.14	610.61	300.04	303.94	200.02	202.60	150.01	151.94
−0.04	602.14	610.98	300.04	304.12	200.02	202.72	150.01	152.02
−0.02	602.14	611.34	300.04	304.30	200.02	202.84	150.01	152.11
0.02	602.14	611.34	300.04	304.30	200.02	202.84	150.01	152.11
0.04	602.14	610.98	300.04	304.12	200.02	202.72	150.01	152.02
0.06	602.14	610.61	300.04	303.94	200.02	202.60	150.01	151.94
0.08	602.14	610.25	300.04	303.77	200.02	202.48	150.01	151.85
0.1	602.14	609.89	300.04	303.59	200.02	202.36	150.01	151.76
0.2	602.14	608.08	300.04	302.69	200.02	201.77	150.01	151.32
0.3	602.14	606.29	300.04	301.80	200.02	201.19	150.01	150.88
0.4	602.14	604.50	300.04	300.92	200.02	200.60	150.01	150.44
0.5	600.18	600.18	300.04	300.04	200.02	200.02	150.01	150.01
0.6	589.11	586.55	300.04	299.17	200.02	199.44	150.01	149.58
0.7	572.63	567.83	300.04	298.30	200.02	198.87	150.01	149.15
0.8	553.68	546.91	300.04	297.44	200.02	198.30	150.01	148.73
0.9	533.87	525.38	300.04	296.57	200.02	197.73	150.01	148.30
1.0	514.08	504.09	299.23	294.69	200.02	197.16	150.01	147.88

(ii) $V_P = -3$ V and $I_{DSS} = 15$ mA

	$R_{XY}(\Omega)$							
	$v_{C1} = -0.25$ V (Calc. $R_{XY} = 600\ \Omega$)		$v_{C1} = -0.50$ V (Calc. $R_{XY} = 300\ \Omega$)		$v_{C1} = -0.75$ V (Calc. $R_{XY} = 200\ \Omega$)		$v_{C1} = -1.00$ V (Calc. $R_{XY} = 150\ \Omega$)	
v_{XY} (V)	λ = 0 (Obsrvd. v_A = −5.00 V)	λ = 0.03 (Obsrvd. v_A = −5.01 V)	λ = 0 (Obsrvd. v_A = −3.99 V)	λ = 0.03 (Obsrvd. v_A = −4.02 V)	λ = 0 (Obsrvd. v_A = −2.97 V)	λ = 0.03 (Obsrvd. v_A = −3.01 V)	λ = 0 (Obsrvd. v_A = −1.95 V)	λ = 0.03 (Obsrvd. v_A = −2.01 V)
−1.0	600.17	591.48	300.04	295.73	200.02	197.16	150.01	147.88
−0.9	600.17	593.21	300.04	296.58	200.02	197.73	150.01	148.30
−0.8	600.17	594.93	300.04	297.44	200.02	198.30	150.01	148.73
−0.7	600.17	596.67	300.04	298.30	200.02	198.87	150.01	149.15
−0.6	600.17	598.42	300.04	299.17	200.02	199.44	150.01	149.58
−0.5	600.17	600.17	300.04	300.04	200.02	200.02	150.01	150.01
−0.4	600.17	601.94	300.04	300.92	200.02	200.60	150.01	150.44
−0.3	600.17	603.72	300.04	301.80	200.02	201.19	150.01	150.88
−0.2	600.17	605.51	300.04	302.69	200.02	201.77	150.01	151.32
−0.1	600.17	607.31	300.04	303.59	200.02	202.36	150.01	151.76
−0.08	600.17	607.67	300.04	303.76	200.02	202.48	150.01	151.85
−0.06	600.17	608.03	300.04	303.94	200.02	202.60	150.01	151.94
−0.04	600.17	608.39	300.04	304.12	200.02	202.72	150.01	152.02
−0.02	600.17	608.75	300.04	304.30	200.02	202.84	150.01	152.11
0.02	600.17	608.75	300.04	304.30	200.02	202.84	150.01	152.11
0.04	600.17	608.39	300.04	304.12	200.02	202.72	150.01	152.02
0.06	600.17	608.03	300.04	303.94	200.02	202.60	150.01	151.94
0.08	600.17	607.67	300.04	303.76	200.02	202.48	150.01	151.85
0.1	600.17	607.31	300.04	303.59	200.02	202.36	150.01	151.76
0.2	600.17	605.51	300.04	302.69	200.02	201.77	150.01	151.32
0.3	600.17	603.72	300.04	301.80	200.02	201.19	150.01	150.88
0.4	600.17	601.94	300.04	300.92	200.02	200.60	150.01	150.44
0.5	600.17	600.17	300.04	300.04	200.02	200.02	150.01	150.01
0.6	600.17	598.42	300.04	299.17	200.02	199.44	150.01	149.58
0.7	600.17	596.67	300.04	298.30	200.02	198.87	150.01	149.15
0.8	600.17	594.93	300.04	297.44	200.02	198.30	150.01	148.73
0.9	600.17	593.21	300.04	296.58	200.02	197.73	150.01	148.30
1.0	600.17	591.48	300.04	295.73	200.02	197.16	150.01	147.88

(iii) $V_P = -4$ V and $I_{DSS} = 15$ mA

	$R_{XY}(\Omega)$							
	$v_{C1} = -0.25$ V (Calc. $R_{XY} = 600\ \Omega$)		$v_{C1} = -0.50$ V (Calc. $R_{XY} = 300\ \Omega$)		$v_{C1} = -0.75$ V (Calc. $R_{XY} = 200\ \Omega$)		$v_{C1} = -1.00$ V (Calc. $R_{XY} = 150\ \Omega$)	
v_{XY} (V)	λ = 0 (Obsrvd. v_A = −6.22 V)	λ = 0.03 (Obsrvd. v_A = −6.24 V)	λ = 0 (Obsrvd. v_A = −4.42 V)	λ = 0.03 (Obsrvd. v_A = −4.47 V)	λ = 0 (Obsrvd. v_A = −2.61 V)	λ = 0.03 (Obsrvd. v_A = −2.69 V)	λ = 0 (Obsrvd. v_A = −0.79 V)	λ = 0.03 (Obsrvd. v_A = −0.90 V)
−1.0	600.17	591.49	300.04	295.73	200.02	197.16	150.01	147.88
−0.9	600.17	593.21	300.04	296.58	200.02	197.73	150.01	148.30
−0.8	600.17	594.93	300.04	297.44	200.02	198.30	150.01	148.73
−0.7	600.17	596.67	300.04	298.30	200.02	198.87	150.01	149.15
−0.6	600.17	598.42	300.04	299.17	200.02	199.44	150.01	149.58
−0.5	600.17	600.17	300.04	300.04	200.02	200.02	150.01	150.01
−0.4	600.17	601.94	300.04	300.92	200.02	200.60	150.01	150.44
−0.3	600.17	603.72	300.04	301.80	200.02	201.19	150.01	150.88
−0.2	600.17	605.51	300.04	302.69	200.02	201.77	150.01	151.32
−0.1	600.17	607.31	300.04	303.59	200.02	202.36	150.01	151.76
−0.08	600.17	607.67	300.04	303.76	200.02	202.48	150.01	151.85
−0.06	600.17	608.03	300.04	303.94	200.02	202.60	150.01	151.94
−0.04	600.17	608.39	300.04	304.12	200.02	202.72	150.01	152.02
−0.02	600.17	608.75	300.04	304.30	200.02	202.84	150.01	152.11
0.02	600.17	608.75	300.04	304.30	200.02	202.84	150.01	152.11
0.04	600.17	608.39	300.04	304.12	200.02	202.72	150.01	152.02
0.06	600.17	608.03	300.04	303.94	200.02	202.60	150.01	151.94
0.08	600.17	607.67	300.04	303.76	200.02	202.48	150.01	151.85
0.1	600.17	607.31	300.04	303.59	200.02	202.36	150.01	151.76
0.2	600.17	605.51	300.04	302.69	200.02	201.77	150.01	151.32
0.3	600.17	603.72	300.04	301.80	200.02	201.19	150.01	150.88
0.4	600.17	601.94	300.04	300.92	200.02	200.60	150.01	150.44
0.5	600.17	600.17	300.04	300.04	200.02	200.02	150.01	150.01
0.6	600.17	598.42	300.04	299.17	200.02	199.44	150.01	149.58
0.7	600.17	596.67	300.04	298.30	200.02	198.87	150.01	149.15
0.8	600.17	594.93	300.04	297.44	200.02	198.30	150.01	148.73
0.9	600.17	593.21	300.04	296.58	200.02	197.73	150.01	148.30
1.0	600.17	591.49	300.04	295.73	200.02	197.16	150.01	147.88

(iv) $V_P = -3$ V and $I_{DSS} = 10$ mA

	$R_{XY}(\Omega)$							
	$v_{C1} = -0.25$ V (Calc. $R_{XY} = 600\ \Omega$)		$v_{C1} = -0.50$ V (Calc. $R_{XY} = 300\ \Omega$)		$v_{C1} = -0.75$ V (Calc. $R_{XY} = 200\ \Omega$)		$v_{C1} = -1.00$ V (Calc. $R_{XY} = 150\ \Omega$)	
v_{XY} (V)	λ = 0 (Obsrvd. v_A = −4.50 V)	λ = 0.03 (Obsrvd. v_A = −4.52 V)	λ = 0 (Obsrvd. v_A = −2.98 V)	λ = 0.03 (Obsrvd. v_A = −3.02 V)	λ = 0 (Obsrvd. v_A = −1.45 V)	λ = 0.03 (Obsrvd. v_A = −1.52 V)	λ = 0 (Obsrvd. v_A = 0.08 V)	λ = 0.03 (Obsrvd. v_A = −0.01 V)
−1.0	600.18	591.49	300.04	295.73	200.02	197.16	149.28	147.76
−0.9	600.18	593.21	300.04	296.58	200.02	197.73	149.89	148.28
−0.8	600.18	594.94	300.04	297.44	200.02	198.30	149.99	148.72
−0.7	600.18	596.67	300.04	298.30	200.02	198.87	150.01	149.15
−0.6	600.18	598.42	300.04	299.17	200.02	199.44	150.01	149.58
−0.5	600.18	600.18	300.04	300.04	200.02	200.02	150.01	150.01
−0.4	600.18	601.94	300.04	300.92	200.02	200.60	150.01	150.44
−0.3	600.18	603.72	300.04	301.80	200.02	201.19	150.01	150.88
−0.2	600.18	605.51	300.04	302.69	200.02	201.77	150.01	151.32
−0.1	600.18	607.31	300.04	303.59	200.02	202.37	150.01	151.76
−0.08	600.18	607.67	300.04	303.77	200.02	202.48	150.01	151.85
−0.06	600.18	608.03	300.04	303.94	200.02	202.60	150.01	151.94
−0.04	600.18	608.39	300.04	304.12	200.02	202.72	150.01	152.02
−0.02	600.18	608.76	300.04	304.30	200.02	202.84	150.01	152.11
0.02	600.18	608.75	300.04	304.30	200.02	202.84	150.01	152.11
0.04	600.18	608.39	300.04	304.12	200.02	202.72	150.01	152.02
0.06	600.18	608.03	300.04	303.94	200.02	202.60	150.01	151.94
0.08	600.18	607.67	300.04	303.77	200.02	202.48	150.01	151.85
0.1	600.18	607.31	300.04	303.59	200.02	202.37	150.01	151.76
0.2	600.18	605.51	300.04	302.69	200.02	201.77	150.01	151.32
0.3	600.18	603.72	300.04	301.80	200.02	201.19	150.01	150.88
0.4	600.18	601.94	300.04	300.92	200.02	200.60	150.01	150.44
0.5	600.18	600.18	300.04	300.04	200.02	200.02	150.01	150.01
0.6	600.18	598.42	300.04	299.17	200.02	199.44	150.01	149.58
0.7	600.18	596.67	300.04	298.30	200.02	198.87	150.01	149.15
0.8	600.18	594.94	300.04	297.44	200.02	198.30	150.01	148.73
0.9	600.18	593.21	300.04	296.58	200.02	197.73	150.01	148.31
1.0	600.18	591.49	300.04	295.73	200.02	197.16	150.02	147.89

(v) $V_P = -3$ V and $I_{DSS} = 20$ mA

	$R_{XY}(\Omega)$							
	$v_{C1} = -0.25$ V (Calc. $R_{XY} = 600\ \Omega$)		$v_{C1} = -0.50$ V (Calc. $R_{XY} = 300\ \Omega$)		$v_{C1} = -0.75$ V (Calc. $R_{XY} = 200\ \Omega$)		$v_{C1} = -1.00$ V (Calc. $R_{XY} = 150\ \Omega$)	
v_{XY} (V)	λ = 0 (Obsrvd. v_A = −5.25 V)	λ = 0.03 (Obsrvd. v_A = −5.26 V)	λ = 0 (Obsrvd. v_A = −4.49 V)	λ = 0.03 (Obsrvd. v_A = −4.51 V)	λ = 0 (Obsrvd. v_A = −3.73 V)	λ = 0.03 (Obsrvd. v_A = −3.76 V)	λ = 0 (Obsrvd. v_A = −2.96 V)	λ = 0.03 (Obsrvd. v_A = −3.00 V)
−1.0	588.50	578.77	300.04	295.73	200.02	197.16	150.01	147.88
−0.9	595.57	587.87	300.04	296.58	200.02	197.73	150.01	148.30
−0.8	599.67	594.15	300.04	297.44	200.02	198.30	150.01	148.73
−0.7	600.17	596.67	300.04	298.30	200.02	198.87	150.01	149.15
−0.6	600.17	598.42	300.04	299.17	200.02	199.44	150.01	149.58
−0.5	600.17	600.17	300.04	300.04	200.02	200.02	150.01	150.01
−0.4	600.17	601.94	300.04	300.92	200.02	200.60	150.01	150.44
−0.3	600.17	603.72	300.04	301.80	200.02	201.19	150.01	150.88
−0.2	600.17	605.51	300.04	302.69	200.02	201.77	150.01	151.32
−0.1	600.17	607.31	300.04	303.59	200.02	202.36	150.01	151.76
−0.08	600.17	607.67	300.04	303.76	200.02	202.48	150.01	151.85
−0.06	600.17	608.03	300.04	303.94	200.02	202.60	150.01	151.94
−0.04	600.17	608.39	300.04	304.12	200.02	202.72	150.01	152.02
−0.02	600.17	608.75	300.04	304.30	200.02	202.84	150.01	152.11
0.02	600.17	608.75	300.04	304.30	200.02	202.84	150.01	152.11
0.04	600.17	608.39	300.04	304.12	200.02	202.72	150.01	152.02
0.06	600.17	608.03	300.04	303.94	200.02	202.60	150.01	151.94
0.08	600.17	607.67	300.04	303.76	200.02	202.48	150.01	151.85
0.1	600.17	607.31	300.04	303.59	200.02	202.36	150.01	151.76
0.2	600.17	605.51	300.04	302.69	200.02	201.77	150.01	151.32
0.3	600.17	603.72	300.04	301.80	200.02	201.19	150.01	150.88
0.4	600.17	601.94	300.04	300.92	200.02	200.60	150.01	150.44
0.5	600.17	600.17	300.04	300.04	200.02	200.02	150.01	150.01
0.6	600.17	598.42	300.04	299.17	200.02	199.44	150.01	149.58
0.7	600.17	596.67	300.04	298.30	200.02	198.87	150.01	149.15
0.8	599.67	594.15	300.04	297.44	200.02	198.30	150.01	148.73
0.9	595.57	587.87	300.04	296.58	200.02	197.73	150.01	148.30
1.0	588.50	578.77	300.04	295.73	200.02	197.16	150.01	147.88

Table A.8: Circuit simulation (LT Spice) results for a precision linear floating VCR using matched JFET device pair with SD-bootstrapped gate and self-tracking arrangement considering the effect of mismatch in the device pair (Circuit in Figure 3.6 with $R_2 = R_3 = 1$ MΩ, $R_4 = R_5 = R_7 = 10$ kΩ, $R_8 = 5$ kΩ): R_{XY} as a function of v_{XY}, with $R_1 = 210$ Ω, $v_{C2} = 0.5$ V, and v_{C1} as the voltage for controlling the VCR value. Q1 has $V_P = -1$ V and $I_{DSS} = 6$ mA while Q2 has V_P and I_{DSS} with mismatch of ±20 mV and ±0.18 mA, respectively.

(i) Q1: $V_P = -1$ V and $I_{DSS} = 6$ mA, Q2: $V_P = -1$ V and $I_{DSS} = 6$ mA

	R_{XY} (Ω)			
v_{XY} (V)	$v_{C1} = -0.25$ V (Calc. $R_{XY} = 420$ Ω) λ = 0 (Obsrvd. $v_A = -1.61$ V)	$v_{C1} = -0.50$ V (Calc. $R_{XY} = 210$ Ω) λ = 0 (Obsrvd. $v_A = -1.20$ V)	$v_{C1} = -0.75$ V (Calc. $R_{XY} = 140$ Ω) λ = 0 (Obsrvd. $v_A = -0.79$ V)	$v_{C1} = -1.00$ V (Calc. $R_{XY} = 105$ Ω) λ = 0 (Obsrvd. $v_A = -0.38$ V)
−1.0	346.35	207.70	140.01	105.01
−0.9	361.57	209.43	140.01	105.01
−0.8	377.31	210.02	140.01	105.01
−0.7	393.07	210.02	140.01	105.01
−0.6	407.94	210.02	140.01	105.01
−0.5	420.09	210.02	140.01	105.01
−0.4	425.90	210.02	140.01	105.01
−0.3	425.92	210.02	140.01	105.01
−0.2	425.92	210.02	140.01	105.01
−0.1	425.92	210.02	140.01	105.01
−0.08	425.92	210.02	140.01	105.01
−0.06	425.92	210.02	140.01	105.01
−0.04	425.92	210.02	140.01	105.01
−0.02	425.92	210.02	140.01	105.01
0.02	425.92	210.02	140.01	105.01
0.04	425.92	210.02	140.01	105.01
0.06	425.92	210.02	140.01	105.01
0.08	425.92	210.02	140.01	105.01
0.1	425.92	210.02	140.01	105.01
0.2	425.92	210.02	140.01	105.01
0.3	425.92	210.02	140.01	105.01
0.4	425.90	210.02	140.01	105.01
0.5	420.09	210.02	140.01	105.01
0.6	407.94	210.02	140.01	105.01
0.7	393.07	210.02	140.01	105.01
0.8	377.31	210.02	140.01	105.01
0.9	361.57	209.43	140.01	105.01
1.0	346.35	207.70	140.01	105.01

(ii) Q1: $V_P = -1$ V and $I_{DSS} = 6$ mA, Q2: $V_P = -0.98$ V and $I_{DSS} = 6$ mA

	$R_{XY}(\Omega)$			
v_{XY} (V)	$v_{C1} = -0.25$ V (Calc. $R_{XY} = 420\ \Omega$) $\lambda = 0$ (Obsrvd. $v_A = -1.61$ V)	$v_{C1} = -0.50$ V (Calc. $R_{XY} = 210\ \Omega$) $\lambda = 0$ (Obsrvd. $v_A = -1.20$ V)	$v_{C1} = -0.75$ V (Calc. $R_{XY} = 140\ \Omega$) $\lambda = 0$ (Obsrvd. $v_A = -0.79$ V)	$v_{C1} = -1.00$ V (Calc. $R_{XY} = 105\ \Omega$) $\lambda = 0$ (Obsrvd. $v_A = -0.38$ V)
−1.0	352.62	208.68	139.08	103.43
−0.9	369.80	210.98	139.08	103.43
−0.8	387.96	212.20	139.08	103.43
−0.7	406.74	212.28	139.08	103.43
−0.6	425.36	212.28	139.09	103.43
−0.5	442.16	212.28	139.09	103.43
−0.4	453.61	212.28	139.09	103.43
−0.3	455.24	212.28	139.09	103.43
−0.2	455.24	212.28	139.09	103.43
−0.1	455.24	212.28	139.08	103.43
−0.08	455.24	212.28	139.08	103.43
−0.06	455.24	212.28	139.08	103.43
−0.04	455.24	212.28	139.08	103.43
−0.02	455.24	212.28	139.09	103.43
0.02	455.24	212.28	139.09	103.43
0.04	455.24	212.28	139.09	103.43
0.06	455.24	212.28	139.09	103.43
0.08	455.24	212.28	139.09	103.43
0.1	455.24	212.28	139.08	103.43
0.2	455.24	212.28	139.08	103.43
0.3	455.24	212.28	139.08	103.43
0.4	453.61	212.28	139.08	103.43
0.5	442.16	212.28	139.09	103.43
0.6	425.36	212.28	139.09	103.43
0.7	406.74	212.28	139.09	103.43
0.8	387.96	212.20	139.09	103.43
0.9	369.80	210.98	139.09	103.43
1.0	352.62	208.68	139.09	103.43

(iii) Q1: $V_P = -1$ V and $I_{DSS} = 6$ mA, Q2: $V_P = -1.02$ V and $I_{DSS} = 6$ mA

	$R_{XY}(\Omega)$			
v_{XY} (V)	$v_{C1} = -0.25$ V (Calc. $R_{XY} = 420\ \Omega$) $\lambda = 0$ (Obsrvd. $v_A = -1.61$ V)	$v_{C1} = -0.50$ V (Calc. $R_{XY} = 210\ \Omega$) $\lambda = 0$ (Obsrvd. $v_A = -1.20$ V)	$v_{C1} = -0.75$ V (Calc. $R_{XY} = 140\ \Omega$) $\lambda = 0$ (Obsrvd. $v_A = -0.79$ V)	$v_{C1} = -1.00$ V (Calc. $R_{XY} = 105\ \Omega$) $\lambda = 0$ (Obsrvd. $v_A = -0.38$ V)
−1.0	340.48	206.77	140.98	106.58
−0.9	353.92	207.96	140.98	106.58
−0.8	367.48	208.13	140.98	106.58
−0.7	380.58	208.13	140.98	106.58
−0.6	392.20	208.13	140.98	106.58
−0.5	400.40	208.13	140.98	106.58
−0.4	402.32	208.13	140.98	106.58
−0.3	402.32	208.13	140.98	106.58
−0.2	402.32	208.13	140.98	106.58
−0.1	402.32	208.13	140.98	106.58
−0.08	402.32	208.13	140.98	106.58
−0.06	402.32	208.13	140.98	106.58
−0.04	402.32	208.13	140.98	106.58
−0.02	402.32	208.13	140.98	106.58
0.02	402.32	208.13	140.98	106.58
0.04	402.32	208.13	140.98	106.58
0.06	402.32	208.13	140.98	106.58
0.08	402.32	208.13	140.98	106.58
0.1	402.32	208.13	140.98	106.58
0.2	402.32	208.13	140.98	106.58
0.3	402.32	208.13	140.98	106.58
0.4	402.32	208.13	140.98	106.58
0.5	400.40	208.13	140.98	106.58
0.6	392.20	208.13	140.98	106.58
0.7	380.58	208.13	140.98	106.58
0.8	367.48	208.14	140.98	106.58
0.9	353.92	207.96	140.98	106.58
1.0	340.48	206.77	140.98	106.58

(iv) Q1: $V_P = -1$ V and $I_{DSS} = 6$ mA, Q2: $V_P = -1$ V and $I_{DSS} = 5.82$ mA

	$R_{XY}(\Omega)$			
v_{XY} (V)	$v_{C1} = -0.25$ V (Calc. $R_{XY} = 420\ \Omega$) $\lambda = 0$ (Obsrvd. $v_A = -1.61$ V)	$v_{C1} = -0.50$ V (Calc. $R_{XY} = 210\ \Omega$) $\lambda = 0$ (Obsrvd. $v_A = -1.20$ V)	$v_{C1} = -0.75$ V (Calc. $R_{XY} = 140\ \Omega$) $\lambda = 0$ (Obsrvd. $v_A = -0.79$ V)	$v_{C1} = -1.00$ V (Calc. $R_{XY} = 105\ \Omega$) $\lambda = 0$ (Obsrvd. $v_A = -0.38$ V)
−1.0	356.97	214.06	144.28	108.19
−0.9	372.67	215.84	144.28	108.19
−0.8	388.89	216.46	144.28	108.19
−0.7	405.15	216.46	144.28	108.19
−0.6	420.48	216.46	144.28	108.19
−0.5	433.01	216.46	144.28	108.19
−0.4	439.01	216.46	144.28	108.19
−0.3	439.03	216.46	144.28	108.19
−0.2	439.03	216.46	144.28	108.19
−0.1	439.03	216.46	144.28	108.19
−0.08	439.03	216.46	144.28	108.19
−0.06	439.03	216.46	144.28	108.19
−0.04	439.03	216.46	144.28	108.19
−0.02	439.03	216.46	144.28	108.19
0.02	439.03	216.46	144.28	108.19
0.04	439.03	216.46	144.28	108.19
0.06	439.03	216.46	144.28	108.19
0.08	439.03	216.46	144.28	108.19
0.1	439.03	216.46	144.28	108.19
0.2	439.03	216.46	144.28	108.19
0.3	439.03	216.46	144.28	108.19
0.4	439.01	216.46	144.28	108.19
0.5	433.01	216.46	144.28	108.19
0.6	420.48	216.46	144.28	108.19
0.7	405.15	216.46	144.28	108.19
0.8	388.89	216.46	144.28	108.19
0.9	372.67	215.84	144.28	108.19
1.0	356.97	214.06	144.28	108.19

(v) Q1: $V_P = -1$ V and $I_{DSS} = 6$ mA, Q2: $V_P = -1$ V and $I_{DSS} = 6.18$ mA

	$R_{XY}(\Omega)$			
v_{XY} (V)	$v_{C1} = -0.25$ V (Calc. $R_{XY} = 420\ \Omega$) $\lambda = 0$ (Obsrvd. $v_A = -1.61$ V)	$v_{C1} = -0.50$ V (Calc. $R_{XY} = 210\ \Omega$) $\lambda = 0$ (Obsrvd. $v_A = -1.20$ V)	$v_{C1} = -0.75$ V (Calc. $R_{XY} = 140\ \Omega$) $\lambda = 0$ (Obsrvd. $v_A = -0.79$ V)	$v_{C1} = -1.00$ V (Calc. $R_{XY} = 105\ \Omega$) $\lambda = 0$ (Obsrvd. $v_A = -0.38$ V)
−1.0	336.34	201.72	135.99	102.01
−0.9	351.12	203.39	135.99	102.01
−0.8	366.39	203.96	135.99	102.01
−0.7	381.70	203.96	135.99	102.01
−0.6	396.13	203.96	135.99	102.01
−0.5	407.92	203.96	135.99	102.01
−0.4	413.55	203.96	135.99	102.01
−0.3	413.57	203.96	135.99	102.01
−0.2	413.57	203.96	135.99	102.01
−0.1	413.57	203.96	135.99	102.01
−0.08	413.57	203.96	135.99	102.01
−0.06	413.57	203.96	135.99	102.01
−0.04	413.57	203.96	135.99	102.01
−0.02	413.57	203.96	135.99	102.01
0.02	413.57	203.96	135.99	102.01
0.04	413.57	203.96	135.99	102.01
0.06	413.57	203.96	135.99	102.01
0.08	413.57	203.96	135.99	102.01
0.1	413.57	203.96	135.99	102.01
0.2	413.57	203.96	135.99	102.01
0.3	413.57	203.96	135.99	102.01
0.4	413.55	203.96	135.99	102.01
0.5	407.92	203.96	135.99	102.01
0.6	396.13	203.96	135.99	102.01
0.7	381.70	203.96	135.99	102.01
0.8	366.40	203.96	135.99	102.01
0.9	351.12	203.39	135.99	102.01
1.0	336.35	201.72	135.99	102.01

APPENDIX B

PRACTICAL RESULTS FOR JFET BASED VCR CIRCUITS

Table B.1: Circuit simulation (LT Spice) results for JFET-based floating VCR using single device with SD-bootstrapped gate (Circuit in Figure 3.2 with $R_1 = R_2 = R_3 = R_5 = 10$ kΩ, $R_4 = 5$ kΩ): R_{XY} as a function of v_{XY}, with different values of v_C and λ as a parameter. (i) $V_P = -1.032$ V & $I_{dss} = 0.8987$ mA, and (ii) $V_P = -1.028$ V & $I_{dss} = 0.8842$ mA.

(i) Q1: Device 1: $V_P = -1.032$ V and $I_{DSS} = 0.8987$ mA

	R_{XY} (Ω)							
V_{XY} (V)	$V_C = 0$ V		$V_C = -0.5$ V		$V_C = -1$ V		$V_C = -1.5$ V	
	λ = 0	λ = 0.03	λ = 0	λ = 0.03	λ = 0	λ = 0.03	λ = 0	λ = 0.03
−1.0	573.41	556.91	759.75	737.73	1115.8	1083.4	1940.5	1884.1
−0.9	575.73	560.71	759.75	739.88	1115.8	1086.6	1993.0	1940.8
−0.8	576.11	562.70	759.75	742.03	1115.8	1089.8	2040.7	1993.0
−0.7	576.17	564.40	759.75	744.20	1115.8	1093.0	2079.2	2036.5
−0.6	576.18	566.06	759.75	746.38	1115.8	1096.2	2101.3	2064.2
−0.5	576.18	567.73	759.75	748.58	1115.8	1099.4	2103.3	2072.2
−0.4	576.18	569.40	759.75	750.78	1115.8	1102.6	2103.3	2078.4
−0.3	576.18	571.08	759.75	753.00	1115.8	1105.9	2103.3	2084.5
−0.2	576.18	572.77	759.75	755.24	1115.8	1109.2	2103.3	2090.7
−0.1	576.18	574.47	759.75	757.49	1115.8	1112.5	2103.3	2097.0
−0.08	576.18	574.81	759.75	757.94	1115.8	1113.2	2103.3	2098.2
−0.06	576.18	575.16	759.75	758.39	1115.8	1113.8	2103.3	2099.5
−0.04	576.18	575.50	759.75	758.84	1115.8	1114.5	2103.3	2100.7
−0.02	576.18	575.84	759.75	759.29	1115.8	1115.2	2103.3	2102.0
0.02	576.18	575.84	759.75	759.29	1115.8	1115.2	2103.3	2102.0
0.04	576.18	575.50	759.75	758.84	1115.8	1114.5	2103.3	2100.7
0.06	576.18	575.16	759.75	758.39	1115.8	1113.8	2103.3	2099.5
0.08	576.18	574.81	759.75	757.94	1115.8	1113.2	2103.3	2098.2
0.1	576.18	574.47	759.75	757.49	1115.8	1112.5	2103.3	2097.0
0.2	576.18	572.77	759.75	755.24	1115.8	1109.2	2103.3	2090.7
0.3	576.18	571.08	759.75	753.01	1115.8	1105.9	2103.3	2084.5
0.4	576.18	569.40	759.75	750.78	1115.8	1102.6	2103.3	2078.4
0.5	576.18	567.73	759.75	748.58	1115.8	1099.4	2103.3	2072.2
0.6	576.18	566.07	759.75	746.38	1115.8	1096.2	2101.3	2064.2
0.7	576.18	564.41	759.75	744.20	1115.8	1093.0	2079.2	2036.5
0.8	576.18	562.77	759.75	742.03	1115.8	1089.8	2040.7	1993.0
0.9	576.18	561.14	759.75	739.88	1115.8	1086.6	1993.0	1940.8
1.0	576.19	559.53	759.75	737.73	1115.8	1083.4	1940.5	1884.1

(ii)Device Pair 1: J2, $V_P = -1.028$ V and $I_{dss} = 0.8842$ mA

V_{XY} (V)	$R_{XY}(\Omega)$							
	$V_C = 0$ V		$V_C = -0.5$ V		$V_C = -1$ V		$V_C = -1.5$ V	
	λ = 0	λ = 0.03	λ = 0	λ = 0.03	λ = 0	λ = 0.03	λ = 0	λ = 0.03
−1.0	580.47	563.76	770.10	747.79	1133.8	1100.9	1977.1	1919.7
−0.9	582.85	567.64	770.10	749.96	1133.8	1104.1	2032.1	1978.8
−0.8	583.23	569.66	770.10	752.15	1133.8	1107.3	2082.3	2033.6
−0.7	583.30	571.38	770.10	754.35	1133.8	1110.6	2123.6	2080.0
−0.6	583.31	573.06	770.10	756.56	1133.8	1113.8	2148.5	2110.6
−0.5	583.31	574.75	770.10	758.78	1133.8	1117.1	2151.6	2119.8
−0.4	583.31	576.44	770.10	761.02	1133.8	1120.4	2151.6	2126.1
−0.3	583.31	578.14	770.11	763.27	1133.8	1123.7	2151.6	2132.4
−0.2	583.31	579.85	770.11	765.54	1133.8	1127.1	2151.6	2138.8
−0.1	583.31	581.58	770.11	767.81	1133.8	1130.4	2151.6	2145.2
−0.08	583.31	581.92	770.11	768.27	1133.8	1131.1	2151.6	2146.4
−0.06	583.31	582.27	770.11	768.73	1133.8	1131.8	2151.6	2147.7
−0.04	583.31	582.61	770.11	769.19	1133.8	1132.4	2151.6	2149.0
−0.02	583.31	582.96	770.11	769.65	1133.8	1133.1	2151.6	2150.3
0.02	583.31	582.96	770.11	769.65	1133.8	1133.1	2151.6	2150.3
0.04	583.31	582.61	770.11	769.19	1133.8	1132.4	2151.6	2149.0
0.06	583.31	582.27	770.11	768.73	1133.8	1131.8	2151.6	2147.7
0.08	583.31	581.92	770.11	768.27	1133.8	1131.1	2151.6	2146.4
0.1	583.31	581.58	770.11	767.81	1133.8	1130.4	2151.6	2145.2
0.2	583.31	579.85	770.11	765.54	1133.8	1127.1	2151.6	2138.8
0.3	583.31	578.14	770.11	763.27	1133.8	1123.7	2151.6	2132.4
0.4	583.31	576.44	770.11	761.02	1133.8	1120.4	2151.6	2126.1
0.5	583.31	574.75	770.11	758.78	1133.8	1117.1	2151.6	2119.9
0.6	583.31	573.07	770.11	756.56	1133.8	1113.8	2148.5	2110.6
0.7	583.31	571.39	770.11	754.35	1133.8	1110.6	2123.6	2080.0
0.8	583.31	569.73	770.11	752.15	1133.8	1107.3	2082.3	2033.6
0.9	583.31	568.08	770.11	749.96	1133.8	1104.1	2032.1	1978.8
1.0	583.32	566.44	770.11	747.79	1133.8	1100.9	1977.1	1919.7

Table B.2: Circuit simulation (LT Spice) results for a floating precision linear VCR using matched JFET device pair with SD-bootstrapped gate and self-tracking arrangement (Circuit in Figure 3.6 with $R_2 = R_3 = 1$ MΩ, $R_4 = R_5 = R_7 = 10$ kΩ, $R_8 = 5$ kΩ): R_{XY} as a function of v_{XY}, with $R_1 = 1000$ Ω, $v_{C2} = 0.5$ V, and v_{C1} as the voltage for controlling the VCR value. Device Pair: Q1 with $V_P = -1.032$ V and $I_{DSS} = 0.8987$ mA and Q2 with $V_P = -1.028$ V and $I_{DSS} = 0.8842$ mA.

Device Pair: Q1 with $V_P = -1.032$ V and $I_{DSS} = 0.8987$ mA and Q2 with $V_P = -1.028$ V and $I_{DSS} = 0.8842$ mA

	R_{XY} (Ω)							
	$v_{C1} = -0.25$ V (Calc. $R_{XY} = 2000$ Ω)		$v_{C1} = -0.50$ V (Calc. $R_{XY} = 1000$ Ω)		$v_{C1} = -0.75$ V (Calc. $R_{XY} = 666$ Ω)		$v_{C1} = -1.00$ V (Calc. $R_{XY} = 500$ Ω)	
v_{XY} (V)	λ = 0 (Obsrvd. $v_A = -1.47$ V)	λ = 0.03 (Obsrvd. $v_A = -1.48$ V)	λ = 0 (Obsrvd. $v_A = -0.88$ V)	λ = 0.03 (Obsrvd. $v_A = -0.89$ V)	λ = 0 (Obsrvd. $v_A = -0.28$ V)	λ = 0.03 (Obsrvd. $v_A = -0.31$ V)	λ = 0 (Obsrvd. $v_A = 0.31$ V)	λ = 0.03 (Obsrvd. $v_A = 0.39$ V)
−1.0	1906.6	1871.7	1015.8	1001.2	675.54	665.81	192.81	267.42
−0.9	1954.7	1926.0	1015.8	1004.1	675.55	667.75	391.71	435.44
−0.8	1997.4	1975.5	1015.8	1007.0	675.55	669.70	482.63	489.62
−0.7	2030.2	2015.9	1015.8	1010.0	675.55	671.65	502.08	501.11
−0.6	2046.2	2040.1	1015.8	1012.9	675.55	673.62	505.47	504.30
−0.5	2046.6	2047.0	1015.8	1015.9	675.55	675.60	506.05	506.07
−0.4	2046.6	2053.0	1015.8	1018.9	675.55	677.59	506.15	507.61
−0.3	2046.6	2059.1	1015.8	1021.9	675.55	679.59	506.16	509.12
−0.2	2046.6	2065.3	1015.8	1025.0	675.55	681.61	506.17	510.63
−0.1	2046.6	2071.4	1015.8	1028.0	675.55	683.63	506.17	512.14
−0.08	2046.6	2072.7	1015.8	1028.6	675.55	684.04	506.17	512.45
−0.06	2046.6	2073.9	1015.8	1029.2	675.55	684.45	506.17	512.75
−0.04	2046.6	2075.1	1015.8	1029.9	675.55	684.86	506.17	513.06
−0.02	2046.6	2076.4	1015.8	1030.5	675.55	685.26	506.17	513.36
0.02	2046.6	2076.4	1015.8	1030.5	675.55	685.26	506.17	513.36
0.04	2046.6	2075.1	1015.8	1029.9	675.55	684.86	506.17	513.06
0.06	2046.6	2073.9	1015.8	1029.2	675.55	684.45	506.17	512.75
0.08	2046.6	2072.7	1015.8	1028.6	675.55	684.04	506.17	512.45
0.1	2046.6	2071.4	1015.8	1028.0	675.55	683.63	506.17	512.14
0.2	2046.6	2065.3	1015.8	1025.0	675.55	681.61	506.17	510.63
0.3	2046.6	2059.1	1015.8	1021.9	675.55	679.59	506.17	509.12
0.4	2046.6	2053.0	1015.8	1018.9	675.55	677.59	506.17	507.62
0.5	2046.6	2047.0	1015.8	1015.9	675.55	675.60	506.17	506.13
0.6	2046.2	2040.1	1015.8	1012.9	675.55	673.62	506.17	504.66
0.7	2030.2	2015.9	1015.8	1010.0	675.55	671.65	506.18	503.19
0.8	1997.4	1975.5	1015.8	1007.0	675.55	669.70	506.23	501.76
0.9	1954.7	1926.0	1015.8	1004.1	675.55	667.75	506.57	500.48
1.0	1906.6	1871.8	1015.8	1001.2	675.55	665.82	508.49	500.09

Table B.3: Practical results for a precision linear floating VCR using matched JFET device pair with SD-bootstrapped gate and self-tracking arrangement (Circuit in Figure 3.6 with $R_2 = R_3 = 1$ MΩ, $R_4 = R_5 = R_7 = 10$ kΩ, $R_8 = 5$ kΩ, two 10 kΩ in parallel): R_{XY} as a function of v_{XY}, with $R_1 = 992$ Ω (measured value), $v_{C2} = 0.5$ V, and v_{C1} as the voltage for controlling the VCR value. Device Pair: Q1 with $V_P = -1.032$ V and $I_{DSS} = 0.8987$ mA and Q2 with $V_P = -1.028$ V and $I_{DSS} = 0.8842$ mA.

Device Pair: Q1 with $V_P = -1.032$ V and $I_{DSS} = 0.8987$ mA and Q2 with $V_P = -1.028$ V and $I_{DSS} = 0.8842$ mA

	R_{XY} (Ω)			
v_{XY} (V)	$v_{C1} = -0.2535$ V (Calc. R_{XY} = 1955.37 Ω, Observd. $v_A = -1.3540$ V)	$v_{C1} = -0.5057$ V (Calc. R_{XY} = 980.19 Ω, Obsrvd. $v_A = -0.7001$ V)	$v_{C1} = -0.7541$ V (Calc. R_{XY} = 657.32 Ω Observd. $v_A = -0.0228$ V)	$v_{C1} = -1.0023$ V (Calc. R_{XY} = 494.55 Ω Observd. $v_A = 0.5400$ V)
−1.0	1846.45	995.45	678.79	158.74
−0.9	1908.55	1001.11	684.30	276.16
−0.8	1993.28	1009.79	688.86	422.15
−0.7	2060.78	1021.60	688.23	487.96
−0.6	2146.16	1036.13	686.91	503.78
−0.5	2277.93	1044.59	686.14	508.67
−0.4	2451.00	1059.47	685.92	509.33
−0.3	2797.79	1083.01	688.70	506.32
−0.2	3439.07	1120.72	689.53	499.52
−0.1	11378.95	1253.16	687.82	477.12
0.1	11093.75	1236.36	686.51	476.19
0.2	3575.39	1112.24	683.77	497.71
0.3	2865.48	1083.99	683.41	505.40
0.4	2537.44	1054.16	683.04	505.33
0.5	2326.53	1037.21	681.43	503.72
0.6	2175.17	1026.32	678.27	498.09
0.7	2084.89	1017.75	675.19	465.93
0.8	1994.54	1007.54	673.42	379.50
0.9	1904.90	1000.33	671.33	240.89
1.0	1839.15	986.00	668.26	130.76

APPENDIX C

SIMULATION AND PRACTICAL RESULTS FOR MOSFET BASED VCR CIRCUITS

Table C.1: Circuit simulation (LT Spice) results for a floating precision linear VCR using matched MOSFET device pair with SD-bootstrapped gate, SD-bootstrapped substrate and self-tracking arrangement (Circuit in Figure 4.4 with R_1 = 1 kΩ, R_2 to R_4 = R_6 to R_9 = R_{11} to R_{14} = R_{16} to R_{19} = R_{21} = 10 kΩ, R_5 = R_{10} = R_{15} = R_{20} = 5 kΩ) for v_{C2} and λ: R_{XY} as a function of V_{XY}, R_1 = 1000 Ω, v_{C1} = 1 V, v_{C3} = 0 V, V_{BB} = –2 V. Device parameters: (i) V_T = 0.7 V and k = 0.52 mA/V^2, and (ii) V_T = 0.4 V and k = 0.28 mA/V^2.

(i) V_T = 0.7 V and k = 0.52 mA/V^2

	R_{XY} (Ω)							
	v_{C2} = −0.5 V (Calc. R_{XY} = 2000 Ω)		v_{C2} = −1.0 V (Calc. R_{XY} = 1000 Ω)		v_{C2} = −1.5 V (Calc. R_{XY} = 666.67 Ω)		v_{C2} = −2.0 V (Calc. R_{XY} = 500 Ω)	
v_{XY} (V)	λ = 0 (Obsrvd. v_A = 3.91 V)	λ = 0.03 (Obsrvd. v_A = 3.86 V)	λ = 0 (Obsrvd. v_A = 5.86 V)	λ = 0.03 (Obsrvd. v_A = 5.75 V)	λ = 0 (Obsrvd. v_A = 7.81 V)	λ = 0.03 (Obsrvd. v_A = 7.65 V)	λ = 0 (Obsrvd. v_A = 9.76 V)	λ = 0.03 (Obsrvd. v_A = 9.54 V)
−2.0	1551.7	1499.4	873.76	846.71	608.10	589.92	466.32	452.65
−1.9	1592.2	1543.7	886.49	861.71	614.23	597.67	469.91	457.49
−1.8	1633.5	1589.1	899.15	876.75	620.28	605.38	473.45	462.30
−1.7	1675.7	1635.5	911.77	891.84	626.26	613.07	476.92	467.07
−1.6	1718.7	1683.3	924.37	907.00	632.18	620.74	480.35	471.82
−1.5	1762.8	1732.3	936.96	922.24	638.05	628.40	483.73	476.55
−1.4	1807.9	1782.8	949.56	937.59	643.86	636.05	487.06	481.27
−1.3	1854.2	1834.8	962.17	953.05	649.64	643.71	490.36	485.98
−1.2	1901.8	1888.4	974.82	968.64	655.38	651.39	493.63	490.68
−1.1	1950.7	1943.8	987.51	984.37	661.09	659.07	496.86	495.37
−1.0	2001.0	2001.0	1000.3	1000.3	666.78	666.78	500.06	500.06
−0.9	2052.9	2060.3	1013.1	1016.3	672.44	674.51	503.24	504.76
−0.8	2106.4	2121.6	1025.9	1032.5	678.09	682.27	506.40	509.46
−0.7	2161.8	2185.3	1038.9	1048.9	683.72	690.06	509.53	514.16
−0.6	2219.0	2251.4	1051.9	1065.5	689.34	697.89	512.65	518.87
−0.5	2278.2	2320.0	1065.0	1082.3	694.95	705.75	515.75	523.59
−0.4	2339.5	2391.5	1078.2	1099.3	700.56	713.66	518.83	528.32
−0.3	2403.2	2465.9	1091.6	1116.5	706.16	721.61	521.89	533.07
−0.2	2469.3	2543.5	1105.0	1133.9	711.76	729.60	524.94	537.83
−0.1	2538.0	2624.5	1118.6	1151.6	717.36	737.65	527.98	542.60
0.1	2538.0	2624.5	1118.6	1151.6	717.36	737.65	527.98	542.60
0.2	2469.3	2543.5	1105.0	1133.9	711.76	729.60	524.94	537.83
0.3	2403.2	2465.9	1091.6	1116.5	706.16	721.61	521.89	533.07
0.4	2339.5	2391.5	1078.2	1099.3	700.56	713.66	518.83	528.32
0.5	2278.2	2320.0	1065.0	1082.3	694.95	705.75	515.75	523.59
0.6	2219.0	2251.4	1051.9	1065.5	689.34	697.89	512.65	518.87
0.7	2161.8	2185.3	1038.9	1048.9	683.72	690.06	509.53	514.16
0.8	2106.5	2121.6	1025.9	1032.5	678.09	682.27	506.40	509.46
0.9	2052.9	2060.3	1013.1	1016.3	672.44	674.51	503.24	504.76
1.0	2001.0	2001.0	1000.3	1000.3	666.78	666.78	500.06	500.06
1.1	1950.7	1943.8	987.51	984.37	661.09	659.07	496.86	495.37
1.2	1901.8	1888.4	974.82	968.64	655.38	651.39	493.63	490.68
1.3	1854.2	1834.8	962.17	953.05	649.64	643.71	490.36	485.98
1.4	1807.9	1782.8	949.56	937.59	643.86	636.05	487.06	481.27

1.5	1762.8	1732.3	936.96	922.25	638.05	628.40	483.73	476.55
1.6	1718.7	1683.3	924.37	907.00	632.18	620.74	480.35	471.82
1.7	1675.7	1635.5	911.77	891.84	626.26	613.07	476.92	467.07
1.8	1633.5	1589.1	899.15	876.75	620.28	605.38	473.45	462.30
1.9	1592.2	1543.7	886.49	861.71	614.23	597.67	469.91	457.49
2.0	1551.7	1499.4	873.77	846.71	608.10	589.92	466.32	452.65

(ii) V_T = 0.4 V and k = 0.28 mA/V^2

	R_{XY} (Ω)							
	v_{C2} = −0.5 V (Calc. R_{XY} = 2000 Ω)		v_{C2} = −1.0 V (Calc. R_{XY} = 1000 Ω)		v_{C2} = −1.5 V (Calc. R_{XY} = 666.67 Ω)		v_{C2} = −2.0 V (Calc. R_{XY} = 500 Ω)	
v_{XY} (V)	λ = 0 (Obsrvd. v_A = 4.93 V)	λ = 0.03 (Obsrvd. v_A = 4.83 V)	λ = 0 (Obsrvd. v_A = 8.50 V)	λ = 0.03 (Obsrvd. v_A = 8.30 V)	λ = 0 (Obsrvd. v_A = 12.1 V)	λ = 0.03 (Obsrvd. v_A = 11.8 V)	λ = 0 (Obsrvd. v_A = 15.6 V)	λ = 0.03 (Obsrvd. v_A = 15.2 V)
−2.0	1733.2	1679.0	929.57	902.12	635.09	616.75	482.30	468.54
−1.9	1760.5	1710.8	937.37	912.39	638.72	622.08	484.39	471.92
−1.8	1787.8	1742.7	945.03	922.59	642.27	627.35	486.43	475.27
−1.7	1815.0	1774.8	952.58	932.73	645.75	632.59	488.43	478.59
−1.6	1842.2	1807.2	960.03	942.83	649.16	637.79	490.38	481.88
−1.5	1869.5	1839.7	967.39	952.90	652.52	642.96	492.29	485.16
−1.4	1896.9	1872.6	974.66	962.94	655.82	648.11	494.17	488.42
−1.3	1924.3	1905.8	981.86	972.97	659.07	653.24	496.01	491.67
−1.2	1951.9	1939.3	989.00	982.99	662.28	658.35	497.82	494.90
−1.1	1979.7	1973.2	996.07	993.01	665.45	663.44	499.61	498.12
−1.0	2007.6	2007.5	1003.1	1003.0	668.57	668.53	501.37	501.34
−0.9	2035.7	2042.2	1010.1	1013.1	671.66	673.61	503.11	504.55
−0.8	2064.1	2077.3	1017.0	1023.1	674.72	678.68	504.82	507.75
−0.7	2092.7	2113.0	1023.9	1033.2	677.75	683.75	506.51	510.95
−0.6	2121.5	2149.1	1030.7	1043.3	680.74	688.82	508.19	514.15
−0.5	2150.6	2185.7	1037.6	1053.4	683.71	693.90	509.84	517.34
−0.4	2180.0	2222.9	1044.4	1063.5	686.66	698.97	511.47	520.54
−0.3	2209.7	2260.7	1051.1	1073.7	689.58	704.05	513.09	523.74
−0.2	2239.8	2299.0	1057.9	1083.9	692.48	709.14	514.70	526.94
−0.1	2270.2	2337.9	1064.6	1094.2	695.36	714.23	516.28	530.14
0.1	2270.2	2337.9	1064.6	1094.2	695.36	714.23	516.28	530.14
0.2	2239.8	2299.0	1057.9	1083.9	692.48	709.14	514.70	526.94
0.3	2209.7	2260.7	1051.1	1073.7	689.58	704.05	513.09	523.74
0.4	2180.0	2222.9	1044.4	1063.5	686.66	698.97	511.47	520.54
0.5	2150.6	2185.7	1037.6	1053.4	683.72	693.90	509.84	517.34
0.6	2121.5	2149.1	1030.7	1043.3	680.74	688.82	508.19	514.15
0.7	2092.7	2113.0	1023.9	1033.2	677.75	683.75	506.51	510.95
0.8	2064.1	2077.3	1017.0	1023.1	674.72	678.68	504.82	507.75
0.9	2035.7	2042.2	1010.1	1013.1	671.66	673.61	503.11	504.55
1.0	2007.6	2007.5	1003.1	1003.0	668.57	668.53	501.37	501.34
1.1	1979.7	1973.2	996.07	993.01	665.45	663.44	499.61	498.12
1.2	1951.9	1939.3	989.00	982.99	662.28	658.35	497.82	494.90
1.3	1924.3	1905.8	981.86	972.97	659.07	653.24	496.01	491.67
1.4	1896.9	1872.6	974.66	962.94	655.82	648.11	494.17	488.42
1.5	1869.5	1839.7	967.39	952.90	652.52	642.96	492.29	485.16
1.6	1842.2	1807.2	960.03	942.83	649.17	637.79	490.38	481.88
1.7	1815.0	1774.8	952.58	932.73	645.75	632.59	488.43	478.59
1.8	1787.8	1742.7	945.03	922.59	642.27	627.35	486.43	475.27
1.9	1760.5	1710.8	937.37	912.39	638.72	622.08	484.39	471.92
2.0	1733.2	1679.0	929.57	902.12	635.09	616.75	482.30	468.54

Table C.2: Circuit simulation (LT Spice) results for a floating precision linear VCR using matched MOSFET device pair with SD-bootstrapped gate, SD-bootstrapped substrate and self-tracking arrangement (Circuit in Figure 4.4 with R_1 = 1 kΩ, R_2 to R_4 = R_6 to R_9 = R_{11} to R_{14} = R_{16} to R_{19} = R_{21} = 10 kΩ, R_5 = R_{10} = R_{15} = R_{20} = 5 kΩ) for V_{BB} and λ: R_{XY} as a function of v_{XY}, R_1 = 1000 Ω, v_{C1} = 1 V, v_{C2} = –1 V, v_{C3} = 0 V. Device parameters: V_T = 0.7 V and k = 0.52 mA/V^2.

R_{XY} (Ω)

v_{XY} (V)	V_{BB} = −2.0 V (Calc. R_{XY} = 1000 Ω)		V_{BB} = −4.0 V (Calc. R_{XY} = 1000 Ω)	
	λ = 0 (Obsrvd. v_A = 5.86 V)	λ = 0.03 (Obsrvd. v_A = 5.75 V)	λ = 0 (Obsrvd. v_A = 6.71 V)	λ = 0.03 (Obsrvd. v_A = 6.60 V)
−2.0	873.76	846.71	909.03	881.78
−1.9	886.49	861.71	917.91	893.07
−1.8	899.15	876.75	926.84	904.48
−1.7	911.77	891.84	935.82	916.00
−1.6	924.37	907.00	944.84	927.64
−1.5	936.96	922.24	953.93	939.41
−1.4	949.56	937.59	963.07	951.31
−1.3	962.17	953.05	972.27	963.33
−1.2	974.82	968.64	981.53	975.50
−1.1	987.51	984.37	990.86	987.80
−1.0	1000.3	1000.3	1000.3	1000.3
−0.9	1013.1	1016.3	1009.7	1012.9
−0.8	1025.9	1032.5	1019.3	1025.6
−0.7	1038.9	1048.9	1028.9	1038.5
−0.6	1051.9	1065.5	1038.6	1051.6
−0.5	1065.0	1082.3	1048.3	1064.8
−0.4	1078.2	1099.3	1058.2	1078.2
−0.3	1091.6	1116.5	1068.2	1091.8
−0.2	1105.0	1133.9	1078.2	1105.6
−0.1	1118.6	1151.6	1088.3	1119.5
0.1	1118.6	1151.6	1088.3	1119.5
0.2	1105.0	1133.9	1078.2	1105.6
0.3	1091.6	1116.5	1068.2	1091.8
0.4	1078.2	1099.3	1058.2	1078.2
0.5	1065.0	1082.3	1048.3	1064.8
0.6	1051.9	1065.5	1038.6	1051.6
0.7	1038.9	1048.9	1028.9	1038.5
0.8	1025.9	1032.5	1019.3	1025.6
0.9	1013.1	1016.3	1009.7	1012.9
1.0	1000.3	1000.3	1000.3	1000.3
1.1	987.51	984.37	990.86	987.80
1.2	974.82	968.64	981.53	975.50
1.3	962.17	953.05	972.27	963.33
1.4	949.56	937.59	963.07	951.31
1.5	936.96	922.25	953.93	939.41
1.6	924.37	907.00	944.84	927.64
1.7	911.77	891.84	935.82	916.00
1.8	899.15	876.75	926.84	904.48
1.9	886.49	861.71	917.91	893.07
2.0	873.77	846.71	909.03	881.78

Table C.3: Circuit simulation (LT Spice) results for a floating precision linear VCR using matched MOSFET device pair with SD-bootstrapped gate, SD-bootstrapped substrate and self-tracking arrangement (Circuit in Figure 4.4 with R_1 = 1 kΩ, R_2 to R_4 = R_6 to R_9 = R_{11} to R_{14} = R_{16} to R_{19} = R_{21} = 10 kΩ, R_5 = R_{10} = R_{15} = R_{20} = 5 kΩ) : R_{XY} as a function of v_{XY}, R_1 = 1000 Ω, v_{C1} = 1 V, v_{C2} = –1 V, v_{C3} = 0 V, and V_{BB} = –2 V. To observe the effect of device parameters V_T, k, and λ. Device parameters: (i) V_T = 0.7 V and k = 0.52 mA/V^2 and (ii) V_T = 0.4 V and k = 0.28 mA/V^2.

	R_{XY} (Ω)			
	(i) V_T = 0.7 V and k = 0.52 mA/V^2 (Calc. R_{XY} = 1000 Ω)		(ii) V_T = 0.4 V and k = 0.28 mA/V^2 (Calc. R_{XY} = 1000 Ω)	
v_{XY} (V)	λ = 0 (Obsrvd. v_A = 5.86 V)	λ = 0.03 (Obsrvd. v_A = 5.75 V)	λ = 0 (Obsrvd. v_A = 6.71 V)	λ = 0.03 (Obsrvd. v_A = 6.60 V)
−2.0	873.76	846.71	927.13	899.81
−1.9	886.49	861.71	934.89	910.04
−1.8	899.15	876.75	942.51	920.19
−1.7	911.77	891.84	950.02	930.29
−1.6	924.37	907.00	957.43	940.34
−1.5	936.96	922.24	964.75	950.36
−1.4	949.56	937.59	971.98	960.36
−1.3	962.17	953.05	979.14	970.34
−1.2	974.82	968.64	986.24	980.31
−1.1	987.51	984.37	993.27	990.28
−1.0	1000.3	1000.3	1000.3	1000.3
−0.9	1013.1	1016.3	1007.2	1010.2
−0.8	1025.9	1032.5	1014.1	1020.2
−0.7	1038.9	1048.9	1020.9	1030.3
−0.6	1051.9	1065.5	1027.7	1040.3
−0.5	1065.0	1082.3	1034.5	1050.4
−0.4	1078.2	1099.3	1041.3	1060.5
−0.3	1091.6	1116.5	1048.0	1070.6
−0.2	1105.0	1133.9	1054.7	1080.8
−0.1	1118.6	1151.6	1061.4	1091.0
0.1	1118.6	1151.6	1061.4	1091.0
0.2	1105.0	1133.9	1054.7	1080.8
0.3	1091.6	1116.5	1048.0	1070.6
0.4	1078.2	1099.3	1041.3	1060.5
0.5	1065.0	1082.3	1034.5	1050.4
0.6	1051.9	1065.5	1027.7	1040.3
0.7	1038.9	1048.9	1020.9	1030.3
0.8	1025.9	1032.5	1014.1	1020.2
0.9	1013.1	1016.3	1007.2	1010.2
1.0	1000.3	1000.3	1000.3	1000.3
1.1	987.51	984.37	993.27	990.28
1.2	974.82	968.64	986.24	980.31
1.3	962.17	953.05	979.14	970.34
1.4	949.56	937.59	971.98	960.36
1.5	936.96	922.25	964.75	950.36
1.6	924.37	907.00	957.43	940.34
1.7	911.77	891.84	950.02	930.29
1.8	899.15	876.75	942.51	920.19
1.9	886.49	861.71	934.89	910.04
2.0	873.77	846.71	927.13	899.81

Table C4: Practical results for a floating precision linear VCR using matched MOSFET device pair with SD-bootstrapped gate, SD-bootstrapped substrate and self-tracking arrangement (Circuit in Figure 4.4 with R_1 = 1 kΩ, R_2 to R_4 = R_6 to R_9 = R_{11} to R_{14} = R_{16} to R_{19} = R_{21} = 10 kΩ, R_5 = R_{10} = R_{15} = R_{20} = 5 kΩ) for v_{C2} and V_{BB} : R_{XY} as a function of v_{XY}, R_1 = 992 Ω, v_{C1} = 1 V, and v_{C3} = 0 V. Measured device parameter for the device pair with mismatch: M1: V_T = 0.396 V and k = 0.575 mA/V^2 and M2: V_T = 0.389 V and k = 0.614 mA/V^2.

	R_{XY} (Ω)			
	V_{BB} = −2 V		V_{BB} = −4 V	
v_{XY} (V)	v_{C2} = −0.5016 V (Calc. R_{XY} = 1980.2 Ω, Obsrvd. v_A = 2.875 V)	v_{C2} = −1.0070 V (Calc. R_{XY} = 991.1 Ω, Obsrvd. v_A = 4.148 V)	v_{C2} = −0.5010 V (Calc. R_{XY} = 1980.9 Ω, Obsrvd. v_A = 3.430 V)	v_{C2} = −1.0101 V (Calc. R_{XY} = 984.9 Ω, Obsrvd. v_A = 4.734 V)
−2.0	1582.36	986.78	1549.21	951.31
−1.9	1607.30	985.38	1561.91	948.12
−1.8	1638.79	987.57	1580.04	952.29
−1.7	1666.73	987.54	1604.41	949.72
−1.6	1694.81	951.42	1622.51	948.78
−1.5	1726.30	988.55	1644.72	948.70
−1.4	1752.88	990.28	1661.91	948.72
−1.3	1782.53	990.21	1686.85	948.69
−1.2	1810.43	988.46	1699.55	948.99
−1.1	1839.33	989.27	1714.09	949.13
−1.0	1863.48	991.12	1727.46	949.80
−0.9	1891.90	995.82	1739.48	950.27
−0.8	1916.53	1008.51	1748.49	951.41
−0.7	1942.63	1023.20	1756.48	953.39
−0.6	1965.47	1041.11	1761.92	954.96
−0.5	1995.25	1045.61	1763.72	958.48
−0.4	2029.56	1052.63	1761.72	963.01
−0.3	2079.32	1056.21	1754.67	971.49
−0.2	2187.57	1038.18	1730.57	987.00
−0.1	2497.60	958.12	1654.04	1034.85
0.1	2514.56	945.69	1657.85	1034.92
0.2	2207.53	1040.85	1738.76	989.86
0.3	2099.30	1068.57	1764.98	974.02
0.4	2049.54	1042.95	1776.75	966.83
0.5	2018.41	1028.97	1782.84	963.52
0.6	1993.39	1020.58	1783.47	960.24
0.7	1971.33	1013.66	1781.04	959.03
0.8	1947.13	1009.93	1776.33	958.12
0.9	1924.66	1006.01	1769.09	957.82
1.0	1899.94	1003.18	1758.57	957.73
1.1	1872.09	1000.73	1746.64	957.94
1.2	1844.75	999.09	1732.57	958.55
1.3	1816.62	997.41	1717.02	958.61
1.4	1787.42	996.02	1699.89	958.97
1.5	1757.72	996.17	1683.52	959.40
1.6	1728.08	993.32	1671.88	959.66
1.7	1693.61	991.94	1650.05	959.92
1.8	1664.31	966.40	1630.61	960.20
1.9	1640.17	988.91	1601.87	960.01
2.0	1608.42	985.18	1570.83	959.24

APPENDIX D

SCHEMATIC OF BIOIMPEDANCE SIMULATOR

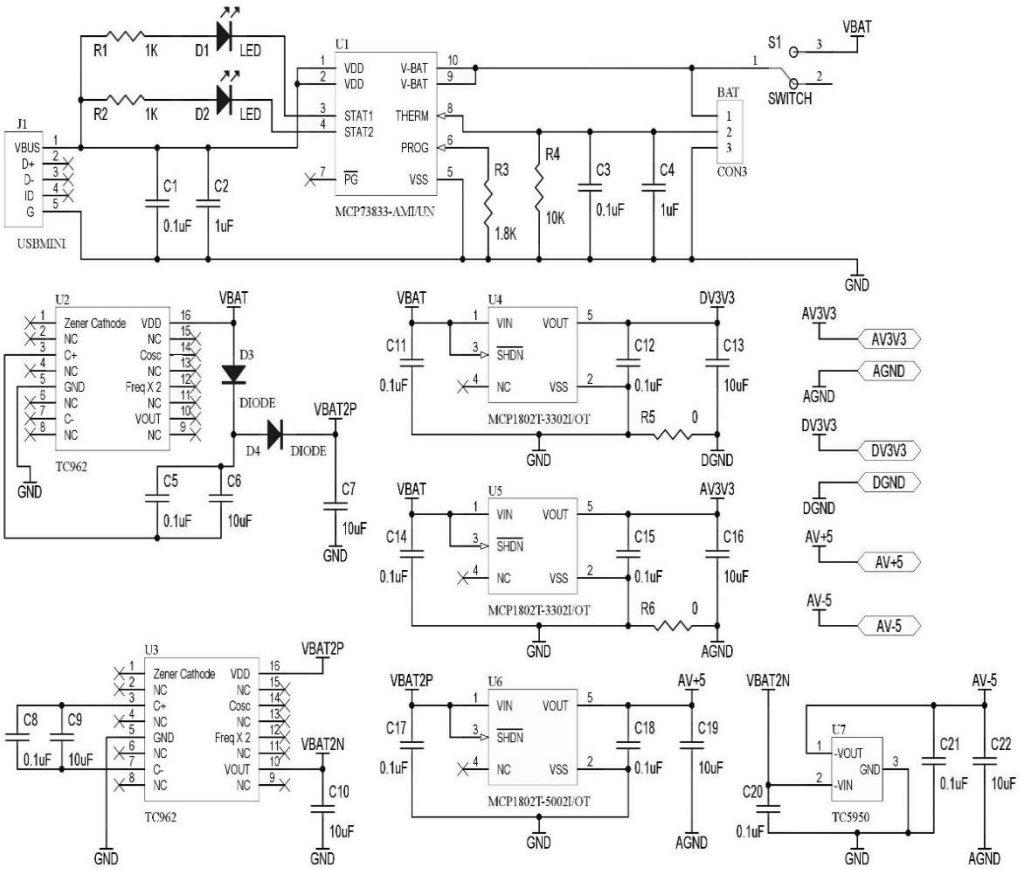

Figure D.1: The power supply circuit.

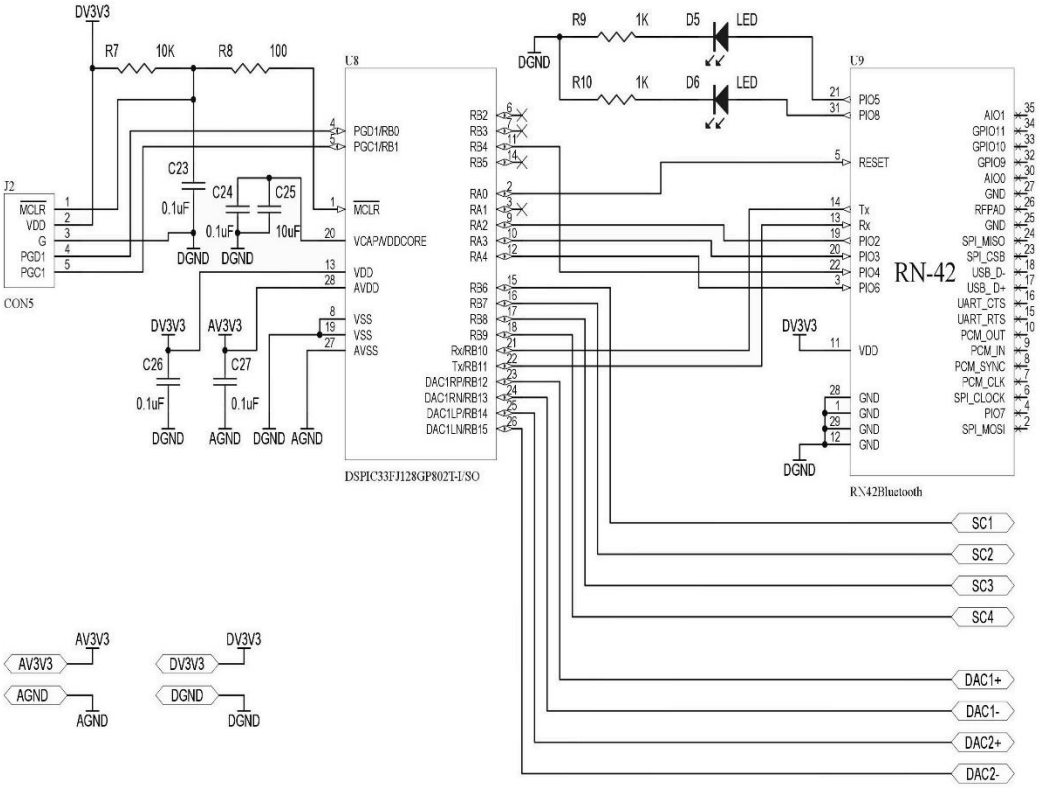

Figure D.2: The controller circuit.

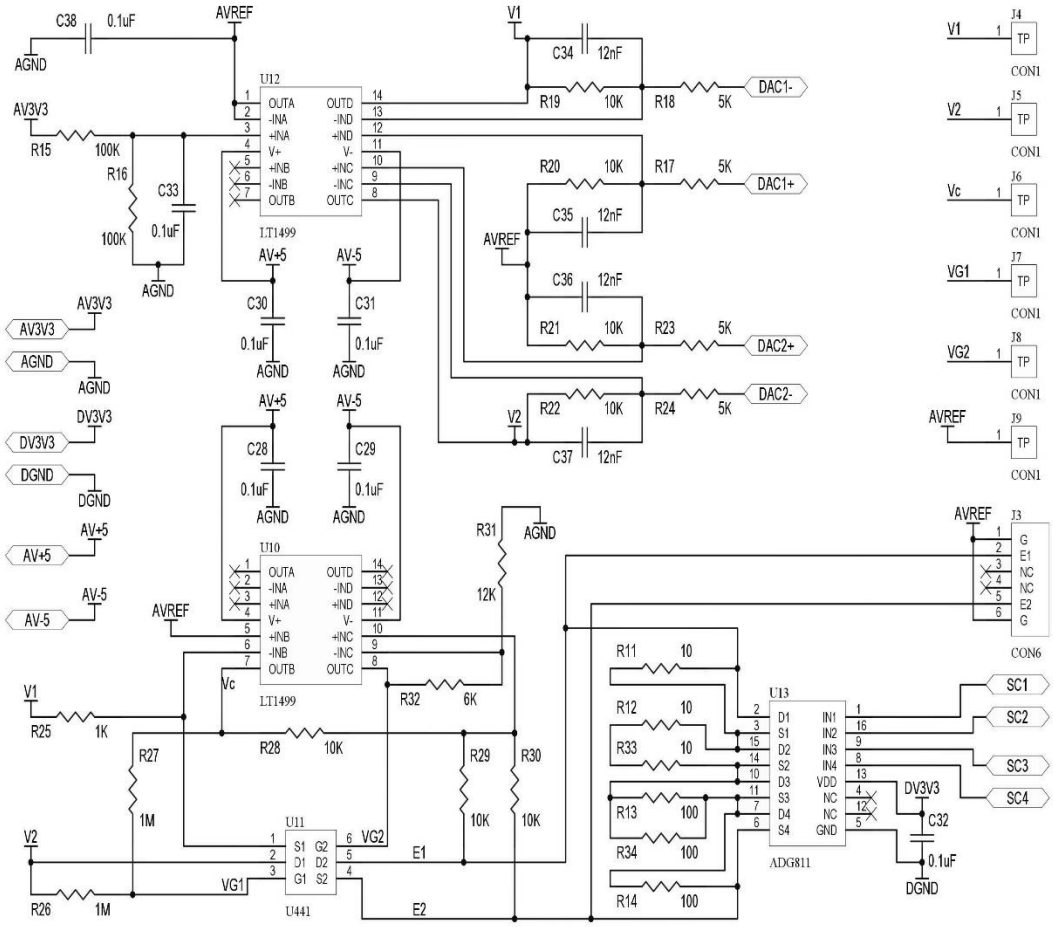

Figure D.3: The impedance variation circuit.

APPENDIX E

PCB LAYOUT OF BIOIMPEDANCE SIMULATOR

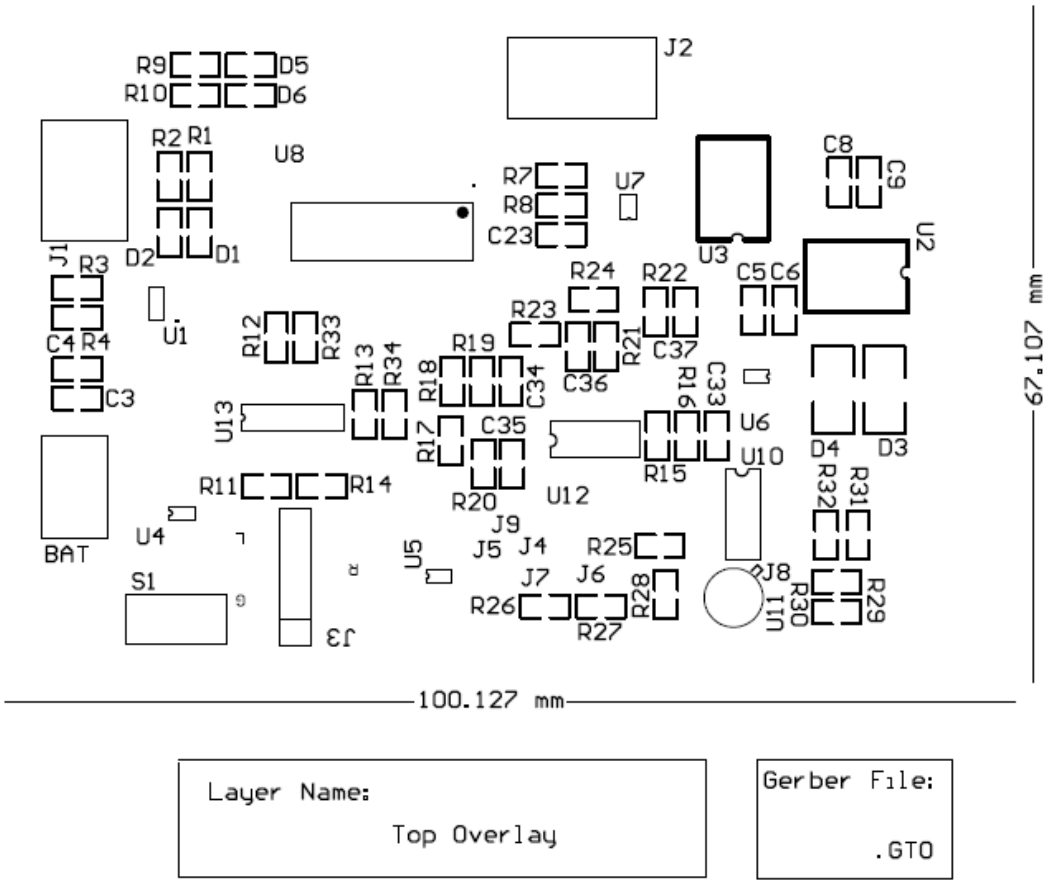

Figure E.1: Top overlay of PCB.

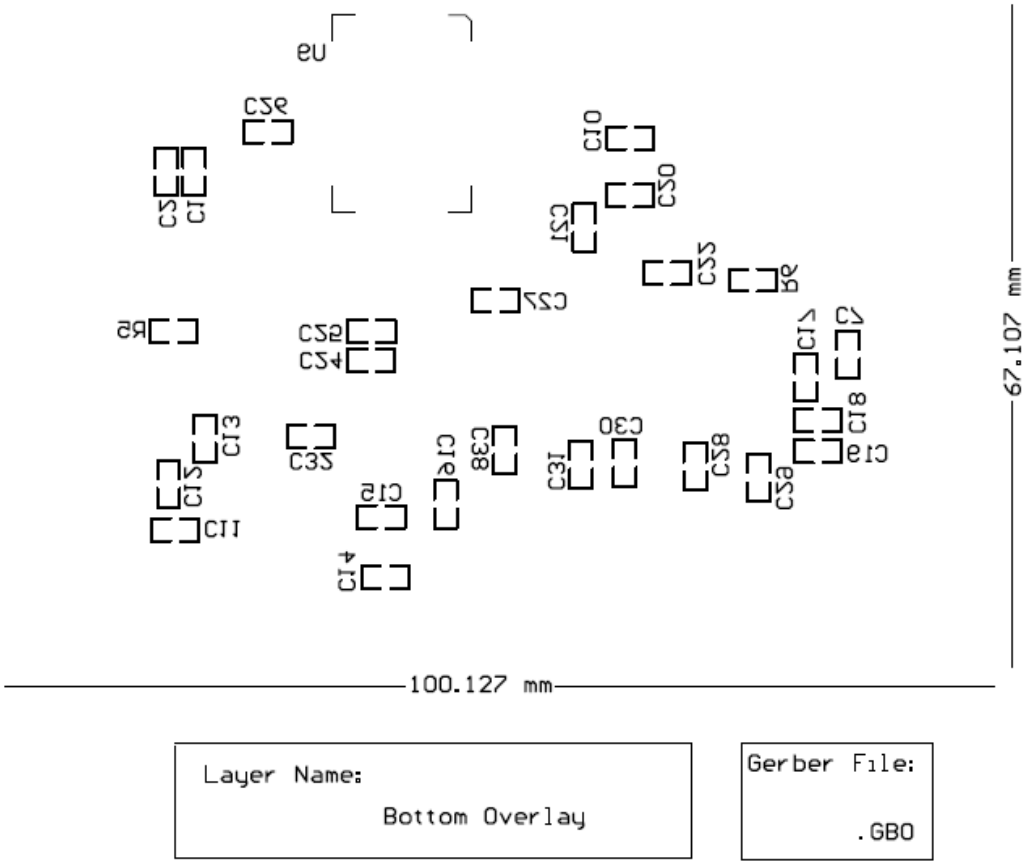

Figure E.2: Bottom overlay of PCB.

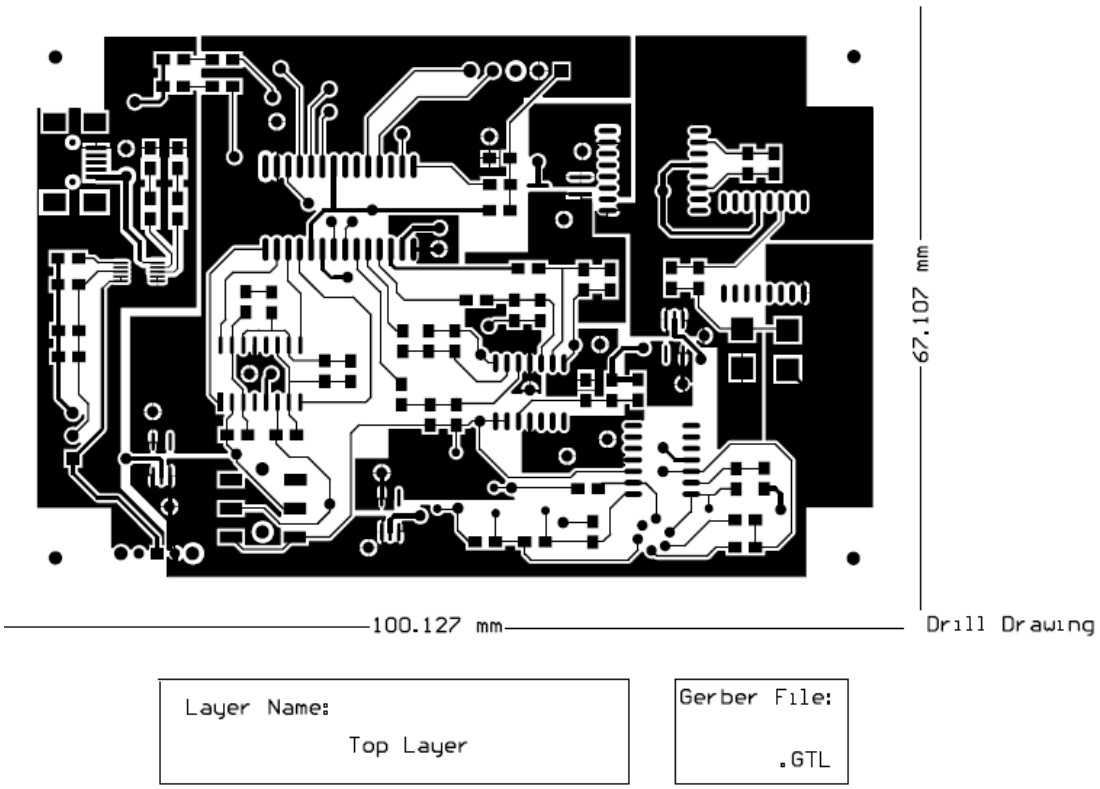

Figure E.3: Top layer of PCB.

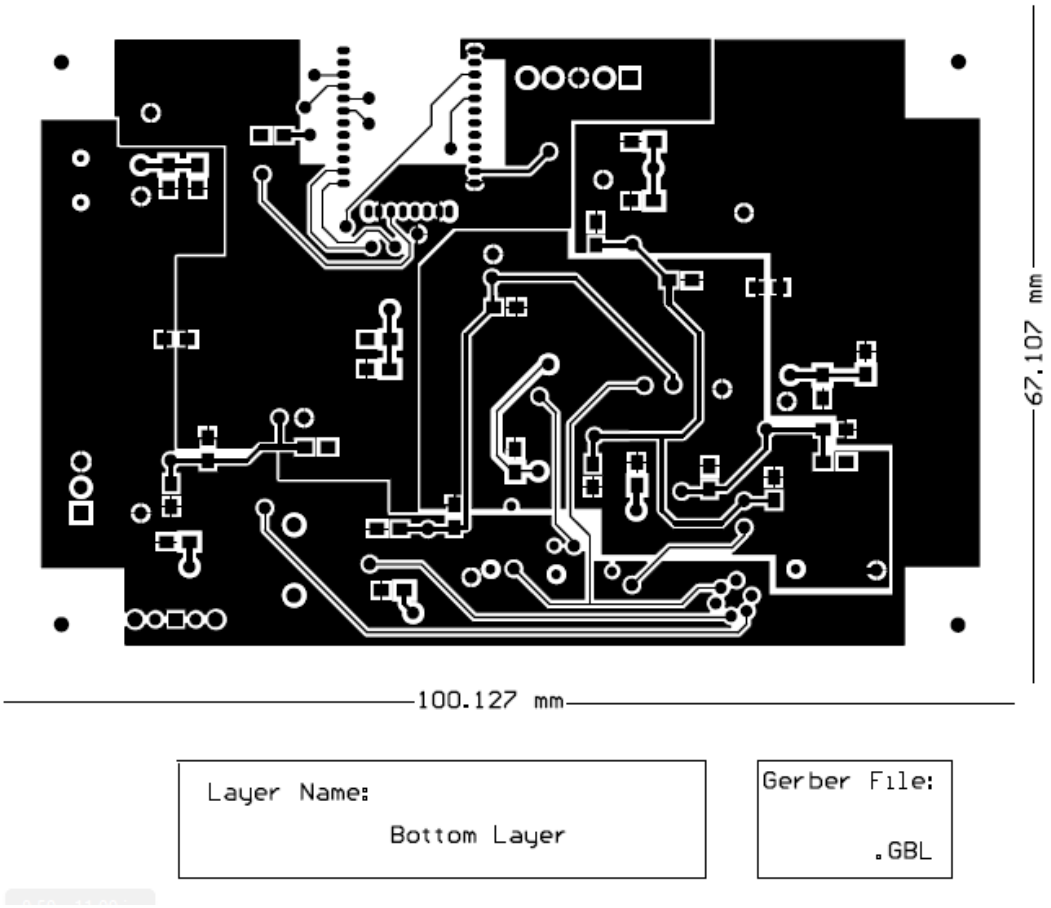

Figure E.4: Bottom layer of PCB.

APPENDIX F

COMPONENT LIST FOR BIOIMPEDANCE SIMULATOR

Table F.1: Component list for the bioimpedance simulator

Component designator	Component description	Part Number / value	Quantity
C1, C3, C4, C5, C8, C11, C12, C14, C15, C17, C18, C20, C21, C23, C24, C26, C27, C28, C29, C30, C31, C32, C33, C38	Capacitor, ceramic, chip	0.1 µF	24
C2, C4	Capacitor, ceramic, chip	1 µF	2
C6, C7, C9, C10, C13, C16, C19, C22, C25	Capacitor, ceramic, chip	10 µF	9
C34, C35, C36, C37	Capacitor, ceramic, chip	12 nF	4
R1, R2, R9, R10, R25	Resistor	1 kΩ	5
R3	Resistor	1.8 kΩ	1
R17, R18, R23, R24, R32	Resistor	5 kΩ	5
R4, R7, R28, R29, R30, R31	Resistor	10 kΩ	6
R15, R16	Resistor	100 kΩ	2

R26, R27	Resistor	1 MΩ	2
R11, R12, R33	Resistor	10 Ω	3
R8, R13, R14, R34	Resistor	100 Ω	4
U1	IC, Li–ion charge management controller	MCP73833	1
U2, U3	IC, Charge pump dc to dc converter	TC962	2
U4, U5	IC, LDO	MCP1802–3.3	2
U6	IC, LDO	MCP1802–5	1
U7	IC, Negative LDO	TC5950	1
U7, U8	IC, LDO	MCP1802-3.3	2
U9	IC, LDO	MCP1802-5	1
U11	IC, LDO	TC5950	1
U8	IC, Microcontroller	DSPIC33FJ128GP802	1
U9	Bluetooth Module	RN42	1
U10, U12	IC, Op amp	LT1499	2

U11	Matched pair JFET	U441	1
U13	IC, Analog Switch	ADG811	1
D1, D2, D5, D6	LED	LED	2
D3, D3	Diode	Diode	2
J1	USBMINI	USBMINI	1
J2	Connector, 5 Pin	DEBUG	1
J3	Stereo Phone Jack	PHONEJACK	1
BAT	Li-ion Battery	Li-ion Battery	1
S1	Switch	Switch	1
TP	Connector, 1 Pin	Test Pin	6

REFERENCES

[1] S. Grimnes and O. G. Martinsen, *Bioimpedance and Bioelectricity Basics*, 2nd ed., Oxford, UK, Elsevier, 2008.

[2] H. P. Schwan and C. F. Kay, “Specific resistance of body tissues,” *Circulation Research*, vol. 4 (6), pp. 664−670, 1956.

[3] R. P. Patterson, “Fundamentals of impedance cardiography,” *IEEE Eng. Med. Biol. Mag.*, vol. 8 (1), pp. 35–38, 1989.

[4] Z. Lababidi et al., “The first derivative thoracic impedance cardiogram,” *Circulation Research*, vol. 41 (4), pp. 651–658, 1970.

[5] L. E. Baker, “Applications of impedance technique to the respiratory system,” *IEEE Eng. Med. Biol. Mag.*, 1989, vol. 8 (1), pp. 50–52.

[6] B. Sramek, "Noninvasive continuous cardiac output monitor." U.S. Patent 4450527, May 22, 1984.

[7] H. H. Woltjer et al., “The technique of impedance cardiography,” *Euro. Heart J.*, 1997, vol. 18 (9), pp. 1396–1403.

[8] D. P. Bernstein and H. J. M. Lemmens. "Stroke volume equation for impedance cardiography." *Med. Biol. Eng. Comput.*, 2005, vol. 43 (4), pp. 443-450.

[9] L. E. Baker, “Principles of the impedance technique,” *IEEE Eng. Med. Biol. Mag.*, 1989 vol. 8 (1), pp. 11–15.

[10] H. H. Woltjer et al., “Optimalisation of the spot electrode array in impedance cardiography,” *Med. Biol. Eng. Comput.*, 1996, vol. 34 (1), pp. 84−87.

[11] Medis, “NICCOMO – non-invasive continuous cardiac output monitor,” Available online, medis.company/cms/uploads/PDF/niccomo.pdf, accessed: June 9, 2016.

[12] Philips, “Phillips ICG – impedance cardiography,” Available online, incenter.medical.philips.com/doclib/enc/fetch/2000/4504/577242/577243/577247/582646/583147/PM_-_ICG_Brochure.pdf, accessed: June 9, 2016.

[13] V. K. Pandey et al., “Impedance simulator for testing of instruments for bioimpedance sensing,” *IETE J. Research*, vol. 54 (3), pp. 203−207, 2008.

[14] M. Ulbrich et al., "A thorax simulator for complex dynamic bioimpedance measurements with textile electrodes," *IEEE Trans. Biomed. Circuits Syst.*, vol. 9 (3), pp. 412–420, 2015.

[15] J. Millman and C. C. Halkias, *Integrated Electronics*, 2nd ed., New York: McGraw Hill, 2010, pp. 322−327.

[16] A. S. Sedra and K. C. Smith, *Microelectronic Circuits*, 5th ed., New York: Oxford University Press, 2004, pp 248–259.

[17] M. Banu and Y. Tsividis, "Floating voltage controlled resistors in CMOS technology," *Electronics Letters*, vol. 18 (15), pp. 678−679, July 22, 1982.

[18] K. Nay and A. Budak, "A voltage-controlled resistance with wide dynamic range and low distortion," *IEEE Trans. Circuits Syst.*, vol. CAS-30, pp. 770-772, Oct. 1983.

[19] K. Nay and A. Budak, "A variable negative resistance," *IEEE. Trans. Circuits Syst.*, vol. CAS-32, pp. 1193-1194, Nov. 1985.

[20] R. Senani and D. R. Bhaskar, "A simple configuration for realizing voltage-controlled impedances', *IEEE Trans. Circuits Syst.*, vol 39 (1), pp. 52-59, Jan. 1992.

[21] R. Senani, "Realisation of linear voltage-controlled resistance in floating form," *Electronics Letters*, vol. 30 (23), pp. 1909−1911, Nov. 10, 1994.

[22] T. L. Clarke, "FET pair and op amp linearize voltage controlled resistor," *Electronics Letters*, pp. 111, Apr. 28, 1977.

[23] N. Tadic, "Resistive mirror based voltage controlled resistor," in *Proc. IEEE Instrum. Meas. Technol. Conf.*,St. Paul, Minnesota, USA, pp. 760– 765, May 1998.

[24] R. Holani et al., "A JFET-based circuit for realizing a precision and linear floating voltage-controlled resistance," in *Proc. 11th Annu. Conf. IEEE India Council (IEEE Indicon 2014)*, Pune, India, Dec. 2014, paper no. 1098.

[25] Vishay, "Matched n-channel JFET pairs," Available online, pdf.datasheetcatalog.com/datasheet/vishay/70251.pdf, accessed: Apr. 30, 2015.

[26] Linear Systems. (2016, Mar. 31). jfet2003_ls5911familyspicemodels.zip [Online]. www.linearsystems.com/products_details.php?pr=jfet-amplifiers--duals&pro_i d = 27.

[27] Texas instruments, "General-purpose operational amplifiers," Available online, www.ti.com/lit/ds/symlink/ua741.pdf, accessed: June 22, 2016.

[28] M. Ismail and T. Fiez, *Analog VLSI: Signal and Information Processing*, New York: McGraw-Hill, 1994, pp. 13−22.

[29] Y. Tsividis, *Operation and Modelling of the MOS Transistor*, 2nd ed., Singapore:WCB/McGraw Hill, 1999.

[30] I. M. Filanovsky and A. Allam, “Mutual compensation of mobility and threshold voltage temperature effects with applications in CMOS circuits,” *IEEE Trans. Circuits Syst.*, vol. 48 (7), pp. 876−884, Jul. 2001.

[31] G. Moon, M. E. Zaghloul, and R. W. Newcomb, “An enhancement-mode MOS voltage-controlled linear resistor with large dynamic range,” *IEEE Trans. Circuits Syst.*, vol. 37 (10), pp. 1284−1288, Oct. 1990.

[32] J. Fort, “MOS resistor with second or higher order compensation,” U. S. Patent 8 067 975, Nov. 29, 2011.

[33] J. K. Greason, “Voltage-controlled resistance element with superior dynamic range,” U.S. Patent 5 264 785, Nov. 23, 1993.

[34] B. White and M. N. Hagh, “Precision MOS resistor,” U. S. Patent 5 345 118, Sep. 6, 1994.

[35] A. Bilotti, “Operation of a MOS transistor as a variable resistor,” *IEEE Proc. Letters*, pp. 1093−1094, Aug. 20, 1966.

[36] A. C. Barber, “Linearization of voltage-controlled amplifier using MOSFET gain control circuit,” U. S. Patent 5 808 516, Sep. 15, 1998.

[37] Advanced Linear Devices, “Quad/dual n-channel matched pair MOSFET array,” Available online, http://www.aldinc.com/pdf/ALD1116.pdf, downloaded on May 29, 2015.

[38] Advance Linear Devices. (2016, May. 15). Model_ALDMOSFET.zip [Online]. http://www.aldinc.com//pdf/Model_ALDMOSFET.zip.

[39] N. S. Manigandan, “Development of hardware for impedance cardiography,” M.Tech. dissertation, Biomedical Eng., IIT Bombay, Mumbai, India, 2004.

[40] N. K. S. Naidu, “Hardware for impedance cardiography,” M.Tech. dissertation, Biomedical Eng., IIT Bombay, Mumbai, India, 2005.

[41] L. Venkatachalam, “Development of hardware for impedance cardiography,” M.Tech. dissertation, Biomedical Eng., IIT Bombay, Mumbai, India, 2006.

[42] B. B. Patil, “Instrumentation for impedance cardiography,” M. Tech. dissertation, Biomedical Eng., IIT Bombay, Mumbai, India, 2009.

[43] R. Holani, “A bioimpedance simulator for impedance cardiography,” M.Tech. dissertation, Biomedical Engg., IIT Bombay, Mumbai, India, 2012.

[44] M. D. Desai, “Development of an impedance cardiograph,” M.Tech. dissertation, Biomedical Eng., IIT Bombay, Mumbai, India, 2012.

[45] Analog Devices, “< 0.5 Ω CMOS, 1.65V−3.6V, quad SPST switches,” Available online, www.analog.com/static/imported-files/data_sheets/ADG811_812_813. pdf, accessed: Apr. 30, 2015.

[46] Linear Technology, “10MHz, 6V/μs, dual/quad rail-to-rail input and output precision C-load op amps,” Available online, cds.linear.com/docs/en/datasheet/ 14989fg.pdf, accessed: Apr. 30, 2015.

[47] Microchip, “High performance, 16-bit digital signal controller,” Available online, www.microchip.com/downloads/en/DeviceDoc/70292E.pdf, accessed: April 30, 2015.

[48] Microchip, “Class 2 Bluetooth module with EDR support,” Available online, ww1.microchip.com/downloads/en/DeviceDoc/rn-42-ds-v2.32r.pdf, accessed: May 26, 2015.

[49] Microchip, “300 mA, 16V, high-performance LDO,” Available online, ww1.microchip.com/downloads/en/DeviceDoc/25160A.pdf, accessed: Apr. 30, 2015.

[50] Microchip, “Low dropout, negative output voltage regulator,” Available online, ww1.microchip.com/downloads/en/DeviceDoc/21438C.pdf, accessed: Apr. 30, 2015.

[51] Microchip, “High current charge pump DC-to-DC converter,” Available online, ww1.microchip.com/downloads/en/DeviceDoc/21484D.pdf, accessed: Apr. 30, 2015.

[52] Microchip, “Stand-alone linear Li-ion / Li-polymer charge management controller,” Available online, ww1.microchip.com/downloads/en/DeviceDoc/22005a.pdf, accessed: May 26, 2015.

ACKNOWLEDGEMENT

I would like to acknowledge my sincere gratitude to my supervisor Prof. P. C. Pandey for his invaluable and constant guidance throughout the journey of my M.Tech. program. I am very thankful to him for giving me the opportunity to work with him, knowledge for doing my project, and moral support. I really enjoyed and learned a lot from the discussions with him about my project work and important lessons about life.

I would like to thank Mr. Nandkumar Pai for his invaluable guidance during the practical implementation of my project and learned a lot about PCB designing. I am grateful to Mr. Vidyadhar Kamble for his constant support for helping me in this project and availing the required components and facilities whenever required. I would like to thank my senior Amritanshu Gupta for encouraging me to take up this project and for giving moral support throughout this journey. I would like to thank Nitya Tiwari, K. S. Natraj, Yogesh, Saketh, Prachir, Vikas, and all my friends for their help and support.

Last but not the least, I am thankful to my parents for their love and constant support in my life. I am thankful to GOD for giving me such prestigious opportunity in my life.

AUTHOR'S RESUME

Shibam Debbarma: He has received his B.Tech. degree in Electronics and Communication Engineering from the National Institue of Technology, Agartala in 2012. Presently he is pursuing his M.Tech. program in Biomedical Engineering from the Indian Institute of Technology Bombay. His area of interest includes electronic system design, embedded systems and software development.